INCREASING FRESHWATER RECOVERY UPON AQUIFER STORAGE

A field and modelling study of dedicated aquifer storage and recovery configurations in brackish-saline aquifers

Koen G. Zuurbier

INCREASING FRESHWATER RECOVERY UPON AQUIFER STORAGE

A field and modelling study of dedicated aquifer storage
and recovery configurations in brackish-saline aquifers

PROEFSCHRIFT

ter verkrijging van de graad van doctor
aan de Technische Universiteit Delft,
op gezag van de Rector Magnificus prof. ir. K.Ch.A.M. Luyben;
voorzitter van het College voor Promoties,
in het openbaar te verdedigen op dinsdag 10 mei 2016 om 15:00 uur
door

Koen Gerardus ZUURBIER
Master of Science in Earth Sciences
(Vrije Universiteit Amsterdam)
geboren te Heerhugowaard, Nederland

Dit proefschrift is goedgekeurd door de promotor:
Prof. Dr. P. J. Stuijfzand en Dr. N. Hartog

Samenstelling promotiecommissie:

Rector Magnificus	voorzitter
Prof. dr. P.J. Stuijfzand	promotor
Dr. N. Hartog	copromotor

onafhankelijke leden:
Prof. dr. G. Massmann (Carl von Ossietzky University, Oldenburg)
Prof. dr. R.J. Schotting (Universiteit Utrecht)
Prof. dr. ir. T.N. Olsthoorn (Technische Universiteit Delft)
Prof. dr. ir. T.J. Heimovaara (Technische Universiteit Delft)
Dr. A. Vandenbohede (De Watergroep, Universiteit Gent)

Dit onderzoek is gefinancierd vanuit:
- Het onderzoeksprogramma Kennis voor Klimaat, binnen het thema 'Zoetwatervoorziening' (www.kennisvoorklimaat.nl)
- Het bedrijfstakonderzoek van de Nederlandse Drinkwaterbedrijven (BTO, www.kwrwater.nl/BTO)
- Het EU-project DESSIN (grant agreement no. 619039)
- Het EU-project SUBSOL (grant agreement no. 642228)

Het onderzoek is uitgevoerd bij KWR Watercycle Research Institute, de Amsterdam Critical Zone Hydrology Group en de TU Delft.

ISBN 978-90-74741-00-2
KWR2015.061

Illustratie voorzijde: Flow Design, Utrecht
Opmaak/vormgeving: WarmGrijs, Hilversum
Druk: Print Service Ede

TABLE OF CONTENTS

Summary

The subsurface may provide opportunities for robust, effective, sustainable, and cost-efficient freshwater management solutions. For instance, via aquifer storage and recovery (ASR; Pyne, 2005): "the storage of water in a suitable aquifer through a well during times when water is available, and the recovery of water from the same well during times when it is needed". This can be successful in storing and recovering both potable and irrigation water. ASR is attractive due to the limited space requirements above ground and the generally successful conservation of water quality (Maliva and Missimer, 2010).

The recovery efficiency (RE) of ASR is defined as the part of the injected water that can be recovered with a satisfying quality. Several factors can limit the RE during ASR in brackish-saline aquifers, such as the simultaneous abstraction of injected freshwater and ambient, more saline groundwater. This can be a result of 'bubble drift', which happens when the infiltrated bubble is transported away from the ASR well by the local or regional hydraulic gradient. However, the RE can be particularly limited in brackish–saline aquifers by the density difference between the injected freshwater and ambient brackish or saline groundwater. This is because this density difference causes the freshwater to float upwards in the aquifer ('buoyancy effect'), while denser saline water is recovered by lower parts of the well (Esmail and Kimbler, 1967; Merritt, 1986; Ward et al., 2007). Both water types are thus blended in the ASR well to produce a brackish, generally unsuitable water quality.

Freshwater availability is more and more stressed in coastal areas, where brackish and saline groundwater is commonly present. Therefore, the ability to increase the RE of ASR systems provides a true benefit because it would significantly amplify the potential of freshwater management. The general objective of this study is therefore *to quantify and increase the performance (indicated by RE) of relatively small-scale ASR systems in areas with brackish-saline groundwater, taking into account recently developed well configurations for performance optimization*.

Methods

To achieve this research's objective, a broad range of research techniques was applied to the Dutch coastal area. This included a validation of theoretical performance estimation methods proposed by Ward et al. (2009) and Bakker (2010) using recorded data of existing small-scale ASR systems. This was followed by spatial performance mapping using regional hydrogeological data in a geographic information system (GIS).

An advanced, small-scale ASR system was realized in the Nootdorp area. Here, a moderate to low ASR performance was predicted as a consequence of buoyancy effects. Independently operating multiple partially penetrating wells (MPPW) were

installed in a single borehole. The purpose was to improve the system's RE by enhanced deep infiltration and shallow recovery. Very strict water quality limits (Na concentrations <0.5 mmol/l or <11.5 mg/l and Fe and Mn <0.05 mg/l) implied that the injected rainwater had to be recovered practically unmixed. Prior to this field pilot, the target aquifer was characterized by obtaining undisturbed sediment cores, performing high-resolution core-scans and sampling, followed by physical and chemical analysis of sediment and groundwater samples. The ASR operation and the residence and transport of the freshwater in the brackish target aquifer (150 – 1,100 mg/l Cl) were extensively monitored and recorded via online sensors, a programmable logic controller, geophysical measurements, and groundwater sampling and analysis.

A similar, second pilot was realized in a more saline aquifer (Westland area, 4,000 – 5,000 mg/l Cl). The ASR operation was simulated using SEAWAT groundwater transport modelling (Nootdorp, Westland) and PHT3D (Nootdorp only). This put the performance of the MPPW-ASR systems with respect to more conventional well configurations into perspective.

Finally, a dedicated 'Freshmaker' system was realized in the south-western delta of the Netherland. A pair of 70 m long, superimposed horizontal directionally drilled wells (HDDWs) was installed to inject freshwater at 7 m depth during winter and intercept saltwater at 14.5 m depth. This way, an approximately 9 m thick freshwater lens was thickened over a long aquifer strip, storing up to 4,500 m^3 of freshwater in the process. The same freshwater volume was abstracted by the shallow HDDW in the summer season, while maintaining the deep saltwater interception. Again, a detailed characterization of the target aquifer was performed using geophysical measurements, physical and chemical sediment analysis, and groundwater sampling and analysis. During operation, geophysical borehole measurements and groundwater sampling and analysis were frequently performed. A 2-D groundwater transport model was set up using SEAWAT to evaluate the Freshmaker's performance in relation to other simulated ASR strategies at the site.

Results spatial analysis of ASR performance

ASR performance of existing systems in the study area showed good agreement with the predicted performance using the two ASR performance estimation methods. Deviations between actual and predicted ASR performance may originate from simplifications in the conceptual model and uncertainties in the hydrogeological and hydrochemical input. As the estimation methods proved suitable to predict ASR performance, meaningful feasibility maps were generated to identify favourable ASR sites. The success of actual small- to medium-scale ASR systems displayed a strong spatial

variability in the study area. This emphasizes the relevance of reliable a priori spatial mapping. Even in brackish aquifers (< 1,000 mg/l Cl), the performance of small- to medium-scale ASR may already be low.

Results MPPW-ASR systems

The MPPW operating with deep injection and shallow recovery helped to reduce freshwater losses during ASR at the Nootdorp pilot. The SEAWAT modelling showed that the simulated Cycle 1 freshwater recovery of fully penetrating and single partially penetrating wells is 15 and 30% of the injected water, respectively. This is significantly less than the 40% recovered by the MPPW. Modelling indicated that, in subsequent cycles, 60% could be recovered by the MPPW, which is significantly more than the predicted <20 and <35% by the conventional well types. The system will, however, never attain an RE of 100%, as mixing in the lower half of the aquifer remains a source of freshwater losses. However, in less ideal ASR conditions, a viable system can still be realized using the MPPW, while additional costs are limited. The unrecoverable freshwater will move laterally from the ASR well in the upper zone of the target aquifer.

Freshwater injected by the deepest of four well MPPW screens became enriched with sodium (Na) and other dominant cations from the brackish groundwater. This was due to cation exchange triggered by 'freshening'. This enriched freshwater was predominantly recovered at the shallowest well, thanks to the buoyancy effects. During recovery periods, the breakthrough of Na was retarded in the deeper and central parts of the aquifer during 'salinization'. The buoyancy effects precluded a progressively improving water quality with subsequent cycles, which is generally observed during ASR systems not suffering from buoyancy effects. The process of cation exchange can either increase or decrease the RE of MPPW-ASR operation, depending on the maximum concentration limits set for Na, the cation exchange capacity, and native groundwater and injected water composition.

Dissolution of Fe and Mn-containing carbonates in deeper sections of the aquifer led to contamination with Fe^{2+} and Mn^{2+} in injected water. Proton-buffering upon pyrite oxidation in at this aquifer interval stimulated this dissolution. In Cycle 1, carbonate dissolution was further stimulated by CO_2-production by oxidation of (adsorbed) Fe^{2+} and Mn^{2+}. Since pyrite consumed virtually all oxygen in the deeper aquifer sections, Fe^{2+} and Mn^{2+} remained mobile in the anoxic water upon release. During recovery, Fe^{2+} precipitated via reduction of MnO_2. Recovery at this interval was therefore marked by a severe and continuous contamination with predominantly Mn^{2+}. However, the field pilot indicated that recovery of Mn^{2+} and Fe^{2+} could be prevented

by frequent injections of small volumes of oxygen-rich water via the normally recovering, shallowest well, as this triggered local subsurface iron removal.

The essentially upward flow paths in the MPPW-ASR system expose a significant part of the injected water to the pronounced vertical geochemical stratification of the aquifer. It was demonstrated that the vertical stratification of reactive layers controls the mobilization of undesired elements during MPPW-ASR, rather than the average geochemical composition of the target aquifer. Especially the deep aquifer intervals control the water quality development shortly after injection, while later also intercalated, potentially reactive intervals are flushed prior to recovery. This justifies a more detailed geochemical characterization of target aquifers for MPPW-ASR, as well as an optimized operation of its injection and recovery wells, depending on which elements control the recovery efficiency.

Connections between originally separated coastal aquifers ('conduits') had a negative effect on the freshwater RE during ASR in brackish-saline aquifers at the Westland ASR pilot. The saline ASR target aquifer was underlain there by a deeper more saline aquifer, which was used for aquifer thermal energy storage (ATES). Although both aquifers were considered properly separated based on lithology and groundwater composition, intrusion of deeper saltwater quickly terminated the freshwater recovery. The most likely pathway identified by field measurements, hydrochemical analyses, and SEAWAT transport modelling was the borehole of the ATES well. This borehole provided a pathway for short-circuiting of deeper saltwater. Transport modelling underlined that the potentially rapid short-circuiting during storage and recovery can reduce the RE to null. When virtually no mixing with ambient groundwater is allowed, a linear RE decrease by short-circuiting with increasing distance from the ASR well within the radius of the injected freshwater body was observed in the simulations. Field observations and groundwater transport modelling showed that the intentional interception of deep short-circuiting water (via the deepest MPPW screens) can mitigate the observed RE decrease. However, complete compensation of the RE decrease will generally be unattainable since also injected freshwater gets intercepted. Finally, it was found that brackish water upconing from the underlying aquitard towards the shallow recovery wells of the MPPW-ASR system can also occur and counteract an increased RE by the use of MPPWs.

Results Freshmaker HDDW system

Groundwater transport modelling preceding the ASR operation demonstrated that the Freshmaker system is able to abstract a freshwater volume of at least 4,200 m^3, equal to the infiltrated freshwater volume, without exceeding strict salinity limits. This would

be unattainable with conventional ASR set-ups. Even when infiltration via the upper HDDW is omitted, a similar freshwater volume can eventually be abstracted thanks to the increased infiltration of freshwater upon deep interception of saline groundwater. The field pilot supported the model outcomes, as almost 4,500 m^3 of freshwater could be successfully abstracted during the Summer of 2014 upon infiltration of an equal freshwater volume. During the ASR operation, a clear increase and decrease of the freshwater lens was observed by geophysical measurements. It was also found that freshwater recovery should be distributed over longer timeframes to achieve successful abstraction.

Conclusions

In this thesis, a broadened scientific understanding of the recovery efficiency (RE) of ASR systems in brackish-saline aquifers is described. A meaningful *a priori* indication of the ASR performance can be obtained by existing performance estimation methods, which have therefore been included in a mapping tool to identify potential and unviable ASR sites. Application of this mapping tool in the coastal Westland-Oostland area highlighted that the predicted ASR-performance in coastal areas can be spatially highly-variable.

There is a potential RE increase that can be attained by implementing dedicated well configurations at ASR-systems in brackish-saline aquifers, which would otherwise achieve moderate to low REs. The dedicated well configurations are primarily based on an increased vertical control on freshwater injection and recovery, optionally complemented by interception of deeper brackish or saline groundwater. Despite significant improvement, an RE of 100% is unattainable in brackish/saline aquifers, since mixing processes at periodically salinizing aquifer intervals will inevitably remain an ever-present cause of freshwater losses. Compared to conventional, bi-directional ASR with (sub)horizontal flow in fresh water aquifers, the dedicated ASR set-ups lead to a large scale vertical upward (buoyant) flow. This means that horizontal, reactive intervals in the deep intervals of the target aquifer have a much more pronounced impact on the recovered water quality. Another important deviation consists of the repeating processes of freshening and salinization induced by buoyancy of the injected bubble.

The findings in this thesis provide important means to achieve a local, self-reliant freshwater supply in especially coastal areas using temporally available freshwater sources via ASR. In these areas, which suffer most from decreasing freshwater availabilities and growing demands, ASR can now become a viable cost-effective freshwater management option, whereas it was previously neglected due to the limited success of conventional ASR systems.

Samenvatting

De ondergrond biedt kansen om te komen tot een robuust, effectief, duurzaam en kostenefficiënt zoetwaterbeheer. Een voorbeeld hiervan is de techniek aquifer storage and recovery (ASR; Pyne, 2005): “het opslaan van tijdelijke zoetwateroverschotten middels infiltratie via een put, gevolgd door terugwinning via dezelfde put bij een zoetwatervraag.” Deze opslag vindt plaats in aquifers: watervoerende grondlichamen. Met deze techniek kan succesvolle opslag en terugwinning van bijvoorbeeld drinkwater en irrigatiewater plaatsvinden. ASR is een interessante techniek vanwege het beperkte ruimtebeslag bovengronds en het behoud van waterkwaliteit ondergronds (Maliva and Missimer, 2010).

De ‘recovery efficiency’ (RE) duidt aan hoe groot het aandeel is dat van het geïnfiltreerde water met een acceptabele kwaliteit kan worden teruggewonnen tijdens ASR. Verschillende factoren kunnen deze RE limiteren wanneer ASR wordt toegepast in brakke of zoute aquifers, zoals het terugwinnen van brak of zout grondwater tezamen met geïnfiltreerd zoetwater. Dit kan bijvoorbeeld het gevolg zijn van ‘afdrijving’, waarbij het geïnfiltreerde zoetwater door regionale grondwaterstroming zich verplaatst tot buiten het bereik van de ASR-put. Echter, ook in niet-stromend grondwater kan in brakke-zoute aquifers een verlies van winbaar zoetwater ontstaan. Dit wordt veroorzaakt door het dichtheidsverschil tussen geïnfiltreerd zoetwater en zouter omringend grondwater. Dit veroorzaakt opdrijving van het zoetwater naar de bovenzijde van de aquifer, en tegelijkertijd verdringing van zoetwater onderin de aquifer (Esmail and Kimbler, 1967; Merritt, 1986; Ward et al., 2007). Het gevolg is dat het water dat gewonnen wordt via de ASR-put bestaat uit een mengsel van geïnfiltreerd zoetwater en zouter grondwater. Dit mengsel zal door de zoute bijmenging al snel niet meer aan de gangbare kwaliteitseisen voldoen.

Ondertussen neemt de zoetwaterbeschikbaarheid juist in kustgebieden, waar brakke en zoute grondwatervoorkomens domineren, steeds verder af. Het is daarom van belang om de doorgaans geringe RE van ASR-systemen in deze gebieden te vergroten, om zo echt een bijdrage aan de zoetwatervoorziening te kunnen realiseren. Watergebruikers kunnen hierdoor een hoge mate van zelfvoorzienendheid bereiken, zoals bijvoorbeeld beoogd binnen het Nederlandse Deltaprogramma Zoetwater. Het doel van dit onderzoek was dan ook om *de prestaties (op basis van RE) van relatief kleinschalige ASR-systemen in gebieden met brakke en/of zoute aquifers te kwantificeren en te verbeteren met behulp van recent ontwikkelde putsystemen*.

Methoden

Verschillende onderzoekstechnieken zijn toegepast in de Nederlandse kustgebieden om het onderzoeksdoel te behalen. Zo zijn theoretische inschattingsmethoden voor de prestaties van ASR zoals voorgesteld door Ward et al. (2009) en Bakker (2010) gevalideerd met behulp van geregistreerde prestaties van kleinschalige ASR-systemen. Hierop volgend zijn met behulp van een geografisch informatie systeem (GIS) en ruimtelijke geohydrologische data de te verwachten ASR-prestaties in het studiegebied Westland-Oostland gekarteerd.

Vervolgens is een geavanceerd, kleinschalig ASR-system gerealiseerd in het studiegebied (Nootdorp). Een beperkte RE kon hier worden verwacht als gevolg van opdrijvingseffecten. Als 'ASR-put' werd gekozen voor onafhankelijk opererende putfilters, boven elkaar geplaatst in één boorgat (MPPW: multiple partially penetrating wells). Het doel hiervan was om de RE te verhogen door met name onderin de aquifer te infiltreren en bovenin terug te winnen. Strikte waterkwaliteitseisen ten behoeve van de hoogwaardige glastuinbouw ter plaatse (natrium concentratie <0.5 mmol/l of <11.5 mg/l en Fe en Mn <0.05 mg/l) hadden tot gevolg dat geïnfiltreerd regenwater alleen vrijwel ongemengd onttrokken mocht worden. De doelaquifer werd vooraf uitvoerig gekarakteriseerd middels het nemen van ongestoorde kernen, hoge-resolutie analyse van deze kernen, en fysisch-chemische analyses van sediment en grondwater. De bedrijfsvoering van het ASR-systeem en het verblijf en transport van zoetwater in de brakke aquifer (150 – 1,100 mg/l Cl) werden uitvoerig gemonitord via online sensoren en computerregistratie, geofysische metingen en grondwatermonstername en analyse.

Een vergelijkbaar proefsysteem werd gerealiseerd in een zoutere aquifer in het Westland (4,000 – 5,000 mg/l Cl). Het verblijf en transport van geïnfiltreerd regenwater gedurende enkele ASR-cycli werden gemodelleerd met behulp van SEAWAT (Nootdorp en Westland) en PHT3D (alleen Nootdorp). Zodoende konden de gerealiseerde veldprestaties voor het MPPW-ASR systeem worden vergeleken met de potentiële prestaties van conventionelere ASR-systemen op de dezelfde locatie.

Als laatste werd de 'Freshmaker' gerealiseerd in de Nederlandse Zuidwestelijke Delta (Ovezande). Twee boven elkaar gelegen, horizontale putten (horizontal directionally drilled wells; afgekort HDDWs) met een lengte van 70 m werden hierbij geïnstalleerd om op 7 m diepte zoet oppervlaktewater te infiltreren en op 14.5 m zoutwater af te vangen. Hiermee werd een ongeveer 9 m dikke zoetwater lens over een grote lengte verdikt en zo'n 4.500 m^3 zoetwater opgeslagen. Eenzelfde volume zoetwater werd in de zomer onttrokken bij zoetwatervraag, waarbij de diepe afvang van zoutwater in stand werd gehouden. Ook hier werd de doelaquifer uitvoerig gekarakteriseerd met behulp van geofysica, fysisch-chemische sedimentanalyses en grondwaterbe-

monstering en -analyse. Een 2-D grondwatertransport model (SEAWAT) werd ingezet om de prestaties van de Freshmaker af te zetten tegen alternatieve ASR-strategieën op de onderzoekslocatie.

Resultaten ruimtelijke analyse ASR-prestaties

De ASR-prestaties van bestaande systemen in het studiegebied kwamen goed overeen met de voorspelde prestaties op basis van twee theoretische inschattingsmethodes. Afwijkingen werden mogelijk veroorzaakt door de noodzakelijke simplificaties en onzekerheden in de geohydrologische en hydrochemische data. Omdat de inschattingsmethodes geschikt lijken om ASR-prestaties in het gebied in te schatten, kon een betekenisvolle kartering uitgevoerd worden om zo de meest geschikte gebieden voor ASR te identificeren. Er werd aangetoond dat de ASR-prestaties in het gebied ruimtelijk sterk variëren. Zelfs in brakke aquifers (< 1.000 mg/l Cl) bleek de RE van kleinschalige tot middelgrote ASR-systemen al sterk tegen te kunnen vallen. Het belang van betrouwbare a priori analyse van de te verwachten ASR-prestaties wordt hierdoor benadrukt.

Resultaten MPPW-ASR systemen

Het diep infiltreren en ondiep terugwinnen met de MPPW zorgden voor een afname van het zoetwaterverlies bij het ASR-systeem in Nootdorp. De modellering met SEAWAT toonde aan dat bij keuze voor een enkelvoudige volkomen of onvolkomen put de RE in de eerste ASR-cyclus respectievelijk 15 en 30% zou zijn. Dit is aanmerkelijk minder dan de RE van 40% behaald door het MPPW-ASR systeem. Op basis van de modellering wordt in volgende cycli een rendement van 60% verwacht voor het MPPW-ASR system, tegenover <20 en <35% voor resp. een enkelvoudige volkomen en onvolkomen put. Ook het MPPW-ASR systeem zal echter nooit een RE van 100% bereiken, omdat menging in de telkens weer verziltende onderste helft van de doelaquifer een bron van zoetwaterverlies blijft. Wel leidt de MPPW duidelijk eerder tot een rendabel ASR-systeem op locaties die voor ASR minder gunstig zijn, terwijl de meerkosten beperkt zijn. Zoetwater dat niet teruggewonnen kan worden tijdens MPPW-ASR verzamelt zich aan de bovenzijde van de aquifer.

Het in Nootdorp op diepte geïnjecteerde zoetwater raakte deels verontreinigd met natrium en andere kationen uit het verdrongen brakwater. Dit was een gevolg van kationuitwisseling tijdens verzoeting. Dit 'verrijkte' zoetwater werd met name bovenin de aquifer weer onttrokken als gevolg van opdrijving. Retardatie van de doorbraak van Na werd waargenomen tijdens terugwinning en kan worden verklaard door opnieuw kationuitwisseling, maar dan tijdens verzilting. Door de opdrijving en voortdurende

periodieke verzilting vond geen vermindering van deze aanrijking en retardatie plaats, hetgeen wel het geval zou zijn in een situatie zonder opdrijving. Het uiteindelijke effect van deze kationuitwisseling op de RE is afhankelijk van de geaccepteerde Na-concentratie, de kationuitwisselingscapaciteit (CEC), en de samenstelling van het omringende grondwater en het injectiewater.

Oplossing van Fe- en Mn-houdende carbonaten in de onderste helft van de Nootdorpse doelaquifer leidde tot verontreiniging van geïnjecteerd water met Fe^{2+} en Mn^{2+}. Proton-buffering na pyrietoxidatie in dit interval stimuleerde deze oplossing. Met name in de eerste ASR-cyclus werd deze carbonaatoplossing tevens gestimuleerd door CO_2-productie als gevolg van oxidatie van (geadsorbeerde) Fe^{2+} en Mn^{2+}. Doordat pyrietoxidatie bleef zorgen voor snelle en volledige consumptie van zuurstof uit het injectiewater, bleef gemobiliseerde Fe^{2+} en Mn^{2+} in oplossing in anoxisch zoetwater. Bij terugwinning vond rondom eerder nog infiltrerende putfilters reductie van eerder gevormde MnO_2 plaats via oxidatie van Fe^{2+}. Met name in de onderste helft was het teruggewonnen zoetwater dan ook continu verontreinigd met voornamelijk Mn^{2+}. Echter, de veldproef toonde aan dat door terugwinning bovenin de aquifer en periodieke infiltratie van kleine volumes zuurstofhoudend water aldaar, het zoete water toch met voldoende kwaliteit kon worden teruggewonnen als gevolg van ondergrondse ontijzering.

De verticale, opwaartse stroming tijdens MPPW-ASR zorgt ervoor dat een groot deel van het ingebrachte water in contact komt met de verticale geochemische stratificatie van het doelpakket. Deze stratificatie is bepalend voor de waterkwaliteitsontwikkeling na infiltratie, meer nog dan de gemiddelde reactiviteit van het doelpakket. Met name vlak na infiltratie in het diepe interval van de aquifer vinden de meeste waterkwaliteitsveranderingen plaats. Daarna worden ook tussenliggende reactieve intervallen doorspoeld tot aan de uiteindelijke terugwinning. Een nadere geochemische karakterisatie van de doelaquifer voor MPPW-ASR is dan ook op zijn plaats, evenals een optimale bedrijfsvoering van de injectie and onttrekkingsputten, afhankelijk van de elementen die de RE bepalen.

Connecties tussen oorspronkelijk gescheiden, kustnabije aquifers bij de Westland ASR-proef hadden een duidelijke negatief effect op de RE. De doelaquifer voor ASR was gelegen boven een zoutere aquifer, welke werd benut voor warmte- en koudeopslag (WKO). Hoewel de aquifers gescheiden konden worden geacht op basis van de bodemopbouw en grondwatersamenstelling, moest door intrusie van dieper zoutwater de terugwinning spoedig beëindigd worden. De meest waarschijnlijke oorsprong hiervan bleek het boorgat van het nabijgelegen WKO-systeem te zijn op basis van veldmetingen, hydrochemische analyses en SEAWAT transportmodellering. Dit boorgat

faciliteerde kortsluitstroming van dieper zout grondwater. Het desastreuze effect van dergelijke kortsluitstroming op de RE van ASR werd bevestigd door de transportmodellering. Als praktisch geen menging met omringend grondwater is toegestaan, dan blijkt de afname in RE door kortsluitstroming lineair te zijn. Uit de veldproef Westland en de modellering bleek dat, dankzij de diepe MPPW putfilters, de zoutwaterintrusie kan worden afgevangen, waardoor winning van zoetwater bovenin de aquifer door kan gaan. Echter, een verlies in RE zal blijven ten opzichte van een onverstoorde situatie, doordat ook een deel van het ingebrachte zoetwater via de afvangput wordt afgevoerd. Als laatste suggereerde de modellering van het Westlandse ASR-systeem dat opkegeling van brakwater ook vanuit de slechtdoorlatende, onderliggende kleilaag plaats kan vinden, hetgeen de prestatieverbetering bij toepassing van MPPW tegenwerkt.

Resultaten Freshmaker HDDW systeem

De grondwatertransportmodellering van de Freshmaker toonde aan dat minimaal 4.200 m^3 zoetwater na infiltratie succesvol te onttrekken zou moeten zijn. Andere ASR-strategieën bleken niet in staat om dit op dezelfde locatie te bereiken. Zelfs zonder infiltratie van zoetwater, zou uiteindelijk eenzelfde volume zoetwater jaarlijks winbaar worden door de toename van natuurlijke infiltratie als gevolg van de diepe interceptie van zoutwater. De waarnemingen tijdens de veldproef ondersteunen de eerdere modellering, aangezien 4,500 m^3 zoetwater succesvol onttrokken kon worden in de zomer van 2014. De verdikking en exploitatie van de zoetwaterlens konden in beeld gebracht worden met de geofysische boorgatmetingen. Spreiding van de zoetwateronttrekking in de tijd bleek een randvoorwaarde voor succesvolle winning van het beoogde volume.

Conclusies

In deze thesis is het verkregen wetenschappelijke inzicht in de prestaties van ASR in brakke en zoute aquifers gepresenteerd. Gebleken is dat *a priori* een redelijk betrouwbare indicatie van de ASR-prestaties te verkrijgen valt. Hiermee is het mogelijk om via kartering zowel potentieel geschikte als bij voorbaat kansloze locaties voor ASR in beeld te krijgen. Deze potentiële ASR-prestaties kunnen ruimtelijk sterk variëren, zoals gebleken in het Westland-Oostland.

De normaal gesproken tegenvallende prestaties van ASR-systemen in brakke/zoute aquifers kunnen worden verbeterd door de uitgekiende putconfiguraties. Belangrijke pijler onder de verbeterde putconcepten is het verkrijgen van controle op de diepte van infiltratie en onttrekking, eventueel gecomplementeerd door interceptie van dieper brak- of zoutwater. Ondanks een significante toename, blijft een RE van 100%

in volledig brakke of zoute aquifers buiten bereik. Dit komt doordat menging in met name diepe intervallen een eeuwige bron van zoetwaterverliezen blijft. In vergelijking met ASR-toepassingen in zoete aquifers vindt met de uitgekiende putconfiguraties veel meer interactie met de geochemische intervallen rondom de infiltratieputten plaats. Daarnaast wordt, zeker bij MPPW-ASR, een groot volume van het zoete water door verschillende, horizontaal gelegen reactieve bodemeenheden getransporteerd. Als laatste heeft kationuitwisseling in door opdrijving periodiek verziltende delen van de doelaquifer een langdurig, negatief effect op een deel van het injectiewater.

De bevindingen zoals beschreven in deze thesis bieden handvatten om lokale, zelfvoorzienende zoetwatervoorziening in met name kustgebieden tot stand te brengen door tijdelijke zoetwateroverschotten te benutten via ASR. In deze gebieden werd ASR in het verleden door onzekerheid over de prestaties nog vaak genegeerd. Juist nu de waterschaarste hier steeds nijpender wordt, kan ASR hierdoor een kansrijke, kosteneffectieve maatregel worden.

Chapter **1**

General Introduction

"Er moet, ook in perioden van droogte,
voldoende zoet water beschikbaar zijn"

Beatrix Wilhelmina Armgard, Prinses der Nederlanden.
Troonrede, 21 september 2010.

1.1 Background

Coastal zones are the most densely populated and economically productive regions of the world. It was estimated that about half of the world's population lives within 200 kilometres of a coastline (United Nations, 2010). While these areas produce many economic benefits, the associated high water demand puts a tremendous pressure on freshwater resources and coastal ecosystems. This leads to problems like seasonal water shortage, overexploitation of groundwater resources, saltwater intrusion, and disappearance of wetlands. Further economic growth, population increase, and climate change will aggravate these problems, ultimately blocking the sustainable development of coastal zones in industrialized, emerging, and developing countries (European Commission, 2012). In 2015, water crises were therefore identified as the main global risk (World Economic Forum, 2015).

Traditionally, aboveground solutions are sought to solve freshwater problems, such as construction of reservoirs or saltwater desalination. However, the subsurface may provide options for more robust, effective, sustainable, and cost-efficient freshwater management solutions. For instance, artificial recharge of aquifers with temporary freshwater surpluses, also known as *managed aquifer recharge (MAR)*, is increasingly applied worldwide for water storage and treatment (Dillon et al., 2010). *Aquifer storage and recovery (ASR)* is one of the various MAR techniques, and is defined as "the storage of water in a suitable aquifer through a well during times when water is available, and the recovery of water from the same well during times when it is needed" (Pyne 2005). It can be a successful technique for storage and recovery of both potable and irrigation water (Maliva and Missimer, 2010). The advantages of ASR consist of the limited space requirement above ground, the lack of losses by evaporation, the protection from atmospheric, biologic and anthropogenic contamination, and the protection from earthquake damage. Related MAR techniques are aquifer transfer and recovery (ATR), using separate, synchronously operating infiltration and abstraction wells and *aquifer storage transfer and recovery (ASTR)*, again using separate infiltration and abstraction wells, but abstracting only after a period of infiltration (Stuyfzand et al., 2012).

ASR may have many purposes, including supply during peak demands, seasonal or diurnal storage, and purification. The fraction of the injected water that can be recovered with a certain accepted quality is called the recovery efficiency (RE, often expressed in percentages). This RE can be derived per cycle (infiltration, storage, recovery), or for the total operation of the ASR system (various cycles). The RE is an

important performance indicator of ASR. ASR systems that yield low REs may be unable to meet the water demand, or require a much larger injection volume to compensate for freshwater losses during storage. Such a large volume may not be available or make the system economically or hydrologically unviable.

1.2 Performance of ASR in brackish-saline aquifers

1.2.1 RE decrease by admixing of ambient groundwater

The RE of ASR can particularly be negatively impacted in brackish–saline aquifers, which are often found in coastal areas. The origin of this reduced RE is the simultaneous abstraction of injected freshwater and more saline, ambient groundwater. Recovery is ceased when too much ambient groundwater is admixed with the injected water and critical water quality standards are no longer met. Besides dispersive mixing at the fringe of the injected freshwater bubble, the density difference between the injected freshwater and ambient brackish or saline groundwater is a major cause for contamination with ambient groundwater in brackish-saline aquifers. This difference in density causes the freshwater to float upwards through the aquifer ('buoyancy effect'), while denser saline water is recovered by lower parts of the well (Esmail and Kimbler, 1967; Merritt, 1986; Ward et al., 2007). Both water types are blended in the ASR well to produce a brackish, generally unsuitable water quality.

The loss of recoverable freshwater may be exacerbated by lateral groundwater flow, causing injected freshwater to move outside the capture zone of the ASR well, where it cannot be recovered (Bear and Jacobs, 1965). Both processes are schematized in Figure 1-1. Although the extent with which lateral flow occurs in coastal areas is location-specific, mixing at the bubble's fringe will always occur. Buoyancy effects will always be present to some extent once density differences between injected freshwater and ambient groundwater are present.

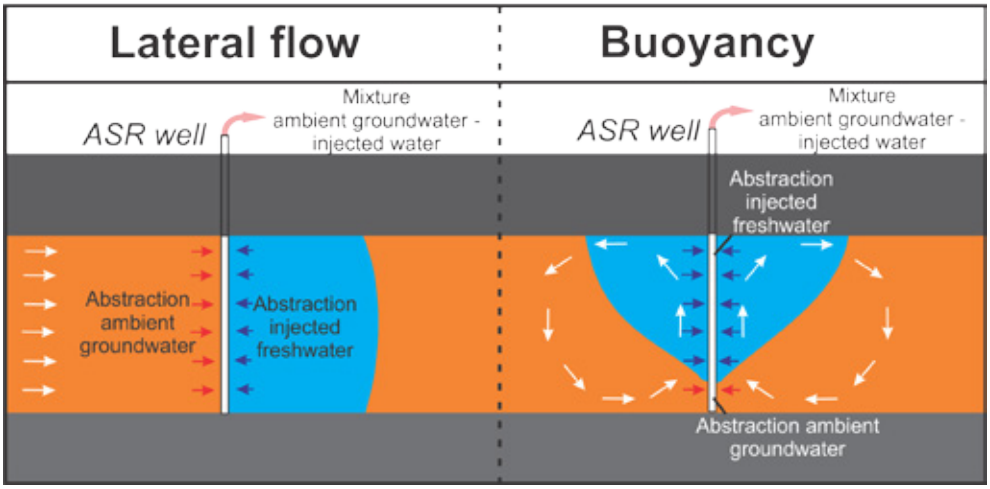

Figure 1-1: Admixing of more saline, ambient groundwater during recovery of injected freshwater by lateral flow and buoyancy effects.

1.2.2 Controlling factors for RE decrease by buoyancy effects

Recent studies have elaborated on the controlling factors for the RE decrease when buoyancy effects are present (Figure 1-2). Ward et al. (2007, 2008, 2009) used numerical modelling and dimensionless ratios for a semi-quantitative analysis of the RE, while Bakker (2010) used a new analytical solution for radial Dupuit interface flow. Based on these studies, which assume fully penetrating ASR wells, it can be derived that two types of factors control the RE. The first type comprises the target aquifer characteristics and can be separated in lithological characteristics (thickness, hydraulic conductivity, anisotropy, heterogeneity) and groundwater characteristics (density of the ambient groundwater). The lithological characteristics are set by the geological development of the target aquifer, while the density of the ambient groundwater is controlled by the temperature and total concentration of dissolved solids (TDS). Operational parameters are the second type of controlling factors and comprise the pumping rate at the ASR well during injection and recovery, the operational scheme (relative duration of injection, storage, and recovery period) and the density of the injection water.

A small density-difference between injection water and ambient groundwater, a thin target aquifer, a low hydraulic conductivity, and strong anisotropy theoretically all have a positive effect on the system's RE. Furthermore, a relatively short storage

period with respect to the injection and recovery period is preferred over long storage periods. Finally, a high pumping rate will yield higher REs for the same operational scheme. This indicates that large-scale ASR systems should perform better than small-scale systems.

It is important to recognize that even when density differences are small, buoyancy effects can lead to low REs. For example in coarse-grained aquifers (high hydraulic conductivity), or in cases with a long storage period or long injection and/or recovery periods with a low pumping rate. The latter is the case when ASR is applied on a small-scale for seasonal storage. Furthermore, an RE increase in subsequent ASR cycles can be expected during multiple cycle operation. This is because the ambient groundwater freshens when unrecoverable injected water is left behind every cycle. The initial conditions for the next ASR cycle therefore improve over time. The largest RE increase will be present in the first ASR cycles (Bakker, 2010).

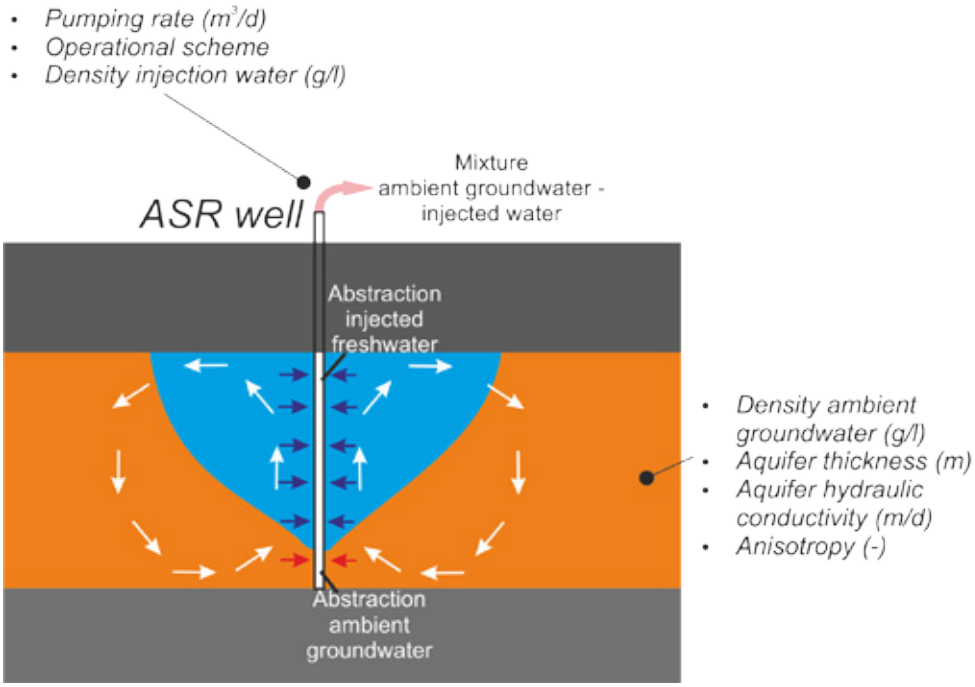

Figure 1-2: Controlling factors for an RE decrease induced by buoyancy effects during ASR, assuming a homogeneous target aquifer.

1.2.3 RE decrease by geochemical interaction with the target aquifer

Besides simultaneous abstraction of ambient groundwater and injected water, geochemical interactions within the aquifer during residence may lead to recovery of an unacceptable water quality. Injected water can get enriched with solutes released from the aquifer matrix. This can be caused by, for instance, dissolution, cation-exchange, desorption, oxidation, and proton-buffering reactions (Pyne, 2005; Stuyfzand, 1998). Typical species of concern are Fe, Mn, As, Ni, Co, Zn, SO_4, Na, Ca, HCO_3, NH_4 and PO_4. For operational, environmental, and/or health concerns, elevated concentrations of these elements can be unacceptable. When one of the critical species exceeds its maximum permissible concentration, recovery has to be terminated early, even if unmixed injected water is recovered. On the other hand, water quality may also improve during aquifer residence, for instance by the reduction of NO_3 in the injection water via oxidation of pyrite and organic matter present in the aquifer, or the degradation of viruses and organic micropollutants (Clinton, 2007).

In brackish-saline (coastal) aquifers, it can be expected that cation-exchange (Appelo, 1994a; Appelo, 1994b) will impact the injected water quality due to the repetitive process of freshening and salinization during ASR cycles. Also, pyrite (FeS_2) is frequently found in coastal aquifers as a consequence of the reduction of SO_4 present in seawater or brackish estuarine water types (Berner, 1984). The subsequent oxidation of pyrite by injection of oxygen- or nitrate-containing water during ASR may lead to mobilisation of low concentrations of As, Ni, Co, and Zn, besides the mobilisation of SO_4 (Pyne, 2005; Stuyfzand, 1998).

1.3 Small-scale ASR as a solution for freshwater supply in coastal areas

To cope with rising freshwater demands and droughts, ASR may be a meaningful solution to provide freshwater availability in coastal areas. Whether this is the case depends to a large extent on the ability to mitigate the risks of poor ASR performance in brackish-saline, coastal aquifers. In this study, focus is therefore on coastal areas, with the Netherlands as the study area. Here, high water demands are present in the agricultural, industrial, and drinking water sectors. As elsewhere, the freshwater availability by precipitation is often increasingly out-of-phase with the demand, freshwater reserves are limited due to the presence of shallow, brackish-saline groundwater, and salinization of river inlets occurs in dry periods.

One of the most important future strategies to combat freshwater shortages in the

Dutch coastal areas is to make end-users independent of external freshwater supply using local, decentralized storage of the winter freshwater surplus ('self-reliancy'; Delta Commission, 2014). Small-scale ASR systems (infiltrating <1 Mm^3) may provide useful freshwater storage facilities to obtain self-reliance thanks to their limited claim on above ground land. An example of such an ASR system to provide freshwater to greenhouse horticulturists is shown in Figure 1-3. In this sector, strict water quality limits are set for maximal recirculation in the greenhouse water system. Enrichment of injected rainwater with especially Na, Mn, Fe, and As is therefore virtually unacceptable. Given the uncertain recovery performance of especially small-scale ASR systems due to the aforementioned reasons and the absence of well-documented small-scale ASR systems in coastal areas, a scientific analysis of the potential ASR performance in this area is required. Additionally, new well techniques such as multiple partially penetrating wells (MPPW) and the horizontal directional drilled well (HDDW) recently became available. They allow better control of the injection and recovery during ASR, which may significantly improve ASR performance in coastal areas by enabling the counteraction of buoyancy effects.

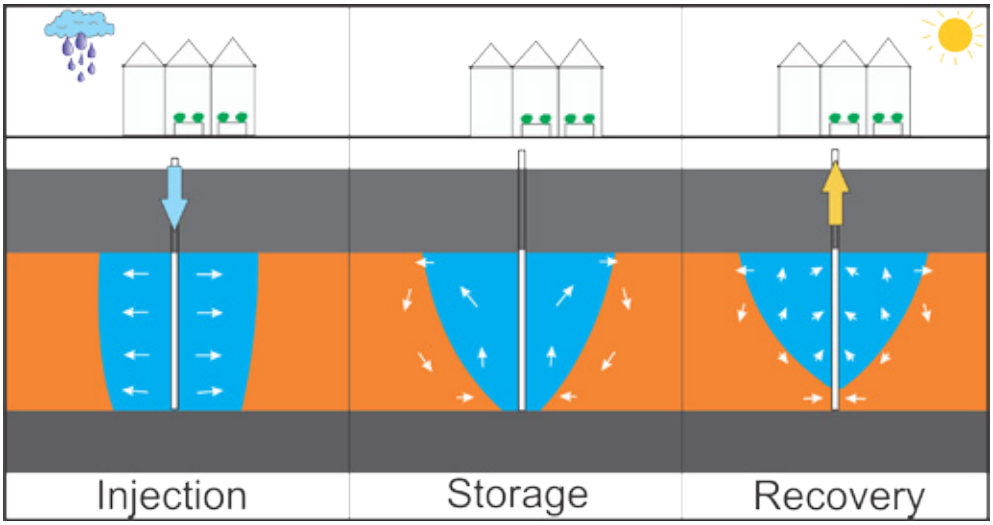

Figure 1-3: The use of small-scale ASR in a brackish-saline aquifer to store the rainwater surplus collected on greenhouse roofs. Buoyancy effects may lead to an early recovery of a brackish, unusable mixture.

1.4 Research objective and questions, methodology, and outline of this thesis

The general objective of this PhD study is *to quantify and increase the potential performance of relatively small-scale ASR systems in coastal areas with brackish-saline aquifers, taking into account recently developed well configurations for performance optimization*. To achieve this objective, a broad range of research techniques was applied to the Dutch coastal area (Figure 1-4). This included a spatial performance analysis using a geographic information system (GIS), field monitoring of advanced ASR configurations, and groundwater transport modelling. With this, the aim was to answer the following specific research questions, which are addressed in separate chapters:

- **Chapter 2**: *What is the predicted ASR performance in the coastal Westland-Oostland area as assessed by ASR performance estimation methods, how does this compare with the measured performance of existing ASR sites, and what are the applicability and drawbacks of the performance estimation methods?*
  The outcomes of the ASR performance estimations were compared with the recorded performance of nine existing small-scale ASR systems in the study area, to identify suitable ASR sites. Based on geohydrological and hydrochemical data, maps of the predicted ASR performance were generated based on the ASR performance estimation methods by Ward et al. (2009) and Bakker (2010).

- **Chapter 3**: *Can the small-scale ASR performance in brackish-saline aquifers be improved by the use of dedicated, independently operating multiple partially penetrating wells (MPPW) and if so, how much improvement can be achieved?*
  To obtain a reliable indication of the true performance and reliability of the MPPW for ASR, a field pilot was realized in the Oostland area (Nootdorp) and extensively monitored. Based on the field observations during ASR in the brackish target aquifer, a density dependent SEAWAT groundwater transport model was set up. The model was used to predict the development of the ASR performance and to compare the performance of the MPPW-ASR system with alternative well configurations.

- **Chapter 4**: *How do reactive transport processes affect the recovered water quality and recovery efficiency (RE) for multiple water quality parameters, what*

controls the development of recovered water quality over time, and how do site-specific or operational conditions of the MPPW-ASR system affect the recovered water quality?
The target aquifer geochemistry and the hydrochemical development of injected water at the Nootdorp MPPW-ASR field pilot presented in Chapter 3 was monitored during two ASR cycles. Based on the results, mass balance equations, and reactive transport modelling, the controls on the water quality development of this new ASR configuration were assessed. Focus was on Na, Fe, Mn, and As, which were the most critical elements in the recovered water, which was used for greenhouse irrigation.

- **Chapter 5**: *What are the potential consequences of short-circuiting for coastal aquifer storage and recovery (ASR) systems and how can negative effects be mitigated?*
  Use of subsurface may lead to short-circuiting due to the formation of conduits in penetrated aquitards as a consequence of improper drilling and well installation. A second MPPW-ASR pilot in a saltwater aquifer demonstrated the consequence of an unexpected artificially induced hydraulic connection with a deeper aquifer used for aquifer thermal energy storage. A potential mitigation strategy is presented.

- **Chapter 6**: *Can ASR become successful in (unconfined) coastal aquifers with saline groundwater by using horizontal directional drilled wells (HDDWs)?*
  Recently developed horizontal directional drilled wells (HDDWs) allow a new ASR strategy by simultaneous, shallow injection of freshwater and deep interception of saltwater over a long aquifer strip (called 'Freshmaker'). In this chapter, the resulting ASR performance at a recently realized field pilot on the island of Zuid-Beveland in the southwest of The Netherlands is analysed.

A synthesis of the research is presented in Chapter 7 and is accompanied by a discussion of the implications and applications of the results for the future freshwater management and ASR research in coastal areas.

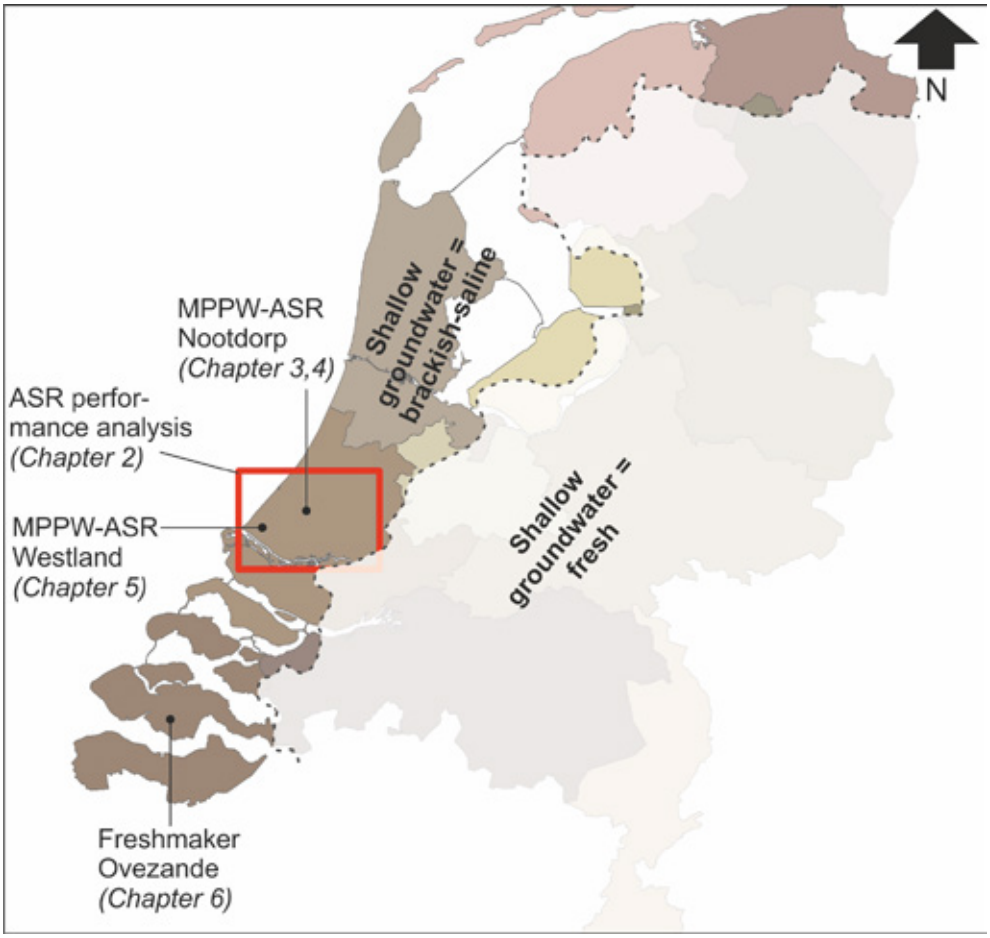

Figure 1-4: Location of the study area (marked by presence of shallow brackish and/or saline groundwater), the spatial ASR performance analysis, and the field pilots discussed in each chapter.

Chapter **2**

Identification of potential sites for aquifer storage and recovery (ASR) in coastal areas using ASR performance estimation methods

Slightly modified from:

Zuurbier, K., Bakker, M., Zaadnoordijk, W., Stuyfzand, P., 2013. Identification of potential sites for aquifer storage and recovery (ASR) in coastal areas using ASR performance estimation methods. Hydrogeology Journal, 21(6): 1373-1383.

2.1 Abstract

Performance of freshwater aquifer storage and recovery (ASR) systems in brackish or saline aquifers is negatively affected by lateral flow, density effects and/or dispersive mixing, causing ambient groundwater to enter ASR wells during recovery. Two recently published ASR performance estimation methods are applied in a Dutch coastal area, characterized by brackish to saline groundwater and locally high lateral flow velocities. ASR performance of existing systems in the study area show good agreement with the predicted performance using the two methods, provided that local vertical anisotropy ratios are limited (<3). Deviations between actual and predicted ASR performance may originate from simplifications in the conceptual model and uncertainties in the hydrogeological and hydrochemical input. As the estimation methods prove suitable to predict ASR performance, feasibility maps are generated for different scales of ASR to identify favorable ASR sites. Successful small- to medium-scale ASR varies spatially in the study area, emphasizing the relevance of reliable a priori spatial mapping.

2.2 Introduction

Aquifer storage and recovery (ASR) is defined as "the storage of water in a suitable aquifer through a well during times when water is available, and the recovery of water from the same well during times when it is needed" (Pyne 2005). It may be a successful technique for storage and recovery of both potable and irrigation water (Dillon, 2005; Dillon et al., 2006; Maliva et al., 2006; Pyne, 2005; Vacher et al., 2006). ASR may have many purposes, including supply during peak demands, seasonal or diurnal storage, and purification. The fraction of the injected water that can be recovered with a certain accepted quality is called the recovery efficiency (RE), which is a performance indicator of ASR. The RE can be reduced in coastal areas due to density differences between the injected freshwater and ambient brackish or saline groundwater. In such cases, freshwater floats upwards through the aquifer (buoyancy effect), while denser saline water is recovered by lower parts of the well (Esmail and Kimbler, 1967; Merritt, 1986; Ward et al., 2007). The loss of recoverable freshwater may be further increased by lateral groundwater flow, causing injected freshwater to move outside the capture zone of the ASR well, where it cannot be recovered (Bear and Jacobs, 1965).

It is important to predict the ASR-performance before large investments are made, considering all the relevant factors. Ward et al. (2007, 2008 and 2009) showed that not only salinity, but also aquifer thickness, hydraulic conductivity, hydraulic gradient,

aquifer anisotropy and hydrodynamic dispersion need consideration. Furthermore, operational parameters such as pumping rates, injection volume and injection-, storage- and recovery durations need to be considered when potential ASR-performance is analyzed. ASR performance estimation therefore traditionally requires extensive and expensive data collection and advanced numerical modeling to reduce uncertainties in important aquifer parameters (Misut and Voss, 2007; Pavelic et al., 2002; Pyne, 2005; Ward et al., 2007; Ward et al., 2008; Ward et al., 2009). Ward et al. (2009) and Bakker (2010) recently proposed two relatively simple methods to predict ASR performance by a fully penetrating well. Potential performance of ASR can be predicted using these methods, without rigorous numerical modeling, taking into account common hydrogeological data and operational parameters. However, there is little field verification and application of these theoretical performance estimation methods known to date in geologically varying brackish and saline aquifers due to a scarcity of monitored ASR systems.

The objective of this paper is to assess the predicted ASR performance by Ward et al. (2009) and Bakker (2010) through comparison with the measured performance of existing ASR sites in a coastal area. The applicability and drawbacks of both methods are analyzed and maps are generated of hydrologically potential ASR sites in the study area. Maps of predicted spatial ASR performance provide important information on the potential use of ASR as a freshwater management strategy in the study area.

2.3 Study area

2.3.1 Westland – Oostland greenhouse area

The combined Westland and Oostland area in The Netherlands (Figure 2-1) is an intensive greenhouse horticultural area facing irrigation water related issues. The salinity requirements of the irrigation water in this area (generally measured using electrical conductivity, EC) are exceptionally strict; drinking water is already too saline for many of the crops and flowers cultivated. Low salinity allows greenhouse owners to reuse drained water from artificial substrates multiple times, without reaching critical sodium concentrations. Fresh irrigation water supply is realized primarily by storing low EC rainwater from greenhouse roofs in basins or tanks, complemented by the use of surface water in periods of low salinity and by desalination of brackish groundwater (Stuyfzand and Raat, 2010).

A mismatch in precipitation and water demand creates a large winter freshwater surplus (Figure 2-2), which is discharged to sea, as only a small part can be stored in

basins or tanks. Surface water is generally unsuitable as a source of freshwater during summer droughts, as they are fed by brackish seepage water (de Louw et al., 2010). Fresh surface water can be brought in from major rivers, but the inlets suffer increasingly from salinization caused by seawater intrusion during summer droughts, which is exacerbated by sea level rise (Barends et al., 1995; Kooi, 2000; Kwadijk et al., 2010; Oude Essink et al., 2010; Post, 2003; Schothorst, 1977). Summer droughts are predicted to become more intense and prolonged, whereas wintertime precipitation is expected to increase 3.5 to 7% (Intergovernmental Panel on Climate Change (IPCC), 2007; van den Hurk et al., 2007). Freshwater availability for irrigation during summer will likely be reduced due to the changing temporal precipitation distribution in combination with a predicted rise in temperature. Up to now, desalination by reverse osmosis is the only proven technology to ensure freshwater supply. Major disadvantages of this technique are the high energy consumption, the required maintenance, and especially the disposal of leftover concentrate. Discharge of this concentrate to sewage systems or surface waters is not allowed and a ban on its disposal in deeper saline aquifers is being prepared.

A more sustainable use of the precipitation surplus collected by greenhouse roofs will improve freshwater availability in the area. ASR is a cost-effective, readily applicable technique to store large water volumes, without the need for large surface areas. In the study area, ASR has been applied on a small scale since the 1980s in the upper, relatively shallow aquifer (10 - 50 m below sea level (m BSL); Figure 2-3), which is the thinnest and least saline aquifer found in the area.

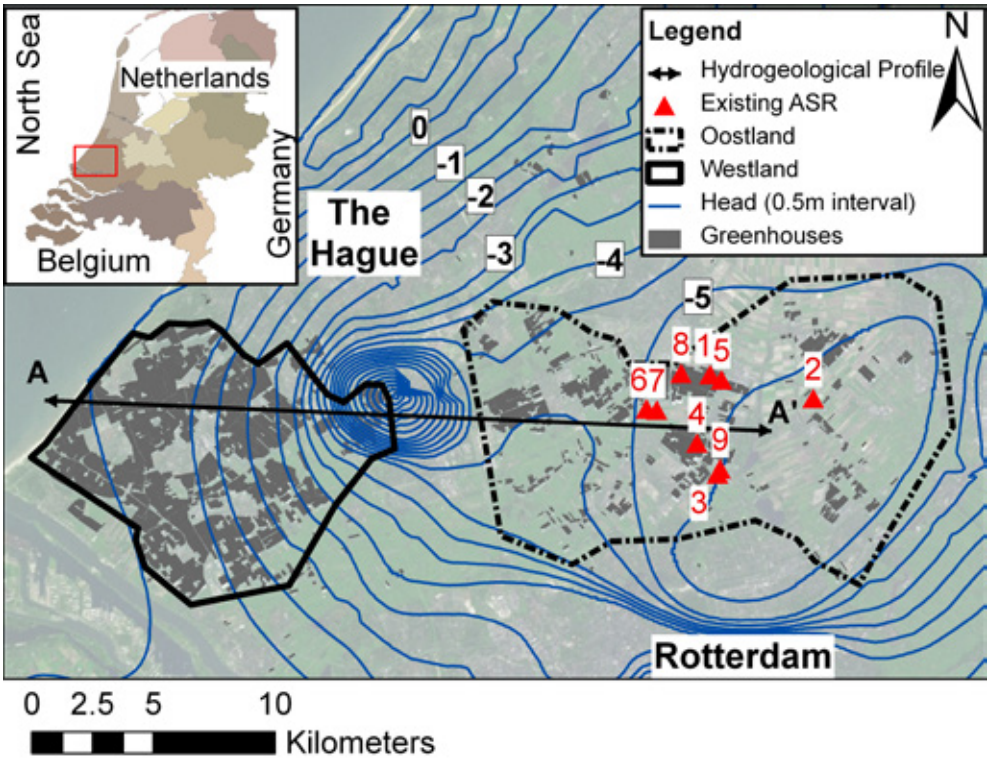

Figure 2-1: Locations of the Westland and Oostland greenhouse areas near The Hague and Rotterdam and hydraulic heads in Aquifer I from the 'Data and information system of the Dutch subsurface' (TNO-NITG). For the hydrogeological profile, see Figure 2-3. Studied ASR systems are coded by no. 1-9.

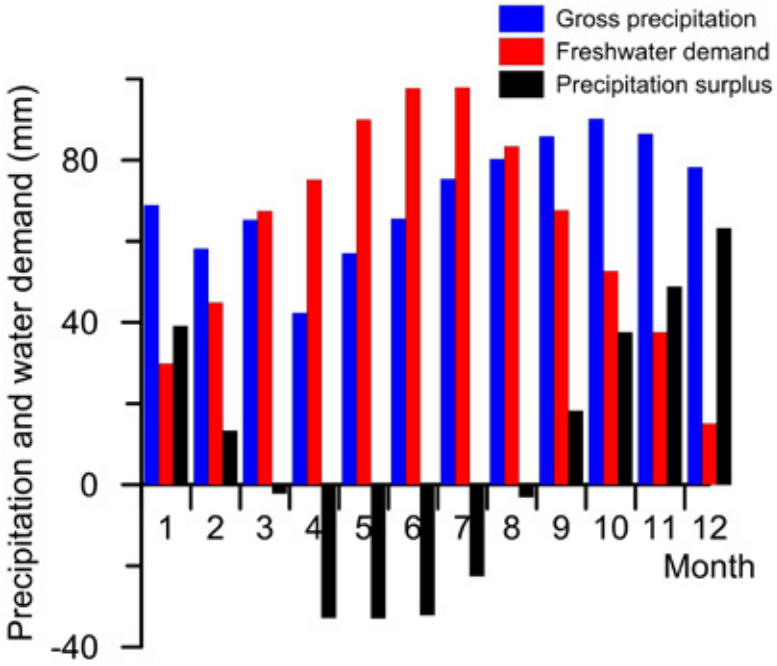

Figure 2-2: Mean gross monthly precipitation (1980-2010) near the study area (weather station Rotterdam, Royal Netherlands Meteorological Institute), estimated monthly water demand of intensive horticulture, and resulting estimate of available water for ASR (Paalman, et al. 2012).

2.3.2 Hydrogeological setting

Unconsolidated Pleistocene and Holocene fluvial and marine deposits are found in the upper ~120 meters of the study area (Figure 2-3, TNO-NITG). These middle to late Pleistocene clays, sands, and gravels were deposited by former Rhine-Meuse fluvial systems and during marine transgressions (Busschers et al., 2005). The transition to groundwater with chloride concentrations >1,000 mg/L is found at a depth of only a few meters in the Westland (Post, 2003), and somewhat deeper in the Oostland (-5 to -40 m BSL). Regional groundwater flow is controlled by the North Sea in the west, the lower drainage level of the deep polders in Oostland, and a large industrial groundwater extraction in the middle areas which results in high flow velocities in its vicinity (Figure 2-1, Figure 2-3). Aquifer I is also exploited for brackish water to supply desalinated greenhouse irrigation water; the concentrate is injected in Aquifers II and III (Figure 2-3).

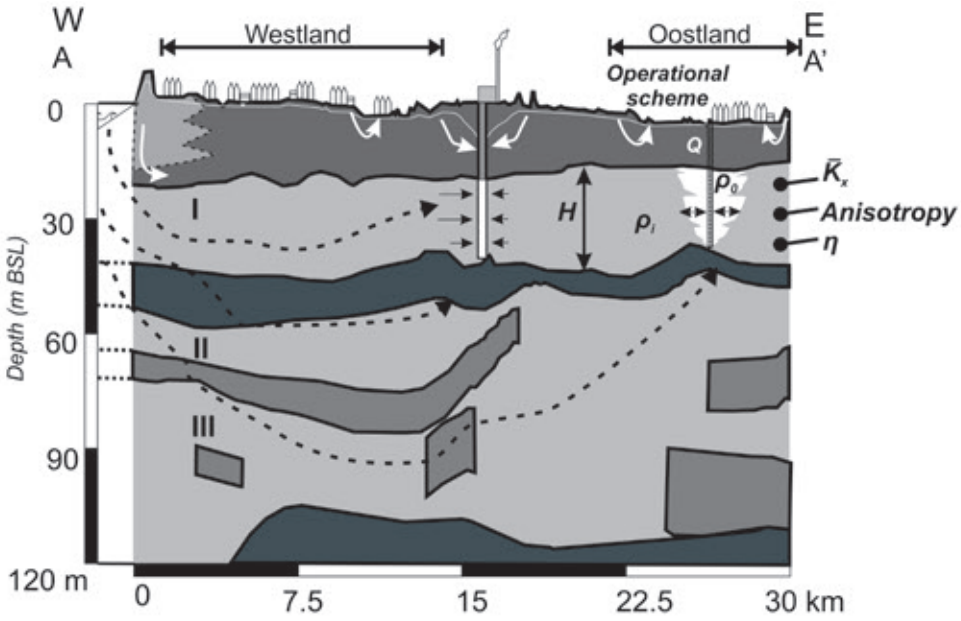

Figure 2-3: Cross-section of the study area based on the REGIS II.1 hydrogeological model from the 'Data and information system of the Dutch subsurface' (TNO-NITG). Flow lines interpreted from regional hydrological system analysis (Negenman et al., 1996). Important factors for ASR performance are highlighted for an example ASR system in the Oostland area (not to scale). *I*, *II* and *III* are aquifers. *H* is the aquifer thickness, $\bar{K}_x$ is the average horizontal conductivity, η is the effective porosity, ρ_i is the ambient groundwater density and ρ_0 is the injection water density. *Q* is the pumping rate during ASR operation (L^3/T).

2.4 ASR performance estimation

ASR performance has been measured at nine existing ASR systems. First, the measured performance is compared to the predicted performance using two recently presented ASR estimation methods. Next, a spatial ASR feasibility analysis is performed and ASR feasibility maps are generated.

Detailed ASR operational parameters have not been recorded. General ASR operational parameters are estimated from the mean monthly precipitation record (1980 – 2010) registered near the Westland-Oostland area and from the estimated mean monthly water demand of the local horticulture by Paalman et al. (2012). Total mean yearly gross precipitation is 853 mm, while the mean yearly water demand

is 679 mm. The estimated ASR operational parameters and water availability and demand (both in m^3/m^2 per year) are presented in Table 2-1.

Table 2-1: General ASR operational parameters and mean water availability and demand in the study area.

Period	Duration (d)	General water availability (+) or demand (-) (m^3/m^2)
Injection	150	+ 0.2
Storage	30	0
Recovery	120	- 0.12
Idle	65	0

2.4.1 Performance of existing ASR systems, Oostland

The total injected and recovered volumes of nine systems outfitted with water meters (for locations, see Figure 2-1) were inventoried at the end of the summer recovery period in August 2011 (Table 2-2). The studied systems were at the end of Cycle 2, 4, 5, 6, or 9. The injected and recovered volumes of multiple cycles are used to calculate the total RE during the lifespan of each system. This total RE is considered the minimum total RE for the ASR lifespan, as it is unknown whether freshwater was recovered until a maximum EC was reached, or whether recovery was terminated because water demand was met. Based on the maximum EC, the allowed mixing fraction is calculated. The mixing fraction f (-) is defined as the proportion of injected water in the recovered water as a function of time during recovery (Pavelic et al., 2002; Ward et al., 2007):

$$f = \frac{C_i - C(t)}{C_i - C_0} \tag{2.1}$$

where C_i is the concentration of the ambient groundwater, $C(t)$ is the concentration at time t in the recovery phase and C_0 is the concentration of the injection water. The mixing factor varies per system due to differences in background salinity of the aquifer and allowed maximum salinity of the recovered water. If a relatively low mixing ratio is allowed, measured ASR performance can be higher than predicted.

The mean pumping rate for each system during injection and recovery is based on the general durations of the injection and recovery period (Table 2-1), the regis-

tered injected and recovered volumes, and the age of each system. In case a system was installed during an injection period, injected volumes are distributed over fewer months of operation.

Table 2-2: Age, allowed mixing fraction, injected and recovered volumes/rates, and the total recovery efficiency (RE) of measured ASR systems in the Oostland area.

ASR system (no., Fig. 1)	Age (yrs)	Allowed mixing fraction *f* (-)	Yearly injection volume (x1000 m^3)	Injection rate (m3/d)	Yearly recovery volume (x1000 m^3)	Recovery rate (m^3/d)	Total RE (%)
1	6.0	0.56	28.3	188	17.1	143	61
2	8.8	0.72	35.3	235	29.2	243	83
3	4.0	0.79	46.0	307	23.4	195	51
4	1.9	0.83	22.4	150	10.2	85	45
5	5.7	0.66	44.4	296	26.4	220	59
6	4.0	0.77	24.6	164	14.8	123	60
7	4.4	0.41	16.9	113	9.2	77	55
8	5.8	0.51	86.7	578	54.4	453	63
9	4.8	0.87	47.5	317	30.0	250	63

2.4.2 ASR performance estimation methods

2.4.2.1 Method of Ward et al. (2009)

Ward et al. (2009) proposed four dimensionless ratios for the qualitative prediction of ASR performance: a technical viability ratio, focusing on the lateral drift during storage, a dispersivity ratio for the effect of dispersive mixing, a mixed convection ratio to characterize the density effects during injection and recovery, and a storage tilt ratio to determine the significance of density-driven flow during storage. All parameters equally contribute to the overall indicator of ASR performance.

The technical viability ratio (R_{TV}) is defined as:

$$R_{TV} = \left| \frac{\bar{K}_x I t_s}{\eta x_{i,u}} \right| \tag{2.2}$$

where $\bar{K}_x$ is the average horizontal hydraulic conductivity (L/T), I is the hydraulic gradient (-), t_s is the duration of storage (T), η is the porosity (-) and $x_{i,u}$ is the location of the injected freshwater in the centre of the aquifer in the upstream direction at the end of the injection period (L).

The dispersivity ratio (R_{disp}) is defined as:

$$R_{disp} = \frac{\beta_L}{x_{i,u}} \tag{2.3}$$

where β_L is the longitudinal dispersivity (L).

The mixed convection ratio (M) is defined by Ward et al. (2009) as:

$$M = \frac{\bar{K}_z \alpha}{\left| \frac{Q}{2\pi H \eta x_{i,u}} \right| - \left| \frac{\bar{K}_x I}{\eta} \right|} \tag{2.4}$$

where $\bar{K}_x$ is the average vertical hydraulic conductivity (L/T), α is the density difference ratio (-), Q is the pumping rate (L^3/T) and H is the aquifer thickness (L). However, after a critical review of the derivation of M it is concluded that the equation to calculate M in Ward et al. (2009) should be:

$$M = \frac{\bar{K}_z \alpha}{\left| \frac{Q}{2\pi H x_{i,u}} \right| - \left| \bar{K}_x I \right|} \tag{2.5}$$

In this equation, η is eliminated from the equation, such that it also matches M as it was introduced by Ward et al. (2007).

The storage tilt ratio (R_{ST}) is defined as:

$$R_{ST} = \frac{\bar{K}_z \alpha H t_s}{\eta \left(x_{i,u} \right)^2} \tag{2.6}$$

The overall indicator R_{ASR} is defined as:

$$R_{ASR} = R_{TV} + R_{disp} + M + R_{ST} \tag{2.7}$$

The density difference ratio (α) is defined as:

$$\alpha = \frac{\rho_i - \rho_0}{\rho_0} \tag{2.8}$$

where ρ_i is the concentration of the ambient groundwater (M/L^3) and ρ_0 is the density of the injected water (M/L^3). Based on modeling results, Ward et al. (2009) concluded for one ASR-cycle that: (a) when R_{ASR} is smaller than 0.1, the mixing ratio f is 1 at the beginning of recovery and at least 0.8 after half of the injected volume is recovered, and ~0.4 at a RE of 100%, (b) the interval $0.1 < R_{ASR} < 10$ is a transitional range in which the dimensionless ratios cannot predict success or failure, and (c) undesirable sites/regimes are marked by an $R_{ASR} \geq 10$, meaning f is around 0 at the start of recovery. This method provides a qualitative prediction of the performance of the first ASR cycle only; the potential RE is not predicted.

R_{TV}, R_{ST} and R_{disp} are calculated following Ward et al. (2009). For calculation of M, Ward et al. (2009) assumed equal pumping rates during the injection and recovery phases. The recovery pumping rate is significantly smaller (33%) than the injection rate for the systems considered here. In this study therefore, $x_{i,u}$ is calculated following Ward et al. (2009) using the injection rate, while M is calculated using the recovery rate. As a consequence, it is possible to obtain negative values for R_{ASR} when the background groundwater velocity exceeds the velocity caused by pumping at $x_{i,u}$. In such cases, counteraction of free convection at the fringe of the freshwater body by pumping is limited, density effects are dominant, and M is set to 10.

2.4.2.2 Method of Bakker (2010)

Bakker (2010) proposed a screening tool considering loss of freshwater by buoyancy effects only. Using interfaces and a new solution for radial Dupuit interface flow, it was

shown that the RE (defined as the part of the injected water recovered until the toe of the fresh-salt interface reaches the well screen) is dependent on the dimensionless parameter *D*:

$$D = \frac{Q}{\bar{K}_x \alpha H^2} \tag{2.9}$$

For each combination of relative lengths of injection, storage and recovery periods, the RE can be calculated for each value of *D* and for each cycle. Groundwater mixing is not taken into account. Hence, this screening tool results in an upper limit of the RE and is intended to assess whether further study of ASR performance is worthwhile. Bakker (2010) does not take into account plume distortion by lateral flow. In this study, zones where plume distortion is expected are identified based on the dimensionless time parameter $\bar{t}$ defined as:

$$\bar{t} = \frac{2\pi t_{inj} H}{\eta Q} (\bar{K}_x I)^2 \tag{2.10}$$

where t_{inj} (T) is the duration of the injection period.
When $\bar{t}$ is < 0.1, lateral flow can be neglected (Ceric and Haitjema, 2005; Ward et al., 2009). The RE was calculated for each D for the injection, storage and recovery durations of Table 2-1, and a 25% higher pumping rate during recovery to get the maximum RE limited by the interface only and not by the duration of recovery. The total estimated RE was calculated for each system, using the injection rate and number of cycles of each system, and compared with the measured total RE.

2.4.3 ASR feasibility in Westland-Oostland

2.4.3.1 Use of ArcGIS

Spatial maps are generated of the required injection rate to achieve successful ASR, indicated by a RE of 60% in cycle 5 (Bakker, 2010) or a R_{ASR} of 0.1 (Ward et al., 2009). The durations of injection, storage and recovery periods are shown in Table 2-1, and the recovery rate is 75% of the injection rate. The Model Builder of ArcGIS (version 9.3) is used to perform all calculation steps on a 100 by 100 m grid (resolution of the hydrogeological input) to predict the required injection rate for each cell. Ten iterations are performed after an initial injection rate of 50 m^3/d using the method by Ward et al. (2009), adapting the injection rate based on the outcome of R_{ASR} in

each step to achieve R_{ASR} = 0.1. For the method of Bakker (2010), a RE of 60% in cycle 5 is achieved when D is higher than 14.3, and the required injection rate is calculated in each cell for this D. Subsequently, the dimensionless corresponding to this pumping rate is calculated to exclude areas with plume distortion from the dataset.

2.4.3.2 Hydrogeological input

Top elevation, bottom elevation, transmissivities and standard deviations of K_x of the hydrogeological units of the Holocene cover, Aquifer I, and Aquitard I were taken from the Regional Geohydrological Information System (REGIS) of the Data and information system of the Dutch subsurface (TNO-NITG). The thickness of Aquifer I (target aquifer) was derived by summation of the hydrogeological units consisting of sand below the Holocene cover, but above the first regional aquitard (Formation of Peize-Waalre, unit Waalre-Clay1). The few cells in which Aquitard I was absent and Aquifer I and II formed one (thick) aquifer were removed from the dataset. Transmissivities of the hydrogeological units were summed to obtain the total transmissivity of the aquifer. A mean horizontal hydraulic conductivity ($\bar{K}_x$) was computed from this aquifer transmissivity and the aquifer thickness. Ward et al. (2008) demonstrated that a homogeneous anisotropy ratio (K_x over K_z) can be used to account for stratification of the aquifer and that higher anisotropy ratios improve ASR performance. As data on these anisotropy ratios are often scarce, a sensitivity analysis is performed using anisotropy ratios of 1 (isotropic) and 3 (anisotropic) in the estimation performance by Ward et al. (2009). A mean porosity (η) of 0.35 was used (Meinardi, 1994). The hydraulic gradient was calculated using the interpolated head data from the 'Data and information system of the Dutch subsurface' of Aquifer I on April 28, 1995 (TNO-NITG, see Figure 2-1). A longitudinal dispersivity (β_L) of 0.1 m was used.

2.4.3.3 Groundwater quality data (chloride concentrations)

Chloride concentrations were used to represent salinity and to estimate groundwater densities. A 3-D interpolation of the chloride concentrations was developed by Oude Essink et al. (2010) based on vertical electrical soundings, geo-electrical well logs, and chloride concentration measurements at observation wells. The interpolated data were stored in a 250 x 250 m raster file with a vertical resolution of 5 m. The chloride concentration at the centre of Aquifer I was estimated using the top and bottom elevations of the aquifer. Those chloride concentrations were converted to groundwater densities using (Oude Essink et al., 2010):

$$\rho(C_{cl}) = \rho_0 + 0.00134 C_{cl} \tag{2.11}$$

where ρ is the density of the water (kg/m^3), C_{cl} is the chloride concentration (mg/l) and ρ_0 is the density of freshwater (1000 kg/m^3). The effect of temperature variations of the injection water on water density was neglected, as this can be presumed limited for the range of temperature differences during the infiltration period (Ma and Zheng, 2010).

2.5 Results

2.5.1 Comparison of the predicted and measured ASR performance

The ASR performance indicator R_{ASR} is plotted versus the total RE from measurements for an isotropic hydraulic conductivity (Figure 2-4a) and for an anisotropy factor of 3 (Figure 2-4b). The parameter R_{ASR} indicates uncertain performance for all systems (i.e., R_{ASR} >0.1) when isotropy is assumed. R_{ASR} is <0.94 (isotropic) and <0.3 (anisotropic; ratio = 3) for all systems. ASR system 3 has a R_{ASR} of 0.20 (anisotropic) to 0.59 (isotropic), and a total RE of 51% in 4 years. It may be expected that this system will recover ~60% of the injected water in cycle 5. Based on measured RE, successful ASR systems are therefore marked by R_{ASR}<0.59 (isotropic), or R_{ASR}<0.2 in the anisotropic case. The results indicate that the qualitative method proposed by Ward et al. (2009) is at least reasonable in the study area, as R_{ASR} is generally low (<1) when ASR performance is moderate to high. It is confirmed that for R_{ASR} <0.1, successful ASR can be expected. Overestimating the anisotropy may result in an unrealistic increase in the predicted performance; R_{ASR} is around or below 0.2 for all systems, with only limited uncertainty.

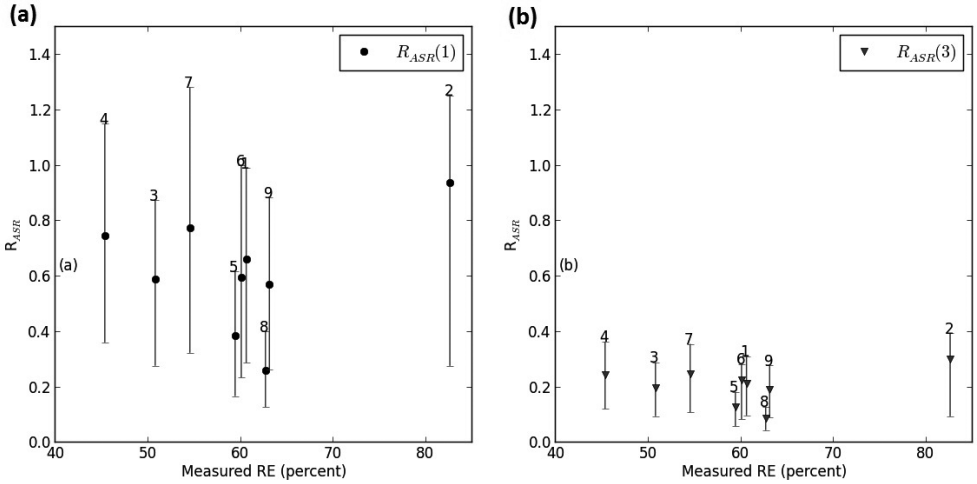

Figure 2-4: Measured RE versus predicted ASR performance. Relation with R_{ASR} is shown for the (a) isotropic and (b) anisotropic case (anisotropy ratio = 3). Error bars represent the results for one standard deviation in uncertainty for the hydraulic conductivity input.

The measured total RE is compared to the predicted total RE with the method of Bakker (2010) in Figure 2-5. At three systems, the measured RE is lower than the predicted RE. Six systems performed better than predicted, even though the estimation method should give an upper limit. For five of these systems the measured RE is within the uncertainty range based on one standard deviation for $\bar{K}_x$.
One ASR system performed significantly better than predicted (83 versus 35%), whereas one system recovered significantly less than predicted (63 versus 78%). In the latter case, this can be due to a low water demand and therefore limited recovery. The system performing better than predicted is installed in a thick, relatively anisotropic aquifer with a relatively fine-grained base, which may have delayed salinization at the bottom of the ASR well. The predicted RE is generally in line with the measured RE. The results suggest that the screening tool by Bakker (2010) can indeed be used to predict a realistic RE in the study area.

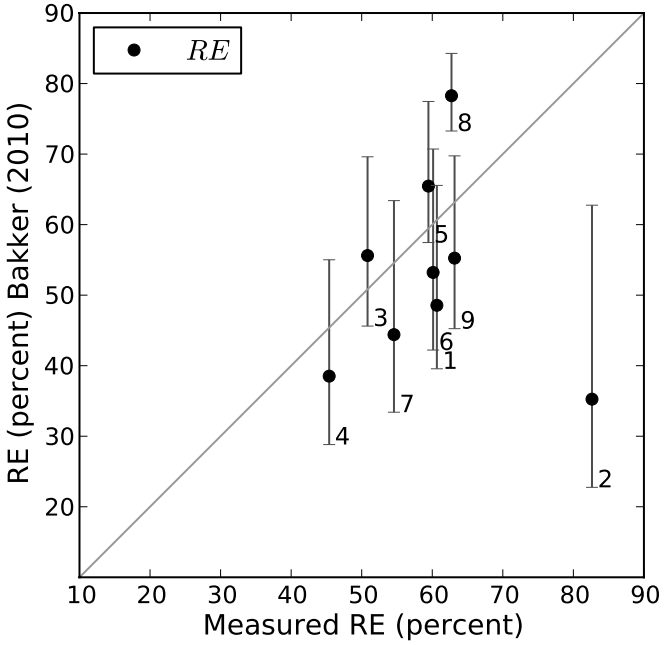

Figure 2-5: Predicted total RE Bakker (2010) versus the measured total RE. Error bars represent the results for one standard deviation in uncertainty for the hydraulic conductivity input. The continuous line indicates predicted RE = measured RE.

2.5.2 Spatial mapping of potential ASR sites

Maps are developed showing the predicted ASR performance for the entire study area. The predicted ASR performance increases with injection rate (or indirectly the ASR scale, as the injection time remains constant), which is therefore used as an indicator for spatial ASR suitability. The required injection rate for successful ASR using Ward et al. (2009) varies up to 4 orders of magnitude (Figure 2-6), highlighting the large variation in potential ASR performance in the study area. For an isotropic case, successful ASR is predicted in only in minor parts of the Oostland. The expected ASR performances is better the anisotropic case, indicating that at least large-scale ASR should be successful in the Oostland area. In the Westland a high mean injection rate of more than 10,000 m^3/d is always required.

The mean required injection rate for successful ASR is ~300 m^3/d in the Oostland area according to Bakker (2010), whereas in the Westland area a mean injection rate of ~800 m^3/d is required. The latter confirms the limited suitability of this particular area for small- to medium-scale ASR application, although projections are better than predicted by Ward et al. (2009). More suitable ASR sites are predicted in general with

this method, compared to the method by Ward et al. (2009). Spatial mapping using Bakker (2010) also illustrates the large variations in aquifer suitability for freshwater ASR, with minimum injection rates increasing from 50 to more than 1000 m^3/d within a distance of 2 km.

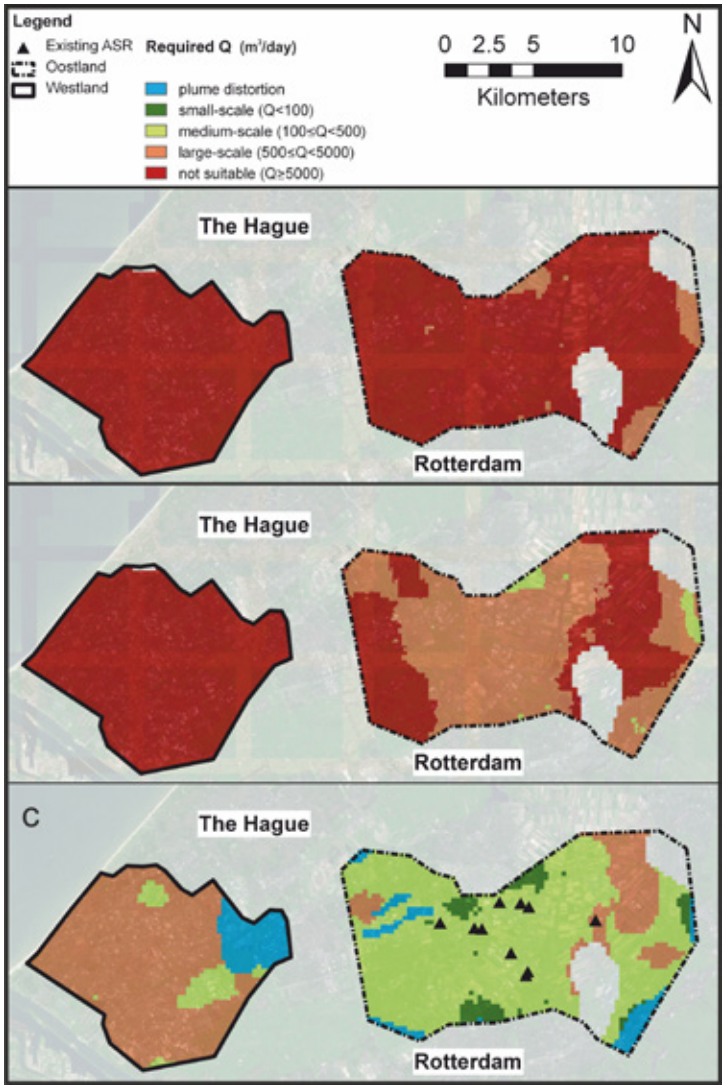

Figure 2-6: Required winter injection rates (m^3/d) for successful ASR (R_{ASR} =0.1) predicted using Ward et al. (2009) for (a) the isotropic case and for (b) anisotropy ratio = 3, and (c) predicted using Bakker (RE = 60% in cycle 5). No mapping is performed where Aquitard 1 is absent.

2.6 Discussion

2.6.1 Comparison of the measured and predicted ASR performance

The ASR performance estimation presented by Ward et al. (2009) cannot be correlated directly to a RE. Based on the existing systems, successful ASR sites are marked by R_{ASR} <0.59 for the isotropic case or <0.20 for an anisotropy ratio of 3. This indicates that this method is suitable for a qualitative performance analysis, and that the proposed required R_{ASR} of 0.1 for certain success is appropriate in the study area, but certainly does not rule out successful ASR when R_{ASR} >0.1. This R_{ASR} value is therefore small enough to ensure ASR success, even though the different ratios are lumped with an equal contribution. The anisotropy ratio should not be overestimated in the area, as a similar ASR performance is predicted at all systems with limited uncertainty for an anisotropy ratio of 3, whereas in reality more differentiation was found. In this comparison, two out of nine systems performed outside the 65% confidence interval (based on the uncertainty in $\bar{K}_x$). One system performed significantly worse, which may be explained by a limited water demand, and therefore limited recovery. Another system performed much better than predicted, but is installed in a relatively thick, potentially anisotropic aquifer, while its well screen may be partially penetrating the aquifer. The latter may also increase the RE (see Chapter 3). Six systems performed better than predicted by Bakker (2010), which should overestimate RE since it does not take into account mixing.

Although the predicted REs, especially by the method presented by (Bakker, 2010), are in line with the measured REs, deviations are observed and potential explanations can be addressed. The performance estimation tools are for instance based on confined aquifers having an impermeable top and base, thus not considering semi-confined aquifers. It is known that the lower confining clay layer of the target aquifer locally has a limited resistance (TNO-NITG), making the ASR-well partially penetrating a thick aquifer. In this study, the performance estimation is limited to areas where the upper aquifer was underlain by a clay layer in the REGIS hydrogeological model, but no further deviations based on the resistance of those aquitards and vertical head gradients are made. Seepage, which is induced in parts of the study area by drainage levels up to 7 m BSL, is therefore neglected and may cause earlier salinization at the bottom of the ASR well than expected based on the estimation methods.

This study can be particularly used to identify unsuitable parts of the target aquifer for future ASR with a specific injection rate, independent of seepage. Furthermore, the potential RE is predicted using Bakker (2010) neglecting aquifer vertical anisotropy, for instance by stratification of isotropic units in the target aquifer with a different

K, which might underestimate the potential RE due to an anisotropy ratio larger than 1 (Ward et al., 2008). The method by Ward et al. (2009) takes into account this (potential) vertical anisotropy, resulting in a significant increase in area where successful ASR is predicted for an anisotropy ratio of 3. Although a limited anisotropy ratio is presumed (<3) based on the measured and the predicted REs using Ward et al. (2009), aquifer stratification may be a cause for the underestimation of the RE at six out of nine sites by Bakker (2010), which was expected to overestimate the RE.

Altogether, both methods have their own advantages and disadvantages, of which the most important ones are given in Table 2-3. These should be taken into account in future ASR feasibility studies.

Table 2-3: Comparison of ASR performance methods for spatial mapping

Ward et al. (2009)	Bakker (2010)
Input - K_x, K_z, η, I, H, α - Operational ASR parameters - Fully penetrating well	Input - K_x, H, α - Operational ASR parameters - Fully penetrating well
Lacks estimation of RE	Lacks lateral flow and mixing
Suitability for spatial mapping: - All factors can be calculated based on common geological data (+) - Takes into account lateral flow and anisotropy (+) - May overestimate minimum injection rates required for certain success (-)	Suitability for spatial mapping: - Easy to calculate D from common geological data (+) - Direct estimation of RE (+) from D, but relation between D and RE needs to be derived first (-) - Lateral flow and anisotropy are not considered (-) - Predicts realistic minimum injection rates required for success (+)

Differences between predicted and measured performance for both methods can also originate from the available hydogeological and hydrochemical data. The regional geological model, which is based on local data (bore logs, pumping tests) has its uncertainties, since interpretation and interpolation of bore log data is required to cover large areas. The same holds for the background salinity distribution. The datasets incorporate the relative regional variations in aquifer thickness, hydraulic conductivity

and salinity, which can be considered sufficient for an initial ASR performance prediction and mapping of potential ASR sites. The latter is confirmed by the agreement between the predicted and measured ASR performance.

2.6.2 ASR operation in the study area

In this study, general durations of injection, storage and recovery periods, and the total injected and recovered volumes of each system in multiple years of operation are used to derive the mean pumping rates for each ASR site. Yearly variations are neglected, which may affect ASR performance; this cannot be investigated further, as no data were recorded. An improved registration using (automatic) logging of (daily) injected and recovered volumes is essential for better assessment of performance.

Both ASR performance estimation methods consider fully penetrating wells. Use of multiple partially penetrating wells in a single borehole (MPPW, see Chapter 3) may lead to higher recovery efficiencies. Although its benefit for freshwater recovery was not quantified during this ASR performance analysis, it is illustrated in Chapter 3 that this ASR well type may increase the RE by enhanced injection at the aquifer base and/or recovery at the aquifer top, delaying salinization at the bottom of the ASR recovery well(s). Especially in the case of small-scale freshwater ASR and a thicker but relatively homogeneous aquifer, injected freshwater bodies have a limited radius, making flow conditions at the fringe of the injected freshwater body significantly different from fully penetrating wells, especially when the aquifer is anisotropic (Hantush, 1966). The loss caused by buoyancy effects may therefore be partly counteracted, as demonstrated for a case with partially penetrating wells for aquifer thermal energy storage (ATES, Buscheck et al., 1983; Molz et al., 1983a; Molz et al., 1983b). Although multiple partially penetrating wells are installed at existing systems, the systems studied were recovering and injecting over the full aquifer thickness, shutting off lower sections only when salinization at those well sections occurred. A limited increase in freshwater recovery is expected by this strategy, which is another explanation for the higher RE of some of the existing ASR systems, compared to their predicted RE. Although quantification of the potential increase in RE by such a well configuration and pumping scheme is a relevant research question, it is beyond the scope of this chapter.

2.6.3 ASR performance in the Westland-Oostland area

Good agreement is obtained between predicted and measured ASR performance, which justifies application of the estimation methods to generate feasibility maps for new ASR sites. Excluding the areas where plume distortion may be expected and

single-well ASR performance is expected to be low (marked by $\overline{t}$ >0.1), the aquifer suitability is best quantified using Bakker (2010). As only a few ASR sites are predicted to be unsuitable due to plume distortion by lateral flow, it was shown that success of ASR in the study area mainly depends on freshwater loss by buoyancy effects.

Conventional small-scale ASR (Q<100 m^3/d) using a fully penetrating well is expected to have a poor performance in large parts of the study area. Spatial maps also show large variations over small distances, which highlight the relevance of *a priori* spatial mapping and site-selection. The required mean pumping rate in the more suitable Oostland area indicates that medium-scale ASR (100<Q<500 m^3/d) is potentially successful in a large part of the area. Only large-scale ASR (Q>500 m^3/d) can be successful in the Westland area, which is caused by the relatively thick and fairly saline aquifer. In this area, rainwater harvesting by a large cluster of greenhouses to feed one central ASR system may result in injection rates large enough for successful ASR.

ASR appears to be a suitable technique for freshwater supply in a large coastal study area, based upon average operational parameters. Between 1980 and 2010, annual precipitation varied between 605 and 1150 mm in the study area, with a mean gross precipitation of 853 mm. This means that in wet years injection rates may be higher, recovery rates need to be lower and larger water volumes are stored for longer periods, and vice versa for relatively dry years. It is well-known that long-term aquifer storage is less efficient, but still higher REs can be expected in the cycle following a wet year with relatively limited recovery, potentially supplying sufficient irrigation water even if the subsequent summer is extremely dry. This study did not quantify the RE under varying operational parameters.

Geochemical reactions during aquifer residence of the fresh, oxic rainwater may severely affect the quality of the stored water and is a well-known pitfall in ASR operation (e.g., Jones and Pichler, 2007; Prommer and Stuyfzand, 2005; Pyne, 2005; Wallis et al., 2010). This feasibility study neglects geochemical changes in the injection water and focuses on hydrological feasibility only. Reactions during aquifer residence may make the recovered water unsuitable irrespective of the EC or chloride concentration. Oxidation of pyrite, a mineral present in the target aquifers in the study area (Busschers et al., 2005) may, for instance, mobilize trace elements, which can make the recovered water unsuitable for further use. Such geochemical studies are needed to determine feasible ASR sites based on the maps in Figure 2-6. Therefore, the geochemical effects on injected rainwater during ASR in the study area were studied. The results are presented in Chapter 4.

2.7 Conclusions

Two recently developed ASR performance estimation tools were applied to predict ASR performance in a coastal area in the Netherlands. Comparison of predicted with measured ASR performance of systems in the study area show good agreement between measured and predicted total RE using the method of Bakker (2010). The performance factor (R_{ASR}) of Ward et al. (2009) correlates with successful ASR systems for R_{ASR} <0.59 for isotropic aquifers, and R_{ASR} <0.20 for a vertical anisotropy factor of 3. This confirms that successful ASR may be at least expected for R_{ASR} lower than ~0.1, provided that the assumed anisotropy ratio is low (<3). Deviations between measured and predicted ASR performance may originate from simplifications in the conceptual model and uncertainties in the hydrogeological and hydrochemical input. Good agreement between measured and predicted performance justifies the use of both methods for spatial analysis of predicted ASR performance in this area. Maps were generated showing areas suitable for small-, medium-, and large-scale ASR systems. Successful small- to medium- ASR application is spatially variable in the study area, highlighting the relevance of *a priori* spatial mapping.

2.8 Acknowledgements

This research was funded by the Knowledge for Climate research programme as part of the theme 'Climate Proof Freshwater Supply' of this program. Dr. Gualbert Oude-Essink is thanked for providing the chloride distribution in the study area.

Chapter 3

How multiple partially penetrating wells improve the freshwater recovery of coastal aquifer storage and recovery (ASR) systems: a field and modelling study

This chapter was published as:

Zuurbier, K.G., Zaadnoordijk, W.J., Stuyfzand, P.J., 2014. How multiple partially penetrating wells improve the freshwater recovery of coastal aquifer storage and recovery (ASR) systems: A field and modeling study. Journal of Hydrology, 509(0): 430-441.

3.1 Abstract

Aquifer storage and recovery (ASR) of freshwater in brackish or saline aquifers can be an efficient technique to bridge freshwater shortages in coastal areas. However, buoyancy effects may cause salinization at the bottom of the ASR well during recovery, making a part of the freshwater irrecoverable. This study shows how such freshwater losses can be reduced by applying deep injection and shallow recovery by independently operated multiple partially penetrating wells (MPPW) in a single borehole. A small-scale ASR system with such an MPPW was installed in January 2012 and its operation was extensively monitored until October 2012. A SEAWAT model was built and calibrated on the field measurements of this first ASR cycle. The model was used to compare the MPPW with a conventional fully and partially penetrating well. The freshwater recovery of those wells was 15 and 30% of the injected water, respectively, which is significantly less than the 40% recovered by the MPPW. In subsequent cycles, no more than 60% could be recovered by the MPPW, as mixing in the lower half of the aquifer remained a source of freshwater losses. However, this recovery is significantly higher than the recovery of the conventional well types. This study therefore shows that for less ideal ASR conditions, a viable system can still be realized using MPPW.

3.2 Introduction

Aquifer storage and recovery (ASR) involves the injection and recovery of water by wells into natural porous media and can be an efficient technique to store and recover large volumes of water (e.g., Maliva and Missimer, 2010; Pyne, 2005). Periods with shortage of for instance drinking, industrial, and irrigation water can be bridged this way, claiming little surface area aboveground. The injected water bubble is less vulnerable to surface contamination (Hermann, 2005) as this storage type is typically applied in deep, confined aquifers. Successful ASR applications were reported by Dillon et al. (2006), Pyne (2005), Vacher et al. (2006), and Ward et al. (2009). About one third of the current ASR systems is already situated in brackish to saline aquifers (Pyne, 2005), as more and more freshwater shortages occur in coastal areas due to climate change, overexploitation, and seawater intrusion (e.g., Arnell, 1999; Schröter et al., 2005; Werner et al., 2013). Success of especially small-scale ASR in those areas may be very limited, as the injected freshwater gets mixed with and displaced by

ambient brackish or saline groundwater due to background lateral flow and buoyancy effects (Bakker, 2010; Kumar and Kimbler, 1970; Ward et al., 2009; Chapter 2). This displacement of fresh by saline water enables saline water to enter the lower parts of the well early during recovery, which may significantly reduce the recovery efficiency (RE). RE is defined as the fraction of the injected water that is recovered by the ASR system. When RE is low, ASR can either not satisfy the water demand, or the costs of the water recovered exceed the benefits.

Strategies were proposed to prevent low REs in brackish and saline aquifers. For instance, a large volume may be injected without recovery, prior to injecting the water that is to be recovered (the so-called target storage volume; Pyne, 2005). A targeted volume of unmixed injection water may be recovered this way. However, the water required for such a first phase without recovery may not be available. In addition, buoyancy effects may still cause early salinization at the bottom of the ASR well, especially in case of small-scale ASR in combination with lateral flow and/or saline seepage. Another method to improve RE can be optimization of the well design, enabling preferential recovery at the aquifer top, which may be combined with preferential injection at deeper parts of the aquifer. This strategy was proposed for improved recovery of hot water by the use of partially penetrating wells during aquifer thermal energy storage, where buoyancy effects may also induce low RE (Buscheck et al., 1983; Molz et al., 1983a; Molz et al., 1983b). More recently, preferential recovery has also been proposed for ASR in brackish aquifers using one-way (flapper) valves, inflatable packers, or an extra partially penetrating well (Maliva et al., 2006). Maliva and Missimer (2010) additionally proposed installation of a deeper partially penetrating well for preferential injection at deeper parts of the aquifer. Miotliński et al. (2013) studied the use of a multiple (rhombic) injection and recovery well system for aquifer transfer and recovery in a brackish aquifer, using four partially penetrating injection and two production wells. In this study, focus was on mixing with brackish background water and the attenuation of contaminants through adequately long residence times. However, density effects were not considered. Optimization of freshwater recovery by this well system under conditions where buoyancy effects otherwise negatively influence RE was therefore not studied.

The potential benefits of optimized well designs for ASR under conditions where density effects may cause a significantly lower RE are practically still unexplored. Nevertheless, many small greenhouse ASR systems in Dutch coastal areas are already equipped with multiple partially penetrating wells in a single borehole (MPPW) to inject and recover roofwater surpluses. This way, lower well segments can be closed off once salinization occurs. ASR owners may be able to achieve a higher RE this way

than predicted by recent ASR performance tools (Chapter 2), but there are neither field nor modeling studies known to date that quantify the potential benefits.

The objectives of this study are to validate and quantify the potential benefits of MPPW for a small-scale freshwater ASR system suffering from buoyancy effects. A greenhouse ASR system injecting less than 14,000 m^3/y in a Dutch brackish coastal aquifer was extensively monitored for this purpose from January to October 2012. Using MPPW, freshwater was injected preferentially at deeper parts of the aquifer, whereas recovery was performed in the upper part of the aquifer. The monitoring results were used to calibrate a SEAWAT transport model, simulating the aquifer injection, storage, and recovery. Both a fully penetrating and a single shallow partially penetrating well was simulated with this model for equal ASR operational parameters, to quantify the long-term RE increase by an MPPW-equipped ASR system.

3.3 Study area

3.3.1 Irrigation water demand and supply

The study area is dominated by greenhouse horticulture with a typically high water demand, using on average 759 mm of the mean yearly gross precipitation of 853 mm (Paalman et al., 2012). With the average distribution of water availability and demand throughout the year, a mean freshwater shortage of 60% of the winter surpluses exists (Chapter 2). Furthermore, there are high water quality standards concerning salinity, with especially sodium concentrations being critical (maximum permissible NaCl concentrations: 0.5 to 3.0 mmol/l, depending on plant species). Fresh irrigation water supply in this area is currently realized by storage of rainwater in basins or tanks, use of surface water, and desalination of brackish groundwater. ASR can be a valuable technique to store more of the large (winter) precipitation surplus to bridge water shortages in the area during (summer) droughts, but its use is limited to date because of expected low REs in the brackish to saline coastal aquifers (Chapter 2).

3.3.2 Hydrogeological setting

Unconsolidated Pleistocene and Holocene fluvial and marine deposits are found in the upper ~120 meters in the study area (Busschers et al., 2005). Regional groundwater flow is controlled by the North Sea in the west and the drainage levels of the low polders in the Oostland area and a large industrial groundwater extraction, as illustrated by the regional head contours (Figure 3-1). Groundwater in the shallow ASR target aquifer (10 – 50 m below sea level (m BSL)) is typically brackish to saline

(Figure 3-1), with highest salinities (up to ~5,000 mg/l Cl) found near the coast and in low-lying polders (Oude Essink et al., 2010).

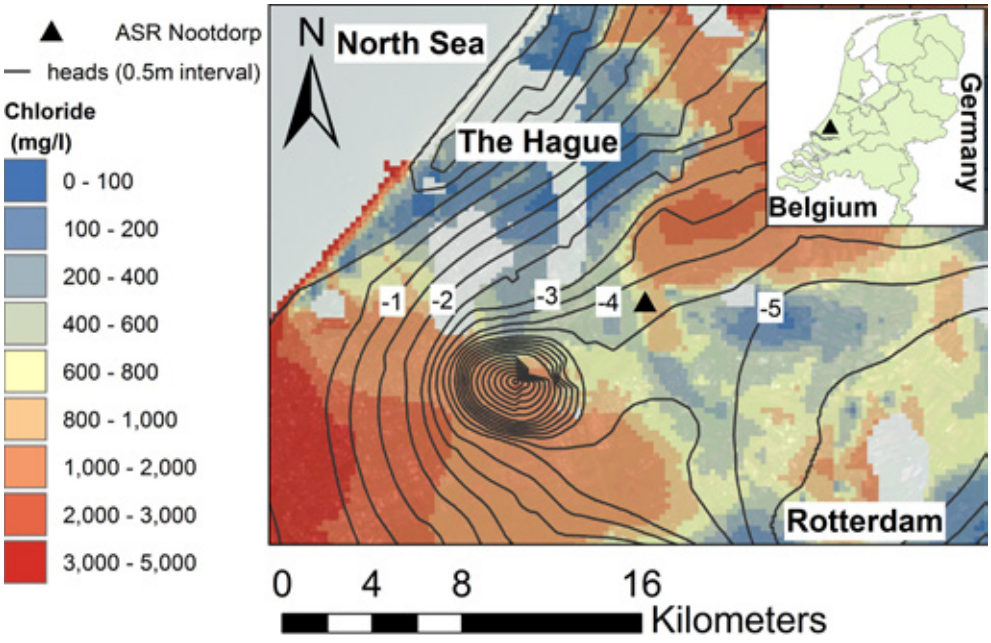

Figure 3-1: Regional piezometric head contours (TNO, 1995) and chloride concentrations (Oude Essink et al., 2010) in the centre of the ASR target aquifer and location of the Nootdorp ASR field trial (black triangle).

3.3.3 Nootdorp ASR field trial

The ASR field trial is situated near the village of Nootdorp, where chloride concentrations in the target aquifer are typically around 1,000 mg/l (Figure 3-1). Based on regional mapping of the groundwater heads on April 28, 1995 (TNO-NITG), a hydraulic gradient of $2.7*10^{-4}$ m/m was deduced. This gradient corresponds to a moderate southwestern regional groundwater flow of about 11 m/y, based on an estimated hydraulic conductivity (K) of ~40 m/d (TNO-NITG). Local groundwater flow velocities may be higher than this regional velocity due to either local abstractions or abrupt transitions in drainage levels, for instance at the boundaries of high peat lands and deep polders in the study area. Local lateral flow velocities can also be reduced, on the other hand, further away from these transitions. The Nootdorp ASR site is situated in one of the latter areas having a constant drainage level of 4.8 (summer) to 5.0 m BSL (winter), which is maintained by discharging rainwater surpluses to sea and inlet

of fresh river water in periods of drought. This means it is situated in a deep polder with brackish seepage to the surface waters (de Louw et al., 2010), but negligible lateral background flow. Brackish groundwater extractions for reverse osmosis around the ASR site may induce some lateral flow during summer.

The ASR system has been installed to supply a greenhouse with a surface of 20,000 m^2 with an estimated yearly water demand of 400 mm (8,000 m^3/yr) in an area with a mean gross annual precipitation of 853 mm (Royal Netherlands Meteorological Institute) or 17,060 m^3/yr. However, the water recovered from the aquifer after storage must have a chlorinity <0.5 mmol/l (~18 mg/l Cl) as water quality requirements are strict. This means only a very limited contribution of ambient brackish water to the injected rainwater is allowed.

3.4 Materials and methods

3.4.1 ASR configuration and operation

In the target aquifer, a 34 m deep, 350 mm diameter borehole was drilled by reverse-circulation rotary in November 2011, in which the MPPW with a diameter of 75 mm (screens 1- 3) and 90 mm (screen 4) was installed (see Figure 3-2 for the screened intervals). Bentonite clay plugs of 0.4 to 0.7 m thickness were installed using pellets at a minimum vertical distance of approximately 0.5 m away from each screen top or where clay layers were pierced. Each well was outfitted with a valve in the injection and recovery pipeline, allowing manual adjustment of injection and recovery rates per well. Rainwater collected by the greenhouse roof was stored in a 400 m^3 rainwater storage tank, which could thus store 20 mm of rainfall. Prior to injection, the roofwater was pre-treated by rapid and slow sand filtration to prevent well clogging by suspended particles (see Figure 3-2 for a cross-section).

ASR operation started in February 2012. Injection automatically started with a rate of ~12 m^3/h once a predefined level in the rainwater storage tank was reached (30%, to prevent overflow during intense rainfall). Injection ceased when a set minimum level (20%) was reached. Recovery started automatically with a pumping rate of ~8 m^3/h when the predefined minimum level (40%) in a 90 m^3 irrigation water tank was reached, and was stopped once the predefined maximum level in this tank was reached (60%). The size of the tanks, their predefined minimum and maximum levels, and the precipitation distribution resulted in a highly dynamic ASR operation with frequent alternation of injection and recovery stages.

Figure 3-2: Set-up of the ASR field trial. *MW* = monitoring well, *CTD* = electric conductivity, temperature, and pressure datalogger, *R.S.F.* = rapid sand filtration, *S.S.F.* = slow sand filtration.

3.4.2 Field monitoring

3.4.2.1 Installation of monitoring wells

Three bailer drilled boreholes (MW 1-3, Figure 3-2) with a diameter of 219 mm were realized at locations aligned at 5, 15, and 40 meters from the ASR-well, respectively. There were six (MW1) or five (MW2 and 3) separate piezometers with 1 m screen length installed in each borehole. Bentonite clay plugs of 1 to 2 m thickness were installed using pellets at a minimum vertical distance of 0.5 meter from the screen top, or where clay layers were pierced.

3.4.2.2 Sediment analyses

A 27 meter long (12.8 to 39.8 m BSL, Figure 3-2) continuous, undisturbed core was obtained at MW1 using a core catcher (Oele et al., 1983) and thin-wall tubes of 1 m length and 0.10 m diameter. A total of 114 samples was taken from these thin-wall tubes, at intervals of 0.2 m or smaller where differing lithological units appeared, to analyze vertical variations (Broers, 2001). Samples were taken from the bailer every meter at the other intervals of MW1 (n= 14) and over the full depth of MW2 and 3 (n=29 and n=28, respectively). The samples were prepared for grain size analysis following the methods described by Konert and Vandenberghe (1997). Measurements were done using a HELOS/KR laser particle sizer (Sympatec GmbH, Germany), resulting in grain size distributions in the range of 0.12–2,000 µm. Samples containing gravel were oven-dried and sieved using a 1,600 µm sieve to obtain the fraction >2,000 µm, taking elongated particles into account. The grain size distribution (<2,000 µm) was subsequently corrected for the gravel contribution.

3.4.2.3 (Ground)water quality monitoring

The pretreated ASR injection water was sampled at least monthly. All monitoring screens were first sampled prior to ASR operation (December 19, 2011) and subsequently with a high frequency during the breakthrough of the injection water at MW1. Thereafter, monthly sampling was maintained. Three times the volume of the well casing was removed prior to sampling. All samples were analyzed in the field in a flow-through cell for EC (GMH 3410, Greisinger, Germany), pH, ORP, and temperature (Hanna 9126, Hanna Instruments, USA), and dissolved oxygen (Odeon Optod, Neotek-Ponsel, France). Samples for alkalinity determination on the Titralab 840 (Radiometer Analytical, France) were stored in a 250 ml container and titrated within one day after sampling. Samples for further hydrochemical analysis were passed over a 0.45 µm cellulose acetate membrane (Whatman FP-30, UK) in the field and stored in two 10-ml plastic vials, of which one was acidified with 100 µl 65% HNO_3 (Suprapur, Merck International) for analysis of cations (Na, K, Ca, Mg, Mn, Fe, S, Si, P, and trace elements) using ICP-OES (Varian 730-ES ICP OES, Agilent Technologies, U.S.A.). The other 10 ml vial was used for analysis of F, Cl, NO_2, Br, NO_3, PO_4, and SO_4 using the Dionex DX-120 IC (Thermo Fischer Scientific Inc., USA), and ammonium using the LabMedics Aquakem 250 (Stockport, UK). All samples were cooled to 4 ^{o}C immediately after sampling.

The mixing fraction (*f*) describes the proportion of injected water of the water sample at the time of sampling (Pavelic et al., 2002; Ward et al., 2007):

$$f = \frac{C(t) - C_i}{C_0 - C_i} \tag{3.1}$$

where $C(t)$ is the concentration at time t, C_i is the concentration of the ambient groundwater, and C_0 is the concentration of the injection water. For conservative elements, pure injection water is marked by f=1 and ambient groundwater by f=0. Cl was used as tracer because of its conservative behavior and its low concentration in the injection water (1-19 mg/l), contrary to its high concentrations in the ambient groundwater (115 - 1001 mg/l).

3.4.2.4 Borehole logging

Boreholes MW2 and MW3 were logged via the deepest piezometer to measure changes in formation conductivity outside the standpipe of the well. Such changes should indicate a change in electrical conductivity of the groundwater, as the lithology remains constant (Metzger and Izbicki, 2013). The formation electrical conductivities were recorded using the Robertson DIL-39 probe. Logs were performed on January 18 and of MW2 on October 3, 2012. The 2.3 m long probe could not be lowered into MW1 due to a slight curve in the standpipe.

3.4.2.5 Electronic monitoring of ASR operation and target aquifer

Operation of the ASR system was monitored by electronic data logging with a 30 minutes interval. This included: ASR cycle registration (operating phase), injected volumes per well (based on pipe diameters and flow velocities from Signet 515 Rotor-X Paddlewheel Flow Sensors (Georg Fischer Signet LLC, USA)), recovered volumes per well (idem), EC of recovered water per well (ELMECO, The Netherlands), and the total operation period per pump. Two combined electrical conductivity and pressure transducers (CTD) and two regular pressure transducers (Divers from Schlumberger Water Services, USA) were installed at MW1 (S1-4). Manual head measurements were performed prior to each sampling round to validate the head observations by the Divers.

3.4.3 SEAWAT density-dependent groundwater transport model

3.4.3.1 Model outline and calibration

SEAWAT version 4 is a MODFLOW/MT3DMS-based computer program which simulates three-dimensional variable-density groundwater flow coupled with multi-species solute and heat transport (Langevin et al., 2007). It was used for the simulation of groundwater flow and conservative solute transport, including the effects of densi-

ty differences. Density differences were caused by the significant contrast in total dissolved solids (TDS) in the injection water (44 – 80 mg/L) and ambient groundwater (1424 – 3462 mg/L). Its effect on especially small-scale ASR performance can be significant, even when density differences are small (Ward et al., 2007; Ward et al., 2009). The local hydrogeology and ASR configuration were incorporated into an axial-symmetric model (Langevin, 2008; Wallis et al., 2013), neglecting lateral aquifer heterogeneities and background lateral flow. The head in the upper layer was fixed to simulate the mean drainage level (4.9 m BSL). A fixed head (4.15 m BSL) was applied at the base of aquifer 2 to achieve the measured head in the target aquifer before injection (4.30 m BSL), thereby simulating the natural seepage. Results from grain size analyses were used to define hydrogeological units and a first estimation of hydraulic conductivities (K). Field measurements of head responses to pumping and the breakthrough of chloride at MW1 (S1-4) were used to calibrate the model for K and specific storage (S_s), and dispersivity (D) and effective porosity (η_e), respectively. The resulting SEAWAT model was able to reproduce the head response and breakthrough curve at all well screens, indicating the model was reliable at least for the hydrogeological units in which observation wells were installed.

3.4.3.2 Model set-up

A vertical (Δz) and horizontal discretization (Δr) of 1 m was used close to the well, which was increased to 10 m at radii >100 m. The total model radius was 3,000 m, which was sufficient to prevent edge effects from affecting the simulated flow regime. A no-flow boundary was used at the model boundary where the well was situated (left), whereas constant head boundaries were used for the model top, bottom, and right-hand side. A schematization of the model is shown in Figure 3-3.

A total of 37 stress periods was used for the MPPW field set-up, each lasting 1 to 18 days, simulating nine months of injection and recovery from January 12 till October 11, 2012. The mean pumping rate in each stress period of each well was based on the measured pumped volumes. Each well screen was represented by multiple cells in the well package, of which the discharge was calculated using the discharge of the well screen and the relative transmissivity of the aquifer at each cell. The recovered concentration for each well screen was calculated based on the concentration and contribution of each cell to the well discharge. The third-order total-variation-diminishing (TVD) scheme (Leonard, 1988) was used to simulate advective transport of TDS and chloride. Effective molecular diffusion coefficients (D_e) for TDS and chloride were based on diffusion coefficients in free water (D_f) by Appelo and Postma (2005), assuming $D_e = D_f/2$.

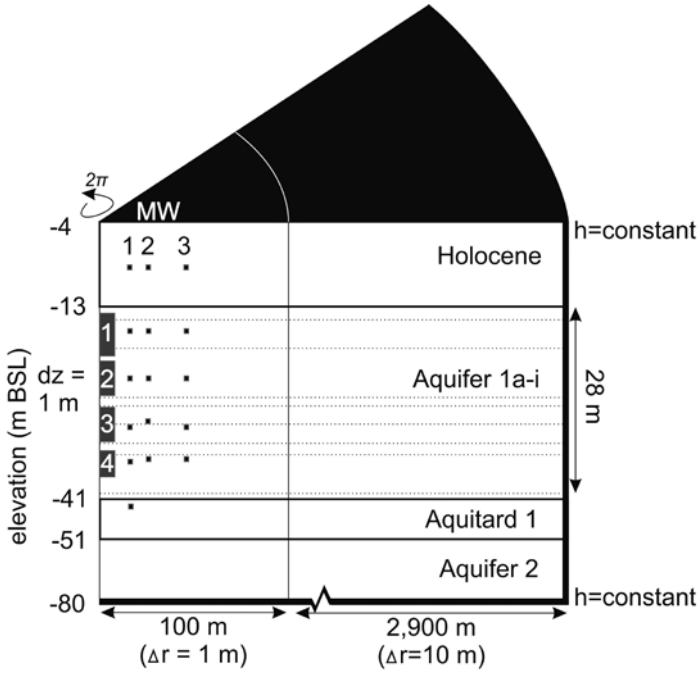

Figure 3-3: Set-up of axial-symmetric ASR model.

3.4.3.3 Model calibration

The parameters for the modelling of groundwater flow and solute transport were derived stepwise. Aquifer hydraulic conductivity (K) was initially assessed using grain size data (e.g., Koltermann and Gorelick, 1995; Vienken and Dietrich, 2011) from MW1, which provided undisturbed samples from the vicinity of the ASR well. The empirical relationship by Bear (1972) based on the Kozeny-Carman equation was used (3.2):

$$K = \frac{\rho g}{\mu} \frac{d_m^{\,2} \eta_e^{\,3}}{180(1-\eta_e)^2} \tag{3.2}$$

where K is the hydraulic conductivity (L/T), ρ is the density of fluid (M/L^3), μ is the dynamic viscosity (M/LT), d_m is the representative (geometric) mean grain size (L), and η_e is the effective porosity (-).

Assumptions were made for η_e (0.35 for sands (Meinardi, 1994), 0.2 for clay and

loam). The hydrogeological boundaries were determined from this first interpretation. The freshwater head response during several pumping stages, as observed at MW1 after freshening of the whole aquifer beyond 5m radius, was used to calibrate the MODFLOW model (Harbough et al., 2000) for hydraulic conductivity (K) and specific storage (S_s). Relative K-values of the aquifer units, as derived from the grain size distributions, were maintained as much as possible.

The initial groundwater composition was based on hydrochemical analysis of samples from MW1 prior to ASR operation. The breakthrough curve of chloride at the well screens of MW1 was used to derive aquifer dispersivity and effective porosity. The anisotropy ratio of specific model layers where clay/peat deposits (interbedded in the aquifer sands) were observed was adjusted in the final calibration step.

3.4.3.4 Density correction for groundwater compositions

Several methods are available to derive groundwater densities, such as direct measurements and relationships with EC or chemical composition (Post, 2011). The algorithm presented by Millero (1971) , Millero (2000), and Millero (2001) in PHREEQC Version 2.18 (Parkhurst and Appelo, 1999) was used to calculate groundwater densities of the samples taken between December 2011 and May 2012. The contribution of all dissolved components (including inorganic carbon) to the groundwater density was taken into account this way. Density showed a linear relation with TDS (Figure 3- 4), which was used to calculate groundwater densities in SEAWAT:

$$\rho(TDS) = 0.0007TDS + 999.8 \tag{3.3}$$

where $\rho(TDS)$ is the density (kg/m^3) based on the TDS and TDS is the total dissolved solids (mg/L). Cl was found unsuitable to base the density upon, as even for low Cl concentrations an increased density of the ambient groundwater was found due to high Ca and HCO_3 concentrations. Dissolution of calcite in the aquifer slightly increased TDS of the injected water, but was negligible.

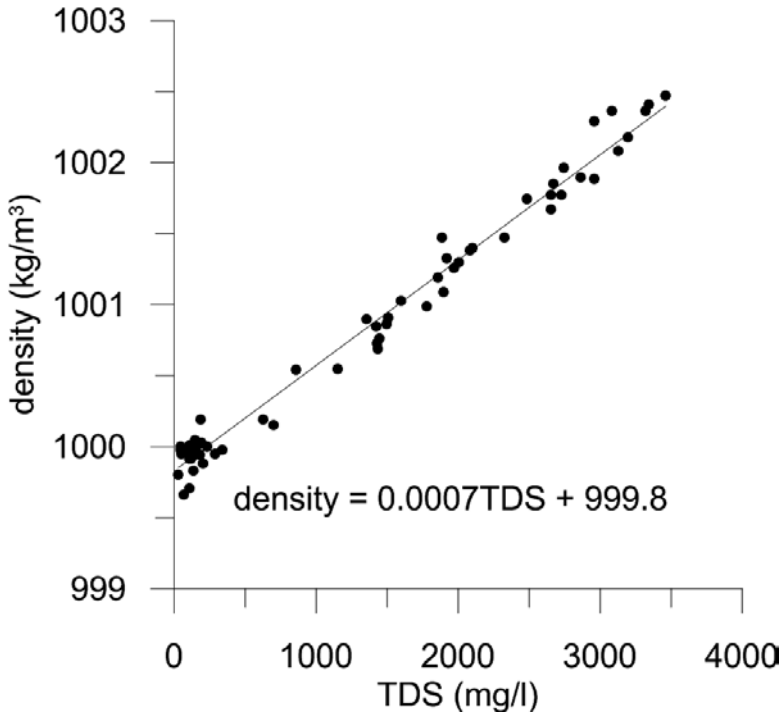

Figure 3-4: Calculated density versus TDS.

3.4.3.5 Comparison of MPPW with fully penetrating (FPW) and single partially penetrating (SPPW) ASR wells

The calibrated model was used to simulate ASR using a fully penetrating (FPW) and single partially penetrating well (SPPW) at the same location. Equal ASR operational parameters were thereby used to compare their performance with ASR using MPPW. The FPW covered the full aquifer thickness, whereas the SPPW was screened only in the upper half of the target aquifer. Pumping rates of each cell were proportional to the contribution of each layer to the total transmissivity, which may cause some overestimation of water injected and recovered by deeper cells (Houben and Hauschild, 2011). Bulk concentrations in the recovered water from the ASR well were calculated likewise based on the concentration and contribution of each cell to the total discharge. Recovery was ceased for the rest of the particular recovery period once recovered concentrations exceeded the irrigation water limits (18 mg/l Cl).

Finally, two subsequent years (or ASR "cycles") were modeled with the operational parameters of 2012 for an FPW, SPPW, and MPPW to estimate future ASR

performance. Therefore, an idle period was added to the last recovery stage to start injecting again on January 12. The last recovery stage in year 2 and 3 was extended until the maximum allowable salinity of the bulk recovered water was exceeded. Three cycles were also modeled for an FPW without buoyancy and seepage. This scenario should give the maximum RE at the particular site for the operational parameters of the 2012 cycle, taking into account the salinity of the ambient groundwater and the allowable mixing fractions. Based on the scenarios with an FPW, SPPW, and MPPW, one can quantitatively compare the benefits of the SPPW and MPPW, and conclude to what extent freshwater losses by buoyancy and seepage can be overcome.

3.5 Results

3.5.1 Nootdorp ASR trial

3.5.1.1 Hydrogeological characterization of the target aquifer

The target aquifer is underlain by a compacted silty loam layer. According to the regional geological model (TNO-NITG), the base of this unit can be found at 55 m BSL, while the K_v should be ~0.02 m/d. The base of the target aquifer (~ 31 to 41 m BSL) is characterized by fine to gravelly very coarse sands and marked by Unit 1f to 1i (Figure 3-5). Most estimated *K*-values of these units based on the grain size distributions are well above 20 m/d, with a maximum of 100 m/d at the basal 1 m (well sorted gravel and coarse sand, Unit 1i). Thin clay layers, reworked peat, and clay pebbles (with a diameter of 1 to 10 cm in the cores of MW1, and mollusks were found in a matrix of middle coarse sand in the central part of the aquifer (Unit 1e, 28 to 31 m BSL). This unit is not considered a continuous clay layer separating the aquifer into two (semi-)confined aquifers (Busschers et al., 2005). A mean K of ~5 to 10 m/d was estimated based on the grain size distributions for this Unit. The top of the target aquifer (Unit 1a to 1c, ~ 13 to 28 m BSL) consists of relatively homogeneous, mainly middle coarse fluvial sands. The estimated *K* of those units was 5 - 15 m/d. The Holocene cover (3.8 to ~ 13 m BSL) consists of marine silty clay and silty loam with thin peat layers. The vertical hydraulic conductivity (K_v) based on grain size distributions of this upper confining unit was estimated 0.01 m/d.

The *K* and S_s values based on freshwater head response in the aquifer are shown given in Figure 3-5. A three to four times higher *K* than estimated using grain size analyses was generally required to simulate the head response in the aquifer. All *K*-values are in line with *K*-values known for the specific sediments (Bear, 1972). The deduced total transmissivity (1,900 m^2/d) was significantly higher than indicated by

the geological model (TNO-NITG), which predicted a much thinner target aquifer with a maximum depth of 35 m BSL. The clay aquitards were considered anisotropic (K_h / K_v = 10). Unit 1e was considered slightly anisotropic (K_h / K_v = 2), to incorporate the clayey intervals in the model. The vertical anisotropy of the whole target aquifer based on the values derived for K_v and K_h is 1.9, indicating the aquifer is relatively isotropic. Effective porosities in the aquifer based on the chloride breakthrough ranged from 0.25 to 0.35.

3.5.1.2 Hydrochemical characterization of the target aquifer

Background groundwater in the target aquifer prior to ASR operation showed a clear salinity stratification (Figure 3-5). Relatively fresh water was observed at the top of the aquifer (Cl: 115 mg/l), allowing a mixing ratio (*f*) of 0.8 here to comply with irrigation water demands. At the base, however, chloride concentrations ranged 860 - 1001 mg/l. This means *f* should remain >0.98 here, allowing no more than 2% of ambient groundwater to be admixed in the water recovered from the deepest ASR well. The vertical TDS zonation in the aquifer was dominated by a NaCl water type at the base of the aquifer, and by a $CaHCO_3$ water type in the upper aquitard. Both water types show a positive Base Exchange Index (BEX; Stuyfzand, 1993, 2008), indicating that the originally saline aquifer was flushed with fresh groundwater.

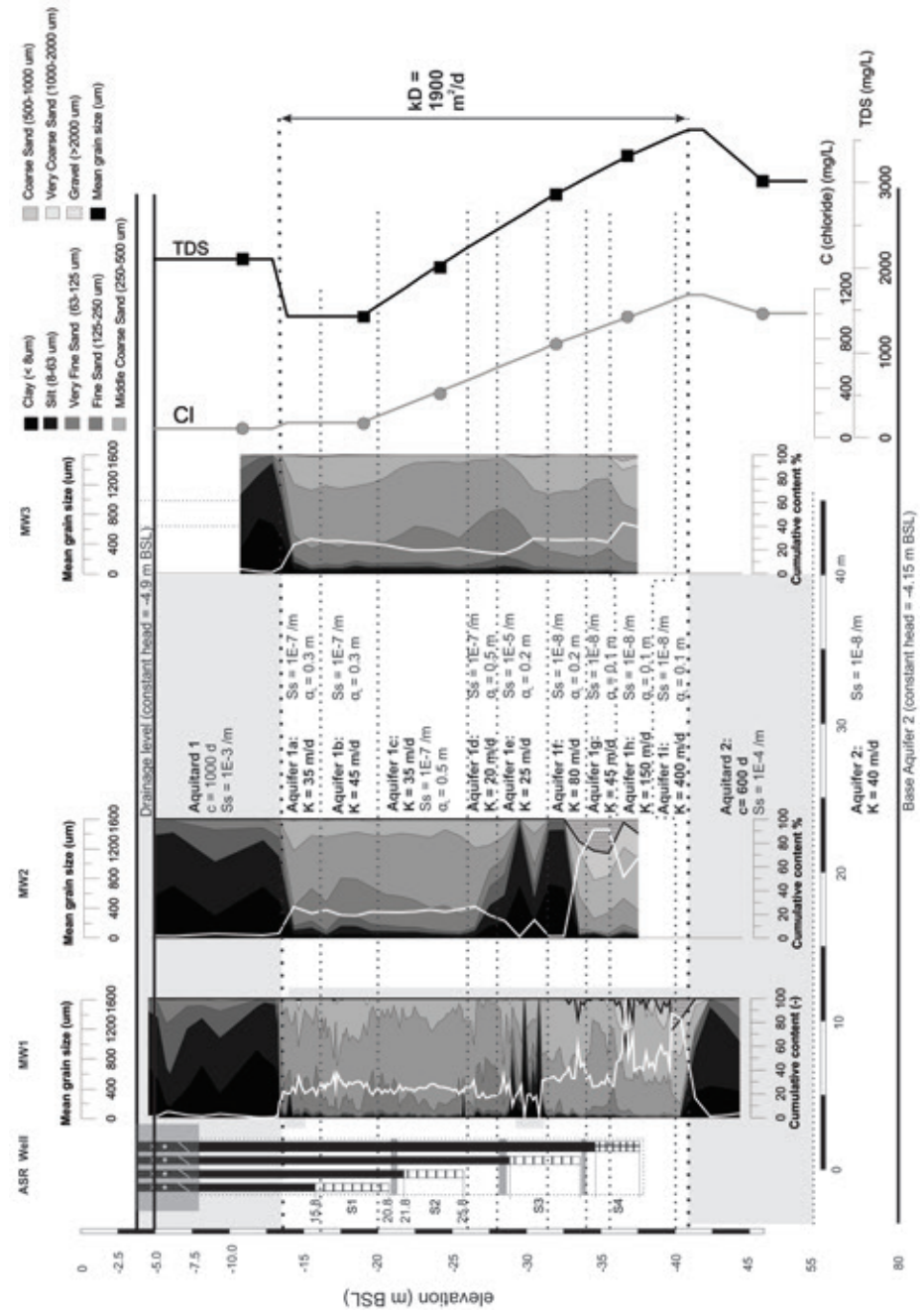

Figure 3-5: Physical characterization of the target aquifer in the monitored flow direction, groundwater salinity (measured at MW1), and calibrated aquifer properties. *c*= hydraulic resistivity, S_s= specific storage, α_L= longitudinal dispersivity, and *TDS*= total dissolved solids.

3.5.1.3 Operation of the ASR system

The pumped volumes per well of the MPPW are shown in Figure 3-6. A large rainwater surplus during the first weeks of January was first infiltrated using all ASR well screens. The infiltration capacity of the wells was tested and the first breakthrough at MW1 in the target aquifer was monitored in this period. Recovery using all ASR wells started after injecting ~3,700 m^3 during the relatively dry months of February and March. It was decided to close off AWS4 after rapid salinization and limit further recovery to the upper two ASR wells mainly, while injection of further surpluses was performed by the lower three wells. A large precipitation surplus was injected from April to August 2012, when recovery was limited to short periods of drought. Almost 11,000 m^3 was injected by early August, whereas only little more than 1,600 m^3 was recovered. Injection and recovery were more or less in equilibrium from August until mid-September. A recovery period was forced as final stage of the ASR cycle to determine the maximum RE of the system. Any precipitation occurring was injected at S2 and S3 in this period, to delay salinization during recovery by S1 and S2. By October 11, 13.700 m^3 was injected and 5,500 m^3 was recovered. This means that an overall recovery efficiency of 40.2% was achieved.

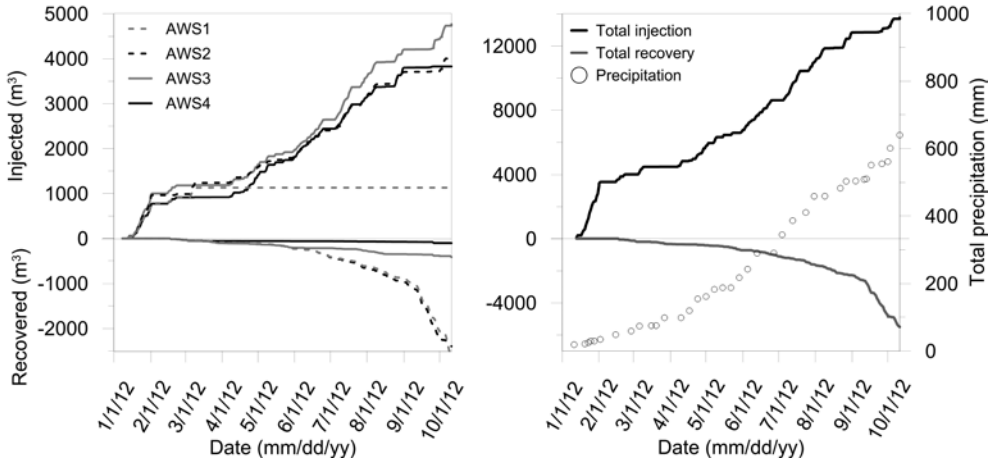

Figure 3-6: Pumping by the ASR system by each well of the MPPW. AWS = ASR well screen.

3.5.1.4 Injection water quality

The quality of the pre-treated roofwater was fairly constant and typically low in chloride and TDS (Figure 3-7). The rooftop water gained minor amounts of Ca^{2+} and

HCO_3 by dissolution of calcite in the slow sand filter, especially during periods without injection. Cl concentrations were typical for precipitation in the area lying ~12 km from the North Sea coast (Stuyfzand, 1993).

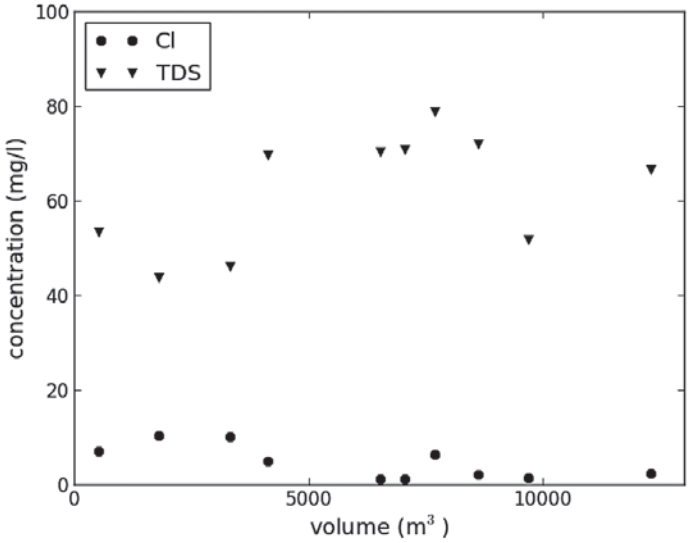

Figure 3-7: Measured chloride (Cl) and total dissolved solids (TDS) in the injection water.

3.5.1.5 Location of the freshwater by the end of the ASR season

The hydrochemical analyses (Figure 3-8) and borehole logging at MW2 (Figure 3-9) indicated that by the end of the ASR season, the injected freshwater was present at the top and center of the aquifer at the ASR well (AW) and MW1 (S1, S2 and S3). No injection water reached the S3 level at 15 m (MW2). MW2S1 and later MW2S2 and MW2S4 showed a clear freshening when the stored volume was at its peak. MW2S2 and MW2S4 salinized subsequently during the final recovery stage. MW2S1 remained fresh, which may be caused by significant buoyancy effects moving fresh water toward the aquifer top and/or by a clay layer in the top of the aquifer just above the specific well screen at a depth of ~17 m BSL, trapping the freshwater locally by preventing upward flow. Indications for such a clay layer can be derived from grain size distributions (Figure 3-5), borehole logging (Figure 3-9), and literature (Busschers et al., 2005). A thin freshwater lens was found by borehole logging just below the fine clayey deposits in the center of the aquifer (Unit 1e). As this lens was situated between MW2S3 and MW2S4, it was not detected by groundwater sampling.

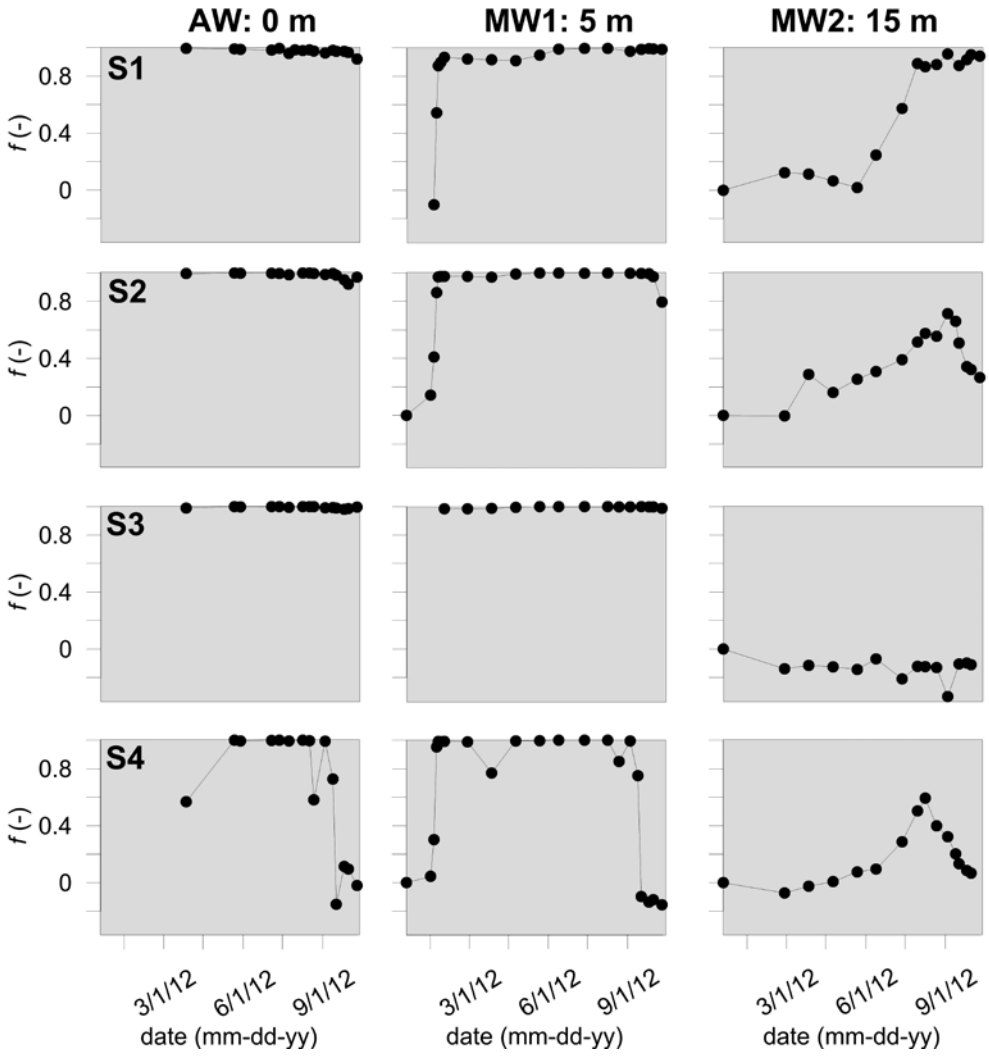

Figure 3-8: Mixing fraction *f* at AW, MW1, and MW2 versus time.

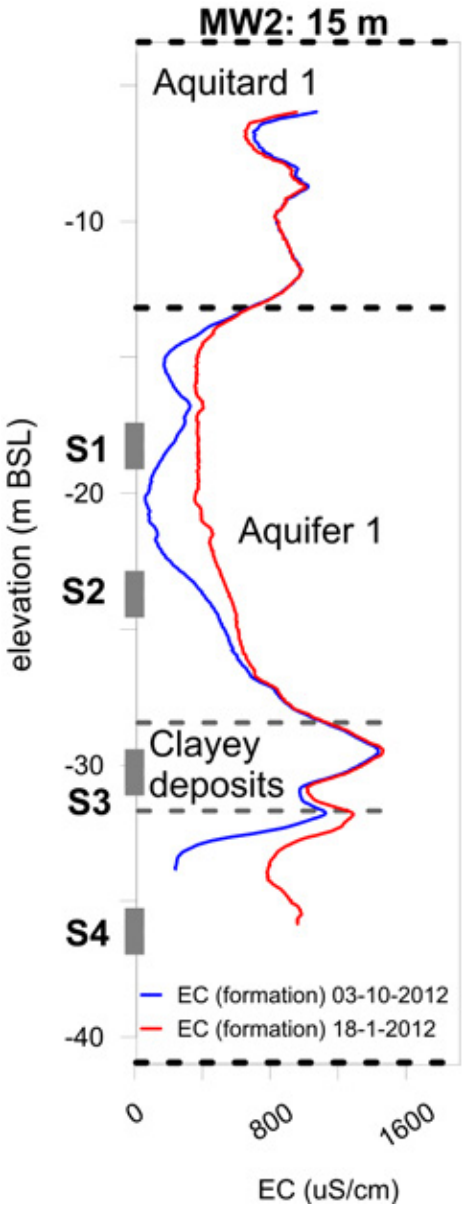

Figure 3-9: Formation electrical conductivity based on borehole logging at MW2.

3.5.2 Solute transport model of the Nootdorp ASR trial

3.5.2.1 Comparison of field and model results

The results of the SEAWAT transport model for the various well screens during ASR operation are shown in Figure 3-10. Most of the observed Cl concentrations at AW,

MW1, and MW2 are in line with the modelled concentrations. Only MW2S3 shows a large deviation with respect to the modelled trend of the Cl concentration, which is presumably caused by the local clay deposits surrounding this particular monitoring well. Further deviations are mainly found in the late summer recovery period (from August onwards). For instance, the shallow monitoring wells at the S1-level (especially MW2S1) salinized later than predicted by the model. This suggests that the lack of salinization at MW2S1 during recovery is not caused by buoyancy effects (which are incorporated in the model), but by a local clay layer just above the monitoring well, trapping the fresh ASR water.

The freshening and salinization of the deepest well screens (S4) are well predicted by the model, although measured Cl concentrations are slightly higher during the final recovery stage. Altogether, the model produced an acceptable simulation, as it was able to reproduce the most important trends in chloride concentrations, while major deviations could be explained by local heterogeneities.

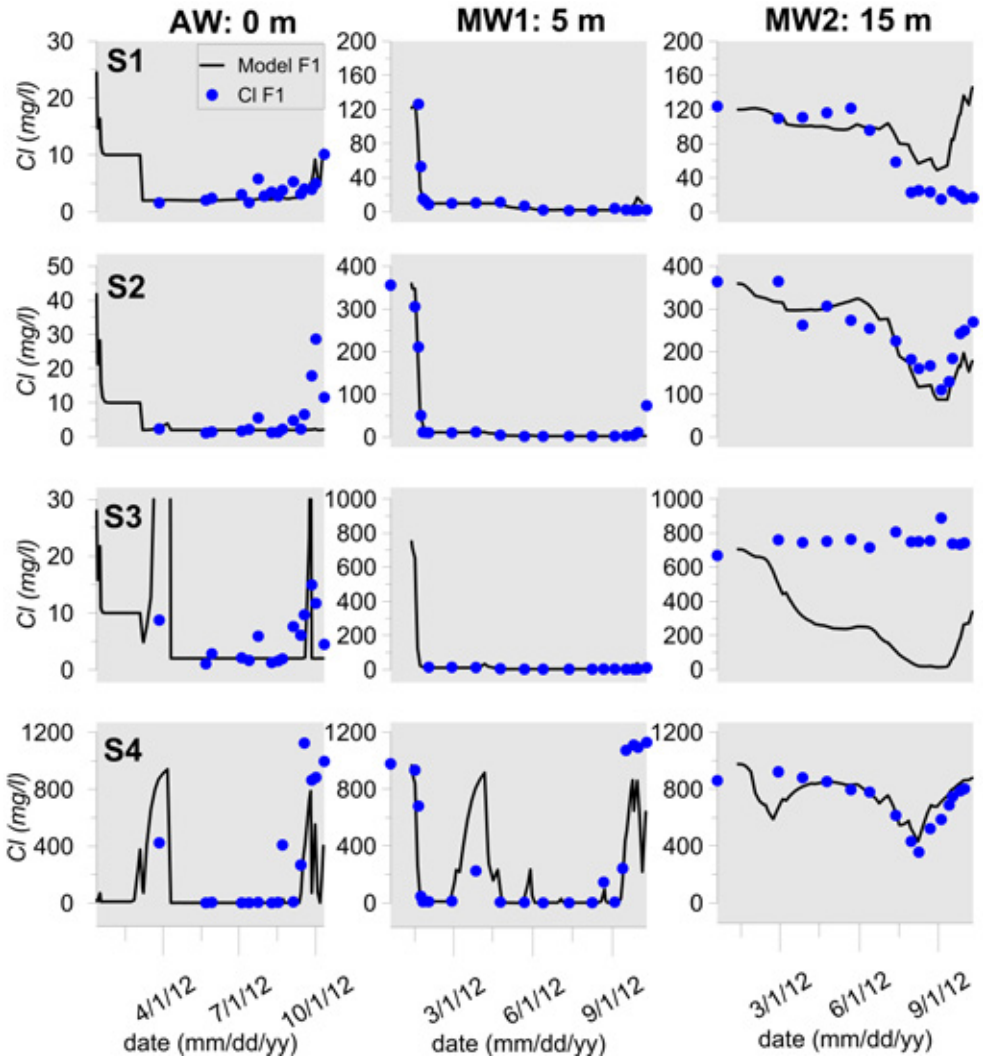

Figure 3-10: Measured and modelled chloride concentrations at the ASR well (AW), and the monitoring wells at 5 and 15 m distance (MW1 and 2 respectively).

3.5.3 Effect of the MPPW on ASR recovery efficiency

3.5.3.1 Comparison with a fully penetrating ASR well (FPW)

A fully penetrating well (FPW) was modelled to test whether the MPPW yields a higher RE than a conventional FPW. This well injected the same freshwater surpluses and recovered with the same pumping rate as the field set-up until the maximum allowable Cl concentration (~18 mg/l, Figure 3-11) was reached. Subsequently, an idle period

was imposed until a new surplus was available for injection. As less days of recovery could take place, less freshwater was recovered and the RE clearly decreased for an FPW (Table 3-1). No ASR water satisfying the quality constraints could be recovered during 77 out of 114 days with irrigation water demand. In total, 2,014 m^3 could be recovered with an FPW, resulting in an RE of 14.7%, which is only one-third of the RE realized by the MPPW.

3.5.3.2 Comparison with a single partially penetrating ASR well (SPPW)

For a single partially penetrating well (SPPW) in the upper half of the target aquifer, the model predicted an RE of 30.2%. This is twice the RE calculated for the FPW (Table 3-1), but still significantly less than the RE achieved with the MPPW (40.2%). Irrigation was not possible during 12 d, which is a clear improvement compared to the FPW. All recovery terminations due to an exceeding salinity took place in the last phase of recovery (September/October 2012,Figure 3-8).

Table 3-1: Recovered volume, recovery efficiency, and recovery duration of a modelled fully (FPW) and single partially penetrating well (SPPW), compared to the multiple partially penetrating wells (MPPW) used at the Nootdorp ASR trial.

	Recovery (m^3)	Recovery efficiency (RE, %)	Recovery (d)
Fully penetrating well (FP)	2,014	14.7	35
Single partially penetrating well (SPPW)	4,136	30.2	102
Multiple partially penetrating wells (MPPW)	5,499	40.2	114

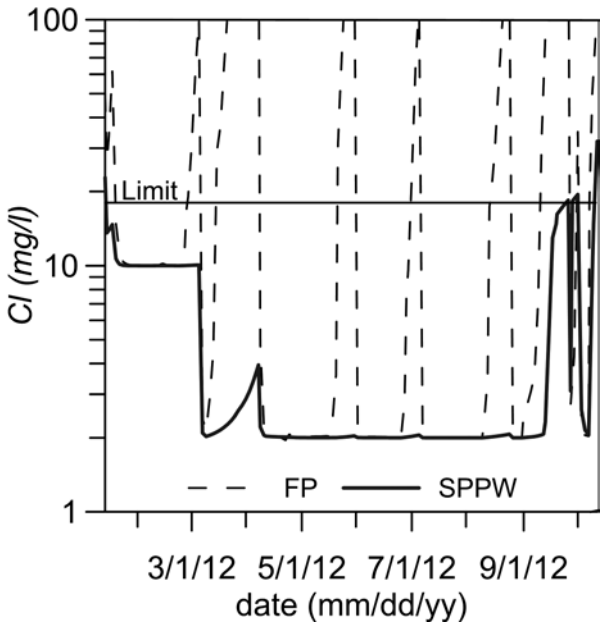

Figure 3-11: Modelled chloride concentrations during recovery with a fully penetrating well (FPW) and a single partially penetrating well (SPPW). Recovery was stopped whenever the limit for irrigation water was exceeded.

3.5.3.3 Quantifying the long-term benefits of SPPW and MPPW

A second and third cycle was modelled to explore the long-term benefits of MPPW on the ASR performance. In case of the MPPW, 80% of the freshwater surplus was injected by AWS3 and AWS4 in the lower half of the aquifer, while AWS1 and AWS2 were used for recovery in the upper half. A scenario was added for the FPW, in which buoyancy and seepage were neglected so that only mixing caused freshwater losses. After many cycles, this results in a theoretical RE approaching 100% (Figure 3-12), since a broad mixing zone is developed around the injected freshwater, protecting it from mixing-induced salinization.

The MPPW can almost overcome the loss by buoyancy and seepage in the first cycle, as the RE approaches the maximum RE. However, the RE of MPPW shows an increasing deviation with the maximum RE in subsequent cycles. The RE of MPPW remains little less than 60% (Figure 3-12), indicating a structural freshwater loss of 40%. The recovery achieved is still almost two and more than three times higher than an SPPW and FPW, respectively.

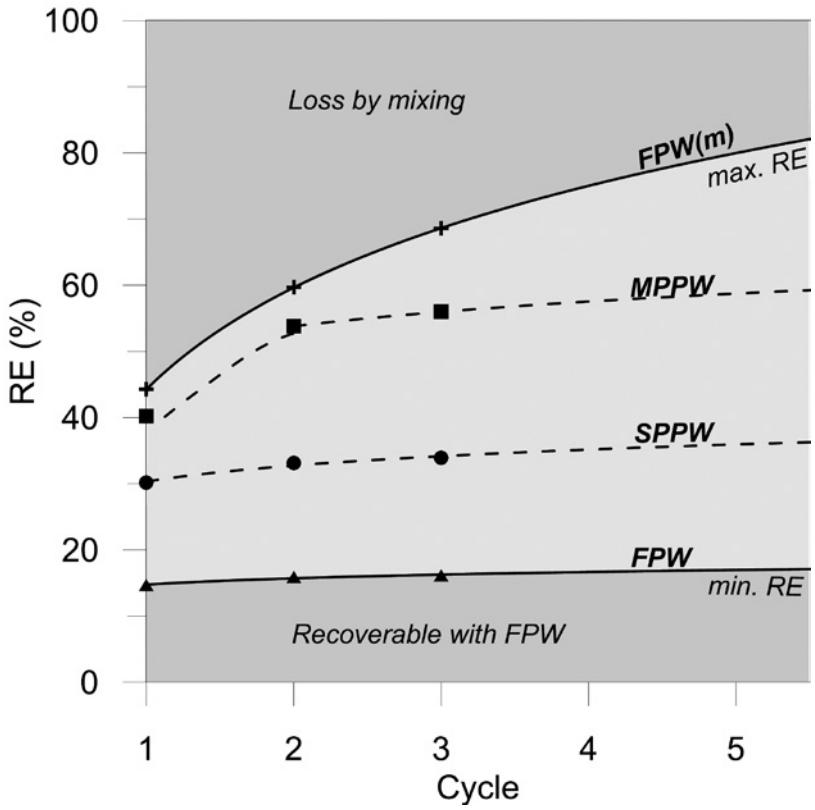

Figure 3-12: Modelled RE per cycle versus cycle number for four scenarios. FPW (m) =scenario with only mixing and a fully penetrating ASR well. The other scenarios take into account mixing, seepage, and buoyancy for multiple partially penetrating wells (MPPW), a single partially penetrating well (SPPW), and a fully penetrating well (FPW). Cycles 1-3 were modelled, cycle 4 and 5 were extrapolated from the modelled cycles.

3.6 Discussion

3.6.1 Water quality development during recovery using MPPW

The deepest ASR well used for recovery (AWS2) salinized first (Figure 3-8), which forced lowering of the pumping rate at AWS2, to attain mixed water with a concentration below the maximum salinity. MW1S2 (same depth) and the deeper wells screens (AWS3 and MW1S3) remained fresh in the same period and were not affected by transport of more saline water towards AWS2. MW1S2 did show a clear salinization in the last stage of recovery. This more saline water entering AWS2 and MW1S2 was not

predicted by the model, and potential causes are discussed here. First of all, some background lateral flow (not included in the axi-symmetrical model) in the south-eastern direction of the monitoring wells can explain this salinization, as it would bring in more saline water to the ASR well screens upstream. This cannot explain, however, the clear salinization of MW1S2 by the end of recovery, as this monitoring well is situated downstream where it should remain fresh. Lateral background flow is therefore excluded as a cause for the unexpected salinization.

Short-circuiting of deeper saline water is considered as a cause, but does not seem a plausible explanation either. The deepest well screens (S4) quickly salinized during periods with a net recovery. At these wells screens, Cl concentrations rose above the concentrations found prior to the ASR operation, which is marked by a negative *f*. This suggests that some upconing of more saline water occurred, or that disturbance of the groundwater during installation of the monitoring wells caused an underestimation of the salinity in the initial sampling. There were no signs of short-circuiting of this brackish water through the gravel pack to the upper three ASR screens as AWS3 remained fresh while the deeper AWS4 fully salinized. So the salinization of the shallower AWS2 in the same period cannot be caused by short-circuiting.

The detailed data of local aquifer heterogeneity and water quality monitoring permits another explanation. In the centre of the aquifer (Unit 1e, see Figure 3-5), reworked clay was found within a sandy matrix. In this unit, preferential flow paths can be expected, while other zones are flushed significantly less, resulting in local brackish groundwater pockets. The latter was found at MW2S3, which remained brackish while the surrounding aquifer freshened. Relatively stagnant brackish pore water in such an interval containing clay or peat pebbles may increase the salinity of the injected water by dispersion and diffusion (Appelo and Postma, 2005; Weber and Smith, 1987). A physical non-equilibrium of the concentrations is likely, considering the average flow velocities in the storage zone of the ASR system (>15 m/yr) and the size of the clay and peat pebbles (1 to 10 cm). Diffusion out of this stagnant water in the pebbles can therefore remain a prolonged supply of salts to the injected freshwater, especially further away from the ASR well or during storage. It is expected that the clay and peat deposits caused the early salinization at AWS2 and later MW1S2.
A model simulation with some extra low conductivity cells created such a salinization of deeper freshwater travelling towards AWS2. The same process may have caused salinization at AWS1 in the last phase of recovery. The water quality development during recovery underlines that the shape of the injected freshwater in a heterogeneous aquifer differs significantly from a typical 'bubble shape' as state by Vacher et al. (2006), which is also illustrated in Figure 3-13.

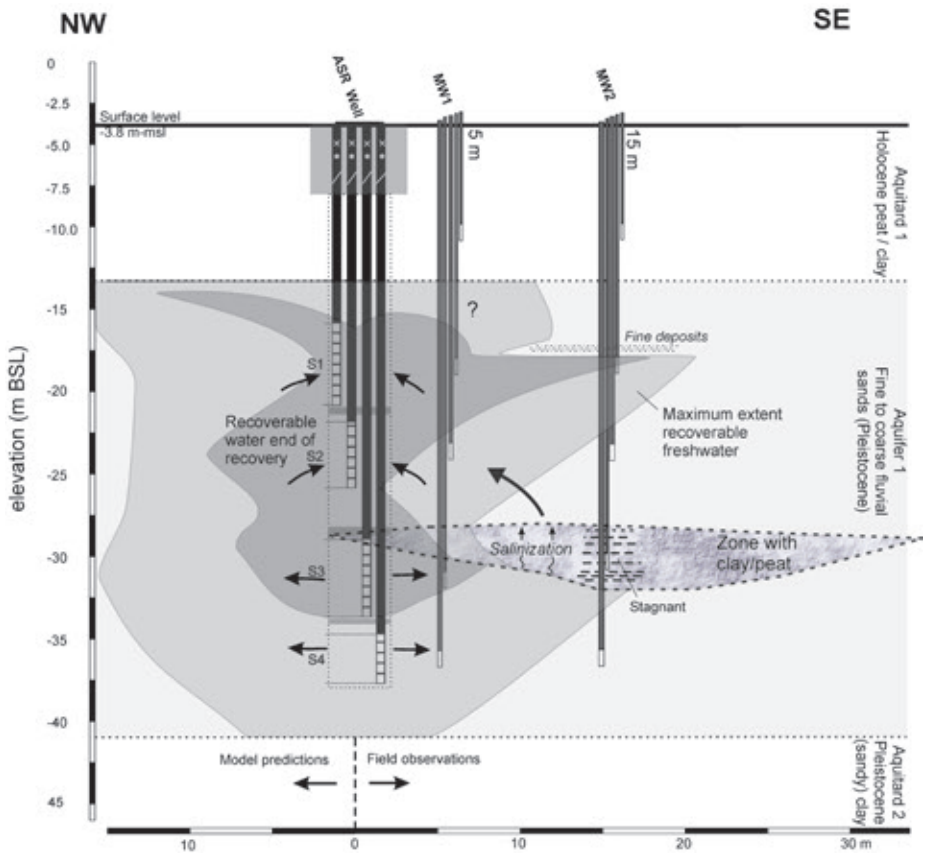

Figure 3-13: Interpreted geometry of the recoverable freshwater (<18 mg/l Cl) based on the SEAWAT model (left-hand side) and hydrochemical data and borehole logging (right-hand side). The maximum stored volume at the end of recovery is shown. In the direction of the monitoring wells, a zone with clay and peat pebbles with brackish pore water limits upward flow and potentially causes salinization of injected freshwater by diffusion and dispersion.

3.6.2 Benefits of the MPPW set-up

This study quantifies the increase in freshwater recovery of an optimized well design in a real-world ASR application. It shows that for a relatively small-scale ASR system in a brackish, relatively homogeneous sand aquifer, the RE in the first cycle was doubled by installation of a single partially penetrating well (SPPW, 30.2% recovered), instead of a fully penetrating well (FPW, 14.7% recovered). An even larger increase in RE was achieved by the use of multiple partially penetrating wells (MPPW), consisting of 4 partially penetrating wells in a single borehole, which were separated by bentonite

clay plugs. By enhanced injection at the base of the injected freshwater bubble and recovery at the top of the aquifer ('skimming'), the RE of this particular ASR system increased to 40.2%. This way, a vulnerable, potentially unviable, small-scale ASR system was optimized to a system able to supply sufficient irrigation water throughout the summer of 2012.

Modelling of subsequent cycles indicated that although buoyancy effects were approximately overcome by the use of MPPW, the yearly RE is expected to be little less than 60%. This can be related to the unavoidable salinization occurring at the lower half of the aquifer during recovery. Starting conditions for subsequent ASR cycles in this zone thus become comparable to the initial conditions. A significant loss of freshwater by mixing results in the subsequent injection phase, making a large part of the injection water unsuitable for recovery. Yet still, a significant increase in freshwater recovery is maintained in subsequent cycles by the MPPW with respect to a set-up with an SPPW (RE: <35%) or an FPW (RE: <20%). It is therefore demonstrated that the use of MPPW is preferred over an SPPW and FPW for ASR in brackish or saline aquifers.

In many (especially small-scale) ASR applications, site-specific data on aquifer properties and groundwater density is lacking (e.g., Ward et al., 2009; Chapter 2), hampering *a priori* optimization of well design and injection/scheme. With the MPPW set-up proposed in this study, however, the ASR scheme can be optimized after the installation based on the EC of the water recovered from each layer. In case of more favorable ASR conditions, e.g., salinity of the ambient groundwater is low or anisotropy is high, the MPPW can still be operated more like an FPW. In case of unfavorable conditions on the other hand, the deeper wells of the MPPW can be used to re-inject part of the recovered water to enable a larger net recovery, comparable to an injection-extraction well pair in coastal aquifers suffering from seawater intrusion (Lu et al., 2013). Alternatively, one can use the deeper well screens for interception of brackish/saline water below the injected freshwater, which will further postpone salinization of the shallower MPPW recovery wells (Stuyfzand and Raat, 2010; Van Ginkel et al., 2010). Installation of an MPPW is therefore preferred over an FPW for ASR in coastal aquifers. As for ASR using an FPW, background lateral flow velocities need to be limited, especially for the small-scale ASR systems considered in this study.

Clustering of local ASR systems to a larger system in combination with MPPW may further improve the RE, as the relative freshwater loss by mixing then becomes less. However, the effect of the partially penetrating wells at the location of the fresh-salt interface at large-scale ASR systems can be limited, as this interface is further from the ASR well (Hantush, 1966), especially in relatively thin, isotropic aquifers. The

MPPW may then act similar to an FPW. It would be helpful for planning purposes, to account for the benefits of MPPW in ASR performance estimation methods, as the current methods (Bakker, 2010; Ward et al., 2009) only consider fully-penetrating ASR wells.

3.6.3 Implications of an optimized well design for ASR operation

3.6.3.1 Installation and operation of the MPPW

The MPPW configuration required three additional clay plugs, standpipes, suction pipes, valves, well heads, and EC-meters, as well as 6 additional flow meters. All requirements could easily be installed to enable varying pumping rates in various sections of the aquifer, while the additional costs (~5 k USD) were negligible compared to the construction costs of the ASR system (~65 k USD). This means that for each m3 of yearly recovered freshwater, almost 9 USD was invested in the MPPW set-up, whereas for the poorly performing FPW this would have been 27 USD per m^3.

An SPPW configuration has the advantage that it does not require any aboveground modification of the ASR set-up, but the capacity of such an ASR well is decreased by approximately 50%. More ASR wells may be required to enable large injection and/or recovery rates. When a reduced well capacity is acceptable, this study shows that an SPPW is to be preferred over an FPW. The well capacity available for injection and recovery of the MPPW set-up is also reduced when water is injected at the base of the aquifer only. However, the full aquifer thickness can still be used incidentally for injection of large freshwater surpluses (for instance, in a period of intense rainfall).

3.6.3.2 Water quality changes and the MPPW set-up

Water quality changes during injection, storage, and recovery of the rainwater in the brackish target aquifer can be anticipated by chemical interaction with the aquifer sediments. For instance, Na and K can be introduced to the injection water by cation exchange with Ca and Mg (Appelo and Postma, 2005). The injection of oxygen-containing rainwater in the deeply anoxic target aquifer also poses a threat for the water quality development by oxidation of pyrite, and is recently reported in ASR studies worldwide (e.g., Antoniou et al., 2012; Jones and Pichler, 2007; Price and Pichler, 2006; Vanderzalm et al., 2011; Wallis et al., 2011; Wallis et al., 2010).
As a consequence, mobilization of SO_4, Fe, Mn (from subsequent siderite dissolution), As, Co, and Ni is observed, which can make the recovered water unsuitable for its purpose. Because these water quality changes can be relevant for the final RE, a further analysis of the water quality development by aquifer interactions is presented in Chapter 4.

3.6.3.3 Comparison with other techniques to improve RE

Other ways to improve RE have been proposed and can be compared to this new MPPW set-up (e.g., Maliva et al., 2006; Maliva and Missimer, 2010). The results hint that a theoretical RE increase may also be realized by the use of a one-way (flapper) valve or inflatable packer installed halfway an FPW, as proposed by Maliva et al. (2006). However, short-circuiting of deeper brackish groundwater via the gravel pack of the ASR well may then still cause early salinization, unless a packer is applied in an open hole. Using the MPPW, no signs of short-circuiting were found. It is presumed that the >0.4 m thick bentonite clay plugs installed are sufficient to prevent this unfavorable process. It is therefore recommended to combine the use of a one-way valve or a packer with the installation of a clay plug during installation of the ASR well just below the targeted depth of the valve/packer, unless the ASR well is realized with an open hole.

Finally, the target aquifer in the current study was relatively isotropic and homogeneous, which may be a prerequisite for all techniques to improve RE. Only then, water injected at the base of the aquifer can be recovered by shallower wells, unhampered by intervening clay layers. If a resistant unit is present, use of the current MPPW set-up (more flexible by the use of four partially penetrating wells) might still enable sufficient recovery, albeit deeper in the aquifer.

3.7 Conclusions

A well-monitored, small-scale ASR system in a brackish aquifer was equipped with multiple partially penetrating wells (MPPW). In the first cycle, at least 40.2% of the injected water was recovered practically unmixed as a result of enhanced injection at the aquifer's base and recovery at the top. A SEAWAT model was set up for the ASR system and calibrated with the monitoring data. The SEAWAT model calculated a recovery efficiency (RE) of only 14.7% when the MPPW was replaced with a conventional fully penetrating well (FPW). Replacement with a single partially penetrating well (SPPW) in the upper half of the aquifer gave an RE of 30.2%. The ASR scheme applied with the MPPW is thus able to recover significantly more freshwater than a conventional and a single partially penetrating ASR well. Modelling showed that in subsequent cycles no more than 60% of the yearly injected water could be recovered by the MPPW (<35% for the SPPW and <20% for the FPW). This is caused by mixing with ambient brackish groundwater in the lower half of the aquifer, where buoyancy effects and seepage prevent the formation of a stable mixing zone. Nevertheless,

a more than three times higher RE is maintained with respect to an FPW. Therefore, (small-scale) ASR becomes a viable freshwater management technique in many brackish coastal aquifers, where it would be ineffective with conventional ASR wells. Further optimization of injection and recovery rates and/or the use of the deeper wells of the MPPW as scavenger wells to further improve the freshwater recovery need further study.

3.8 Acknowledgements

This research is funded by the Knowledge for Climate research program as part of its theme 'Climate Proof Freshwater Supply'. Frans Backer, Michel Groen, John Visser, Martine Hagen, and Guido Beenakker are thanked for their contribution during field and laboratory work. Three anonymous reviewers are acknowledged for their comments on the earlier version of this chapter.

Chapter **4**

Reactive transport impacts on recovered freshwater quality for a field multiple partially penetrating well (MPPW-)ASR system in a brackish heterogeneous aquifer

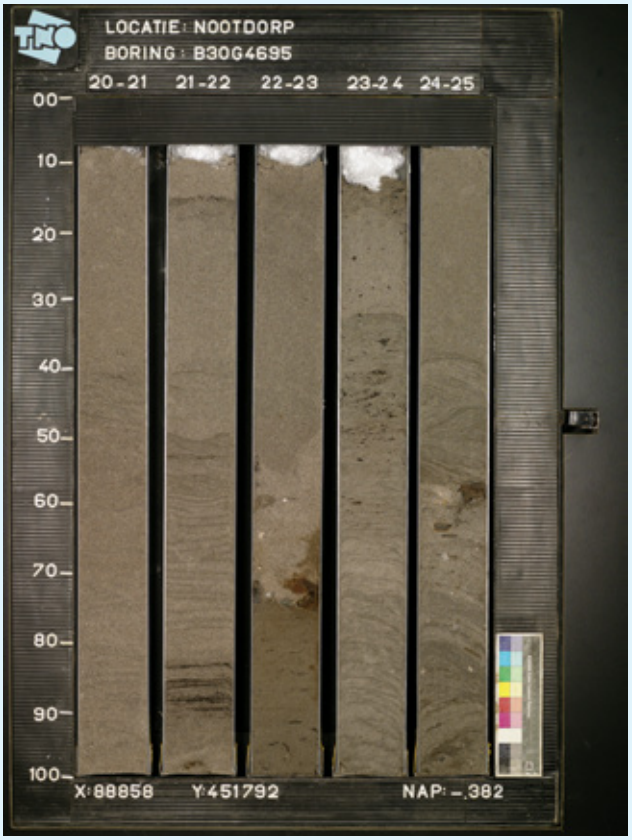

This chapter is based on:

Zuurbier, K.G., Hartog, N., Stuyfzand, P.J., under review. Reactive transport impacts on recovered freshwater quality for a field MPPW-ASR system in a brackish and geochemically heterogeneous coastal aquifer. In revision for Applied Geochemistry.

4.1 Abstract

The use of multiple partially penetrating wells (MPPW) during aquifer storage and recovery (ASR) in brackish aquifers can significantly improve the recovery efficiency (RE) of unmixed injected water (Chapter 3). The water quality changes by reactive transport processes in a field MPPW-ASR system and their impact on RE were analyzed. The oxic freshwater injected in the deepest of four wells was continuously enriched with sodium (Na^+) and other dominant cations from the brackish groundwater due to cation exchange by repeating cycles of 'freshening'. During recovery periods, the breakthrough of Na^+ was retarded in the deeper and central parts of the aquifer by 'salinization'. Cation exchange can therefore either increase or decrease the RE of MPPW-ASR compared to the RE based on conservative Cl^-, depending on the maximum limits set for Na^+, the aquifer's cation exchange capacity, and the native groundwater and injected water composition. Dissolution of Fe and Mn-containing carbonates was stimulated by acidifying oxidation reactions, involving adsorbed Fe^{2+} and Mn^{2+} and pyrite in the pyrite-rich deeper aquifer sections. Fe^{2+} and Mn^{2+} remained mobile in anoxic water upon approaching the recovery proximal zone, where Fe^{2+} precipitated via MnO_2 reduction, resulting in a dominating Mn^{2+} contamination. Recovery of Mn^{2+} and Fe^{2+} was counteracted by frequent injections of oxygen-rich water via the recovering well to form Fe and Mn-precipitates and increase sorption. The MPPW-ASR strategy exposes a much larger part of the injected water to the deeper geochemical units first, which may therefore control the mobilization of undesired elements during MPPW-ASR, rather than the average geochemical composition of the target aquifer.

4.2 Introduction

Aquifer storage and recovery (ASR) using wells can be a successful freshwater management tool in coastal areas worldwide by keeping temporary freshwater surpluses available for periods of shortage (Pyne, 2005). Freshwater surpluses are stored this way for later use in times of demand, creating a self-sufficient freshwater supply which makes external freshwater supply (including infrastructure) and/or costly desalination superfluous. However, application of small-scale ASR systems in aquifers with brackish or saline groundwater often results in a low recovery efficiency (RE: part of the injected water that can be recovered with a satisfying quality) due to buoyancy effects (Ward et al., 2009, Chapter 2). Also, the buoyancy effects may preclude a pro-

gressively improving water quality with subsequent cycles as observed at conventional ASR systems (Ward et al., 2009). Recently, the use of multiple partially penetrating wells (MPPW) installed in a single borehole in a brackish aquifer allowed significantly higher recovery efficiencies by deep injection and shallow recovery, as demonstrated for relatively unmixed rainwater containing <0.5 mmol/l Na^+ (Chapter 3). While that study focused on the buoyancy and mixing effects on the conservative transport of chloride (Cl^-), other water quality parameters may determine the final success of ASR, depending on the intended use. Sodium (Na^+), for example, may threaten the water quality for irrigation since it is toxic in low concentrations for various plants or crops (Kronzucker and Britto, 2011), but also for drinking and industrial purposes. Also, arsenic is known to be toxic for both humans and plants (National Research Council, 1977). Besides toxic effects, operational aspects, such as the clogging of pumps, pipelines, and sprinklers by the precipitation of manganese or iron oxides, may determine the suitability of the recovered water for direct use (Pyne, 2005). Especially for agricultural end users, recovered water upon aquifer storage ought to be directly usable to limit the water costs. Although the elements of concern are typically low in ASR 'injection water' (i.e. the water that is to be injected, after which it becomes 'injected water'), enrichment may occur by freshening and salinization (e.g., Appelo, 1994a; Appelo, 1994b; Stuyfzand, 1993; Valocchi et al., 1981) and dissolution of carbonates (Antoniou et al. 2012, Stuyfzand 1998). Additionally, the injection of oxygen and/or nitrate-containing water in a deeply anoxic target aquifer may induce mobilization of SO_4, Fe, Mn, and As, which has been reported in ASR studies worldwide (e.g., Antoniou et al., 2012; Jones and Pichler, 2007; Neil et al., 2014; Price and Pichler, 2006; Stuyfzand, 1998; Vanderzalm et al., 2011; Wallis et al., 2011; Wallis et al., 2010).

The operation of an MPPW-ASR system does not comply with the more traditional ASR-theories for bi-directional horizontal flow directions during injection and recovery via fully penetrating well screens in aquifers without significant buoyancy effects. During MPPW-ASR, instead, (oxygen-rich) freshwater is predominantly injected in brackish aquifers via the deeper wells while extraction occurs at shallower wells. Consequently, vertical transport exposes the injected water to a vertical range of geochemical heterogeneities in the aquifer and the associated potential sources of water quality deterioration. Additionally, hydrochemical conditions at the deeper wells are highly dynamic, with frequent alternations of freshening (during injection) and salinization (during storage/recovery). In this study, therefore, we analyzed the observed water quality changes by reactive transport processes in a field MPPW-ASR system with a focus on cation-exchange and redox-reactions and their impact on the RE. Hydrochemical data were collected during the field MPPW-ASR pilot in the brackish

aquifer for which described the hydrological aspects and freshwater recoverability based on conservative transport (chloride). The aim of this study was to assess for the same MPPW-ASR system how reactive transport processes affected the concentrations of Na^{+}, Fe^{2+}, Mn^{2+}, and As in the recovered water over time. This provides a more complete analysis of the application and operational optimization of MPPW-ASR systems.

4.3 Materials and methods

The application of an MPPW-ASR system in a brackish aquifer was well-monitored in a field pilot in 2012 and 2013 allowing to closely analyze the water quality development in the aquifer until recovery. This field pilot was preceded by a detailed physical and geochemical characterization of the aquifer to understand the flow patterns and water quality changes.

4.3.1 ASR field site

The Nootdorp MPPW-ASR system was built in 2011 with the aim to store rainwater collected by the roof of a 20,000 m^2 greenhouse, and to recover this water for irrigation purposes in the same greenhouse (more details in Chapter 3). The MPPW, with four independently operated well screens at distinct aquifer intervals installed in a single borehole, were used to maximize the freshwater recovery (Figure 4-1). The ASR system was extensively monitored for this study from January 2012 until September 2013.

The unconsolidated target aquifer is confined by unconsolidated clay and peat. Geological characterization indicated that the target aquifer consists of middle-coarse to very coarse fluvial sands from the Rhine River (Chapter 3). The lower part (HU-f-l, Chapter 3 and Figure 4-4) is a little coarser than the upper part (HU-a-c). A fine sand layer (HU-d) and a sand layer containing reworked clay and peat deposits in a coarse sand matrix (HU-e) are present in the middle of the target aquifer. This HU-e unit is dis-continuous and found only locally in the pilot area. Besides local separation into two compartments by the clayey interval of this HU-e unit, the aquifer is relatively homogeneous, as underlined by geophysical and hydrochemical analysis during the first ASR cycle (Chapter 3).

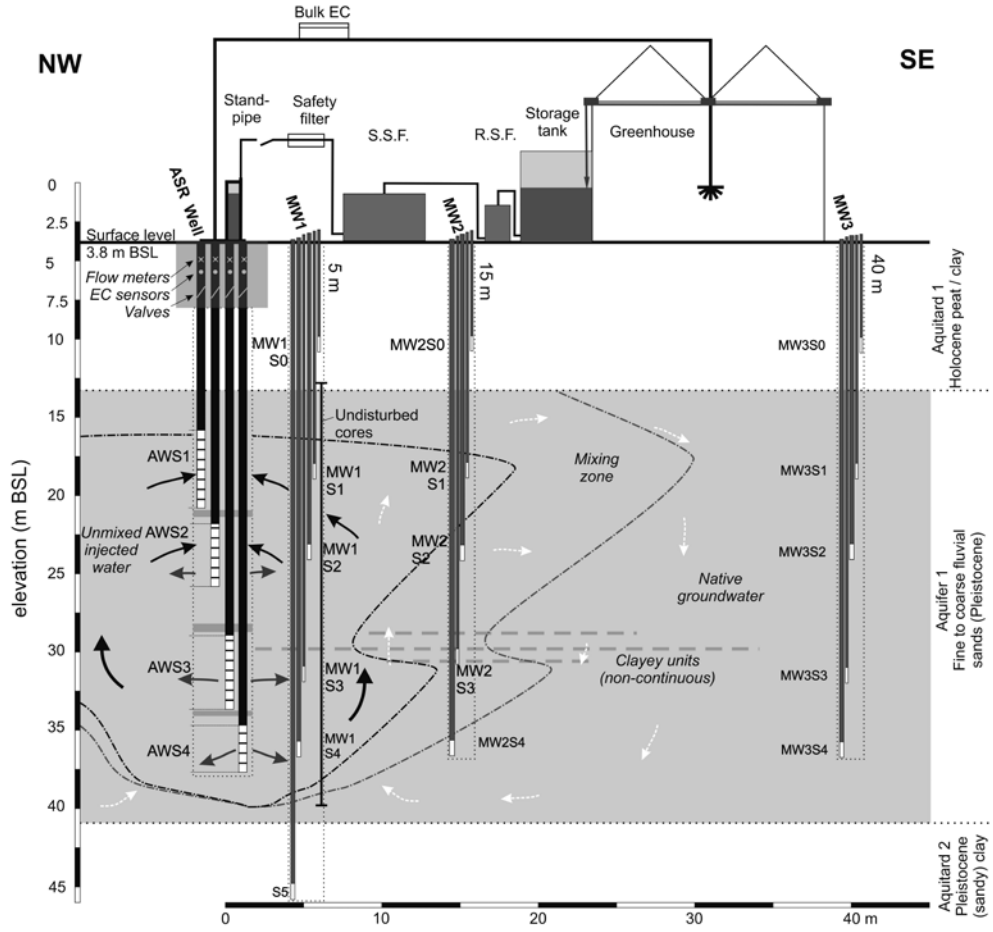

Figure 4-1: Cross-section of the Nootdorp ASR system as presented in Chapter 3. Water from the greenhouse is first pre-treated by rapid sand filtration (*R.S.F.*) and slow sand filtration (*S.S.F.*) and then injected mainly with the deeper wells (AWS3 and AWS4), whereas most recovery occurred with the shallower wells (AWS1 and AWS2). '*MW*'=monitoring well. '*Bulk EC*'= EC of the mixed water from all recovering wells. Indicated distribution of the injected water and the flow paths are based on the findings presented in Chapter 3.

4.3.2 Operation of the MPPW during the Nootdorp ASR pilot

The injection rate was equally distributed over all MPPW screens in the first 3 months (Figure 4-2). From April 2012 until May 2013 only the lower three well screens (AWS2-4) were used for injection, while mainly the shallow AWS1 and AWS2 were used for recovery, accompanied by a low-rate recovery at AWS3 in Cycle 2. The fresh-water surpluses in the last phase (Summer 2013) were injected at AWS1-4 from May 2013 until August and at AWS1-S3 during the last month of the pilot. During the pilot phase, 39.9% (11,591 m^3) of the injected water (29,047 m^3) was abstracted.

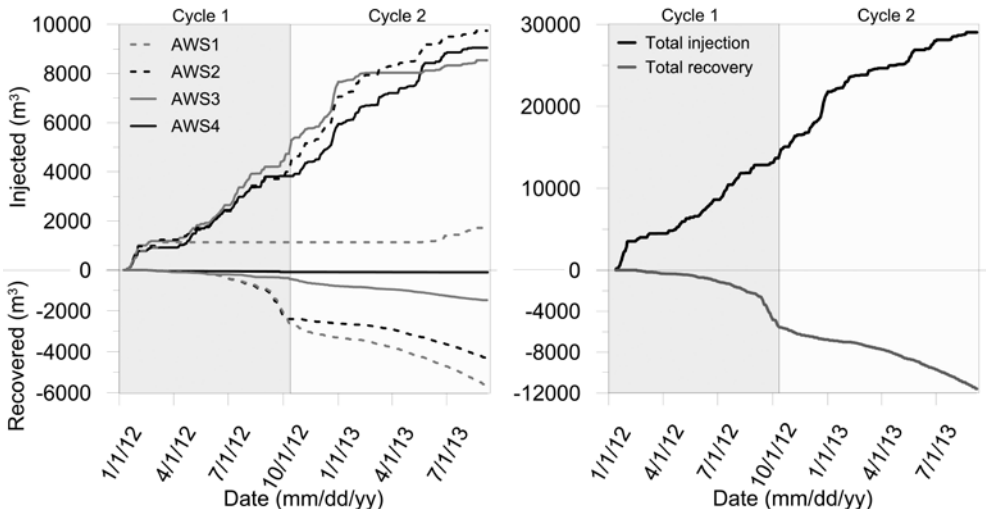

Figure 4-2: Operation of the ASR system during the 611 d pilot. Most of the water was injected at AWS2-4, whereas the bulk of the water was recovered by AWS1-2.

4.3.3 Site characterization and hydrochemical monitoring

4.3.3.1 Physical and geochemical sediment analyses

To characterize the target aquifer and identify potentially reactive intervals 114 samples were taken from thin-wall tubes at intervals of 0.2 m or smaller whenever lithological variations appeared (Chapter 3), or from the bailer at the other intervals of MW1 (every meter, n= 14). Grain size distribution of each sample was determined using a laser particle sizer (Chapter 3). Hydrogeological units (HU-a to HU-h) and their hydraulic properties were derived using the grain size distributions, head responses at MW1 upon pumping, and the breakthrough curves of Cl^- at MW1 (Chapter 3). Sedimentary organic matter (SOM) and total carbonates were deduced from thermo-gravimetry (TGA at 330, 550, 1000 ^oC).

An XRF-core scan (Avaatech, The Netherlands) was executed on the cut cores for a semi-quantitative analysis of Al, S, Ca, Mn, and Fe on a split-core-surface area of 1 cm^2 over a time interval of 10 s using a generator setting of 10 kV. This way, reliable log-ratios of Fe/S, Fe/Ca, Mn/Ca, and S/Ca were obtained, which are linearly related to the log-ratios of quantitative element concentrations (Weltje and Tjallingii, 2008). Sediments samples were taken at 6 distinct depth intervals and sent for laboratory XRF to correct the log-ratios obtained by the high-resolution core-scan. True elemental ratios were subsequently attained via these log-ratios and corrected for molal masses (Figure 4-3). S/Ca was used to derive the part of Fe/Ca that is related to pyrite, assuming Fe=0.5*S. This way the potential relative presence of Ca, Fe, and Mn in the carbonates could be derived. In this approach the presence of these elements in silicates is neglected. Also the contribution of Mg to the carbonates is not considered, since this element is not measured by the XRF core-scan. For Fe/Al, an overestimation and a poor correlation was found with the laboratory analyses due to the relatively short measurement time of the core scan, insufficient to measure all Al present; it was therefore only used as a qualitative indication for the presence of reactive Fe (not bound to silicate minerals).

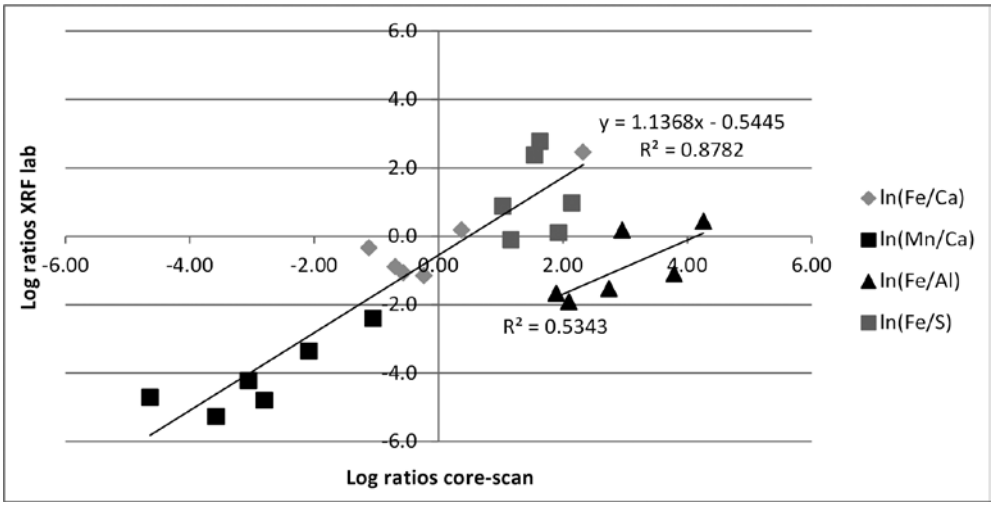

Figure 4-3: Log-ratios derived from XRF analyses on homogenized samples from 1 specific depth interval versus the log-ratios from the XRF core-scan. The recorded log-ratios of Fe/Ca, Mn/Ca, and Fe/S by the XRF core scan were linearly related and could therefore be used to derive true ratios. Due to the short measurement time of the XRF core-scanner, Al was underestimated.

Geochemically similar units (GU-I to GU-V) were defined based on the high-resolution core-scan data. Per GU, 5 (GU-II, IV) or 10 (GU-I, II, V) equally distributed subsamples of approximately 30 g were taken from the core. Sampling depths were slightly adjusted only when equidistant sampling forced sampling of 'unreliable intervals', for instance by slumped sediment at the top 10 cm of each 1 m core. Each subsample was oven-dried and homogenized and then equally contributed (5 g or 10 g) to one mixed sample per GU (50 mg). These mixed samples were analyzed on grain size distribution and SOM and total carbonates using thermogravimetric analysis (TGA). Elemental composition was derived using X-ray fluorescence (XRF), total C and S using LECO Induction Furnace Instruments, and trace elements using ICP-MS following aqua regia digestion.

4.3.3.2 (Ground)water sampling

All monitoring screens were sampled prior to ASR operation (December 19, 2011). MW1 and MW2 were sampled monthly from January 2012 until September 2013 and a higher frequency was maintained during the first breakthrough of the injected water at MW1 (January/February 2012). Three times the volume of the well riser plus well screen was purged from the wells prior to sampling. The pre-treated ASR injection water was sampled 19 times during the pilot runtime. All samples were analyzed in the field in a flow-through cell for EC, pH, temperature, and dissolved oxygen. Samples for lab analysis were passed over a 0.45 µm cellulose acetate membrane in the field. The reader is referred to Chapter 3 for more information on the handling and analysis of the water samples during the Nootdorp ASR pilot.

4.3.4 Geochemical and hydrochemical data analysis

4.3.4.4 Geochemical data analysis

Pyrite content (FeS_2), reactive iron in pyrite (Fe_{py}), total reactive iron (Fe_{TR}), and reactive iron (non-pyrite: Fe_{reac}) were calculated using (4.1):

$$
\begin{aligned}
FeS_2 &= 0.5 \; M_{FeS_2} / M_S \; S \\
Fe_{py} &= 0.5 \; M_{Fe} / M_S \; S \\
Fe_{TR} &= 2 \; M_{Fe} / M_{Fe_2O_3} \; [Fe_2O_3 - 0.1 \; Al_2O_3] \\
Fe_{reac} &= Fe_{TR} - Fe_{py}
\end{aligned}
\qquad (4.1.1\text{-}4.1.4)
$$

Where M_{FeS2}, M_s, and M_{Fe2O3} are the molar masses of FeS_2, S, and Fe_2O_3, respectively. *S* is the total S content by weight as measured by the CS elemental analyzer, and

Fe_2O_3 and Al_2O_3 are contents by weight, as determined by XRF. The correction of Fe_2O_3 for silicate-bounded Fe to determine Fe_{TR} was based on the lowest Fe_2O_3/Al_2O_3 ratio found in the XRF lab analyses. The lowest ratio was found in a single sample at 16.62 m-BSL; this depth corresponds with a zone of relatively low Fe/Al ratios according to the XRF core-scan. Based on the these measurements, Fe_2O_3 amounts to about 10% of the Al_2O_3, which is less than the 22.5% found for these formations by Griffioen et al. (2012).

The cation exchange capacity (CEC) of each GU was calculated using (Appelo and Postma, 2005):

$$CEC(meq/kg) = 7\ (\%clay) + 35\ (\%C) \tag{4.2}$$

Where %clay is the clay fraction (<2 µm) derived from the grain size analyses and (%C) is the fraction of organic carbon, which is derived from TGA (assuming %C = %LOI550/2). Total C from the CS analyses was selected only when %C from TGA exceeded the total C from the CS analyzer.

4.3.4.2 Hydrochemical processes and data analysis

Total dissolved solids (TDS) was calculated based on concentrations measurements to correct for density differences in the groundwater flow model (Chapter 3). The Base Exchange Index (BEX; Stuyfzand, 1993, 2008) was calculated to identify freshening and salinization.

The potentially relevant hydrochemical reactions are shown in Table 1. Since NO_3^- concentrations in rainwater are low, DO is considered the most relevant oxidant in the injection water. Some processes (cation exchange, nitrification, oxidation of adsorbed Fe and Mn) are mainly relevant in the mixing zone and during freshening, but rarely during later injection, while others (pyrite and SOM oxidation, carbonate dissolution) are relatively persistent, or relevant during recovery (MnO_2 and $Fe(OH)_3$ reduction, cation exchange).

The amount of pyrite oxidation was calculated using the maximum SO_4-production observed at the different ASR well screens and was based on the difference between SO_4^{2-} concentration in the injected and recovered water. The amount of oxygen consumption by pyrite was calculated as:

$$\Delta C(O_{2(pyrite)}) = \frac{3.75}{2} \cdot \left[C(SO_4) - C(SO_{4(injected)}) - C(SO_{4(NO_3)}) \right] \tag{4.3}$$

Where $\Delta C(O_{2(pyrite)})$ is the oxygen consumption by pyrite, $C(SO_4)$ is the molal concentration SO_4^{2-} observed in the aquifer upon injection, $C(SO_{4(injection)})$ is the molal SO_4^{2-} concentration in the injection water, and $C(SO_{4(NO3)})$ is the molal SO_4-production from NO_3^- (assuming all NO_3^- is consumed by oxidation of pyrite). The latter was calculated using:

$$C(SO_{4(NO_3)}) = \frac{10}{14}\left[C(NO_{3(injected)}) - C(NO_3)\right] \quad (4.4)$$

Where $C(NO_{3(injected)})$ is the molal concentration of NO_3^- in the injection water (0.05 mmol/L in the collected rainwater) and $C(NO_3)$ is the molal concentration of NO_3^- observed in the aquifer during storage.

4.3.5 Modelling codes and set-up

A reactive transport model was built to verify if alternating freshening and salinization could indeed affect the recovered water quality. This way, also the long-term effects and the effect of injection water modification could be explored.

4.3.5.1 Input flow model

SEAWAT (Langevin et al., 2007) was used to calculate the flow field in an axi-symmetrical model during the two field trial cycles (611 days, January 2012 – September 2013). Three subsequent fictitious cycles were added in a simplified way after Cycle 2. TDS was used to calculate the density in each cell, as described in Chapter 3. The modelled pumping scheme is described in Table 4-2. The three additional cycles contained relatively long periods without injection, resulting in more salinization at the end of each cycle than in Cycle 1 and 2. The results of the SEAWAT flow model were stored in a .FLO file for later use in PHT3D. Pre- and post-processing was performed using PMWIN8.06 (Simcore Software, 2010).

Table 4-1: Potentially relevant hydrochemical reactions involved with the injection of oxic rain-water in the deeply anoxic, brackish target aquifer.

Process	Reaction equation
Pyrite oxidation	
Pyrite-oxidation by O_2	$3.75O_2 + FeS_2 + 3.5H_2O \rightarrow Fe(OH)_3 + 2SO_4^{2-} + 4H^+$
Pyrite-oxidation by NO_3	$14NO_3^- + 5FeS_2 + 4H^+ \rightarrow 5Fe^{2+} + 10SO_4^{2-} + 7N_2 + 2H_2O$
Other redox	
Oxidation of organic matter by O_2	$O_2 + CH_2O \rightarrow CO_2 + H_2O$
Oxidation of organic matter by NO_3	$NO_3^- + 1.25CH_2O \rightarrow 0.5N_2 + HCO_3^- + 0.75H_2O + 0.25CO_2$
Fe-carbonate oxidation	$0.25O_2 + FeCO_3 + 1.5H_2O \rightarrow Fe(OH)_3 + CO_2$
Mn-carbonate oxidation	$0.5O_2 + MnCO_3 \rightarrow MnO_2 + CO_2$
Oxidation of Fe^{2+}	$Fe^{2+} + 0.25O_2 + 2.5H_2O \rightarrow Fe(OH)_3 + 2H^+$ (dissolved Fe^{2+})
	$Fe-X_2 + 0.25O_2 + CaCO_3 + 1.5H_2O \rightarrow Ca-X_2 + Fe(OH)_3 + CO_2$ (adsorbed Fe^{2+})
Mn- oxidation	$Mn^{2+} + 0.5O_2 + H_2O \rightarrow MnO_2 + 2H^+$ (dissolved Mn^{2+})
	$Mn-X_2 + 0.5O_2 + CaCO_3 \rightarrow Ca-X_2 + MnO_2 + CO_2$ (adsorbed Mn^{2+})
$Fe(OH)_3$ reduction by DOC	$Fe(OH)_3 + 0.25CH_2O + 1.75CO_2 \rightarrow Fe^{2+} + 2HCO_3^- + 0.75H_2O$
MnO_2 reduction by Fe^{2+}	$2Fe^{2+} + MnO_2 + 4H_2O \rightarrow 2Fe(OH)_3 + Mn^{2+} + 2H^+$
MnO_2 reduction by DOC	$MnO_2 + 0.5CH_2O + 1.5CO_2 + 0.5H_2O \rightarrow Mn^{2+} + 2HCO_3^-$
Nitrification	$4O_2 + 2NH_4^+ \rightarrow 2NO_3^- + 2H_2O + 4H^+$
Dissolution	
Carbonate dissolution	$2H^+ + (Ca,Fe,Mn)CO_3 \rightarrow (Ca,Fe,Mn)^{2+} + CO_2 + H_2O$ (proton-buffering)
	$CO_2 + (Ca,Fe,Mn)CO_3 + H_2O \rightarrow (Ca,Fe,Mn)^{2+} + 2HCO_3^-$ (following CO_2-production)
Cation exchange	
Freshening	$aCa^{2+} + [bNa,cMg,dK,eNH_4,fFe,gMn]-X \rightarrow$ $bNa^+ + cMg^{2+} + dK^+ + eNH_4^+ + fFe^{2+} + gMn^{2+} + [aCa]-X$
Salinization	$bNa^+ + cMg^{2+} + dK^+ + eNH_4^+ + fFe^{2+} + gMn^{2+} + [aCa]-X \rightarrow$ $aCa^{2+} + [bNa,cMg,dK,eNH_4,fFe,gMn]-X$

Table 4-2: Modeled ASR cycles in this study. Distribution of pumping rates (Q_{tot}) over the MPPW screens (S1 / S2 / S3 / S4) in the added cycles is given in percentages between brackets.

ASR phase	Stress periods	Pumping	Duration (d)
Cycle 1	1-37	As recorded by flowmeters (Figure 4-2)	273
Cycle 2	38-83	As recorded by flowmeters (Figure 4-2)	338
Idle Cycle 2	84	Idle	30
Injection Cycle 3-5	85, 89, 93	Q_{tot} =133.3 m^3/d (0% / 10% / 40% / 50%)	150
Storage Cycle 3-5	86, 90, 94	Idle	30
Recovery Cycle 3-5	87, 91, 95	Q_{tot} = -53.3 m^3/d (60% / 40% / 0% / 0%)	150
Idle Cycle 3-4	88, 92	Idle	35

4.3.5.2 PHT3D model input for reactive transport (cation exchange)

Initial concentrations of Na^+, Cl^-, Ca^{2+}, Mg^{2+}, K^+, NH_4^+, HCO_3^-, and the pH were derived from chemical analyses on samples taken at MW1 prior to ASR operation. The exchanger compositions (Na-X, Ca-X, Mg-X, K-X, NH_4-X) were first calculated by PHREEQC (Parkhurst and Appelo, 1999) batch calculations using the standard PHREEQC database and the initial concentration and CEC at the levels of the MW1 well screens . The conversion of CEC-values to meq/l for PHREEQC was performed assuming a grain density of 2650 kg/m^3 and the porosity of the target aquifer (0.25-0.35) derived from the breakthrough of Cl^- (Chapter 3). A porosity of 0.4 was assumed to calculate the CEC for the confining clay units. The approach discarded some of the geochemical variation found centrally in the target aquifer where MWs were absent (the locally clayey intervals: GU-II and GU-III). The exchanger composition and the calcite content (derived from TGA and assuming all carbonates to be present as calcite) of each cell (converted to attain moles per liter of bulk aquifer volume) were corrected for the axi-symmetry of the model (Wallis et al., 2013). The standard PHREEQC database was used by PHT3D. Equilibrium conditions were assumed for calcite, redox process were not included. This provided an efficient and robust model that included the simulation of freshening and salinization effects in addition to the effects of densi-

ty-driven flow on water quality development in the target aquifer.

To evaluate the influence of the CEC, injection water composition, and flow patterns on water quality development regarding Na^+, four additional scenarios were run:

1. scenario in which GU-III was introduced as a continuous horizontal layer with its potentially high CEC, which was based on geochemical analyses at MW1 (Table 4-3).
2. scenario with three times higher CECs for each hydrogeological unit (which was still within a realistic range according to Breeuwsma et al. (1986)) in the whole target aquifer to assess the sensitivity to CEC;
3. scenario with addition of 5 mmol/l gypsum ($CaSO_4$) to the injection water to test the accelerated release of Na^+ from the exchanger during freshening;
4. scenario in which a fully penetrating well is used, but buoyancy and seepage are neglected. This way, the results of the MPPW can be compared with a conventional, bi-directional ASR system. The CEC was again raised by a factor 3 to emphasize the effect of cation exchange.

4.4 Results

4.4.1 Target aquifer properties

4.4.1.1 Geochemical characterization

The extensive geochemical analyses produced a solid understanding of the aquifers geochemical properties. The following reactive phases were identified (Figure 4-4, Table 4-3):

- *Carbonates* are present mainly in the upper GU's (I-III; ~5% weight) and less in the deeper GU-IV and V (<1% weight). The XRF core-scan results indicated however that the carbonates in the deeper units are potentially enriched with Fe (up to 50%) and Mn (up to 20%), while Ca is the dominant cation in the carbonates in GU-I-III (generally >85%), indicating a relatively pure calcite composition;

- *Pyrite* is relatively low at the shallow GU-I and II and high in the central (GU-III and IV: 0.90 to 1.05% weight) and deeper intervals (GU-IV: 0.28% weight);

- *Sedimentary organic matter (SOM)* is present throughout the target aquifer,

although its content is lowest in GU-IV and V (0.22-0.27% weight) and highest in GU-III (1.02% weight);

- The derived CECs (Table 4-3) are relatively low and in line with CECs observed for this fluvial sediment type (Van Helvoort, 2003).

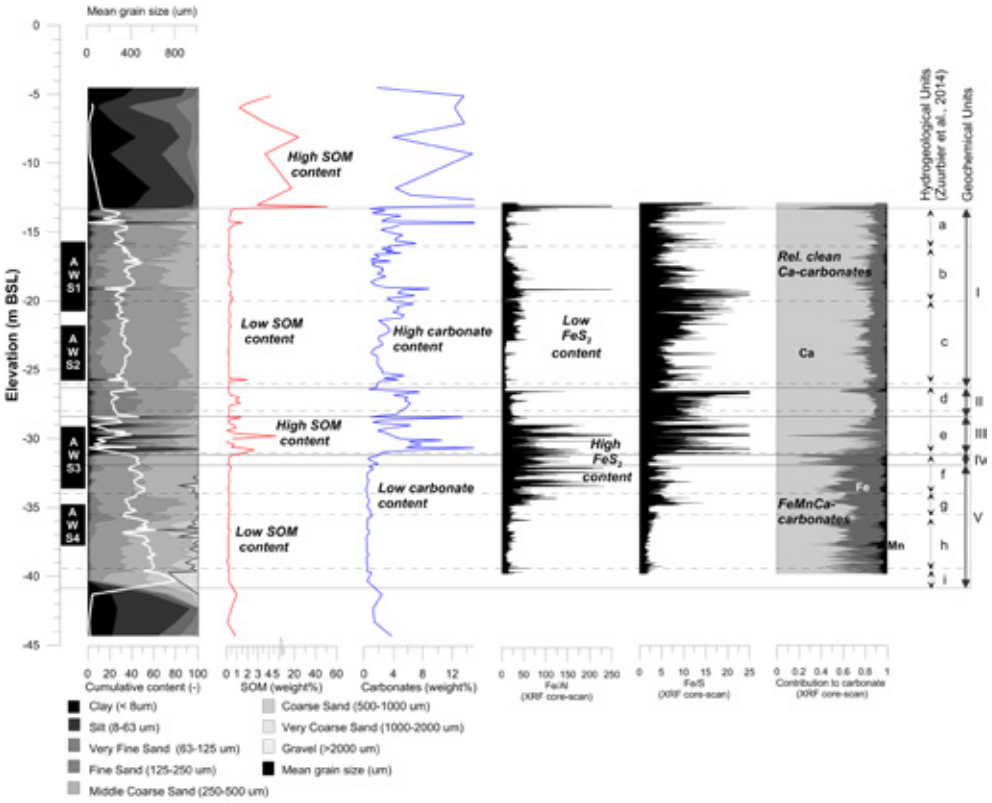

Figure 4-4: High-resolution data from physical and chemical sediment analyses and the XRF core-scan at MW1. Fe/Al and Fe/S were derived from the XRF core-scan and indicator for Fe_{TR} (high Fe/Al) and the presence of Fe_{reac} (high Fe/S). Contribution of Ca, Fe, and Mn to the carbonates was based on the XRF core-scan, neglecting silicate-bound elements and the potential presence of Mg (not measured) in the carbonates.

Table 4-3: Geochemical properties of the target aquifer for the five geochemical units (GU-I-V)

Parameter	Unit	GU-I	GU-II	GU-III	GU-IV	GU-V
Depth	**m BSL**	**13.16-26.57**	**26.57-28.42**	**28.42-31.12**	**31.12-31.82**	**31.82-41.32**
Clay fraction (<2 um)	% d.w.	0.69	0.77	4.75	0.66	0.51
Gravel fraction (>2 mm)	% d.w.	0.00	0.00	0.00	0.00	4.15
SOM	% d.w.	0.41	0.51	1.02	0.27	0.22
Carbonates	% d.w.	4.38	5.32	4.90	0.82	0.44
Total C	% d.w.	0.56	0.69	1.25	0.07	0.07
CEC-calculated	meq/kg	12.0	14.3	51.1	7.1	6.0
Pyrite	% d.w.	0.06	0.09	1.05	0.90	0.28
Fe(total) 0.55 0.71 1.72 0.86 0.40	% d.w.	0.55	0.71	1.75	0.86	0.40
Fe(pyrite)	% d.w.	0.03	0.04	0.49	0.42	0.13
Fe (TR)	% d.w.	0.13	0.28	0.91	0.47	0.15
Fe(react, non-pyrite)	% d.w.	0.10	0.24	0.42	0.05	0.02
MnO	% d.w.	0.1	0.2	0.3	0.1	<0.1
As	ppm	2.2	2.3	14.2	6.1	4

4.4.1.2 Native groundwater and injection water quality.

The native groundwater is marked by a clear salinity stratification (Table 4-4), with relatively freshwater at the aquifer's top (Cl^- = 3.2 mmol/l) and brackish water at the base (Cl^- at least 27.6 mmol/l). A positive BEX index and a positive Na:Cl ratio (up to >2 at the aquifer's top) indicate relatively recent freshening of the aquifer. Deeply anoxic conditions in the native groundwater are reflected by the absence of DO, NO_3^-, and SO_4^{2-} (Table 44), as well as by the high CH_4–concentrations reported for this aquifer (Fortuin and Willemsen, 2005; Stuyfzand, 1994).

The injection water on the other hand was oxic, and had low concentrations of

NO_3^- and SO_4^{2-}. Low concentrations of Ca^{2+} and HCO_3^- resulted from dissolution of calcite in the slow sand filter (Table 4-4). The salinity of the injection water was controlled by wind direction and speed during rainfall close to the coastline (Stuyfzand, 1993). It exceeded 0.25 mmol/l when precipitation coincided with strong western winds (mainly in Autumn, Winter). Since rainwater from Spring and Summer was the first water to be recovered in times of high demands, the average salinity of the unmixed recovered water was lower than in the average injection water. The assimilable organic carbon (AOC, 10 µg/l)) and total suspended solids concentrations (TSS, <1 mg/l) were low, indicating a low risk of well clogging (Russel, 2013), which was confirmed by a constant specific capacity during 20 months of operation.

Table 4-4: Groundwater quality observed in the Nootdorp target aquifer, average quality of the injected and recovered water, and most relevant water quality limits.

Parameter	Unit	Ambient groundwater MW1				Injection AW	Average recovery AW	Quality limits
		S1	S2	S3	S4			
Nr. of samples:	**n**	**1**	**1**	**1**	**1**	**19**	**99**	
EC-20	uS/cm	1448	2177	3159	4062	72	151	250[N], 2500[D]
Temp	°C	10.6	10.5	10.3	10.5	10.4	14.1	
pH	(-)	6.9	7.0	7.0	7.0	7.5	7.9	
DO	mmol/l	0.00	0.00	0.00	0.00	0.32*	0.04	
Na^+	mmol/l	6.6	12.0	19.7	25.8	0.13	0.14	0.5[N], 8.7[D]
K^+	mmol/l	0.3	0.4	0.6	0.9	0.01	0.02	
Ca^{2+}	mmol/l	4.0	4.5	5.4	7.0	0.23**	0.71	
Mg^{2+}	mmol/l	0.8	1.3	2.0	2.8	0.02	0.05	
Fe^{2+}	umol/l	469	335	245	258	0.2	0.41	3.6[N,D]
Mn^{2+}	umol/l	19	19	22	30	0.1	1.95	0.9[N,D]
NH_4^+	mmol/l	1.2	1.6	1.2	1.0	0.0	0.05	0.03[D]
SiO2	mmol/l	0.8	0.8	0.7	0.7	0.0	0.06	
Cl^-	mmol/l	3.2	10.0	21.3	27.6	0.13	0.11	7.1[D]
SO_4^{2-}	mmol/l	0.0	0.0	0.0	0.0	0.03	0.12	2.6[D]
TIC	mmol/l	14	17	21	21	0.56	1.32	
NO_3^-	mmol/l	0.0	0.0	0.0	0.0	0.05	0.02	
PO_4-t	mmol/l	0.06	0.06	0.06	0.05	0.00	0.00	
As-t	umol/l	0.02	0.02	0.00	0.00	0.00	0.05	0.13
DOC	mmol/l	0.4	0.9	1.0	0.5	0.1	-	
BEX	(-)	5.0	4.2	1.5	2.8	0.0	0.13	
SI (calcite)	(-)	0.3	0. 5	0.6	0.6	-2.2	-0.99	
SI (siderite)	(-)	1.9	1.9	1.8	1.8	-2.7	-1.98	

[N] Specific water quality limits horticulture at the Nootdorp ASR site

[D] Drinking water limits (EU drinking water directive 98/83/EG 1998)

* DO range observed: 0.21 – 0.41 mmol/l

**Ca range observed: 0.08-0.47 mmol/l

4.4.2 The behaviour of Na^+ during MPPW-ASR

4.4.2.1 Observed trends in Na^+ concentrations

The effects of the MPPW-ASR on recovered Na^+ concentrations are first explored. While the transport of Cl^- was conservative (Chapter 3), observations at 5 m from the ASR well (MW1; see Figure 4-5) showed that the injected water was enriched with Na^+ and other cations from the ambient groundwater during freshening (injection phases). At the recovery wells (AWS1, AWS2), an earlier arrival of Na^+ at significantly higher concentrations compared to Cl^- was observed during the final recovery phases of Cycle 1 (Figure 4-6). The water was found unsuitable for irrigation $^+$ (Na^+>0.5 mmol/l) before Cl^- concentrations exceeded 0.5 mmol/l. The Na-increase could not be explained by the only limited mixing with ambient water. In Cycle 2, Na^+ concentrations in unmixed recovered water were constantly higher than Cl^- concentrations at AWS1, while they were equal at AWS2, and actually lower during salinization at AWS3 (Figure 4-6). In Figure 4-7, the Na^+ and Cl^- concentrations are plotted on different axes to better indicate the relative increase/decrease of Na^+. The main observation is that Na^+ concentrations in the injected water were significantly affected during MPPW-ASR, despite relatively low CECs in the target aquifer and the native groundwater being only slightly brackish. Na^+-enriched water was recovered at the aquifer top by the shallowest wells, while the arrival of Na^+ was retarded in the deeper wells during salinization.

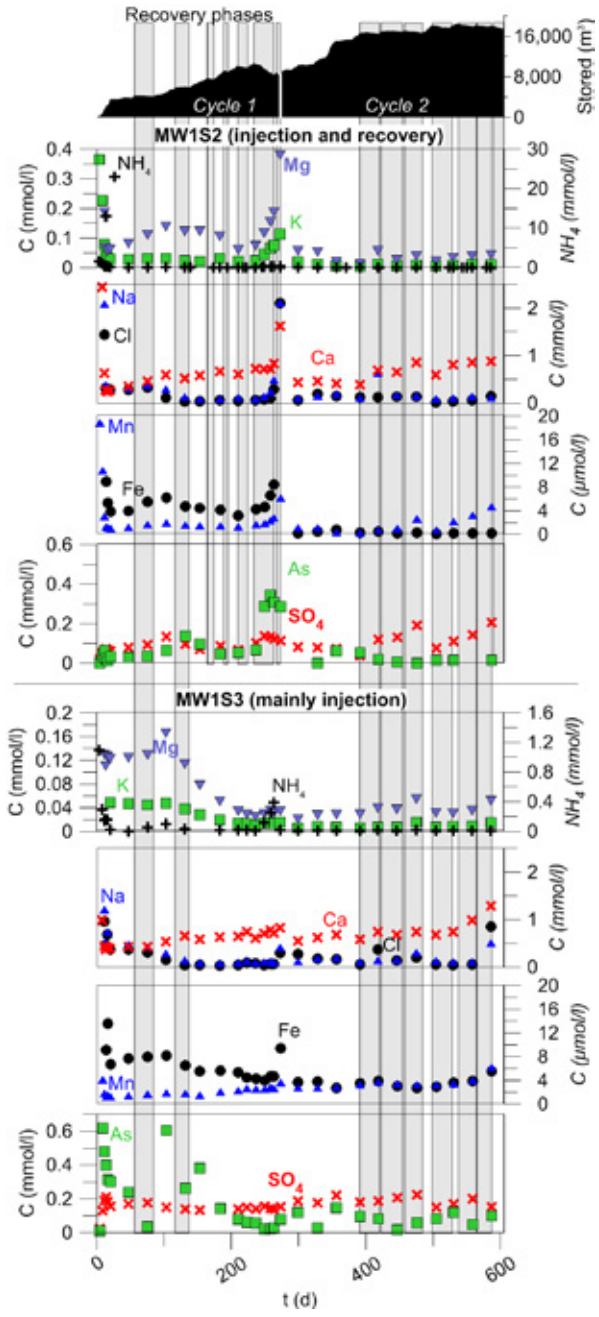

Figure 4-5: Hydrochemical observations at 5 m from the ASR Well (AW), in the upper central part of the aquifer (MW1S2: no pyrite, carbonates contain little Fe and Mn) and the lower central part (MW1S3: containing significant amounts of pyrite and carbonates bear Mn and Fe).

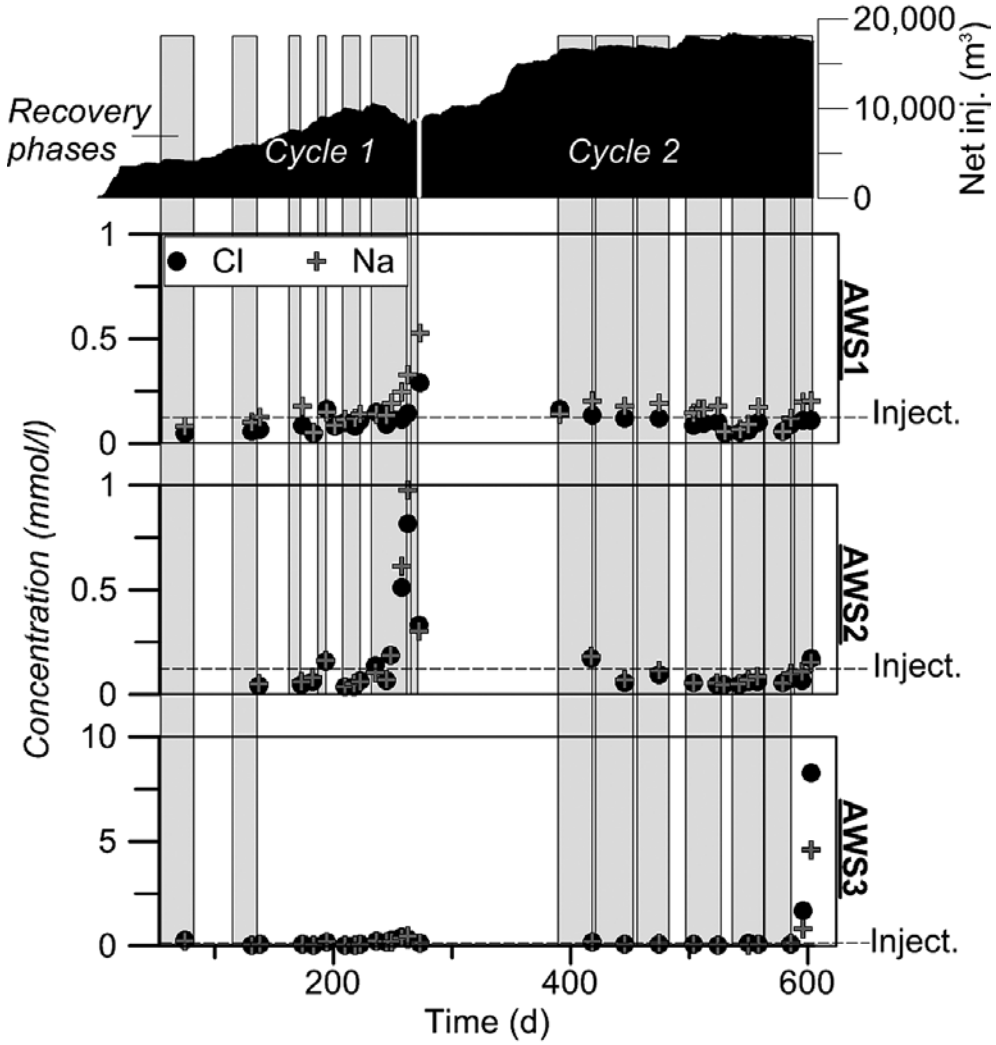

Figure 4-6: Observed Cl^- and Na^+ concentrations at the upper ASR wells (AWS1 – AWS3, where the recovery occurred) during two subsequent ASR cycles (2012-2013). A relatively small volume was recovered at AWS3; the bulk of the freshwater was recovered at AWS1 and AWS2 (Figure 4-2). The 'net injected' volume is calculated using: gross volume(injected) minus gross volume(recovered). 'Inject' marks the average injection concentration.

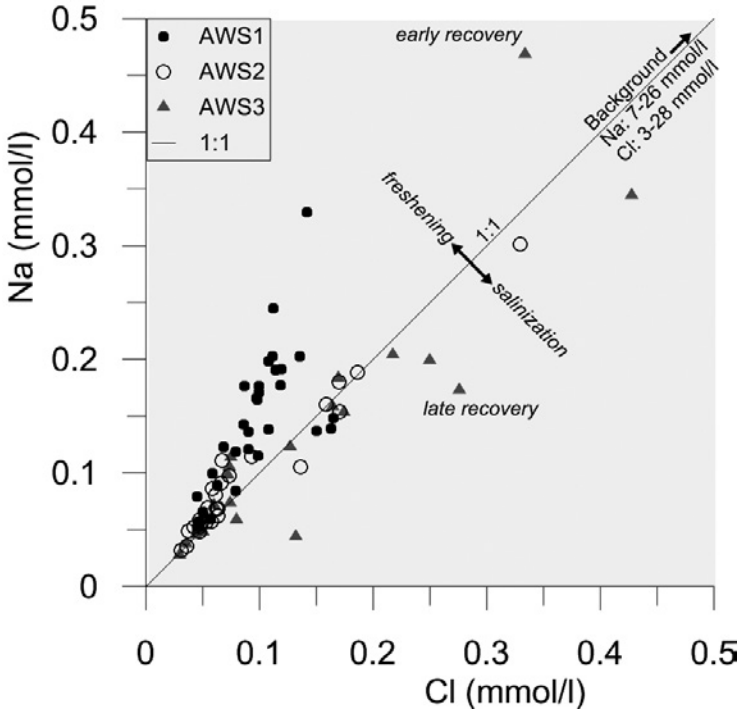

Figure 4-7: Na^+ versus Cl^- indicating that freshening (resulting in concentrations Na>Cl) and salinization (resulting in concentrations Na<Cl) occurred before injected water was recovered at the various wells screens of the MPPW.

4.4.2.2 Assessment of the role of cation exchange on Na^+ during MPPW-ASR

Cation exchange during freshening and salinization was considered the most important mechanism for the enrichment with cations from the brackish water. PHT3D modelling was performed in order to verify the controls of cation exchange during MPPW-ASR and the implications for the recovered water quality and explore the effects of different sediment and injection water compositions.

Reproduction of field observations by the PHT3D-model and simulation of subsequent cycles

First of all, the PHREEQC calculations to derive the exchanger composition showed that since the ambient water is rich in Ca^{2+} (Section 4.4.1.2) and Ca^{2+} is preferred over Na^+ on the exchanger, no more than 11% of the exchanger was occupied by Na^+ even at the base of the aquifer. Ca^{2+} on the other hand occupied 53 to 81% of

the exchanger sites. The straight-forward modelling using PHT3D of cation exchange and equilibrium dissolution of a calcite was able to reproduce the trends observed at the ASR wells: Na^+ concentrations at AWS1 were almost continuously elevated with respect to Cl^- (Figure 4-8), reaching concentrations around and eventually exceeding the limit of 0.5 mmol/l . This limit was not exceeded (Cycle 3) or exceeded 45 days later (Cycle 4 and 5; almost one-third of the total recovery period later) when solely Cl^- was analyzed. Therefore, the recovery at AWS1 would have been limited due to the Na-enrichment instead of an increase in Cl^- concentration.

The Na^+ concentrations at AWS2 produced by the PHT3D-model were significantly lower compared to Cl^- during salinization at the end of recovery periods (Figure 4-8b: Cycle 3-5), supporting the observed retardation at the bottom fringe of the injected freshwater body (AWS3, Figure 4-6). The recovery at AWS2 could therefore be extended with approximately 30 days due to retardation of the Na^+ front.
When GU-III was introduced with its high CEC (51.1 meq/kg), a significant and continuous surplus of Na^+ was observed especially at MW1S2 and MW1S3 (results not shown) and to a lesser extent at AW1S1 (Figure 4-8ab). The modelled degree of Na^+-enrichment was not observed in the field. A high-CEC unit centrally in the target aquifer would have had a negative effect: concentrations at AWS1 would rapidly exceed 0.5 mmol/l (comparable to the high CEC scenario), without sufficient compensation by Na^+ retardation at AWS2.

Implications of cation exchange for Na^+ in the bulk recovered water

It is relevant to examine the net effect on the bulk recovered water, as the recovery of Na^+ deviates in different ways from the recovery of Cl^- at well screens AWS1 (Na^+ enrichment) and AWS2 (Na^+ retardation). The results show that bulk Na^+ concentrations are elevated with respect to Cl^- in the bulk recovered water at the start of recovery periods for an MPPW-ASR system in an aquifer with a 3 times higher CEC than the field situation (Figure 4-8c). This is due to the elevated concentrations at AWS1. In the case of a high CEC, the Na^+ concentrations will never reach the injected concentration. However, bulk Na^+ concentrations are lower than Cl^- concentrations in the recovered water during later stages of recovery due to the retarded arrival at AWS2.

For a theoretical ASR-system with bi-directional flow paths (no buoyancy) in the same aquifer it was found that water quality will improve with consecutive cycles. The zone affected by native groundwater (by mixing and/or cation exchange) is then pushed further and further from the ASR well because of the net injection (only 40% is recovered) and the lack of upward flow paths.

Effect of sediment and injection water composition on Na^+ in the recovered water
A higher CEC in the target aquifer results in higher Na^+ concentrations at AWS1 (Figure 4-8a), qualifying most of the recovered water by this well unsuitable for high-quality irrigation water. The reverse effect was again observed at AWS2, yet stronger than with the 3 times lower field CEC. Here, recovery was now hardly hampered by Na concentrations >0.5 mmol, although Cl^- concentrations reached 8 mmol/l.

Addition of 5 mmol/l gypsum while assuming the low field CECs would lower Na^+ concentrations at AWS1 in the first phase of recovery, but could not increase the recovered water volume with sufficiently low Na^+ concentrations. In this case, the observed Na^+ concentrations were higher at the top of the AWS1 well screen and lower at its base compared to the scenario without addition of gypsum, but the recovered water quality was similar. Raising the addition of gypsum to 20 mmol/l did not result in improvement of the recovered water quality, nor an increase in Na^+ retardation.

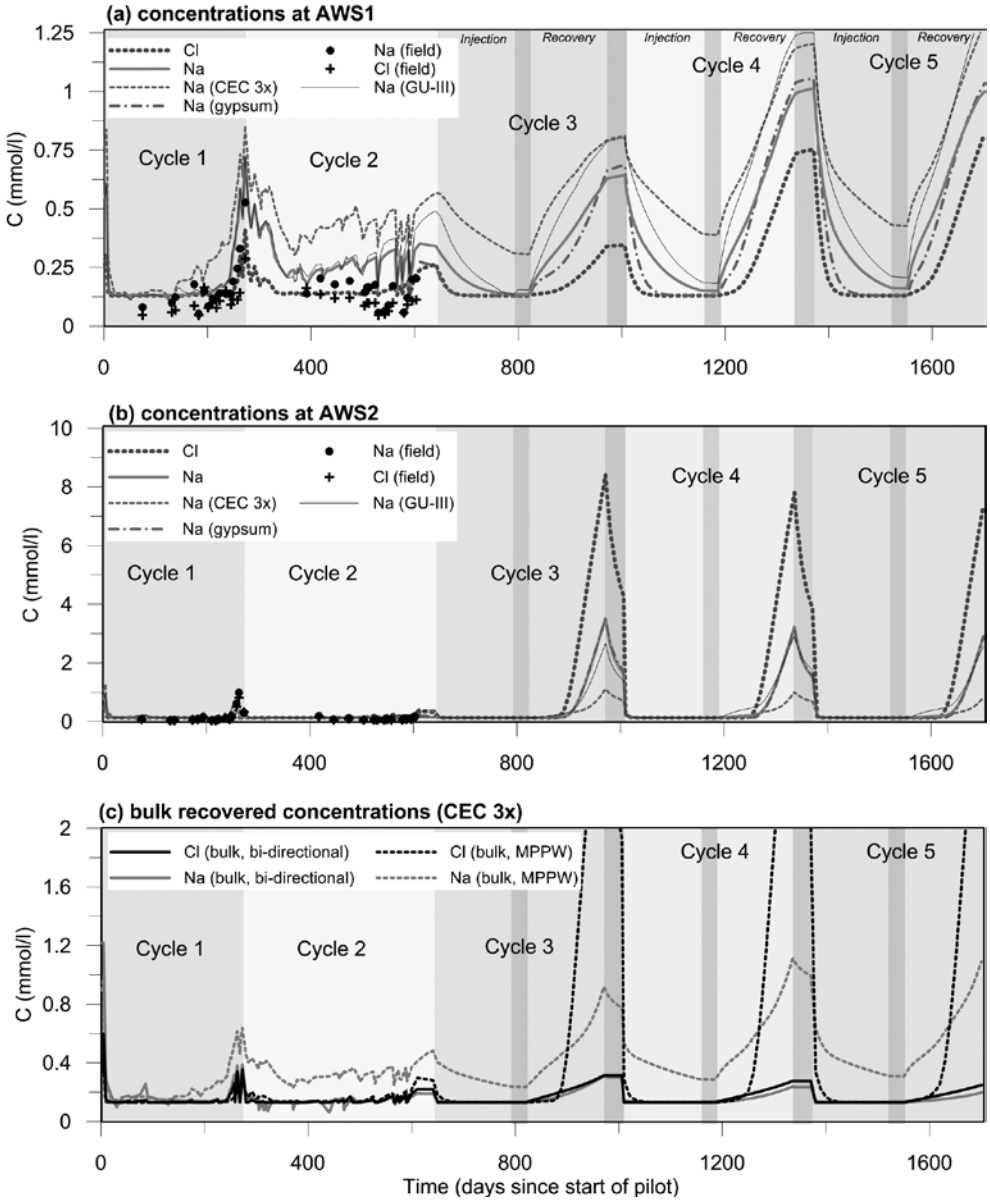

Figure 4-8: Observed and modelled Na+ and Cl- concentrations by PHT3D for the recovery wells AWS1 (a) and AWS2 (b) The modelled concentrations for the bulk recovered water quality assuming a 3 times elevated CEC (c), which can be compared with conventional bi-directional ASR (no buoyancy). Modelling results for an elevated CEC (3 times the CEC derived from aquifer sediments) and a case with injection water enriched with 5 mmol/l gypsum ($CaSO_4$) are shown in (a) and (b) to demonstrate their consequences. Only Cycle 3-5 is shown for the

gypsum enrichment for the sake of clarity and coincides with 'Na' (no enrichment) in (b). Na (GU-III) = scenario with a high CEC at GU-III (51 meq/kg, Table 4-3).

Implications of cation exchange for Na^+ in the bulk recovered water

It is relevant to examine the net effect on the bulk recovered water, as the recovery of Na^+ deviates in different ways from the recovery of Cl^- at well screens AWS1 (Na^+ enrichment) and AWS2 (Na^+ retardation). The results show that bulk Na^+ concentrations are elevated with respect to Cl^- in the bulk recovered water at the start of recovery periods for an MPPW-ASR system in an aquifer with a 3 times higher CEC than the field situation (Figure 4-8c). This is due to the elevated concentrations at AWS1. In the case of a high CEC, the Na^+ concentrations will never reach the injected concentration. However, bulk Na^+ concentrations are lower than Cl^- concentrations in the recovered water during later stages of recovery due to the retarded arrival at AWS2.

For a theoretical ASR-system with bi-directional flow paths (no buoyancy) in the same aquifer it was found that water quality will improve with consecutive cycles. The zone affected by native groundwater (by mixing and/or cation exchange) is then pushed further and further from the ASR well because of the net injection (only 40% is recovered) and the lack of upward flow paths.

Effect of sediment and injection water composition on Na^+ in the recovered water

A higher CEC in the target aquifer results in higher Na^+ concentrations at AWS1 (Figure 4-8a), qualifying most of the recovered water by this well unsuitable for high-quality irrigation water. The reverse effect was again observed at AWS2, yet stronger than with the 3 times lower field CEC. Here, recovery was now hardly hampered by Na concentrations >0.5 mmol, although Cl^- concentrations reached 8 mmol/l.

Addition of 5 mmol/l gypsum while assuming the low field CECs would lower Na^+ concentrations at AWS1 in the first phase of recovery, but could not increase the recovered water volume with sufficiently low Na^+ concentrations. In this case, the observed Na^+ concentrations were higher at the top of the AWS1 well screen and lower at its base compared to the scenario without addition of gypsum, but the recovered water quality was similar. Raising the addition of gypsum to 20 mmol/l did not result in improvement of the recovered water quality, nor an increase in Na^+ retardation.

4.4.3 Concentration increases for Fe^{2+}, Mn^{2+}, and As

4.4.3.1 Observed trends in Fe^{2+}, Mn^{2+}, and As concentrations

Release of Fe^{2+} and/or Mn^{2+} is undesirable for operational reasons (clogging), while

increased As concentrations can have a toxic effect. During recovery in Cycle 1, Mn^{2+} concentrations frequently exceeded the operational limit of 0.9 µmol/l at AWS1 (which was a recovery well after injecting 1,132 m^3). Breakthrough of also Fe^{2+} (analyzed as total Fe, species based on pH) and As (analyzed as total As, species unknown) was observed here later during recovery. At AWS2 (alternating injection/recovery), Mn^{2+} and Fe^{2+} concentrations were significantly lower: an increase of Mn^{2+} was observed only during the first, short recovery stages and at the end of Cycle 1. AWS3 was used mainly for injection and showed high Mn^{2+} and As concentrations during short recovery stages.

In Cycle 2, high Mn^{2+} and elevated Fe^{2+} and As concentrations were observed at AWS1, but concentrations were lower than in Cycle 1, and were lowered further after restoring the injection of small rainwater volumes in the later phase. The recovered water at AWS2 was virtually free of As, Fe^{2+}, and Mn^{2+} in Cycle 2. Mn^{2+} and later Fe^{2+} did cause frequent and severe deterioration of the water recovered at AWS3, despite a significant net injection. The general observation is that most enrichment was observed at the S3 wells (also at MW1, Figure 4-5) and concerns Mn^{2+}. The As mobilization tended to decrease over time. Water reaching AWS1, which was injected at deeper aquifer intervals, was on average slightly enriched with all elements of concern.

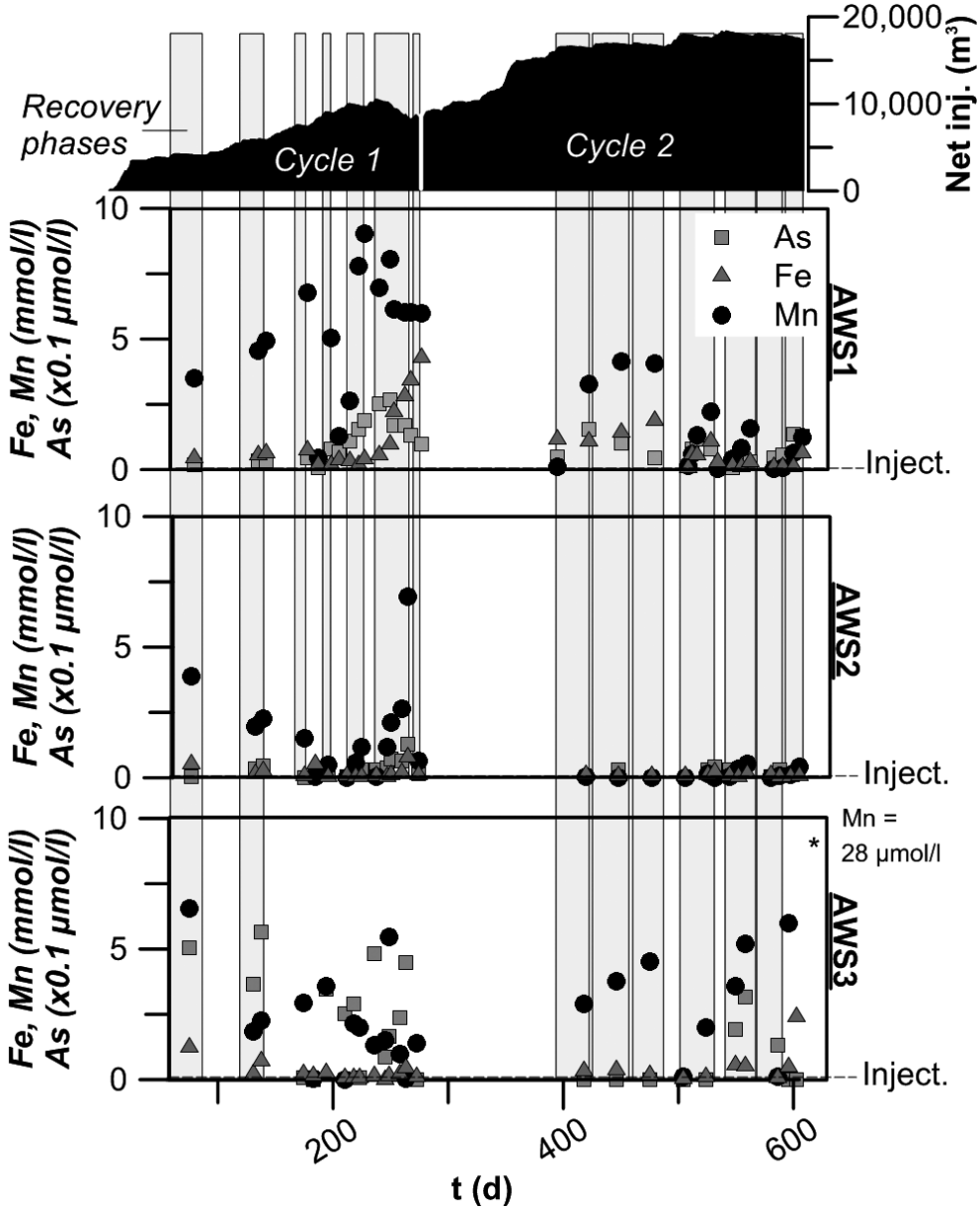

Figure 4-9: Concentrations of Fe, Mn, and As in the water recovered from the recovery wells (AWS1 – AWS3) during two subsequent ASR cycles (2012-2013). Recovery at AWS3 was relatively limited; the bulk of the freshwater was recovered at AWS1 and AWS2 (Figure 4-2). Inject. = concentration in the injection water. The 'net injected' volume is calculated using: gross volume(injected) minus gross volume(recovered).

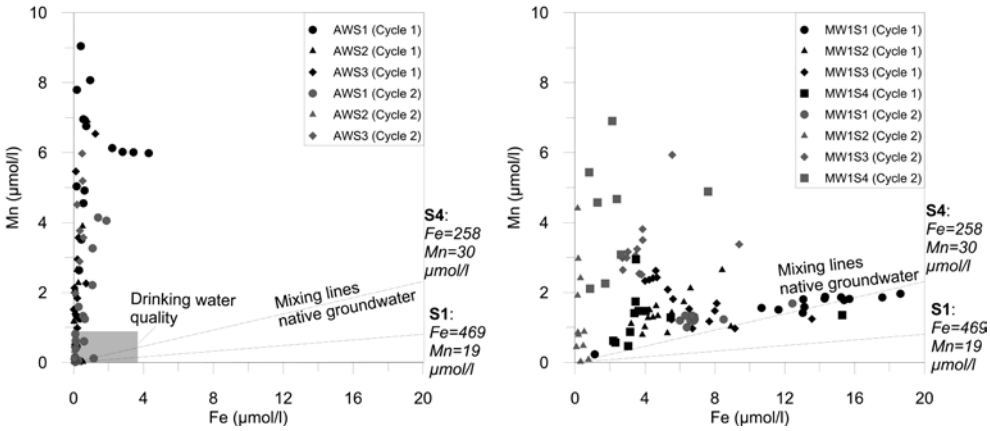

Figure 4-10: Mn versus Fe recovered from the ASR well (AW) and observed in the aquifer at 5 m from the ASR well (MW1).

4.4.3.2 Assessment of the mobilization of Fe^{2+} and Mn^{2+}

Potential processes for elevated Fe^{2+} and Mn^{2+} concentrations

Various processes can be responsible for the observed mobilization of Fe^{2+} and Mn^{2+}, the most relevant being mixing with ambient Fe^{2+}/Mn^{2+}-rich groundwater, cation exchange (similar to the enrichment with Na^{+}), dissolution of Mn and/or Fe-carbonates, and reduction of MnO_2 by Fe, releasing Mn^{2+} while precipitating Fe^{2+} (Table 4-1).

Effect of mixing and cation exchange on Fe^{2+} and Mn^{2+}

Mixing can easily be assessed with the help of the mixing lines for Fe^{2+} and Mn^{2+} in Figure 4-10. Only at MW1, a part of the observed concentrations plot on the mixing line. Release by cation exchange during freshening just behind the mixing zone should be marked by a positive correlation with the base exchange index (BEX). This relation was partly present for Fe^{2+}, but not for Mn^{2+} (Figure 4-11). Enrichment of Fe^{2+} and Mn^{2+} (~3 µmol/l) occurred even in freshwater samples with a neutral BEX (freshening completed).

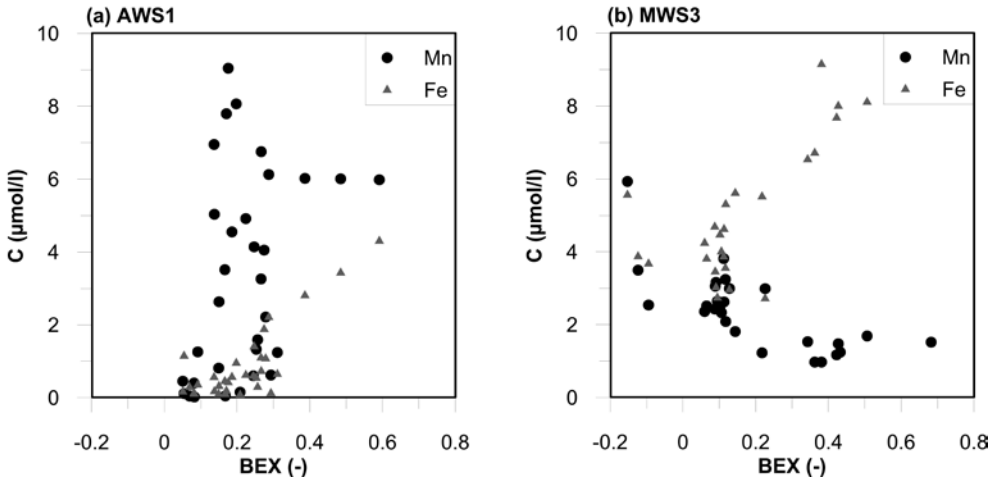

Figure 4-11: Fe and Mn concentration at AWS1 (left) and MWS3 (right) versus the BEX of the corresponding sample.

Effects of carbonate dissolution in combination with pyrite oxidation

The geochemical characterization (Figure 4-4) indicated that potentially a significant amount of the carbonate in the deeper half of the target aquifer is present as a Fe- and Mn-bearing carbonate. However, as the more soluble calcite ($CaCO_3$) is the dominant carbonate in the target aquifer, carbonate dissolution should be primarily marked by an increase in Ca^{2+} and inorganic carbon (primarily HCO_3^- under the pH observed (Appelo and Postma, 2005)) in the aquifer. In it is shown that the increase in Ca^{2+} was generally accompanied by an increase in HCO_3^- with a ± 1:2 ratio ($Ca:HCO_3$,Table 4-1), representing calcite equilibrium under varying CO_2 pressures (from atmospheric ($pCO_2 = 10^{-3.5}$ atm) up to around $10^{-2.4}$ atm). Relatively low Ca^{2+} concentrations accompanied by a relatively high positive BEX suggest freshening occurred before water was recovered by AWS1. Relatively high Ca^{2+} concentrations at the S3-level (generally accompanied by only a slightly positive BEX) on the other hand indicated calcite-dissolution by proton-buffering upon pyrite-oxidation (Hartog et al., 2002; Stuyfzand, 1998). One sample indicated salinization (negative BEX), explaining the relatively high Ca^{2+} concentration (Figure 4-12).

To verify which reactive processes were driving the carbonate dissolution observed, simple PHREEQC batch simulations were performed. The injection water's ionic balance was first attained by adjusting the HCO_3^- concentration, than equilibrated under atmospheric pCO_2, subsequently brought in equilibrium with calcite in a closed system, and finally all dissolved oxygen was used to oxidize pyrite while main-

taining the calcite equilibrium (see reaction equations in Table 4-1). The equilibration dissolution of calcite resulted in a relatively low Ca^{2+} concentration (0.27 mmol/l), close to the lowest Ca^{2+} concentration observed in the recovered freshwater (Figure 4-12). The PHREEQC simulation indicated no more than 0.61 mmol Ca/l and 0.91 mmol HCO_3/l could be attained when pyrite oxidation by oxygen in the average injection water was stimulating carbonate dissolution. The sporadically observed higher DO (up to 0.4 mmol/l), Ca^{2+} (up to 0.47 mmol/l), and HCO_3^- (up to 0.95 mmol/l) concentrations in the injected water were also insufficient to explain the amount of Ca^{2+} and HCO_3^- produced during the field pilot, especially in Cycle 1 (Figure 4-12). So, part of the observed production of Ca^{2+} could not be explained by proton-buffering upon pyrite oxidation or the observed maximum injected Ca^{2+} concentrations.

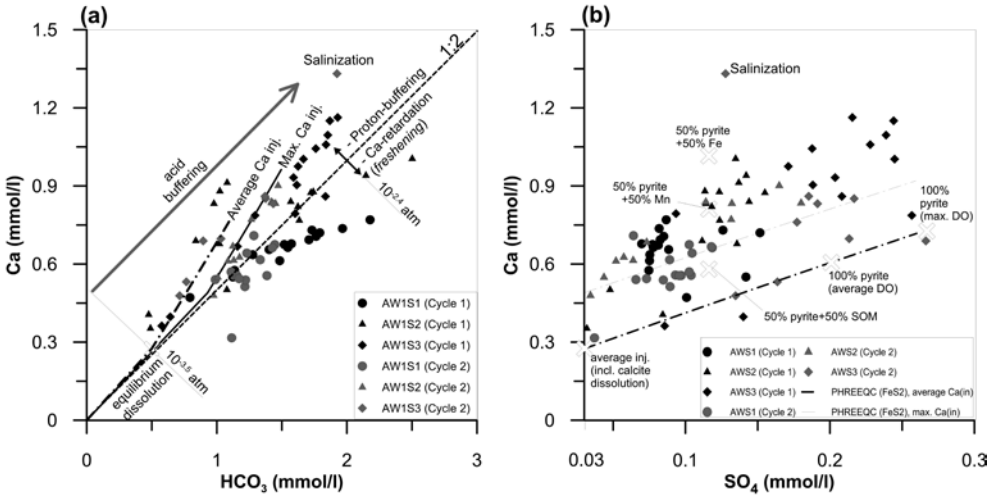

Figure 4-12: Ca^{2+} versus HCO_3^- (a) and Ca^{2+} versus SO_4^- concentrations (b) in the water recovered from the ASR wells. The dashed line in (a) represents calcite equilibrium for increasing CO_2-pressure, the calculated concentrations as a consequence of pyrite oxidation are marked for the average and the maximum observed Ca^{2+} concentrations in the injection water.

To check the assumed contribution of pyrite (FeS_2) oxidation to calcite dissolution, the SO_4-production was analyzed. The calculated oxygen consumption (Table 4-5) based on the observed SO_4-production indicated that virtually all oxygen in the injected water at the lower part of the aquifer (GU-IV and V, level S3 and S4) was used for oxidation of pyrite in Cycle 2 (Table 45), but not in Cycle 1. Furthermore, the Ca:SO_4-ratio

at the S3-level was lower in Cycle 2 than in Cycle 1 (Figure 4-12b), also indicating an increased importance of pyrite-oxidation at the S3/S4-level (GU-III-V) over time.

Table 4-5: O_2 consumption by pyrite based on SO_4-production found at MW1 at the end of long periods of injection.

	O_2 consumed by pyrite oxidation	
MW	**Cycle 1**	**Cycle 2**
S1	48%	33%*
S2	18%	23%
S3	58%	108%
S4	68%	98%

*Based on SO_4^{2+} concentrations observed at AWS1 during recovery after injecting small volumes of freshwater.

Removal of mobilized Fe and Mn by adjustments in the injection scheme

To improve the recovered water quality at AWS1, periodic injection of small rainwater volumes was applied to stimulate subsurface iron removal (SIR; Van Beek, 1985; Van Halem, 2011) during Summer 2013 after 1 year of only recovery at this well. The Mn^{2+} concentrations decreased from 4.1 µmol/l to almost 0 µmol/l. Based on the few SIR-cycles run, about 8 volumes of water could subsequently be recovered with Mn^{2+} concentrations below the limit (0.9 µmol/l) after injection of 1 volume of oxygen-containing rainwater (Figure 4-13). Fe^{2+} was kept below 1 µmol/l. The SO_4-production during SIR injections following abstraction of Mn^{2+} and Fe^{2+}-rich water at S1 level was lower in Cycle 2 (Table 45). This hints that oxidation of (adsorbed) Fe^{2+} and Mn^{2+} during injection led to competition for oxygen and less oxidation of pyrite. Removal of As by SIR appeared less effective, it was immobilized for a short period only after injection of a relatively large freshwater volume.

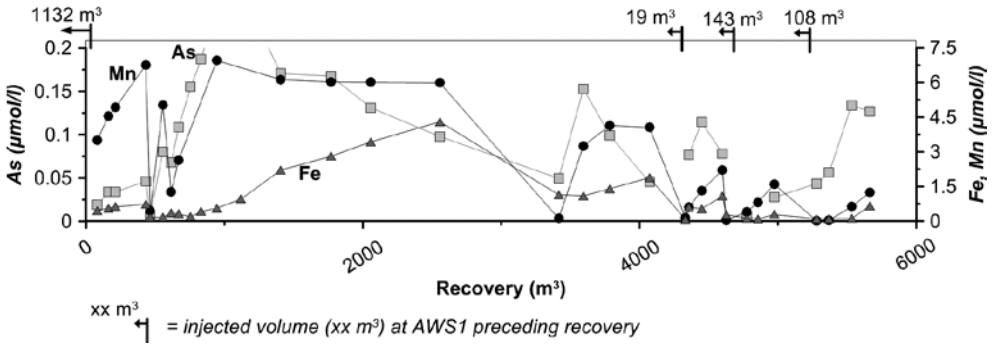

Figure 4-13: Mn, Fe, and As concentrations in recovered water from AWS1 during three SIR tests at the end of cycle 2 plotted versus the net recovery (=injected minus recovered volume at this single well screen).

4.5 Discussion

4.5.1 Increasing Na^+ concentrations during MPPW-ASR in coastal aquifers

Field observations and reactive transport modelling demonstrated a dominance of cation exchange during MPPW-ASR in controlling Na^+ mobility. MPPW-ASR optimizes the recovery of practically unmixed water (low EC, no increase in Cl^-), but repeated salinization of the deeper aquifer intervals during ASR cycles resulted in non-conservative arrival of Na^+ (and other cations from the native groundwater like Mg^{2+}, K^+, Fe^{2+}, Mn^{2+}) at the recovery wells. Since particularly a zone of Na^+-enriched water is undesirable for irrigation water use, the control of Na^+ concentrations cation exchange processes was a critical factor during the MPPW-ASR pilot.

The contamination with Na^+ appears to be relatively persistent during MPPW-ASR, even in the case of a net injection. A cycle-after-cycle water quality improvement is lacking around the deepest wells screens. This is caused by a repeating cycle of Na^+ adsorption when the upward moving infiltrated rainwater is replaced by brackish water during recovery. This is followed by Na^+ desorption when fresh rainwater replaces brackish water during injection. The enrichment with Na^+ may decrease over time thanks to the formation of a $CaCl_2$-water type around the freshwater body during recovery in the lower half of the aquifer. Modeling showed, however, that this water type is diluted and then transported to the shallower parts of the aquifer by density-driven flow, while a native, brackish NaCl water type continues to encroach the deeper part (Figure 4-15).

The net positive or negative effect of Na^+ mobility on the RE depends on the combination of the CEC, native groundwater and injection water composition, and the limits set for Na^+ in the recovered water. The mass of mobilized Na^+ will increase with increasing CEC and native water salinity. The volume of the enriched zone and the Na^+ concentration therein will be controlled by Ca^{2+} concentrations in the injected water. The potential water quality deterioration should be taken into account especially in saline, anisotropic aquifers with intercalated fine sand beds (with a high CEC), which may be preferably targeted over coarse-grained, low-CEC aquifers to limit the freshwater loss by buoyancy effects (van Ginkel, 2015). The retarded arrival during salinization at the deepest recovering well can also positively affect the RE, on the other hand, when slightly elevated Na^+ concentrations are acceptable.

Reactive transport modelling highlighted that a central layer with a high CEC can cause Na^+ contamination of a significant freshwater volume. For the Nootdorp pilot however, the assumption of a relatively low CEC in the whole target aquifer best reproduced field observations, despite the presence of a unit with reworked clay and peat fragments for which a high CEC was determined. Possibly, this contradiction is due to the discontinuous nature of this unit (GU-III) and/or by the fact that the clay and peat in this unit is concentrated in pebbles (Figure 4-14), while most flow will occur in the less reactive surrounding sand matrix of this unit. Affecting the cation-exchange process to reduce or delay the mobilization, e.g. by dosing of Ca^{2+} solution to the injection water may increase the RE. Although this leads to a smaller water volume in which Na^+ is mobilized, the Na^+ concentration will increase proportionally. Therefore, additional Ca^{2+} enrichment does not necessarily lead to an increase in recoverable water. The water with mobilized Na^+ may still reach the top of the recovering wells and hamper later recovery. Also, addition of Ca^{2+} to the injection water will not lead to additional retardation of Na^+ when all Na^+ is already washed from the exchanger sites by Ca^{2+} in the deeper aquifer intervals with the original injection water. A more positive effect of Ca^{2+} dosing on the recovered water quality is expected with higher CECs and/or native salinities. It may at the same time prevent aquifer clogging due to clay swelling and dispersion, which is a risk in clay-bearing aquifer types (Brown and Silvey, 1977; Konikow et al., 2001).

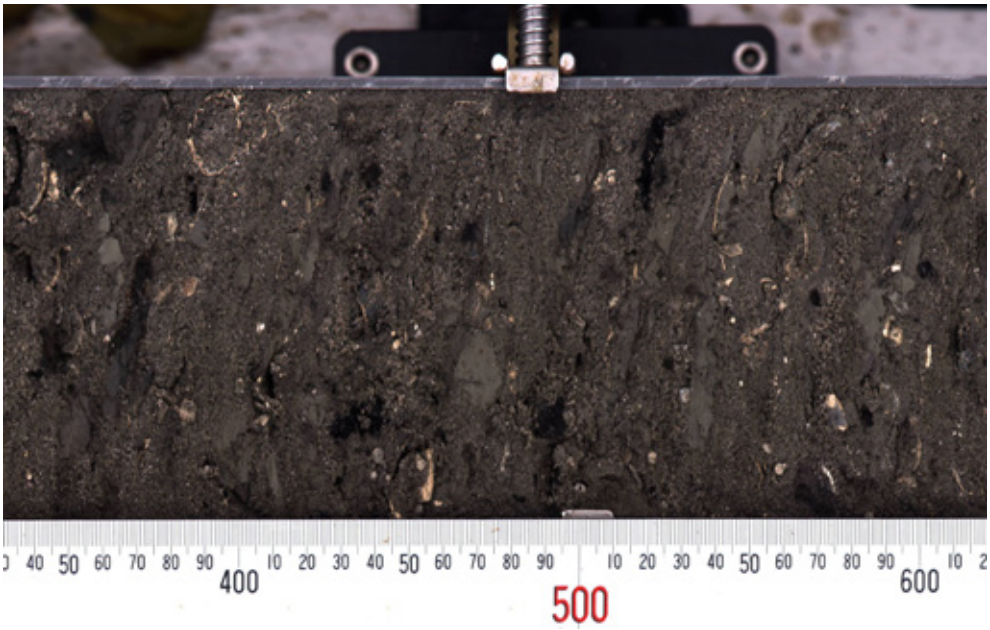

Figure 4-14: Undisturbed core from the GU-III interval, showing presence of peat and clay predominantly in pebbles. The pebbles are present in a coarse sand matrix.

Despite the deterioration by the mobilization of sodium, an MPPW-equipped ASR system will generally still perform significantly better than a conventional ASR-system in a brackish coastal aquifer. This is because the recovered water stays relatively unmixed water to a larger extent, with 3 times larger volumes with still low Na^+ concentrations in the Nootdorp pilot (Chapter 3). Moreover, the effect of cation exchange on the bulk quality of this unmixed water is generally limited. However, a fully-penetrating ASR well in a brackish or saline aquifer may outperform the MPPW when already a small increase of Na^+ concentrations is unacceptable and/or a much larger part of the injected water is forced through high-CEC layers during MPPW-ASR.

4.5.2 Increasing Fe^{2+} and Mn^{2+} concentrations during MPPW-ASR

4.5.2.1 Mobilization during freshwater injection

Both mixing and cation exchange could not explain the observed (continuous) increase in Fe^{2+} and Mn^{2+} in the injected water (Section 4.4.3). Due to the high carbonate content and the potentially significant contribution of Fe and Mn to the carbonates (Figure 4-4), dissolution of Fe and Mn-containing carbonates was suspected to be a source for mobilization. The amount of calcium mobilization in especially

Cycle 1 could be only partly explained by equilibrium calcite dissolution enhanced by proton-buffering upon pyrite oxidation (Figure 4-12). Particularly in Cycle 1, processes other than pyrite-oxidation stimulated calcite dissolution, such as oxidation of Fe^{2+}, $FeCO_3$, and Fe-X, Mn^{2+}, NH_4^+, NH_4-X, $MnCO_3$ and Mn-X, and SOM (reactions in Table 4-1). Based on the Ca^{2+} and HCO_3^- concentrations observed, oxygen was partly consumed by the oxidation of Fe^{2+} and Mn^{2+} rather than SOM (Figure 4-12). Using the observed Ca^{2+} and DO concentrations in the injection water and the dissolution processes, the resulting Ca^{2+} and SO_4^{2-} concentrations could be explained.

Since the observed Ca^{2+} concentrations can explained by equilibrium dissolution and acid buffering upon proton and CO_2-production, it is concluded that the dissolved carbonate was merely pure calcite. The lasting enrichment of Fe^{2+} and Mn^{2+} observed in the deeper aquifer interval (both constantly ~3 µmol/l in Cycle 2) indicates that less than 1% of the dissolved carbonate was in the form of Fe and Mn-carbonates. This was, however, sufficient to create a Fe^{2+} and especially Mn^{2+} enriched water type which was unsuitable for direct use as horticultural irrigation water.

In the upper aquifer interval (GU-I, level S2), the majority of the oxygen was consumed by processes other than pyrite oxidation in both cycles (Table 4-5), which was presumably caused by the lower pyrite and higher SOM content in this unit (Table 4-3). Based on the low Ca^{2+} and SO_4^{2-} production and the geochemical composition here, oxidation of organic matter was the most likely lasting process of oxygen consumption. Mobilization of Fe^{2+} and Mn^{2+} was limited for this reason and due to the presumably purer calcite (Figure 4-4) and the absence of periodic salinization. Sufficient oxygen was available here for oxidation of any (adsorbed) NH_4^+, Fe^{2+}, and Mn^{2+} during injection.

4.5.2.2 Mobilization of Mn^{2+} during recovery

Although equal Fe^{2+} and Mn^{2+} concentrations of ~3 µmol/l were mobilized during injection in the deeper aquifer intervals, these concentrations were not encountered during recovery. Instead, as shown in Figure 4-10, the recovered water at the ASR well (AW) had a much higher Mn:Fe ratio in comparison with the water observed at MW1. Also, a general shift occurred from a Fe^{2+}-dominated water type to a Mn^{2+}-dominated water type. These trends suggest that especially Fe-hydroxides precipitated, which potentially increased the sorption of especially Fe^{2+}. Mn-oxides (like MnO_2) may also have formed close to injecting ASR wells by oxidation of (adsorbed) Mn^{2+} during injection phases. However, they were likely reduced by Fe^{2+} by anoxic water during recovery phases, causing the increase of the Mn:Fe ratio. This process (Table 4-1), which is described by Postma and Appelo (2005), is relatively fast (Postma, 1985). As a

consequence, Fe^{2+} concentrations generally remained below their limits. Part of the Fe^{2+} immobilization and Mn^{2+} enrichment could also have been caused by sorption of Fe^{2+} by $Fe(OH)_3$, inducing proton-buffering via dissolution of Fe- and Mn-carbonates. However, Fe^{2+} concentrations observed at 5 m from the ASR-well were generally half the Mn^{2+} concentrations reaching the ASR well (Figure 4-10). This suggests that MnO_2 reduction was the dominant process driving the mobilization, with 1 mol of Mn^{2+} produced through the oxidation of 2 mol of Fe^{2+} (Table 4-1).

4.5.2.3 Overall effect of MPPW-ASR on Fe^{2+} and Mn^{2+} in the recovered water

In a MPPW-ASR system, injection of (oxic) water occurs predominantly in the deepest well screens. At the Nootdorp site, the deepest levels coincide with an aquifer interval which is pyrite-rich and contains Fe and Mn-bearing carbonates. The oxidation of these species and subsequent carbonate dissolution resulted in a significant and continuous mobilization of Fe^{2+} and Mn^{2+}. The Fe^{2+} and Mn^{2+} released could travel relatively unhampered towards the shallow ASR well (AWS1), where no injection occurred and Fe-hydroxides and Mn-oxides to adsorb Fe^{2+} and Mn^{2+} were absent (Figure 4-15). The positioning of the different reactive aquifer units with respect to the screened intervals at the Nootdorp ASR site is therefore unfavorable as the oxygen in the injected water is consumed by processes that negatively influence the water quality. Geochemically, injection would be preferred in the shallow GU-I, such that oxygen would be mainly consumed by organic matter in presence of a relatively pure calcite to buffer the associated increase in CO_2-pressure.

The Nootdorp MPPW-ASR pilot illustrates that the presence and the exact depth interval of reactive layers have a major impact on the recovered water quality. In contrast with conventional ASR in freshwater aquifers, the bulk recovered water quality is not controlled by the average geochemical composition of the target aquifer, but dominated by the reactivity of deeper aquifer segments where most injection occurs. In the MPPW-ASR, a much larger part of the injected water had to pass the deeper (sub) horizontal reactive units. The (sub)horizontal geochemical stratification of sedimentary aquifers therefore deserves more attention. On the other hand, the enhanced vertical transport or aquifer residence time may also enhance removal of for instance adsorbing ions, organic micropollutants, viruses, and chlorination by-products (Dillon et al., 2006; Miotliński et al., 2014).

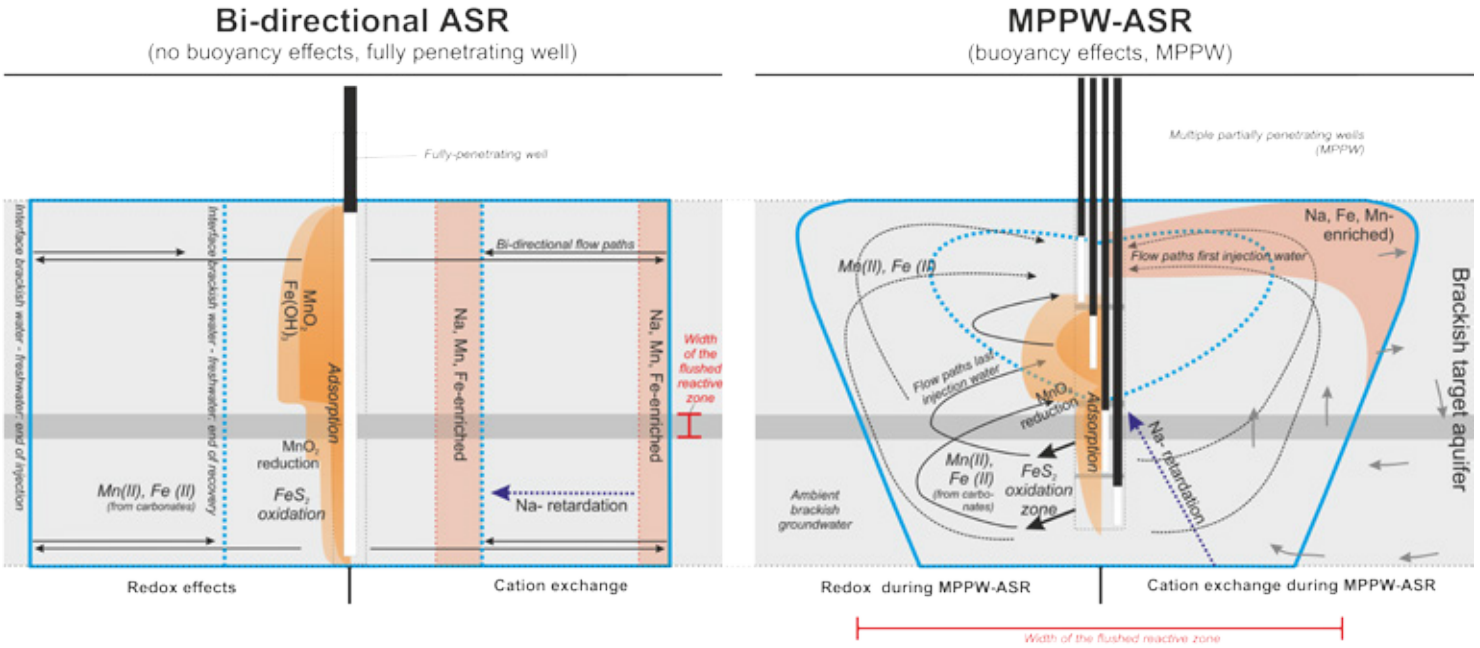

Figure 4-15: Conceptualization of reactive transport processes occurring during the Nootdorp MPPW-ASR pilot, as compared to bi-directional ASR. Also the flushed width of a hypothetical reactive zone in the middle of the aquifer during for both ASR flow regimes is illustrated.

4.5.2.4 Dealing with Mn^{2+} and Fe^{2+} mobilization

The recovery of undesired Mn^{2+} and especially Fe^{2+} (precipitating by reduction of MnO_2) can be controlled by periodically injecting a small portion of the oxic injection water at the shallow recovery well. The system then operates a little more like a conventional ASR-well, creating precipitates around the recovering wells by oxidation of adsorbed and released Fe^{2+} and Mn^{2+} without significantly decreasing the aquifer permeability (Mettler et al., 2001). This process of subsurface iron removal (SIR) may be preferred over aboveground iron removal, as it does not create a waste stream. Antoniou et al. (2014) pre-treated anoxic sediment columns from the GU-V with $KMnO_4$, to create neo-formed Mn-oxides that increase the adsorption of Mn^{2+} and Fe^{2+}. This method has two main advantages: (1) MnO_4^- is a strong oxidant leading to extensive oxidation/depletion of pyrite, SOM, and Fe and Mn-carbonates, and (2) the oxidation reactions increase the pH which accelerates the precipitation of Mn-oxides and raises the sorption capacity for Fe^{2+}, Mn^{2+}, and As.

4.5.2.5 Behaviour of arsenic at the Nootdorp MPPW-ASR pilot

The results suggest that the As concentrations in the recovered freshwater will decrease with subsequent cycles due to a decreasing As-mobilization under more-and-more oxidized conditions around the ASR wells. Sorption of As on Mn-oxides and Fe-hydroxides formed during injection likely facilitate adsorption. The passing of a clear and high As-peak early during injection suggest that a transition of As (III) to As(V) under oxidizing conditions was a boundary condition for As adsorption. The same process was observed during an injection experiment in a similar target aquifer at approximately 30 km from the site (Stuyfzand, 1998; Wallis et al., 2010). Remobilization was not observed in the practically unmixed freshwater that was recovered for irrigation. However, remobilization of As was observed during salinization at the fringe of the injected freshwater body as observed at MW1S4. This As-release can be caused by anion exchange when the anions in the ambient groundwater (such as PO_4^{3-} and HCO_3^- (Stuyfzand et al., 2006)) pass and by reduction of the formed Fe-hydroxides (Lazareva et al., 2015). This may alter the native brackish water around the MPPW-ASR system in Nootdorp, rather than the injected freshwater.

Conclusions

Reactive transport processes impacted the freshwater quality recovered during the MPPW-ASR pilot by increases in Na^+, Fe^{2+}, Mn^{2+}, and As concentrations in the unmixed water. A significant freshwater volume was enriched with especially Na^+ at the start of each injection phase due to cation exchange during freshening at the base of the target aquifer with every injection phase. Na^+-enriched water was subsequently recovered by the shallow recovery wells due to the upward flow paths within the MPPW-ASR-system. As the arrival of Na^+ during salinization of the deeper aquifer interval was retarded by cation exchange, the net effect on the recovery efficiency (RE) during MPPW-ASR is site-specific. Overall, the RE with respect to Na^+ is controlled by the CEC, the composition of the native groundwater and injected water, and the limits set for Na^+ in the recovered water. The Na-enrichment is lasting due to the repeated salinization, filling exchanger sites with Na^+ at the base of the target aquifer during recovery periods. Unlike ASR systems in freshwater aquifers, negative effects from cation exchange on RE do not decrease cycle-after-cycle.

The release of Fe^{2+} and especially Mn^{2+} can cause long-lasting deterioration of injected freshwater. At the Nootdorp ASR-site, this was caused by some Fe^{2+} and Mn^{2+} mobilization by cation exchange during freshening, but primarily and lastingly by dissolution of Fe and Mn-bearing carbonates in the lower half of the target aquifer. At this aquifer interval, this dissolution was promoted by proton-buffering and CO_2 production induced by pyrite oxidation (lasting) and the oxidation of primarily adsorbed Fe^{2+} and Mn^{2+} (mainly Cycle 1) . The lack of injection at the shallowest recovery well prevented formation of precipitates (Fe-hydroxides and Mn-oxides) around this well. Adsorption of Fe^{2+} and Mn^{2+}, which mobilized upon injection at deeper aquifer intervals, prior to recovery was therefore absent around this well. Since MnO_2 was an important oxidant for Fe^{2+}, mobilization of Mn^{2+} was the most prominent threat for the recovered water quality. The formation of sufficient precipitates to adsorb Mn^{2+} and Fe^{2+} close to the shallow recovery well(s) can be stimulated by periodic injections of small oxygen-rich water volumes ('subsurface iron removal'). Arsenic was released during the first ASR-cycle in Nootdorp, but had a stronger tendency to immobilize under oxidizing conditions as a consequence of sorption to Fe-hydroxides and Mn-oxides.

The application of MPPW-ASR in brackish or saline aquifers allows a significant increase in the recovery of injected fresh water compared to conventional ASR wells. However, more so than for ASR systems in freshwater aquifers, the interdependency of geochemical heterogeneity and the different aquifer intervals for deep injection, mobilization, and transport towards recovering wells is crucial for the resulting recov-

ered water quality during MPPW-ASR. Detailed characterization of the vertical variation of geochemical properties rather than the determination of the average geochemical properties of the target aquifer is therefore preferred. This will allow optimal placement of the MPPW well screens and development of a management strategy to combat potential water quality issues, for instance by applying subsurface iron removal or aquifer treatment.

Acknowledgements

The presented research in the chapter was funded by the Knowledge for Climate research program as part of its theme 'Climate Proof Freshwater Supply', the joint research program of the Dutch drinking water companies (BTO), and the EU FP7-project DESSIN. Frans Backer, Michel Groen, John Visser, Martine Hagen, and Guido Beenakker are thanked for their assistance during fieldwork and lab analyses. Codema B-E De Lier and Van der Goes Orchideeën are thanked for their financial and practical support during installation and operation of the Nootdorp ASR-system.

Chapter **5**

Consequences and mitigation of saltwater intrusion induced by short-circuiting during aquifer storage and recovery (ASR) in a coastal, semi-confined aquifer

Based on:

Zuurbier, K.G. and Stuyfzand, P.J., submitted. Consequences and mitigation of saltwater intrusion induced by short-circuiting during aquifer storage and recovery (ASR) in a coastal, semi-confined aquifer. Submitted to: Hydrology and Earth Systems Science.

5.1 Abstract

Aquifers are increasingly used for storage of freshwater and energy and (brackish) water abstractions, while the deeper subsurface is more and more exploited for geothermal energy, CO_2 storage, and oil and gas exploitation. The perturbation of the subsurface has significantly intensified for those purposes, increasing the risk of short-circuiting between originally separated aquifers. This study shows how short-circuiting negatively affects the freshwater recovery efficiency (RE) during aquifer storage and recovery (ASR) in coastal aquifers. ASR was applied in a shallow brackish-saline aquifer overlying a saline aquifer targeted for aquifer thermal energy storage (ATES). Although both aquifers were considered properly separated, intrusion of deeper saltwater quickly terminated the freshwater recovery. The potential pathway was identified by field measurements, hydrochemical analyses, and SEAWAT transport modelling. It was shown that the borehole of an ATES well provided the most presumable pathway for short-circuiting of deeper saltwater. Transport modelling underlined that the potentially rapid short-circuiting during storage and recovery can reduce the RE to null. When limited mixing with ambient groundwater is allowed, a linear RE decrease by short-circuiting with increasing distance from the ASR well within the radius of the injected ASR-bubble was calculated. Field observations and groundwater transport modelling showed that interception of deep short-circuiting water can mitigate the observed RE decrease, although complete compensation of the RE decrease will generally be unattainable since also injected freshwater is intercepted. Finally, it was found that brackish water upconing from the underlying aquitard towards the shallow recovery wells of the MPPW-ASR system can occur. In case of strict water quality limits, this process may cause an earlier termination of freshwater recovery, compared to current ASR performance estimations.

5.2 Introduction

Aquifers are increasingly being used for stormwater infiltration (Ferguson, 1990), brine disposal (Stuyfzand and Raat, 2010; Tsang et al., 2008), and storage of freshwater (aquifer storage and recovery or ASR; Pyne, 2005; Maliva and Missimer, 2010), heat (aquifer thermal energy storage or ATES; Bonte et al., 2011a), and CO_2 (Steeneveldt et al., 2006). Additionally, they are perforated for exploitation of deep fossil and geothermal energy, and traditionally used for abstraction of drinking and irrigation water. The increased use of the subsurface can lead to interference between aquifer

storage systems (e.g., Bakr et al., 2013) or affect the groundwater quality (Bonte et al., 2013a; Bonte et al., 2011a; Bonte et al., 2011b; Bonte et al., 2013b; Zuurbier et al., 2013). These consequences form relevant fields of current and future research.

The widespread perforation of aquifers and aquitards accompanying the subsurface activities imposes an additional risk by the potential creation of hydraulic cross-connections ('conduits') between originally separated aquifers or between aquifers and surface waters. This risk is plausible, as estimations indicate that about two-thirds of the wells may be improperly sealed (Morris et al., 2003), although the attention to this potential risk is limited (Chesnaux, 2012). Additionally, many of the new concepts to use the subsurface (e.g., ATES, ASR, brine disposal) require injection wells, which may cause soil fractures, even when the annulus is initially properly sealed, by exceedance of the maximum-permissible injection pressure (Hubber and Willis, 1972; Olsthoorn, 1982). Although this fracturing has advantages during oil and gas exploitation, it is undesirable for most groundwater wells in the relatively shallow subsurface, especially when this creates new connections between aquifers.

The short-circuiting or leakage process resulting from these connections has been studied at laboratory (Chesnaux and Chapuis, 2007) and field scale (Jiménez-Martínez et al., 2011; Richard et al., 2014; Stuyfzand, 1993), and for deep geological CO_2 storage (Gasda et al., 2008). Santi et al. (2006) evaluated tools to investigate cross-contamination of aquifers. Bonte et al. (2014) provided a simple analytical formula to calculate the flux through a perforated aquitard. Chesnaux et al. (2012) used numerical simulations of theoretical cases to demonstrate the consequences of hydraulic connections between granular and fractured-rock aquifers for pumping tests and hydrochemistry. These clearly demonstrated the significant hydrochemical cross-contamination when short-circuiting aquifers have a distinct chemical composition.

Although the risks of short-circuiting by aquitard perforation are acknowledged by scientists, it seems that the practical and regulatory communities are less aware (Chesnaux, 2012). This is underlined by the fact that certification for mechanical drilling (applied since the Industrial Revolution) in The Netherlands was not obliged before 2011 (Stichting Infrastructuur Kwaliteitsborging Bodembeheer, 2013a), while for the subsurface design and operation of ATES systems (>1500 systems since the nineties (Bonte et al., 2011a; CBS, 2013)) certification was obliged only since early 2014 (Stichting Infrastructuur Kwaliteitsborging Bodembeheer, 2013b). The lack of proper design and regulation of subsurface activities using wells can be partly caused by the lack of clear field examples of how well-intentioned use of the subsurface for sustainability purposes can fail due to earlier activities underground. This lack can

be caused by the fact that short-circuiting may not be easy to observe (Santi et al., 2006), or because failing or disappointing projects often do not make it to public or scientific reports. Careful use of the subsurface is, however, vital to successfully exploit it for sustainable use of energy (Bonte et al., 2011a) and freshwater by bridging periods of surplus and demand via storage (Chapter 1).

In this chapter it is demonstrated how a borehole of a deep ATES system led to failure of freshwater recovery during ASR in a shallow brackish aquifer. Although the boundary conditions were not ideal at this ASR site due to the groundwater's salinity, recovery of at least one-third of the injected water was expected. However, recovery had to be ceased upon recovery of just a few percent of the injected water during two subsequent cycles because of early contamination of injected freshwater with deeper (saline) groundwater.

The objective of this paper is to demonstrate and characterize the potential consequences of conduits for aquifer storage and recovery (ASR) systems. The Westland ASR site in the coastal area of The Netherlands serves as demonstration and reference case. Subsequently, the sensitivity of ASR for short-circuiting from conduits at different distances and a potential mitigation strategy are explored.

5.3 Methods

5.3.1 Set-up Westland ASR system

The Westland ASR system has been installed to inject the rainwater surplus from 270,0000 m^2 of greenhouse roof into a local shallow aquifer (23 - 37 m below sea level (m BSL), surface level = 0.5 m above sea level (m ASL)). Part of the water is recovered in times of demand. For this purpose, two multiple partially penetrating wells (MPPW) were installed (Figure 5-1), such that water can be injected preferably at the aquifer base, and recovered at the aquifer top to increase the recovery (Chapter 3). The ASR wells (AW1 and AW2, installed in 2012) and ATES well (K3, installed in 2006 and replaced close by in 2008, the latter still active) were installed using reverse-circulation rotary drilling. The monitoring wells (MW1-5, Figure 5-2) were installed using bailer drilling. Bentonite clay was applied to seal the ASR and monitoring boreholes (type: Micolite300) and ATES borehole K3 (Micolite000 and Micolite300). The ASR wells use a 3.2 m high standpipe to provide injection pressure, whereas the ATES well is using a pump to meet the designed injection rate of 75 m^3/h.

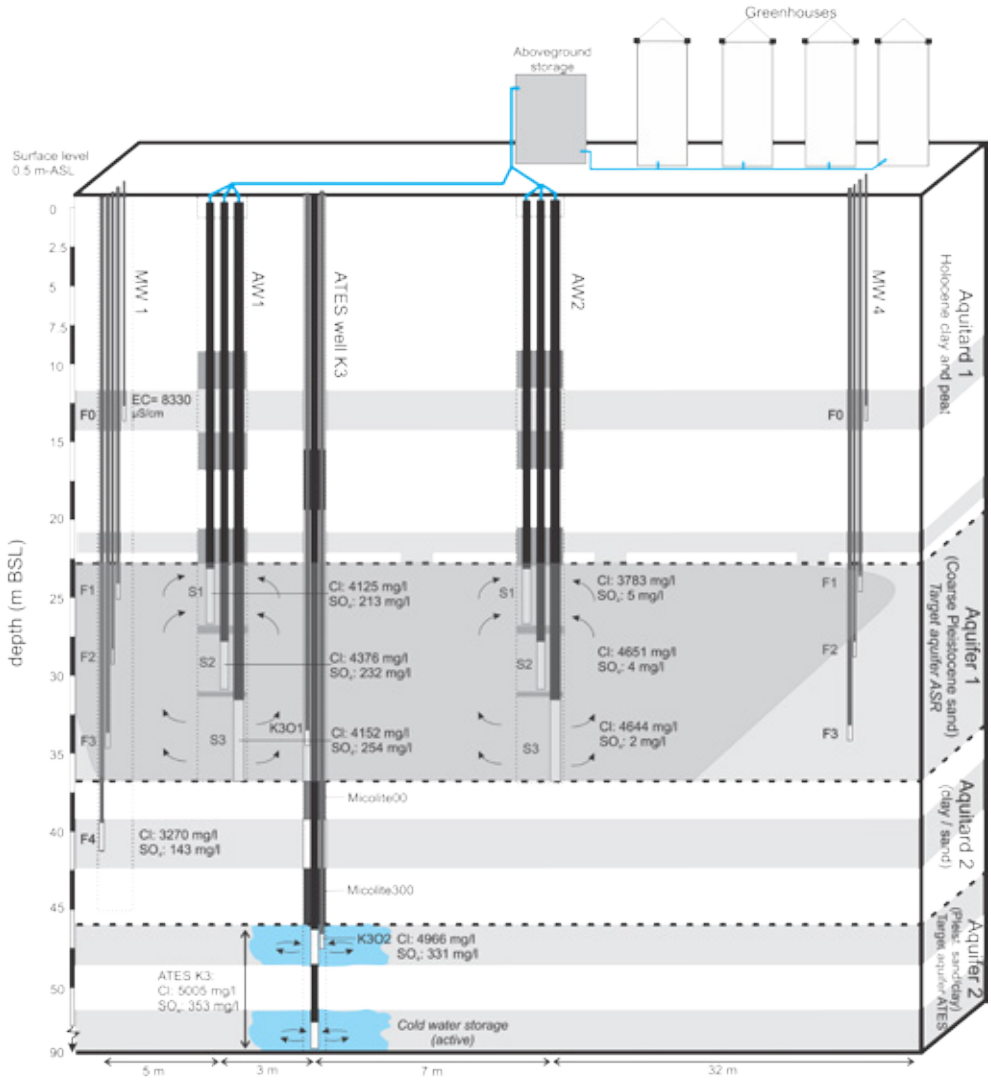

Figure 5-1: Cross-section of the Westland ASR site schematizing the geology, ASR wells, ATES well, and the typical hydrochemical composition of the native groundwater. Horizontal distances not to scale.

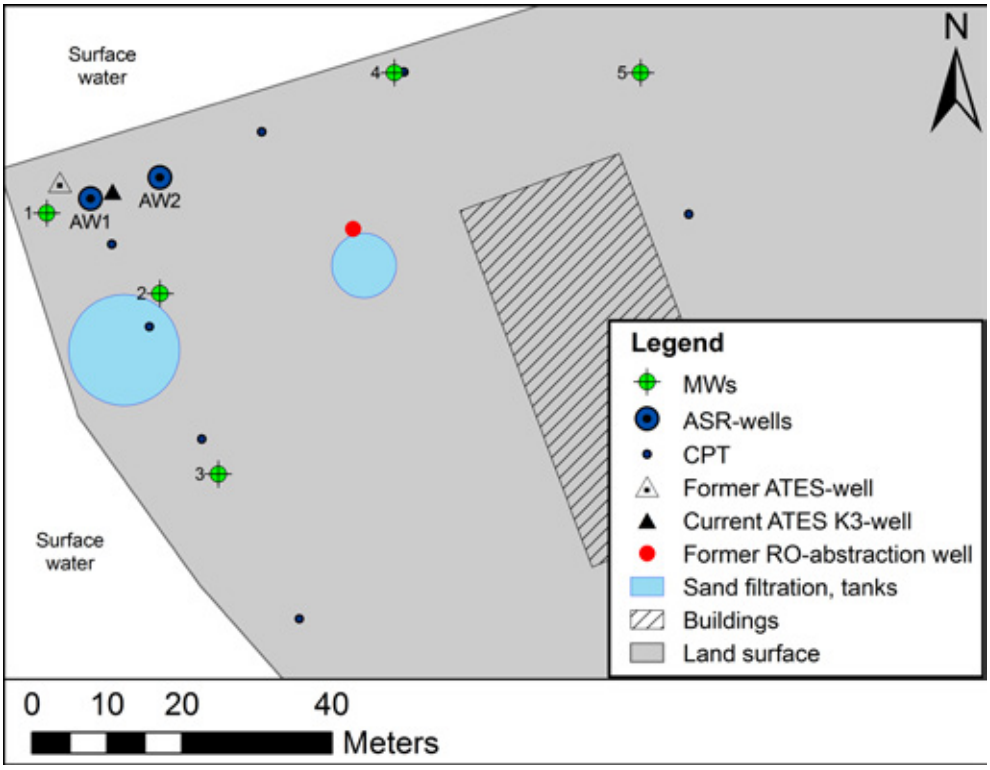

Figure 5-2: Locations of ASR wells (*AW*), ATES wells, and monitoring wells (*MW*). *CPT* = cone penetration test.

5.3.2 Monitoring during the Westland ASR cycle testing

All ASR and monitoring well screens were sampled prior to ASR operation (November and December, 2012). MW1 and 2 were sampled with a high frequency during the first breakthrough of the injection water at MW1 (December 2012, January 2013), while all wells were sampled on a monthly basis. Three times the volume of the well casing was removed prior to sampling. The injection water was sampled regularly during injection phases. All samples were analyzed in the field in a flow-through cell for EC (GMH 3410, Greisinger, Germany), pH and temperature (Hanna 9126, Hanna Instruments, USA), and dissolved oxygen (Odeon Optod, Neotek-Ponsel, France). Samples for alkalinity determination within one day after sampling on the Titralab 840 (Radiometer Analytical, France) were stored in a 250 ml container. Samples for further hydrochemical analysis were passed over a 0.45 µm cellulose acetate membrane (Whatman FP-30, UK) in the field and stored in two 10-ml PE vials, one of which

was acidified with 100 µl 65% HNO_3 (Suprapur, Merck International) for analysis of cations (Na, K, Ca, Mg, Mn, Fe, S, Si, P, and trace elements) using ICP-OES (Varian 730-ES ICP OES, Agilent Technologies, U.S.A.). The second 10 ml vial was used for analysis of F, Cl, NO_2, Br, NO_3, PO_4, and SO_4 using the Dionex DX-120 IC (Thermo Fischer Scientific Inc., USA), and NH_4 using the LabMedics Aquakem 250 (Stockport, UK). All samples were cooled to 4 °C and stored dark immediately after sampling.

CTD-divers (Schlumberger Water Services, Delft, The Netherlands) were used for electronic recording of conductivity, temperature, and pressure in the target aquifer at MW1 (S1-3) and MW2 (S1, 2). Calibrated, electronic water meters were coupled to the programmable logic controller (PLC) of the ASR system to record the operation per well screen.

5.3.3 Set-up Westland ASR groundwater transport model

SEAWAT Version 4 (Langevin et al., 2007) was used to simulate the ASR operation. A half-domain was modelled to reduce computer runtimes. Cells of 1x1 m were applied in an area of 20 x 20 m around the ASR wells. The cell size increased to 2.5 x 2.5 m (30 x 40 m around te well) and was then gradually increased to a maximal cell size of 200 x 200 m at 500 m from the ASR wells (Figure 5-3). The pumping rate of each well screen was distributed over the models cells with the well package based on the transmissivity (thickness x hydraulic conductivity) of each cell. The third-order total-variation-diminishing (TVD) scheme (Leonard, 1988) was used to model advection.

The applied hydrogeological properties loaded in the SEAWAT model are summarized in Table 5-1. Since the regional groundwater flow derived from regional groundwater heads (TNO, 1995) was limited to a few m per year, equal constant heads were imposed at two side boundaries of the aquifers, the top of the model (controlled by drainage) and at the base of the model. No-flow boundaries were given to the other two side boundaries of the model. Constant heads were assigned to the aquifer top based on the local drainage level (top model layer) and the observed heads in Aquifer 2. Initial Cl-concentrations were based on the results of the reference groundwater sampling at MW1. SO_4-concentrations in Aquifer 1 were based on MW2, since these concentration were more representative for the field site. For Aquifer 2, the concentrations in the water abstracted by ATES well K3 and the observation well K3.1 were used (see Figure 5-1). The density of the groundwater was based on the Cl^- concentration using (Oude Essink et al., 2010):

$$\rho_w = 1000 + 0.00134 \cdot Cl \ (mg/l) \tag{5.1}$$

No compensation for temperature was applied, due to the limited temperature differences (average ambient groundwater temperature: 11.4 °C, average injection water temperature: 10.4 °C). A longitudinal dispersivity of 0.1 m was derived from the freshwater breakthrough at MW1 and was applied to the whole model domain.

The recorded pumping rates of the ASR wells and the ATES K3 well were incorporated in the SEAWAT model. The ASR operation was modelled with a properly sealed and an unsealed ATES borehole. In the latter case, a hydraulic conductivity (K) of 1000 m/d was given to the cells (1.0 x 1.0m) in Aquifer 1, Aquitard 2, and Aquifer 2 at the location of the ATES pumping well to force borehole leakage. This K was considered realistic since apart from filter sand around the well screen, the borehole was backfilled with gravel with a grain size of 2-5mm. In other scenarios, the ATES well was moved stepwise towards the fringe of the ASR bubble (10 m further away from AW1 in each scenario), after which Cycle 2 was simulated again.

Table 5-1: Hydrogeological properties of the geological layers in the Westland SEAWAT model. 'VANI' = vertical anisotropy ratio.

Geological Layer	Model layers	Base (m BSL)	K_h (m/d)	VANI (K_h/K_v)	S_s (m^{-1})	n (-)	Initial C (mg/l Cl)	Initial C (mg/l SO_4)
Aquitard 1	6	22.3	0.2 - 1	100	10^{-4}	0.2	2000-3000	4
Aquifer 1 (target aquifer)	12 3	33.7 36.4	35 100	1	10^{-7}	0.3	4000-4800	4
Aquitard 2 (clay-sand)	8	47.5	0.05-10	1-10	10^{-4}	0.2-0.3	3200	160
Aquifer 2 (deeper aquifer)	6	96	12	1	10^{-6}	0.3	4100-7900	331-375

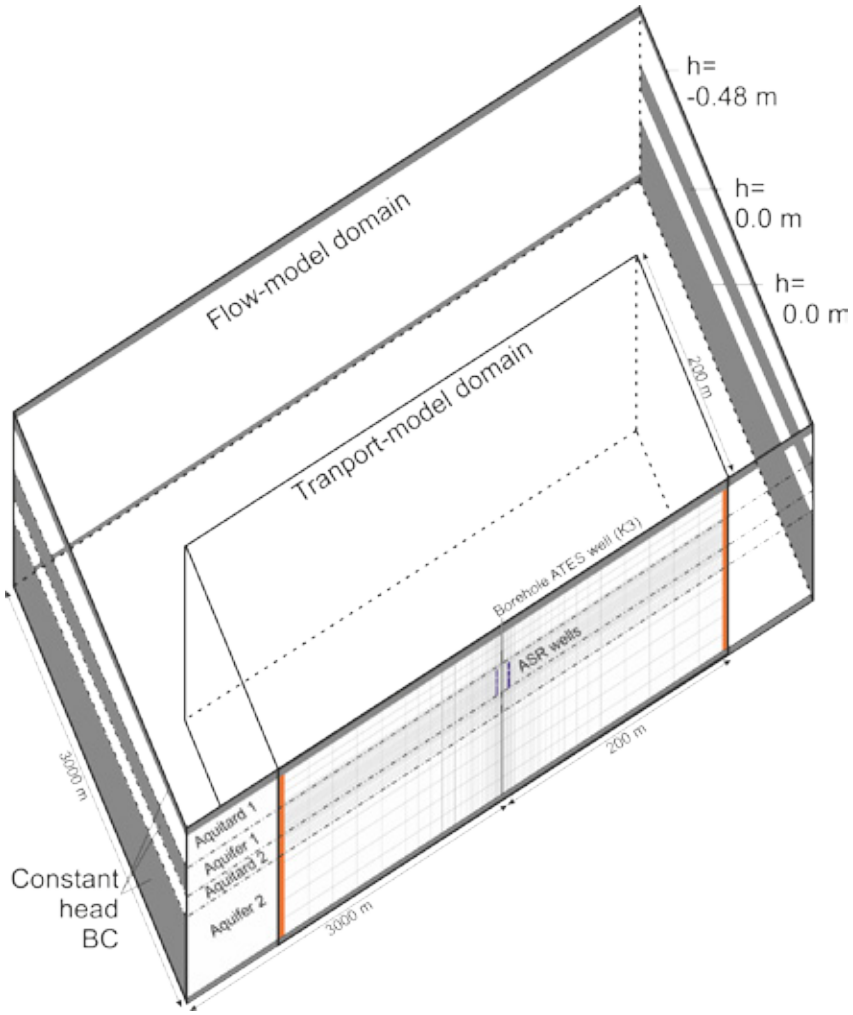

Figure 5-3: Set-up of the Westland ASR groundwater transport model (half-domain). 'BC' = boundary condition.

5.3.4 The maximal recovery efficiency with and without leakage at the Westland ASR site.

The SEAWAT groundwater model, loaded with the aquifer characteristics in Table 5-2, was used to analyze the performance of the MPPW-ASR system for the current and a 'normal field site': i.e. without leakage from deeper aquifers via a perforation, or after sealing of the perforation. The SEAWAT model was used to simulate three ASR-cycles with the representative operational characteristics from Table 5-2 for the Westland

site (Zuurbier et al., 2012). Once the wells salinized in each cycle (Cl>50 mg/l, the Cl limit for this ASR site, indicating water should be recovered practically unmixed), the model was stopped, and the length of the stress period with recovery was adjusted, such that no water with Cl>50 mg/l was recovered. Subsequently the model was run again after adding another cycle.

Table 5-2: Set-up of the modelled, representative ASR-cycle for the Westland ASR trial.

Stage	Duration	Pumping rate
Infiltration	120 days	60,000 / 120 = 500 m^3/d
Storage	30 days	0 m^3/d
Recovery	120 days	-60,000 / 120 = -500 m^3/d
Idle	65 days*	0 m^3/d

** Longer when early salinization occurred during recovery.*

5.4 Results

5.4.1 Hydrogeological setting

The target aquifer for ASR (Aquifer 1) is 14 m thick and consists of coarse fluvial sands (average grain size: 400 µm, Figure 5-4) with a hydraulic conductivity (K) of 30 – 100 m/d derived from head responses upon injection. Aquifer 2 (target aquifer ATES) has a thickness of more than 40 m, but is split up into two parts at the ATES well K3 by a 20 m thick layer of clayey sand and clay. A blind section was installed in this interval, and the borehole was backfilled with coarse gravel in this section. The K-value of the fine sands in Aquifer 2, as derived from a close by pumping test, is 10 to 12 m/d, which is in line with the estimated K-value from grain size distribution (Mos Grondmechanica, 2006). The effective screen length of K3 in this aquifer is only 8 (upper section: 53-61 m-BSL) and 5 m (lower section: 80-85 m-BSL).

The groundwater is typically brackish, with observed Cl-concentrations ranging from 3,795 to 4,650 mg/l in Aquifer 1 and approximately 5,000 mg/l in Aquifer 2. A sand layer in Aquitard 2 contains slightly fresher water (Cl = 3,270 mg/l). SO_4 is a useful tracer to discern the brackish groundwater of Aquifer 1 and 2, as it is typically virtually absent in Aquifer 1, whereas it is high in Aquifer 2. Aquifer 1 contains presumably younger groundwater, infiltrated after the Holocene clay/peat cover was

completely formed, while Aquifer 2 contains older groundwater, infiltrated through a thinner clay cover which limited SO_4-reduction, see Stuyfzand (1993) for more details. Concentrations of 300 to 400 mg/l SO_4 were observed in this deeper aquifer. HCO_3 (approximately 1300 mg/l in Aquifer 1 and 600 mg/l in Aquifer 2) was another suitable tracer, yet less distinct.

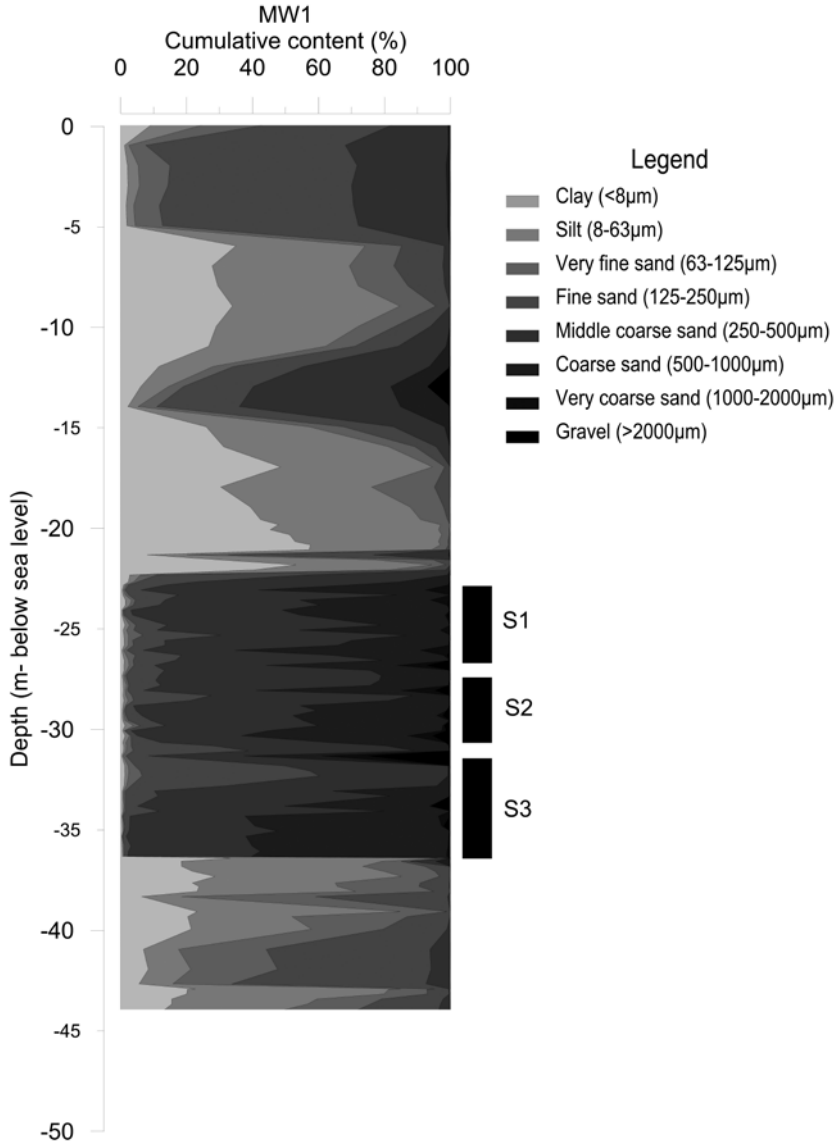

Figure 5-4: Cumulative grain size contents observed at MW1 (at 5 m from ASR well 1). S1-S3 mark the depth intervals of the individual ASR well screens.

5.4.2 Cycle 1 (2012/2013): first identification of borehole leakage

Despite the improved design of the ASR system with the MPPW, a rapid and severe salinization of even shallow recovery wells was observed within the first days of recovery, after injecting freshwater for about 1 month (Figure 5-5). Remarkably, the salinization at ASR well 1 (AW1) preceded salinization of the monitoring wells situated further from the ASR wells (MW1, MW2). High SO_4 concentrations (up to >50 mg/l) were found in the recovered water, which could not be explained by the SO_4-enrichment upon pyrite oxidation by oxygen observed in the injected water, which was observed to be less than 15 mg/l.

The SEAWAT model underlined that tilting of the freshwater-saltwater interfaces at the fringe of the ASR bubble did not cause the early salinization observed, as this would have led to a significantly later salinization (Figure 5-6), even if the recovery period was extended (results not shown). SO_4-production by pyrite oxidation was neglected in the model, but this would not explain the observed SO_4 concentrations >15 mg/l. When the leaky borehole was incorporated in the model (by assigning K=1000 in a 1 x 1 m column at the location of the current ATES well), it was able to introduce the early recovery of deep (SO_4-rich) water (Figure 5-7). Other scenarios that were tested, but were found unable to improve the simulation of the observed SO_4-trends were: leakage via the abandoned ATES K3 well further from the ASR wells (arrival of SO_4 too late), a high-K borehole (2000 m/d; arrival too early, flux too high), a low-K borehole (500 m/d; arrival too late, flux too low), a vertical anisotropy in the aquifers ($K_h/K_z = 2$; arrival too early, flux too high), and omission of the deep cold water abstraction from Aquifer 2 via the ATES well in Aquifer 2 (SO_4-flux too high).

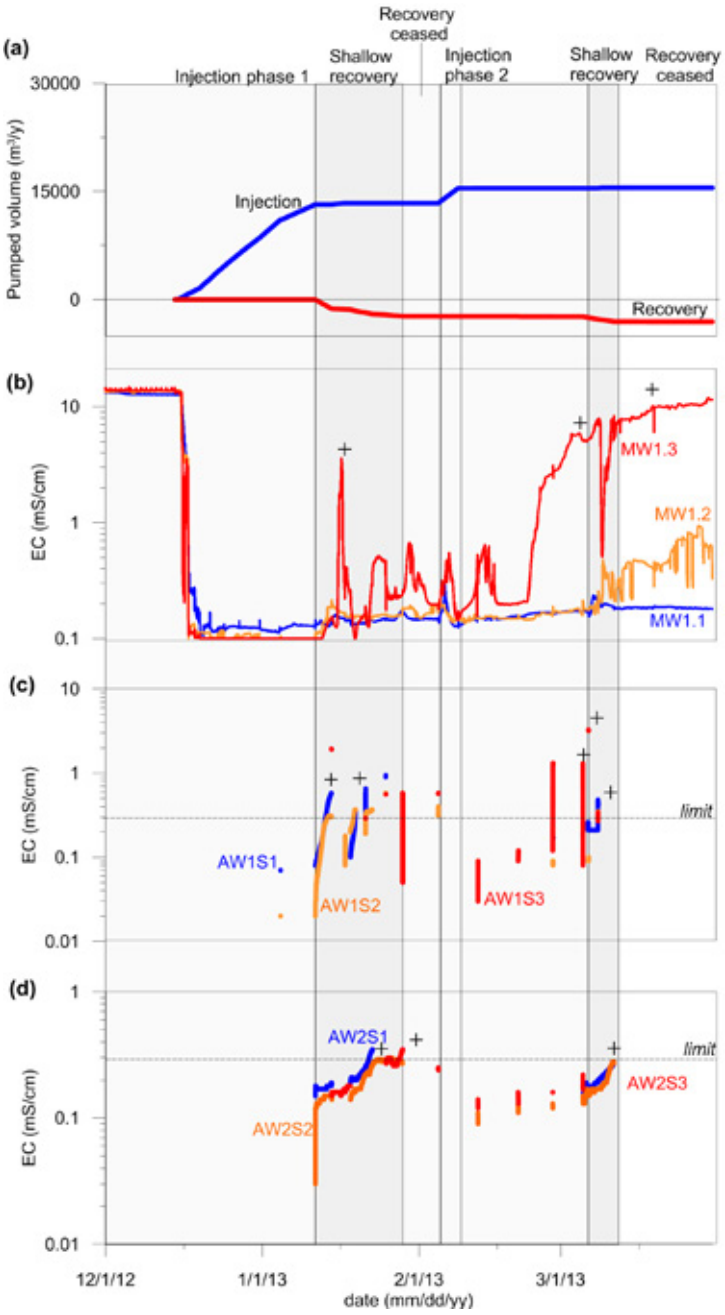

Figure 5-5: Pumping of the ASR system during Cycle 1 (2012/2013), EC observations at MW1 (5 m from AW1), and the EC in the recovered water at AW1 and AW2. MW= monitoring well, AW= ASR well. Presence of increased SO_4 concentrations (>15 mg/l; deep saltwater) are marked by '+', while its absence is marked by '-' (< 15 mg/l; indicating shallow brackish water).

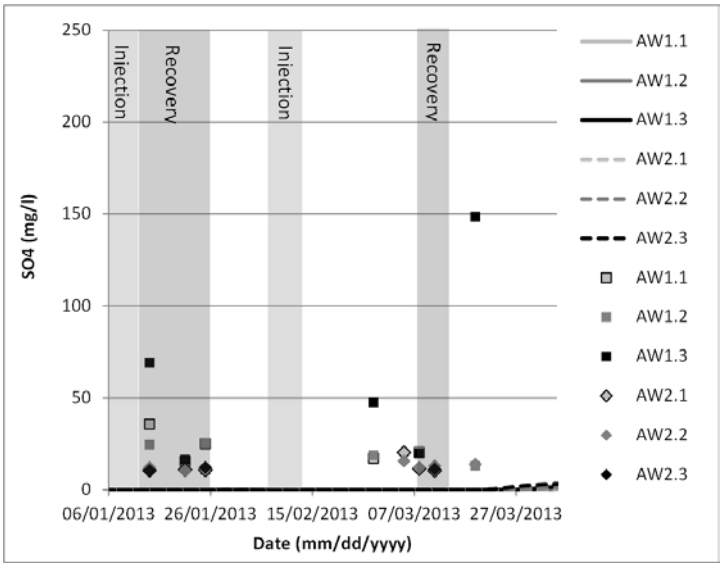

Figure 5-6: Modelled (solid lines) and observed (data points) SO_4 concentrations without borehole leakage. High concentrations indicate admixing of deeper saltwater. Observed SO_4^{2-} concentrations exceed the modelled concentrations by far.

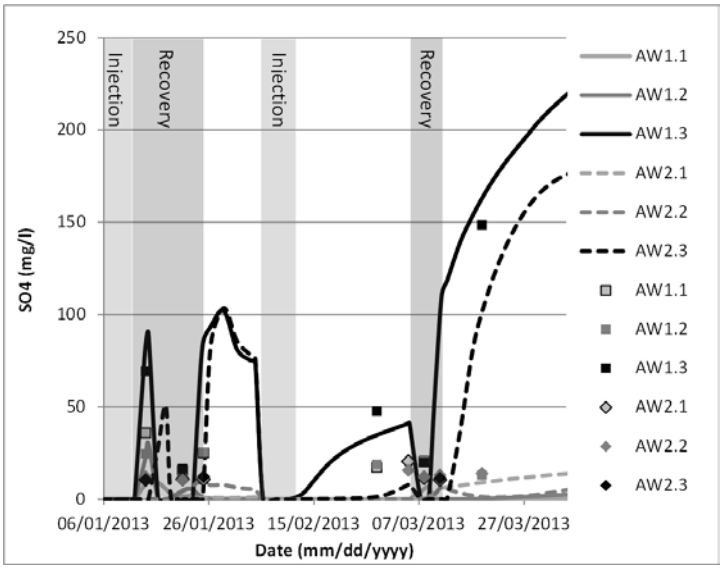

Figure 5-7: Modelled (solid lines) and observed (data points) SO_4 concentrations. Borehole leakage at the location of the current ATES K3 well via a 1x1 m borehole with K=1000 m/d. High concentrations indicate admixing of deeper saltwater. Observed SO_4 concentrations become in line with the modelled concentrations.

The hydrochemical observations and model outcomes of Cycle 1 indicated that the source of the early salinization was the intrusion of saltwater from Aquifer 2. Considering the lithology, thickness, and continuity of Aquitard 2 (confirmed by grain size analyses and cone penetrating tests (n=8, Figure 5-2) on the site), leakage via natural pathways through this separating layer was unlikely. According to the rate and sequence of salinization, the leakage could well be situated at the ATES K3 well close to AW1.

5.4.3 Cycle 2 (2013/2014): improving the ASR operation

Prior to Cycle 2, it was attempted to seal the borehole of the abandoned ATES well K3 (approximately 5 m from ASR well AW1) by injection of Dämmer (Heidelberg Cement, Germany) at the depth interval from 52 to 36 m-BSL. The current ATES well K3 (situated between ASR well AW1 and AW2) was left unaltered as it was still in operation. Cycle 2 started with the injection of 66,178 m^3 of rainwater using both ASR wells between September 2013 and March 2014, which was followed by recovery solely at the downstream AW2 (start: March 5, 2014). A rapid salinization by SO_4-rich brackish water was again observed (Figure 5-8) and the recovery was terminated after 26 days (March 21, 2014) after recovering no more than 2,500 m^3. This time, a monitoring well present in the gravel pack of the ATES K3 well (coded K3O1; a 1 m-well screen at 33 m-BSL) was sampled and equipped with a CTD-diver and continuously pumped with approximately 1 m^3/h, unravelling high ECs and presence of SO_4-rich saltwater from the deeper aquifer (Figure 5-8). This presence of intruding deep saltwater was also found at MW1S3 (5m from the ASR wells), presumably as a consequence of re-injecting part of the abstracted freshwater from the shallow AW2S1 wells screen at the deeper AW2S3 well screen and density-driven flow, which caused lateral displacement of earlier intruded saltwater towards MW1S3. The observed Cl-concentration (268 mg/l) on April 2, 2014 at MW1S4 (situated in Aquitard 2 at 5 m from AW1) was significantly lower than at MW1S3 (2,528 mg/l) and K3O1 (3,341), indicating that salinization of the shallow target aquifer (Aquifer 1) precedes salinization of the deeper Aquitard 2, which suggests a by-pass is present.

To re-enable recovery of freshwater, AW1S3 and AW2S3 were transformed to interception wells or 'Freshkeepers' (Stuyfzand and Raat, 2010; Van Ginkel et al., 2014), abstracting the intruding saltwater and injecting this in a deep injection well in Aquifer 2 at 200 m distance from the ASR-site. This way, the ASR-system could again attain an acceptable water quality (practically unmixed rainwater) at AW2S1 and AW1S2 (from April 15, onwards). As a consequence, the deeper segments of the target aquifer (S3 levels, Figure 5-8bcd) first freshened, followed by again salinization as

recovery proceeded. Saline water was continuously observed at K3O1, indicating that leakage via the K3 borehole continued. After recovery of in total 12,324 m^3 of practically unmixed rainwater (18.6% of the injected water), the recovery had to be ceased due to the increased salinity. During this last salinization, the water at the deeper (S3-)levels of the target aquifer at AW1, MW1, and MW2 showed low SO_4 concentrations, indicating salinization by saltwater from Aquifer 1 caused by buoyancy effects instead of intruding, deeper saltwater. High SO_4 concentrations (>100 mg/l) were only found close to the current K3 ATES well (the presumable conduit) in this phase (at AW1 and K3O1).

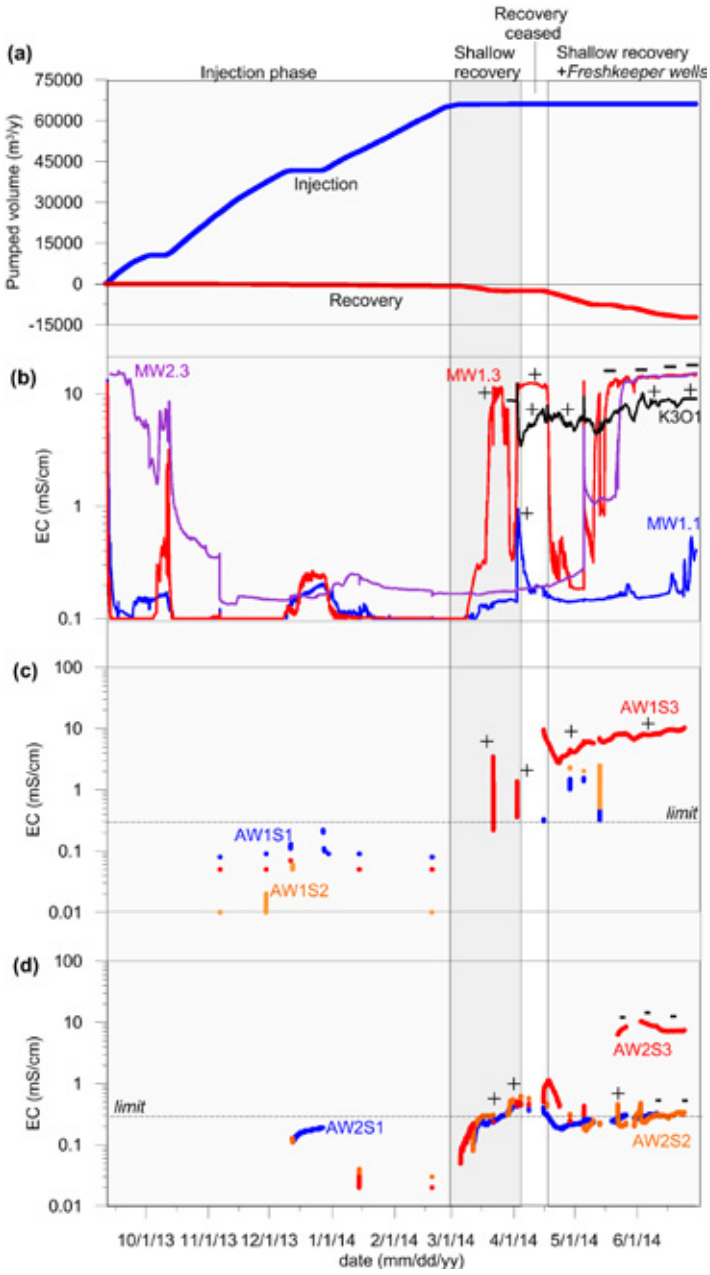

Figure 5-8: Pumping of the ASR system during Cycle 2 (2013/2014), EC observations at MW1 (5 m from AW1), and the EC in the recovered water at AW1 and AW2. AW2.1 and AW2.3 were used for freshwater recovery (12,324 m^3). Presence of increased SO_4 concentrations (>15 mg/l; deep saltwater) are marked by '+', while its absence is marked by '-' (< 15 mg/l; indicating shallow brackish water).

The SEAWAT model with leakage via the borehole of the current ATES well K3 was able to reasonably simulate the water quality trends regarding SO_4 and Cl in Cycle 2 (Figure 5-9 and Figure 5-10). Remaining deviations in observed concentrations were attributed to uncertainties in the model input, mainly aquifer heterogeneity, potential stratification of the groundwater quality in Aquifer 2, and disturbing abstractions and injections in the surroundings, mainly by ATES and brackish water reverse osmosis systems, the latter abstracting in Aquifer 1 and injecting in Aquifer 2.

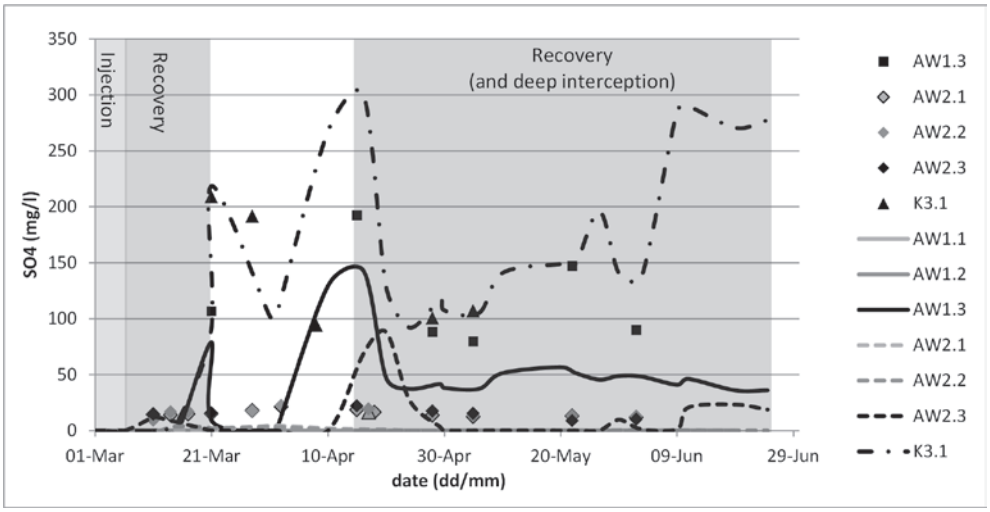

Figure 5-9: Modelled and observed SO_4 concentrations at the most relevant well screens.

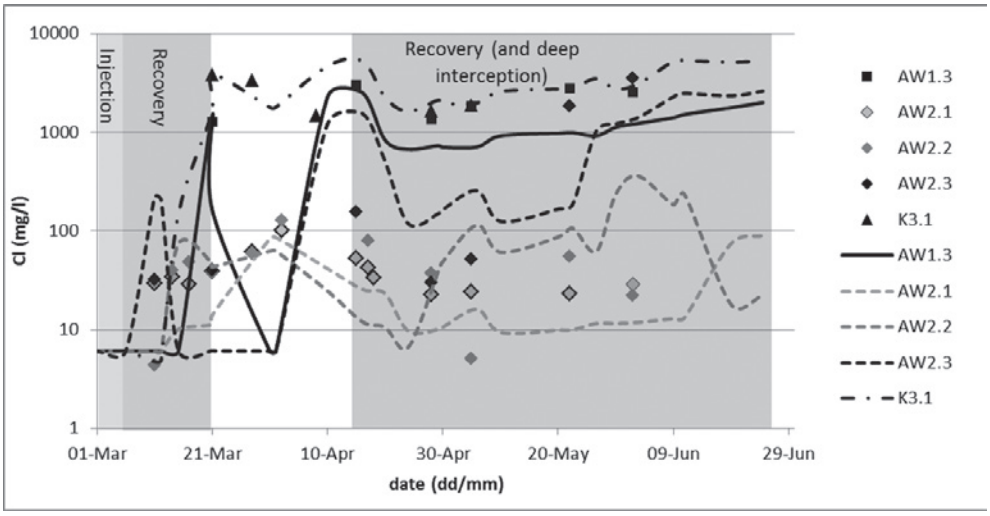

Figure 5-10: Modelled and observed Cl concentrations at the most relevant well screens.

Modelling of Cycle 2 demonstrated that salinization during recovery was independent of the injected freshwater volume. Salinization occurred after recovery with the same rate as in Cycle 1, despite a four times larger injection volume. Analysis of the modelled concentration distribution showed that injected freshwater could not reach deep into the deeper saline aquifers since the freshwater head in the leaky ATES borehole during injection was more or less equal to the freshwater head in the deeper saltwater aquifer. In other words: little freshwater was pushed through the conduit into the deeper aquifer. Further on, the freshwater that did reach the deeper aquifer got rapidly displaced laterally as a result of buoyancy effects (Figure 5-11).

A significant head difference (Δh(fresh)= 0.3 m to 0.65 m) was observed in the model during recovery. In combination with the high permeability of the ATES borehole, this resulted in a significant intrusion of deeper (SO_4-rich) saltwater. Even during storage phases, a freshwater head difference (Δh(fresh)= 0.15 m) was observed in the SEAWAT model as a consequence of the earlier replacement of saltwater by freshwater in the target aquifer, causing intrusion of deep saltwater, yet with a lower rate than during recovery.

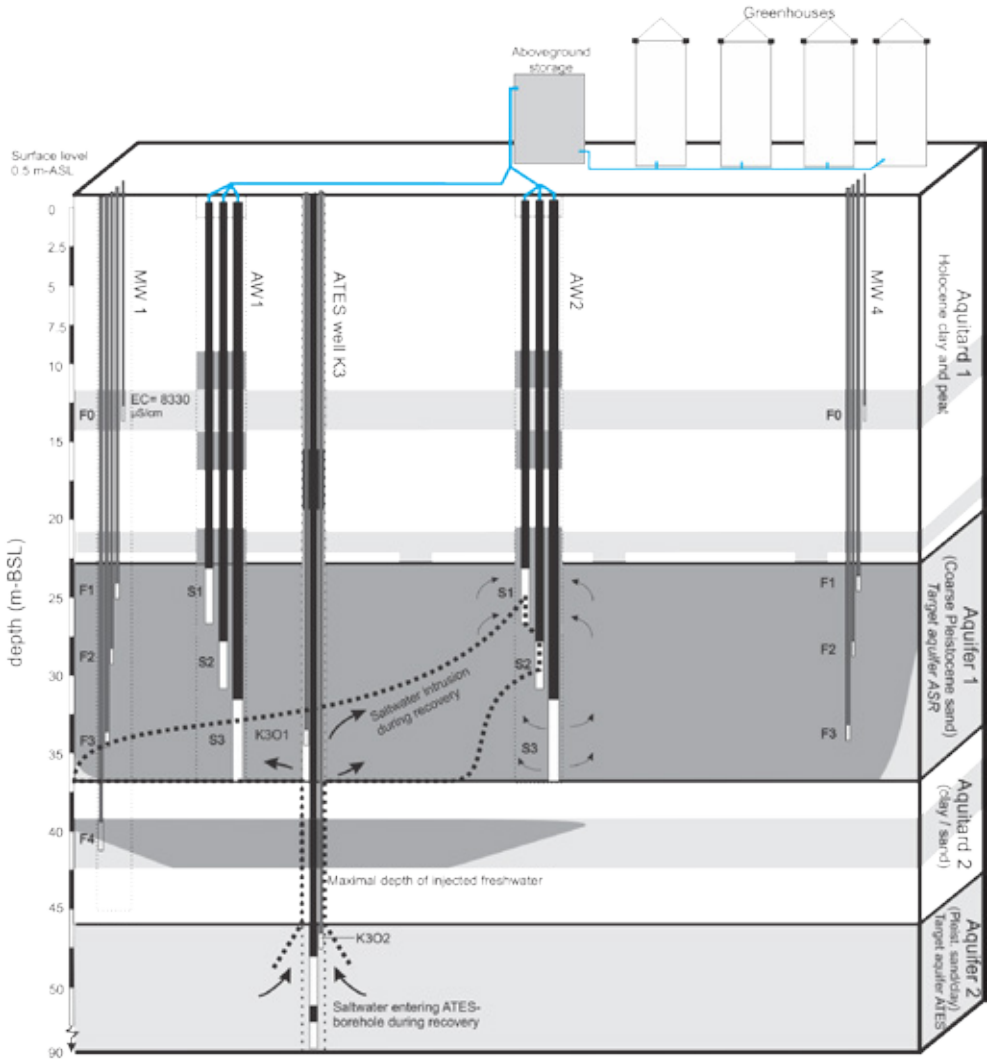

Figure 5-11: Deep saltwater intrusion via the current ATES K3 borehole during shallow recovery of injected freshwater at the Westland ASR site at the start of Cycle 2.

5.4.4 Analysis of the leakage flux via the borehole

An analytical solution was presented by Maas (2011) to calculate the vertical leakage via a gravel or sand pack. In this solution, it is presumed that an aquitard was pierced during drilling and the annulus was filled up with sand or gravel without installing a clay seal. The leakage is then calculated as function of the different hydraulic conductivities, pressure difference, and the radius of the borehole and well screen (5.2):

$$Q_{VGP} = \frac{\Delta h_{GP}}{W} \tag{5.2}$$

where: Q_{VGP} = vertical leakage via gravel pack (m^3/d), Δh_{GP} = hydraulic head difference between 2 sections of the gravel pack, one being the inflow and the other the outflow section (m), and W = leakage resistance (d/m^2) and is calculated as (5.3):

$$W \approx \frac{(0.005(\ln(\alpha))^2 - 0.058\ln(\alpha) + 0.19)}{(r_1\sqrt{K_{HIN}K_{VIN}})} \tag{5.3}$$

And a as (5.4):

$$\alpha = \frac{K_{VGP}(r_1^2 - r_0^2)}{2K_{VIN}r_1^2} / \tag{5.4}$$

where: r_0 = radius of well screen [m]; r_1 = radius of borehole [m]; K_{VGP} = vertical hydraulic conductivity of gravel pack [m/d]; K_{VIN} = vertical hydraulic conductivity of inflow aquifer layer [m/d]; K_{HIN} = horizontal hydraulic conductivity of the inflow aquifer layer [m/d].

Calculating the leakage flux using the Δh_{GP} from the SEAWAT model underlines that the pressure differences induced by density differences and enhanced during abstraction for freshwater recovery in combination with an unsealed borehole leads to a saltwater intrusion (Q_{VGP}) of around 50 to 200 m^3/d (Table 5-3), which is in line with the observed leakage flux in the SEAWAT model.

Table 5-3: Calculated leakage flux QVGP via the (unsealed) borehole based on Maas (2011) for different net recovery rates ($Q_{recovery, net}$).

		Storage (no recovery)	Low recovery rate	High recovery rate
$Q_{recovery, net}$	(m^3/d)	0	77	371
Δh_{GP}	(m)	0.15	0.30	0.66
Q_{VGP}	(m^3/d)	49	99	215
W	(m^2/d)	0.0031	0.0031	0.0031
α		4.7	4.7	4.7
r_0	(m)	0.1	0.1	0.1
r_1	(m)	0.4	0.4	0.4
K_{HIN}	(m/d)	100	100	100
K_{VIN}	(m/d)	100	100	100
K_{VGP}	(m/d)	1000	1000	1000

5.4.5 Obtaining the 'safe distance' from suspect boreholes

When the leaky ATES borehole was located to 10, 20, 30, and 40 m from the nearest ASR well (AW1), the saltwater intrusion in Cycle 2 would obviously decrease while recovery efficiencies (REs) would increase (Figure 5-12). Since the maximal radius of the unmixed freshwater bubble with the yearly injected volume at the Westland ASR site is around 50 m, this can be regarded as the 'safe distance'. In other words, any leakage within the bubble of recoverable freshwater will lead to early termination of recovery. The closer the leakage is to the ASR well, the earlier the arrival of contaminated water and thus the lower the RE will become. From Figure 5-12 it can be derived that there is a virtually linear relationship between the RE decrease and the decrease in the distance of the leakage from the ASR well when low concentrations in the recovered water are desired (little or no mixing allowed). When more mixing is allowed, on the other hand, the negative effects of leakage far from the ASR well becomes less relevant due to the predominating effect of mixing with native groundwater from Aquifer 1. The derived breakthrough curves also indicate that a more or less stationary situation develops after a rapid concentration increase. The contribu-

tion of deep saltwater to the injected water is then almost constant. The second rapid increase marks the arrival of the fringe of the injected freshwater bubble and therefore salinization by saltwater from the target aquifer itself. The contribution of the borehole leakage to salinization then rapidly decreases as Δh_{GP} will decrease.

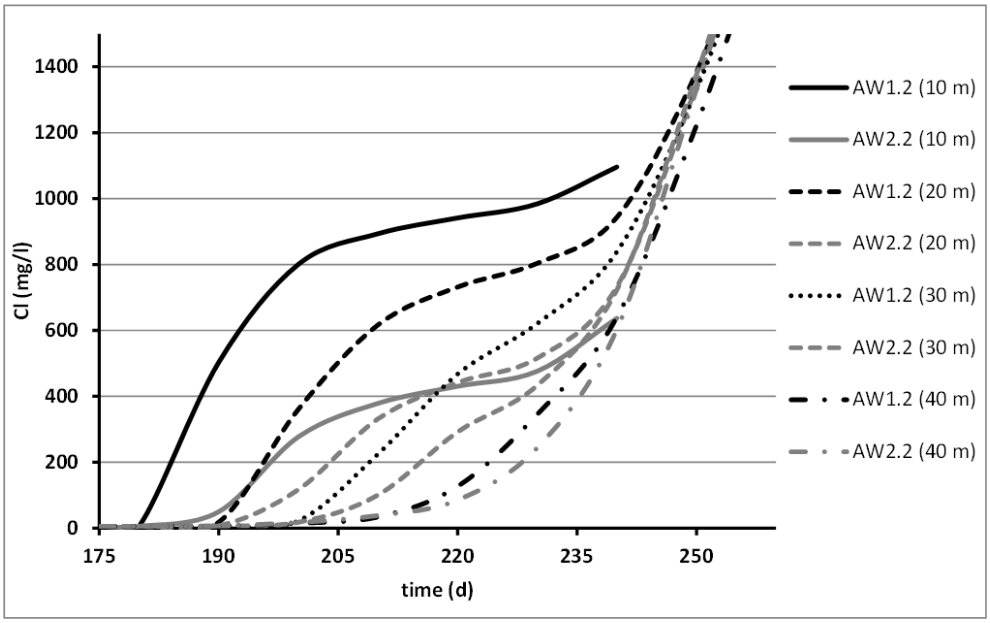

Figure 5-12: Modelled Cl concentrations in the water recovered from the ASR wells in case of borehole leakage at varying distances from the ASR wells.

5.4.6 The maximal recovery efficiency with and without leakage at the Westland ASR site.

The SEAWAT model was used to evaluate the potential ASR performance at the Westland field site with three different ASR strategies (Table 5-4), with and without the saltwater leakage. During the 120 days of recovery it was aimed to recover as much of freshwater (marked by Cl <50 mg/l) as possible. Equal abstraction rates were maintained for both ASR wells (AW1 and AW2) in the scenario's without leakage, while only AW2 was used in the scenario's with leakage.

The RE with conventional, fully penetrating ASR wells will be limited to around 30% of the injected freshwater in a case without the saltwater leakage (Figure 5-13). For the case with leakage, freshwater recovery will be impeded by the short-circuiting during the storage phase: the wells will produce brackish water already at the start of the recovery phase. The use of an MPPW for deep injection and shallow recovery has

a limited positive effect due to the limited thickness of the aquifer: one-third of the injected water can be recovered from an undisturbed subsurface. The improvement of RE by introduction of the MPPW is limited in comparison with the conventional ASR well since some brackish water from Aquitard 2 was found to move up to the shallower recovery wells of the MPPW-system ('upconing') rapidly after the start of recovery. The slight increase in Cl concentrations caused by this process is sufficient to terminate the recovery due to exceedence of the salinity limit. Before the fringe of the freshwater bubble reached the recovery wells, recovery was already terminated. In the case of saltwater leakage and MPPW-ASR, salinization occurred within 2 days, limiting the RE to only 1%.

Table 5-4: Modelled recovery efficiencies at the Westland ASR site without short-circuiting using different pumping strategies. The relative pumping rate per MPPW well screen is given for each particular screen.

Strategy	Distribution pumping rate	RE (short-circuiting / no short-circuiting)	Intercepted brackish water (via deep (S3-) wells)
Conventional ASR-well	In: 100% via one fully penetrating well Out: 100% via one fully penetrating well	Year 1: 0/15% Year 2: 0/25% Year 3: 0/30% Year 4: 0/32%	
Deep injection, shallow recovery (MPPW-ASR)	In: 10/20/70% (Year 1) In : 0/20/80% (Year 2-3) Abstract: 60/40/0% (Year 1-3)	Year 1: 1/19% Year 2: 1/ 29% Year 3: 1/32% Year 4: 1/33%	
MPPW-ASR + 'Freshkeeper'	In: 10/20/70% (Year 1) In : 0/20/80% (Year 2) Abstract: Decreasing from 60/40/0% to 60/0/0% (Year 1-3) Intercept Freshkeeper: increasing from 100 to 500 m^3/d	Year 1: 29/40% Year 2: 32/46% Year 3: 33/47% Year 4: 33/48%	Year 1: 32,700/ 18,500 m^3 Year 2: 33,000 / 20,500 m^3 Year 3: 31,900 / 21,500 m^3 Year 4: 31,500 / 19,300 m^3

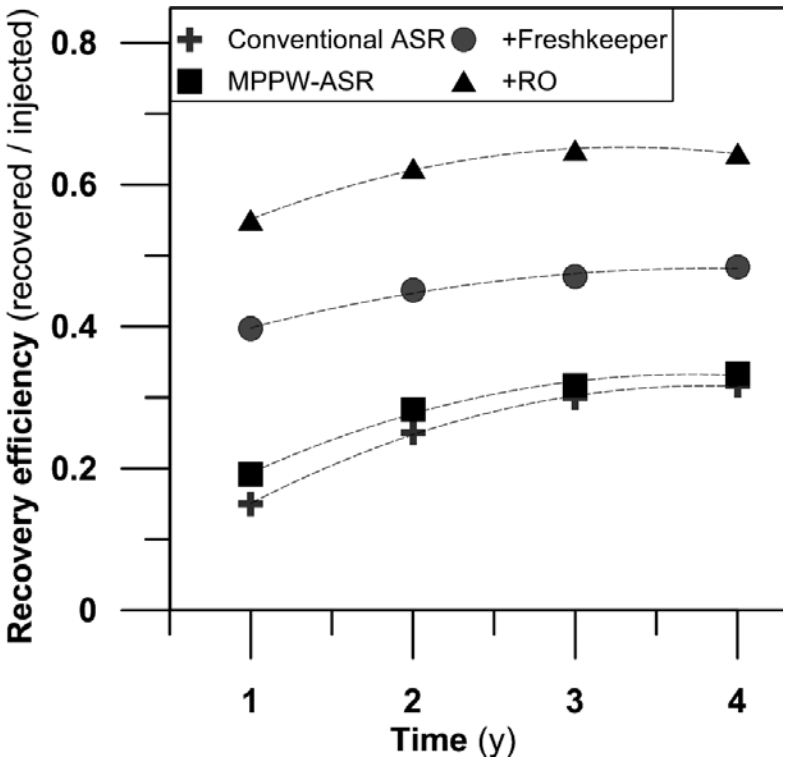

Figure 5-13: Recovery efficiencies at the Westland ASR site with and without the borehole leakage resulting from the SEAWAT groundwater transport model for a conventional ASR well (one well screen, fully penetrating), deep injection and shallow recovery via multiple partially penetrating wells without a 'Freshkeeper' (scenario MPPW-ASR), for a MPPW in combination with a 'Freshkeeper' (scenario Freshkeeper), and for a scenario in which RO is applied on the intercepted brackish water to produce additional freshwater (50% of the abstracted brackish water).

The introduction of the Freshkeeper to protect the shallow recovery wells by interception of this deeper saltwater significantly extended the recovery period, enabling recovery of 40% in the first year for direct use. Ultimately, this will yield a RE of almost 50% of virtually unmixed (Cl <50 mg/l) injected freshwater in Cycle 4. This will require interception of 18,500 m^3 (Cycle 1) to 21,500 m^3 (Cycle 3) of brackish-saline groundwater, while ultimately almost 30,000 m^3 of freshwater is recovered.

When this ASR operational scheme with the Freshkeeper was applied to the field pilot, where short-circuiting saltwater hampered freshwater recovery, approxi-

mately one-third of the injected freshwater could be recovered. The ASR-well close to the leaking borehole (AW1) was unable to abstract freshwater in this case. Only AW2 could be used for freshwater recovery, in the end only via the shallowest well (AW2S1). The freshwater loss by short-circuiting could not be eliminated completely since a large volume of freshwater is also abstracted during the required interception of the intruding deeper saltwater. The RE will therefore remain lower than in an undisturbed geological setting (RE almost 50%). At the same time, the required interception of brackish water will be higher (Table 5-4), with a total intercepted volume of more than 30,000 m^3, while around 20,000 m^3 of freshwater is recovered.

5.5 Discussion

5.5.1 Saltwater intrusion during the Westland ASR pilot

In this study, the first focus was on the causes for the observed significantly lower freshwater RE of the system. This RE was initially less than a few percent, whereas recovery of around one-third of the injected water was expected. The hydrochemical analyses clearly indicated that the observed salinization was caused by unexpected intrusion of deeper saltwater, as marked by substantially higher SO_4 concentrations, which could not be caused by arrival of saltwater from the target aquifer or the upper aquitard, or by the SO_4-release upon oxidation of pyrite in the target aquifer. For this reason, the early salinization could not be caused by stronger buoyancy effects than initially expected, for instance by a higher K or higher ambient salinities in the target aquifer. The high SO_4 concentrations also excluded lateral drift of injected water, as this would also have led to salinization by saltwater with low SO_4 concentrations. Additionally, lateral drift would also result in limited REs after addition of the Freshkeeper, which was not the case.

Knowing the source of the salinization, several transport routes can be presumed. First of all, intrusion of deep saltwater may occur when Aquitard 2 has a significantly higher K than derived from grain size analyses, despite the distinct groundwater qualities observed that suggest a reliable separation. A more diffuse salinization via Aquitard 2 can then be expected. However, this salinization would be more gradual and better distributed around the wells. It would also mean that Aquitard 2 would quickly freshen during injection and salinize first during recovery. However, the slower salinization of Aquitard 2 observed at MW1S4 with respect Aquifer 1 (observed at MW1S3 and K3O1) indicated that Aquitard 2 is by-passed by deeper saltwater during recovery. The presence of (a) conduit(s) provides (a) likely pathway(s) for by-pass-

ing saltwater, meaning short-circuiting was occurring between Aquifer 1 and 2. The SEAWAT model outcomes underlined that this can indeed explain the early and rapid intrusion by deep saltwater. Since the highest Cl and SO_4 concentrations were found in the borehole of the current ATES K3 well (K3O1), this borehole provides the most likely location of one or more conduits. Natural conduits are considered unlikely due to continuity and thickness of Aquitard 2 observed in the surrounding of the ASR wells and the geological genesis (unconsolidated, horizontal lagoonal deposits). The conduit(s) at or around the ATES K3 borehole may originate from the time of installation (improper sealing) or operation, as recorded operation data of the ATES system indicates that the maximum injection pressure in the well of 1 bar (based on Olsthoorn (1982)) was incidentally exceeded during maintenance in 2009.

5.5.2 The consequences of short-circuiting on ASR in coastal aquifers

The potential effects of short-circuiting induced by deep perforation on aquifer storage and recovery (ASR) in a shallower coastal aquifer were subsequently explored. In this case of freshwater storage in a confined, brackish aquifer, pressure differences induced by the difference in density between injected freshwater and native groundwater provoked intrusion of native groundwater in the injected freshwater bubbles via the presumed conduit. It is illustrated that a complete failure of the ASR system can occur when the short-circuiting via such a conduit occurs close to the ASR wells and little mixing with ambient saltwater is allowed.

The negative effects of short-circuiting on ASR in coastal aquifers are mainly related to the hydraulics around the conduits. First, freshwater is not easily transported downwards through the conduits into a deeper aquifer, while it is easily pushed back into the shallower aquifer when infiltration is stopped or paused. Secondly, the freshwater reaching a deeper aquifer is subjected to buoyancy effects and migrates laterally in the top zone of this deeper aquifer. Finally, during storage and especially during recovery, the pressure differences in combination with a high hydraulic conductivity induce a strong flux of saltwater from the whole deeper aquifer into the shallower ASR target aquifer, where a relatively low hydraulic head is present. This short-circuiting induced by such a pressure difference is hampered by the low permeability of the aquitard in a 'pristine situation'. A continuous, undisturbed aquitard is therefore indispensable for the success of ASR in such a setting, as intrusion of deeper saltwater is fatal for the ASR performance.

With an increasing distance between the ASR wells and a nearby conduit, the proportion of mixed saltwater in the recovered water decreases while the arrival time increases. When the conduit is situated outside the radius of the injected freshwater

body in the target aquifer, a decrease in RE is not to be expected.

The Westland field example highlights how design, installation, and operational aspects are vital in the more-and-and more exploited subsurface in densely-populated areas. First of all, old boreholes are unreliable and their presence should better be avoided when selecting new ASR well sites. Secondly, installation and operation of (especially injection) wells should be regulated by strict protocols to prevent the creation of new pathways for short-circuiting. Finally, it is important to recognize that similar processes may occur in unperturbed coastal karst aquifers, where natural vertical pipes can be present (Bibby, 1981; Missimer et al., 2002).

5.5.3 Mitigation of short-circuiting on ASR in coastal aquifers

To mitigate the short-circuiting and improve the freshwater recovery upon aquifer storage under these unfavorable conditions, several strategies can be recognized. Obviously, sealing of the conduits would be the most effective remedy. However, it may not be viable to 1) locate all conduits, for instance when the former wells are decommissioned or when the confining clay layer is fractured upon deeper injection under high pressures, and 2) successfully seal a conduit at a great depth. This underlined by the fact that limited reports of successful sealing of deep conduits can be found.

Apart from sealing, one can also try to deal with these unfavorable conditions. Multiple partially penetrating wells (MPPW) were installed at the Westland ASR site, which enabled interception of intruding saltwater by using the deeper well screens as 'Freshkeepers'. After this intervention, about one-third of virtually unmixed injected freshwater becomes recoverable. This way, the RE is brought to a level similar to the level obtained by an MPPW-equipped ASR system without the Freshkeeper interception and without short-circuiting, while the RE would otherwise remain virtually null. It does require interception of a significant volume of brackish-saline groundwater, however, which must be injected elsewhere or disposed of.

A significant part of the unmixed freshwater is blended with saltwater in the Freshkeeper wells, such that the freshwater recovery becomes lower than in the situation in which the Freshkeeper is applied and saltwater intrusion via short-circuiting is absent. At the Westland field site, this is compensated by desalinating the intercepted brackish-saline groundwater, which is a suitable source water for reverse osmosis (RO) thanks to its low salinity. The freshwater (permeate) produced in this process is used for irrigation, while the resulting saltwater (concentrate) is disposed of in Aquifer 2. The resulting RE increase is plotted in Figure 5-13. Even when no unmixed freshwater is available, desalination of injected water mixed with groundwater can be continued with this technique to further increase the RE. In comparison with conven-

tional RO this leads to a better feed water for RO (lower salinity), while salinization of the groundwater system by a net extraction of freshwater is prevented by balancing the freshwater injection and abstraction from the system.

5.5.4 On the performance of ASR in coastal aquifers without leakage: upconing brackish water from the deeper aquitard

In case of a strict water quality limit and relatively saline groundwater, brackish water upconing from the deeper confining aquitard toward shallow recovery wells is a process to take into account, apart from the buoyancy effects in the target aquifer itself. This was shown by the SEAWAT model runs without short-circuiting, which showed a small increase in Cl^- concentrations at the ASR wells prior to the full salinization caused by arrival of the fringe of the ASR bubble. The SEAWAT model indicated that the (sandy) clay/peat layer (Aquitard 2) below the target aquifer was the source of upconing brackish-saline groundwater. Although this layer has a low hydraulic conductivity, it is not impermeable and salinization via diffusion can occur in this zone, while brackish pore water can physically be extracted from this aquitard. The transport processes in this deeper aquitard are comparable with the borehole leakage water via conduits in this aquitard: freshwater is not easily pushed downwards during injection, but brackish water is easily attracted during recovery. After the recovery phase this zone salinizes until the next injection phase starts, so a gradual improvement in time is limited. Brackish water may also be attracted from the upper aquitard ('downconing'), but this process is counteracted by the buoyancy effects and did not lead to early termination of the freshwater recovery in the Westland case.

The release of brackish water from the deeper aquitard in coastal aquifers can be relevant when quality limits are strict, the native groundwater is saline, and the native groundwater in the target aquifer is displaced far from the ASR wells. The performance of ASR may then be much worse than is predicted by existing ASR performance estimation methods (e.g. Bakker, 2010; Ward et al., 2009), which assume that impermeable aquitards confine the target aquifer. Even in the first MPPW field test (Chapter 3), this process was not observed, due to a smaller radius of the freshwater bubble, resulting in earlier salinization due to buoyancy effects. The upconing water can optionally be intercepted by a (small, deep) Freshkeeper well screen to extend the recovery of unmixed freshwater.

Conclusions

This study shows how short-circuiting negatively affects the freshwater recovery efficiency (RE) during aquifer storage and recovery (ASR) in coastal aquifers. ASR was applied in a shallow saltwater aquifer (23-37 m-BSL) overlying a deeper saltwater aquifer (> 47.5 m-BSL) targeted for aquifer thermal energy storage. Both aquifers were separated by an apparently reliable aquitard, consisting of clay and peat layers. Yet still, a rapid intrusion of deeper saltwater was marked by high SO_4^{2-} concentrations and quickly terminated the freshwater recovery. The most likely pathway for the intruding deeper groundwater was the borehole of an ATES well at 3 m from the ASR well (conduit) and was identified by field measurements, hydrochemical analyses, and SEAWAT transport modelling. Transport modelling underlined that the potentially rapid short-circuiting during storage and recovery can reduce the RE to null. This is caused by a rapid intrusion of the deep saltwater already during storage, and especially during recovery. Transport modelling also showed that when limited mixing with ambient groundwater is allowed, a linear RE decrease by short-circuiting with increasing distance from the ASR well within the radius of the injected ASR-bubble was observed. Old boreholes should therefore rather be avoided during selection of new ASR sites.

Field observations and groundwater transport modelling showed that interception of deep short-circuiting water can mitigate the observed RE decrease, although complete compensation of the RE decrease will generally be unattainable since also injected freshwater is intercepted. At the Westland ASR site, the RE can thus be brought back to around one-third of the injected water, which is comparable to the RE attained with an ASR system without the Freshkeeper in the same, yet undisturbed setting. The same Freshkeeper would be able to abstract around 50% of the injected water unmixed when the setting would be undisturbed, underlining its added value for ASR. Finally, it was found that brackish water upconing from the underlying aquitard towards the shallow recovery wells of the MPPW-ASR system can occur. In case of strict water quality limits, this process may cause an early termination of freshwater recovery, yet it was neglected in many ASR performance estimations to date.

Acknowledgements

The funding agents of the studies discussed in this Chapter are thanked for their support: Knowledge for Climate, the Joint Water Research Program of the Dutch Water Supply Companies (BTO), and the EU FP7 project ‘Demonstrate Ecosystem Services

Enabling Innovation in the Water Sector' (DESSIN) and the EU Horizon2020-project 'SUBSOL'. The tomato growers association 'Prominent' is thanked for facilitating the ASR trial.

Chapter **6**

Enabling successful aquifer storage and recovery (ASR) of freshwater using horizontal directional drilled wells (HDDWs) in coastal aquifers

Based on:

Zuurbier, K.G., Kooiman, J.W., Groen, M.M.A., Maas, B., Stuyfzand, P.J., 2015. Enabling Successful Aquifer Storage and Recovery of Freshwater Using Horizontal Directional Drilled Wells in Coastal Aquifers. Journal of Hydrologic Engineering, 20(3): B4014003.

6.1 Abstract

Aquifer storage and recovery (ASR) of freshwater surpluses can reduce freshwater shortages in coastal areas during prolonged droughts. However, ASR is troublesome in saline coastal aquifers as buoyancy effects generally cause a significant loss of injected freshwater. The use of a pair of parallel, superimposed horizontal wells is proposed to combine shallow ASR with deep interception of underlying saltwater. A shallow, fresh groundwater lens can thereby be enlarged and protected. This 'Freshmaker' set-up was successfully placed in a coastal aquifer in The Netherlands using horizontal directional drilling to install 70 m long horizontal directional drilled wells (HDDWs). The Freshmaker prototype aims to inject a specific volume of freshwater and abstract the same volume of water (consisting of injected water and ambient native groundwater) within the targeted water quality. Groundwater transport modelling preceding ASR operation demonstrated that this this set-up is able to abstract a water volume of 4,200 m^3 equal to the injected freshwater volume without exceeding strict salinity limits, which would be unattainable with conventional ASR. The field pilot supported the model outcomes, as almost 4,500 m^3 of freshwater could be successfully abstracted during the Summer of 2014 upon infiltration of an equal freshwater volume. During the ASR operation, a clear increase and decrease of the freshwater lens was observed. This is the first study to demonstrate the potential benefits of HDDWs for a field ASR application. The outcomes indicate that the feasibility perspectives of ASR in coastal aquifers worldwide require revision thanks to recent developments in hydrologic engineering.

6.2 Introduction

Freshwater supply in coastal areas worldwide is under pressure due to salinization, increasing droughts, and/or increasing freshwater demands (e.g., Werner et al., 2013). With drinking, industrial, and agricultural water supply at stake, efficient exploitation of any available freshwater surpluses is essential to avoid serious shortages. Aboveground storage of such surpluses can be inefficient as the water is prone to evaporation, or because a vast and/or expensive surface area is required. Aquifer storage and recovery (ASR) is defined as 'the injection of water surpluses by a well and recovery by the same well in times of demand' (Pyne, 2005), and it may be an efficient technique to bridge the period in between surplus and demand, without claiming surface area aboveground.

ASR is successfully applied in freshwater aquifers, but storage of freshwater in saline aquifers is troublesome due to mixing and displacement by buoyancy effects in ambient brackish or saline groundwater. Although the loss by mixing can be eliminated by pre-injection of a certain volume to form a buffer zone (Pyne, 2005), buoyancy effects may continuously cause freshwater losses (e.g., Ward et al., 2009; Chapter 1-2). In such cases, the density-difference between injected freshwater (low density) and ambient saline groundwater (high density) will induce upward movement of freshwater. The conventional ASR set-up, which uses a single vertical well for injection and recovery, will therefore generally fail in saline coastal aquifers, as the lower part of the ASR well rapidly abstracts ambient saline groundwater (e.g., Esmail and Kimbler, 1967). Use of upscaling or multiple partially penetrating wells may counteract the freshwater loss by this effect in brackish, confined aquifers, but is presumably insufficient for small-scale ASR in saline aquifers (Chapter 2-3), especially when they are thick and unconfined.

Recent development of horizontal directional drilled wells (HDDWs; Cirkel et al., 2010) may initiate successful ASR in coastal aquifers. Previous studies show that by spreading shallow abstraction of freshwater from a small freshwater lens over a large area, for instance by a HDDW, a larger volume of freshwater can be abstracted (Oude Essink, 2001; Stoeckl and Houben, 2012). Instead of a single HDDW, a parallel, superimposed HDDW pair is proposed in a more advanced set-up to enable both shallow injection and abstraction of freshwater in such a freshwater lens, as well as interception of underlying saltwater. The fresh-salt interface can be actively managed this way to enlarge natural fresh groundwater lenses during injection (the 'Freshmaker' concept), storing large freshwater volumes in the process. During subsequent storage and abstraction, the enlarged freshwater lens can be protected by continuing the deeper abstraction of saltwater. The first Freshmaker prototype was successfully installed in 2013 in a shallow coastal aquifer in the province of Zeeland (The Netherlands, Figure 6-1).

The aim of the study presented in this chapter is to verify and quantify prospective benefits of this innovative ASR configuration based on groundwater transport modelling preceding its first field operation, yet taking into account the local hydrogeological settings. Subsequently, it was aimed to enable a first field validation of the Freshmaker operation with data collected in two test cycles. Moreover, the aim was to demonstrate that even in (unconfined) coastal aquifers with saline groundwater, ASR can be a viable freshwater management technique thanks to recent developments in hydrologic engineering. The latter may have large implications for ASR feasibility worldwide.

6.3 Materials and methods

6.3.1 Study area

The study area is located in the southwest of the Netherlands, in the coastal province of Zeeland. Freshwater is scarce in the study area due to the surrounding Scheldt estuaries (Figure 6-1) and saline seepage. Current freshwater resources are therefore limited to rainwater, local fresh groundwater lenses in sandy creek ridges (Figure 6-1), and some inland river water transported by a pipeline. Due to the large irrigation water demand but limited rainfall in summers, freshwater shortages occur in the local agricultural and horticultural sector, causing a considerable loss of revenue especially for the fruit production sector. On the other hand, large freshwater surpluses are collected by drainage systems and discharged to sea to control the groundwater levels especially in winters, when precipitation rates are high and water use and evapotranspiration are low.

It is aimed to store a part of the local fresh drainage water which is otherwise discharged to sea in a shallow, fine sand aquifer in one of the creek ridges using the Freshmaker in a field trial. The field site is situated on a sandy, relatively young, 5 km wide creek ridge near the village of Ovezande (Figure 6-1). The ridge reaches 0 to 2 m-above sea level (m-ASL) and is surrounded by (older) peat and clay deposits (0 to 1.5 m-below sea level (m-BSL)). The sand in the creek ridge aquifer consists of fine to medium fine sands. Draining water courses on the creek ridge are deep, and have controlled water levels of 0.6 to 0.7 m-BSL. They quickly salinize during dry summers, when electrical conductivities rise to approximately 5,000 µS/cm. The thickness of the fresh groundwater lens in the creek ridge is dependent on surface elevations and the surrounding drainage level (de Louw et al., 2011). Generally, their thickness is less than 15 m, which legally prohibits abstraction from these reserves for irrigation purposes to prevent salinization.

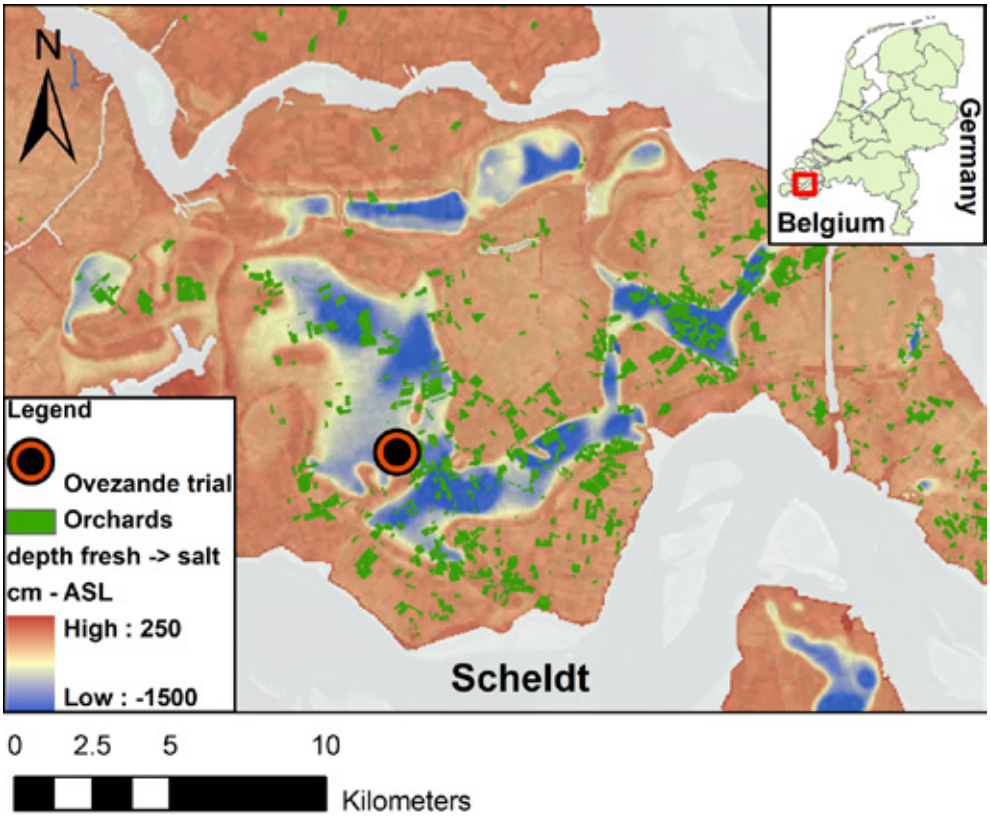

Figure 6-1: Depth of fresh-salt interface (i.e., chloride concentration = 1,000 mg/l) indicating natural freshwater lenses found on the island of Zuid-Beveland (Zeeland, The Netherlands), and the location of the Ovezande Freshmaker trial.

6.3.2 Set-up of the Freshmaker pilot and planned operation

At the field site, the local surface level varies from 0.1 to 0.5 m-ASL. Horizontal directional drilling was used to create two open boreholes with a diameter of approximately 300 mm. The targeted aquifer intervals for the boreholes were based on cone penetration tests to ensure that the HDDWs were placed in sections with a relatively high permeability, without intervening clay layers. The depth profile of the boreholes were recorded in the field using a directional drilling locating system (DigiTrak, USA) and GPS. A bentonite SW drilling fluid (HDD Drilling Fluids, Schoonebeek, The Netherlands) was used to lubricate the drilling, to dispose the cuttings, and to provide borehole stability. A 70 m long HDDW with an inner diameter of 75 mm and four rows with 10 mm holes at 10 cm intervals was wrapped with geotextile. It was then installed in

a borehole at a depth of 13.35 to 14.38 m-BSL (Figure 6-2) to act as the 'interception well'. A perforated casing with an inner diameter of 125 mm and 8 rows of open holes of 10 mm at 10 cm intervals over a length of 70 m surrounded this HDDW during placement for protection and was left around the HDDW. A second, shallow HDDW ('ASR well') with the same properties was installed for artificial recharge and recovery of freshwater surpluses in a second borehole, right above the interception well at 6.68 to 6.93 m-BSL. At this HDDW, a non-perforated casing was used for protection during placement, which was removed after the HDDW was in place. Once the HDDWs were in place, a dispersant was injected, after which 500 m^3 was abstracted to remove the drilling fluid.

During the field pilot, freshwater surpluses from a nearby water course is stored in a ~4,000 m^3 basin, to enable intake of large volumes of freshwater in periods with the highest discharge of fresh surface water in the water course. After settlement of fine particles in the basin, water pumped from the top of the basin is injected by the upper HDDW, using a 3 m high standpipe to provide the pressure for injection. Abstracted saltwater from the deep HDDW is discharged to the local watercourse, with a permitted maximum of 40 m^3/d (Figure 6-3). The recovered freshwater by the Freshmaker is used for irrigation in the growing season at an orchard, where a maximum chloride concentration of 250 mg/l is allowed.

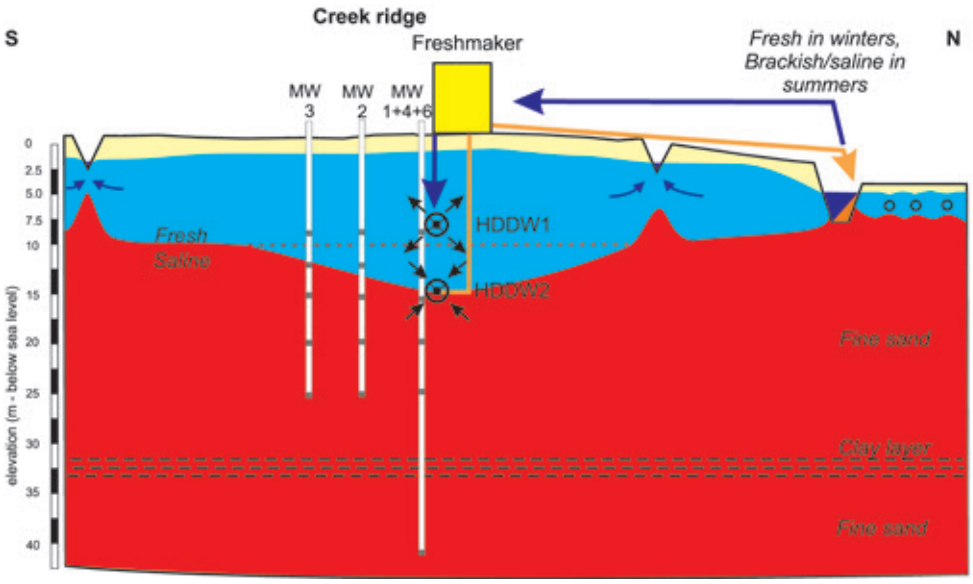

Figure 6-2: Cross section of the Freshmaker set-up at the Ovezande trial. MW = monitoring well, HDDW = horizontal directional drilled well.

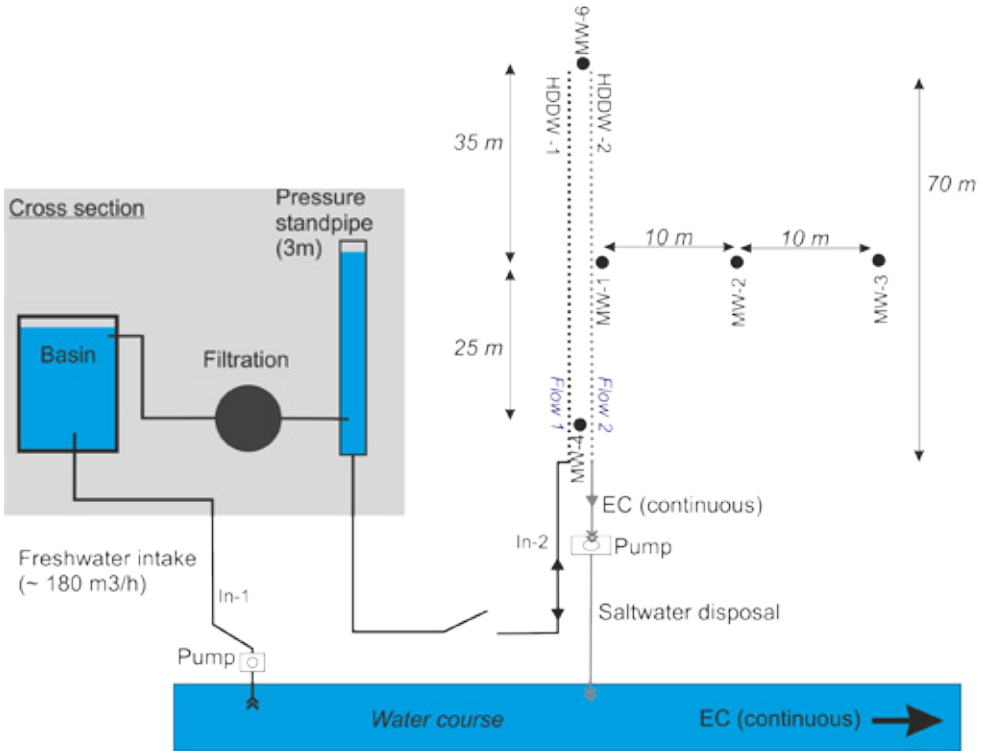

Figure 6-3: Plan view of the Freshmaker set-up at the Ovezande trial.

6.3.3 Characterization of the target aquifer

The target aquifer was characterized using a 40 m deep bailer drilling at the centre of the HDDWs (MW1, Figure 6-2), with samples taken every 1 m. Grain size distributions of these samples were derived using a HELOS/KR laser particle sizer (Sympatec GmbH, Germany), after preparation using the method of Konert and Vandenberghe (1997). It was found that the aquifer is relatively homogeneous and consists of fine to medium fine sand, with a mean grain size of 150 to 200 µm (Figure 6-4).

At three locations (MW1, 2, and 4; see Figure 6-2 and Figure 6-3), electrical conductivities in the aquifer were recorded by geophysical borehole logging using a Robertson DIL-39 probe ('EM-39'; McNeill et al., 1990). The exact location of the fresh-salt interface was found this way. Continuous vertical electrical soundings (CVES) were conducted to map the lateral extent of the freshwater lens. The CVES results indicated the presence of a freshwater lens with a thickness of 0 to 10 m. This thickness was controlled by the elevation of the surface level and the seepage of

saline groundwater towards the draining water course (Figure 6-5). Based on EM-39 measurements, the freshwater lens had a thickness of approximately 9 m and a mixing zone of approximately 6 m at the location of the HDDWs. Below this mixing zone, the high conductivities indicated the presence of groundwater with a salinity equal to local seawater, which has chloride concentration of approximately 16,800 mg/l.

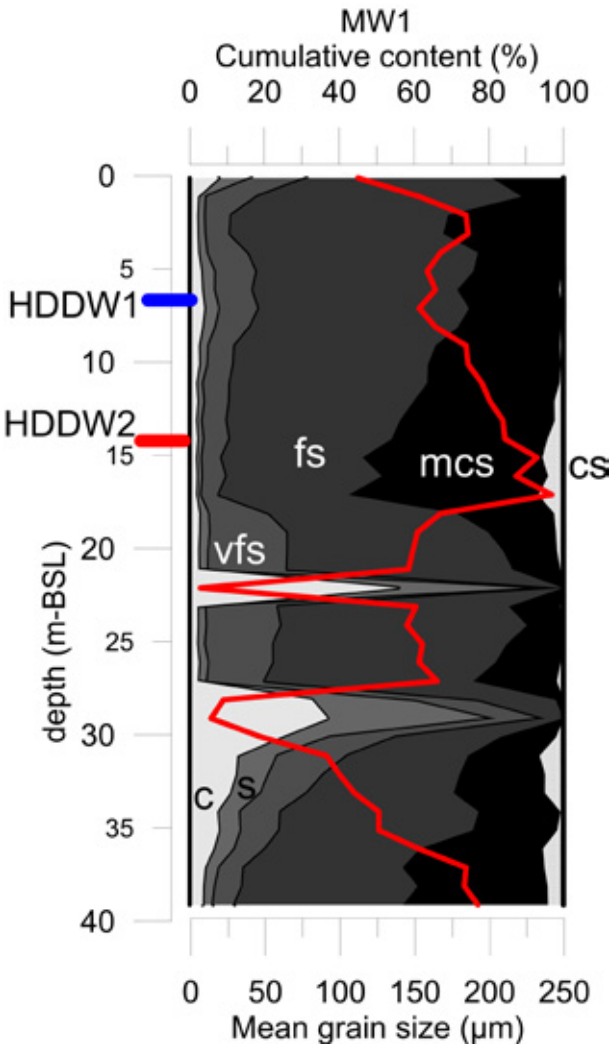

Figure 6-4: Grain size distribution in the target aquifer at MW1. *c* = clay, *s* = silt, *vfs* = very fine sand, *fs* = fine sand, *mcs* = medium coarse sand, *cs* = coarse sand. Mean grain size is indicated in red.

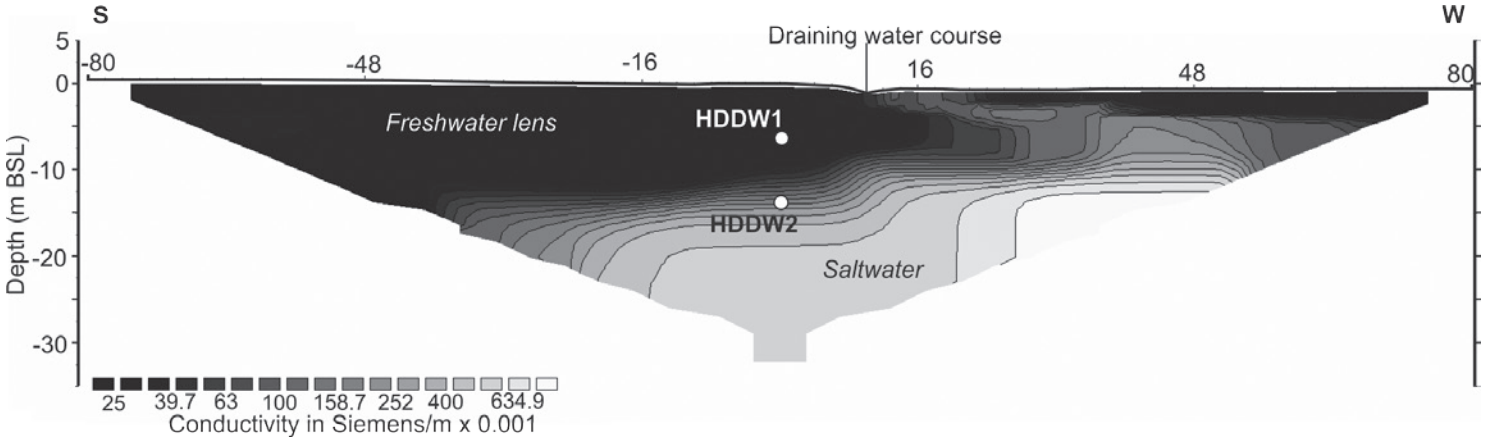

Figure 6-5: Continuous vertical electrical sounding (CVES) at the Ovezande field site. The positions of the HDDWs are marked white (upper) and black (deeper).

6.3.4 Modelling of the Freshmaker benefits

A 2-D SEAWAT (Langevin et al., 2007) model was built prior to the installation of the HDDWs to analyze the efficiency of the Freshmaker set-up and estimate the required pumping rates during operation. A simple slice consisting of only one row comprising 10 m of the HDDW pair was simulated to limit model runtimes (Figure 6-6). Edge effects on the outer ends of the HDDWs were therefore neglected. Hydraulic conductivities were estimated based on the grain size distributions using Bear (1972) and matched typical values for local creek ridge sediments (~5 to 10 m/d). Draining water courses close to the Freshmaker well pair were simulated using MODFLOW's River package. Topography was taken from local elevation measurements. At 850 m from the HDDW pair a constant head boundary was placed. The initial chloride concentration was produced by simulating 100 year with a realistic recharge of 200 mm/yr (Royal Netherlands Meteorological Institute). The conductance of the river beds was modified until the simulation produced the salinity distribution of the reference CVES results (Figure 6-5). A small longitudinal dispersivity of 0.1 m was required to reproduce the mixing zone recorded by borehole logging.

The outcomes of the initial model were used as initial conditions prior to the installation of the Freshmaker HDDW-pair in the model. The HDDWs were simulated by normal single-cell wells with a fixed discharge per stress period in the slice at 6.75 and 14.25 m-BSL. Discharge of each well during 5 years (Table 6-1, Scenario D) was based on the estimated water availability and the minimal well capacity. For each year, five stress periods were simulated: an injection phase, a first recovery phase (sprinkling against frost damage), a storage phase, a second recovery phase (drought irrigation), and an idle period awaiting new freshwater surpluses.

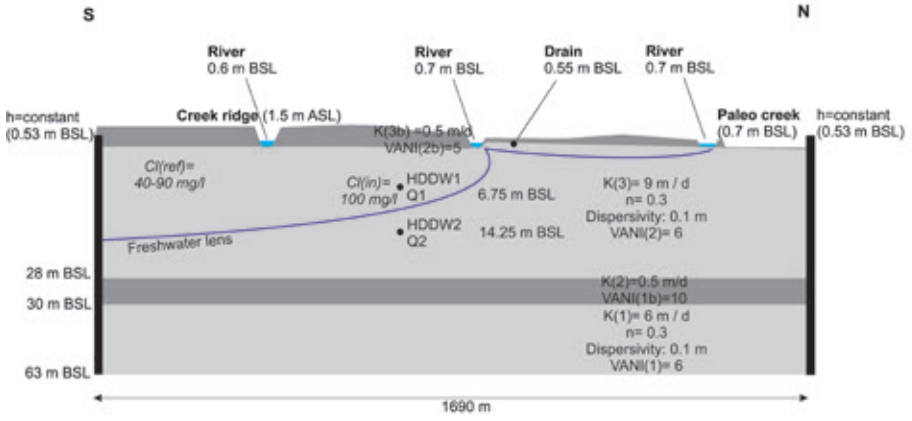

Figure 6-6: Schematization (not to scale) of the 2-D SEAWAT model to evaluate the performance of the Freshmaker. VANI = vertical anisotropy ratio.

Table 6-1: Modeled (yearly) ASR scheme for the Ovezande Freshmaker trial (Scenario D)

Period	t = (d)	Q_{in} (m^3/d) (HDDW1, fresh)	Q_{out} (m^3/d) (HDDW1, fresh)	Q_{out} (m^3/d) (HDDW2, saline)
Winter (infiltration)	120	35	0	35
Spring (recovery 1)	30	0	70	35
Spring (storage)	60	0	0	35
Summer (recovery 2)	60	0	35	35
Idle	95	0	0	0
Total (m^3)		4200	4200	9450

Three additional scenarios were modelled to verify the benefits of Freshmaker configuration. These three scenarios comprised:

- Scenario A: normal ASR operation (simulating ASR), using only the upper HDDW for injection and abstraction of freshwater. No interception of saltwater;
- Scenario B: ASR operation as in Scenario A which is preceded by an additional stress period of 120 d to inject an extra volume equal to the targeted abstraction volume and develop a buffer zone (simulating ASR after injection of a buffer zone). This may reduce freshwater losses during subsequent ASR cycles, as demonstrated by Pyne (2005);
- Scenario C: scenario in which no water was injected by the shallow HDDW, but still deeper saltwater was abstracted in winter prior to, as well as during the abstraction of freshwater in summer (coded "Freshkeeper", as such a set-up is similar to the (vertical) Freshkeeper set-up proposed by Stuyfzand and Raat (2010)).

6.3.5 Field observations

The Freshmaker´s efficiency was recorded using geophysical field measurements (EM-39 borehole logging), EC-sensors, two combined electrical conductivity and pressure transducers (CTDs from Schlumberger Water Services, USA) at MW1 at 7.36 and 12.36 m-BSL, and hydrochemical analyses during operation. The injection, recovery, and interception pipelines were equipped with mechanical water meters (WTII 80 from ARAD, Israel) and were manually recorded at least biweekly.

6.4 Results

6.4.1 Estimated Freshmaker performance by SEAWAT groundwater transport modelling

SEAWAT modelling produced firm insights in the potential performance in the Freshmaker trial. The results indicate that the modelled Freshmaker was able to lower the fresh-salt interface by approximately 5 m, down to the level of the deep HDDW (Scenario D). The thickness of the freshwater lens was increased up to a distance of 30 m away from the HDDW. A targeted freshwater volume of 4,200 m^3 became available for abstraction in this process. During abstraction phases, the fresh-salt interface moved up again, however, not threatening the freshwater abstraction at the upper HDDW (Figure 6-7, scenario D), and a freshwater volume of 4,200 m^3 was abstracted. When only the deepest HDDW was actively intercepting saline groundwater in this scenario (storage phases), the fresh-salt interface was lowered and stabilized. The modelled chloride concentrations at HDDW1 indicated that the abstracted water in spring (recovery 1, see Table 6-1) was merely injected surface water (~100 mg/l Cl^-), whereas in summer (recovery 2) native groundwater from the freshwater lens was abstracted (40 mg/l Cl^-), which was mixed with some upconing saltwater at the end of Cycle 1. In subsequent cycles of Scenario D this upconing was limited and did not impose a risk for the chlorinity of the abstracted water. The results show that the aquifer was slowly freshening, which was underlined by a decrease in saline seepage towards the local water course.

Due to the simultaneous injection of freshwater and abstraction of deeper saline groundwater in Scenario D, the predicted effects increase of the phreatic groundwater level by the model were less than 5 cm during injection. A maximum phreatic drawdown of 7 cm was predicted by the model above the HDDW pair during abstraction, indicating that the hydrological effects remained limited. This highlights another important advantage of the use of HDDWs over vertical wells; hydraulic effects are distributed along a long aquifer strip, preventing major local drawdowns. Potential negative consequences of the ASR operation such as reduced water availability near the plant roots and/or land subsidence are therefore expected to be negligible.

6.4.2 Benefits of the Freshmaker concept over conventional ASR concepts

Significantly less freshwater was found attainable when only a single HDDW (Scenario A: "ASR") was installed at the depth of HDDW1 (6.75 m-BSL), compared with the full Freshmaker set-up in Scenario D. This was evidenced by a firm increase in Cl^- concentrations during both abstraction phases (Figure 6-7, Scenario A), exceeding the local maximum Cl^- concentration for irrigation water after abstraction of a volume which was

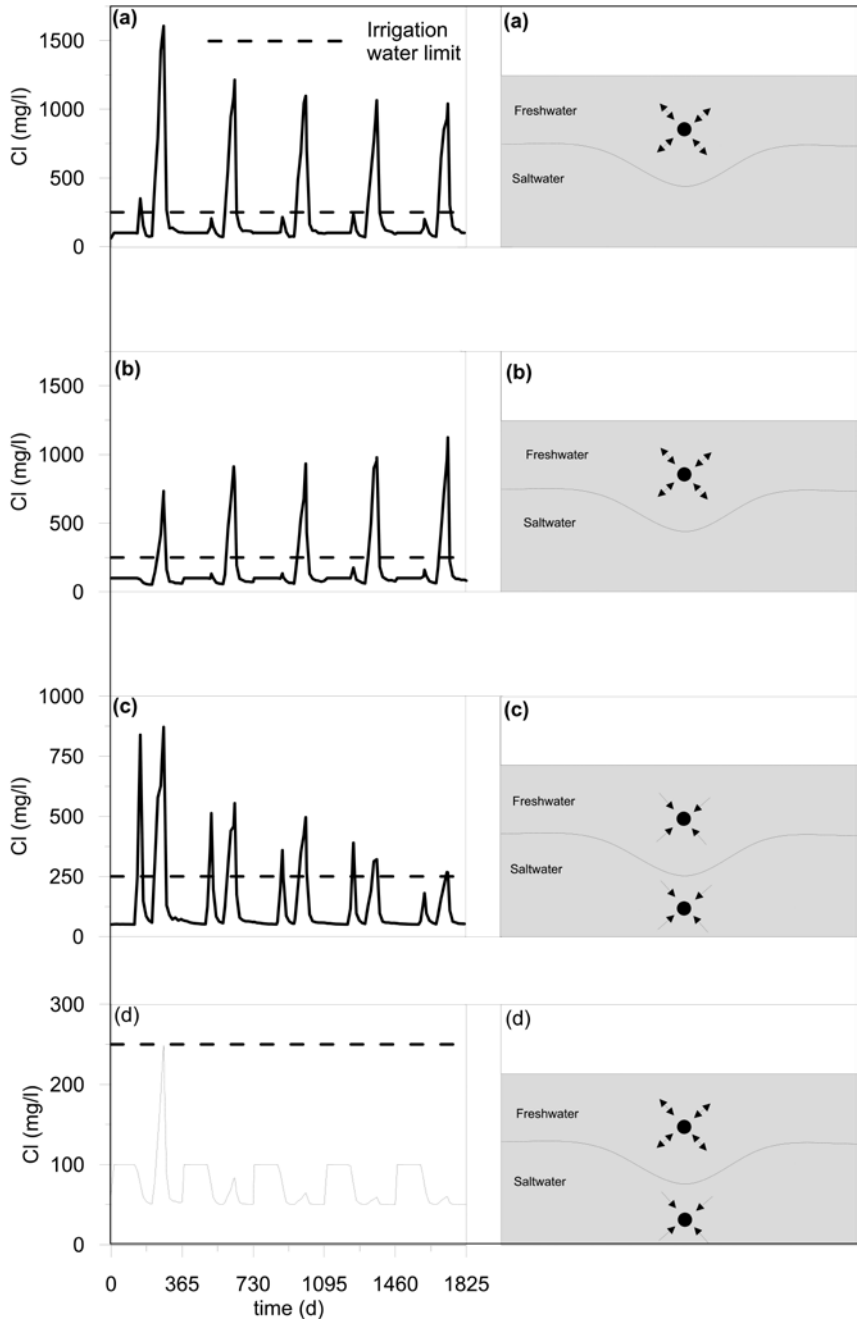

Figure 6-7: Chloride concentrations at the upper HDDW for scenarios without the interception of saline groundwater by a deep HDDW (A (without buffer zone) and B (with buffer zone), without injection (C), and a complete Freshmaker (D).

~50% of the injected volume. The last cycles indicated that no further improvement in the ASR performance could be expected. The results show that buoyancy effects are significant, which causes lateral spreading of injected freshwater during injection, while upconing of saline groundwater occurs already early during the abstraction phase. The introduction of a 'buffer zone' (Scenario B) in this particular setting did not lead to a significant increase in freshwater abstraction. This is demonstrated by the modelled Cl^- concentrations in Cycle 5 (Figure 6-7, Scenario B), which were more or less equal to a case without the injection of a freshwater surplus for the buffer zone formation. This points out that a buffer zone is not maintained in between the HDDWs and cannot provide the desired prolonged protection from underlying saltwater.

6.4.3 The importance of freshwater injection: comparison with a Freshkeeper operation

When a Freshmaker was installed, but no water was injected (scenario C: "Freshkeeper"), a satisfying volume of freshwater could be abstracted from Cycle 5 onwards, due to the almost continuous interception of saltwater by the deep HDDW, increasing infiltration of freshwater and decreasing seepage to the surface water. These results suggest that injection of freshwater is not a requirement for the abstraction of a same volume of freshwater, and that continuous interception of saltwater preceding freshwater abstraction may be sufficient. The latter was confirmed by modelling of an additional scenario in which the first freshwater abstraction was preceded by 1.3 years of deep interception (35 m^3/d) of saltwater. In the following cycles the volume of 4,200 m^3 could be recovered with Cl^- concentrations not exceeding 140 mg/l. A somewhat larger drawdown (13 cm) was observed, however, which might necessitate additional local irrigation near the HDDWs to prevent water shortage in the root zone.

6.4.4 First field results

The Freshmaker field pilot is being executed since June 2013. Operational data, EM-39 borehole measurements, EC, temperature, and pressure data, and hydrochemical data have been collected ever since. In Cycle 1 (June – September 2013), 1,700 m^3 was injected and an equal freshwater volume was successfully abstracted. In Cycle 2 (November 2013 – September 2014), 4,450 m^3 was injected, and 4.400 m^3 of freshwater was abstracted by September 2014. The geophysical EM-39 measurements show that the Freshmaker indeed enlarged the freshwater lens during injection (3 to 4 m, Figure 6-8) and kept the freshwater at its place during storage. The Freshmaker proved able to recover a freshwater volume virtually equal to the injected volume up to at least 4,400 m^3.

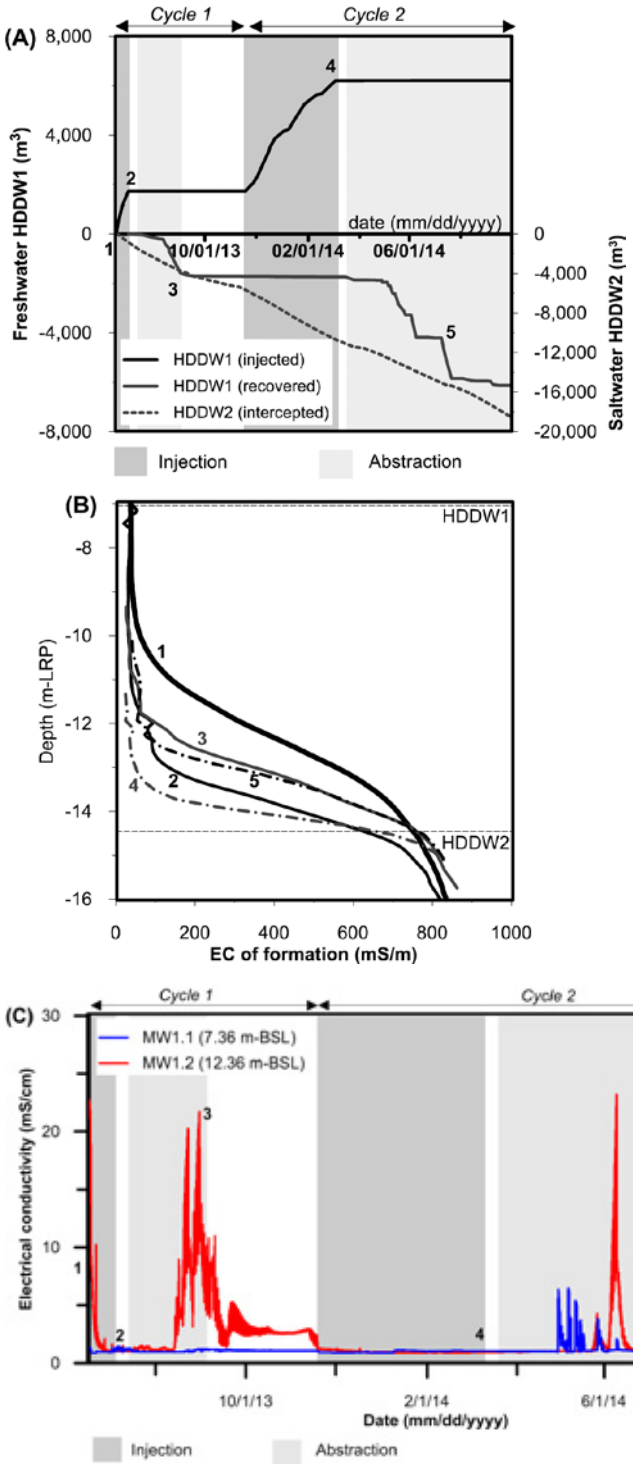

Figure 6-8: (A):Pumping by the Freshmaker (positive=injection, negative=abstraction). (B): changes in the EC of the formation in the target aquifer measured by EM-39 demonstrating freshening (EC decrease) and salinization (EC increase) at the centre of the Freshmaker (halfway the HDDW well screens). m-BSL = meters below sea-level. Numbers 1-5 indicate the moments at which EM-39 recordings were performed. (C): EC as recorded by CTD divers at the monitoring well screens MW1.1 and MW1.2.

The CTD divers installed at MW1.2 clearly recorded the dynamics of the fresh-salt-water transition. Starting at a EC of 23 mS/cm (initial situation), the EC was lowered until it reached the EC of the injected water (approximately 1 mS/cm). Especially during relatively long periods with high-rate freshwater recovery (around 7 m^3/h, i.e. 160 m^3/d), a steep increase in EC was recorded, indicating a rapid rise of saltwater towards the recovering HDDW1, although the recordings at MW1.1 indicated that the saltwater did not reach the zone of recovery. A significant EC increase in this zone was only recorded during and after chemical cleaning of the well in May 2014. In periods with relatively low recovery rates freshening and stabilization was observed in the aquifer section in between both HDDWs, as illustrated by the EC recordings at MW1.2.

The initial freshwater at the depth of HDDW1 is marked by relatively high Na^+ concentrations and a high base exchange index (BEX; Stuyfzand, 1993; Stuyfzand, 2008) of 9.5, indicating freshening of the aquifer. The Cl:Na ratio around HDDW1 was initially 0.4. The injection water (draining water from the study area) shows signs of freshening (BEX: 3.8) and had a Cl:Na ratio of 0.7 to 0.9. The recovered water quality was initially similar to the injected water, but a decrease in the Cl:Na ratio during later recovery marked admixing of native fresh groundwater (Figure 6-9). During high-rate recovery and upconing of saltwater, however, a sudden increase in the Cl:Na ratio was observed, indicating retarded arrival of Na^+ with respect to Cl in the abstraction well, similar to the retarded arrival of Na^+ at the MPPW-ASR pilot in Nootdorp (Chapter 4).

Fe^{2+} and Mn^{2+} concentrations increased in the injected water from virtually 0 to approximately 0.3 and 0.1 mg/l respectively in the bulk of the recovered water (Figure 6-10). This meant that Fe^{2+} concentrations were lower with respect to the native groundwater, whereas Mn^{2+} concentrations were in line with those observed in the native fresh groundwater. During the first phase of recovery upon storage, remarkably higher Fe^{2+} and Mn^{2+} concentrations were observed in deeply anoxic water, however, despite the fact that relatively low concentrations were observed in the injected water at all nearby monitoring wells. Oxygen and nitrate (present with concentrations of several mg/l in the injection water) were completely reduced within the first meters from the injection well (HDDW1), as marked by their absence at MW1.1. No significant changes in SO_4^{2-} concentrations were observed during aquifer residence.

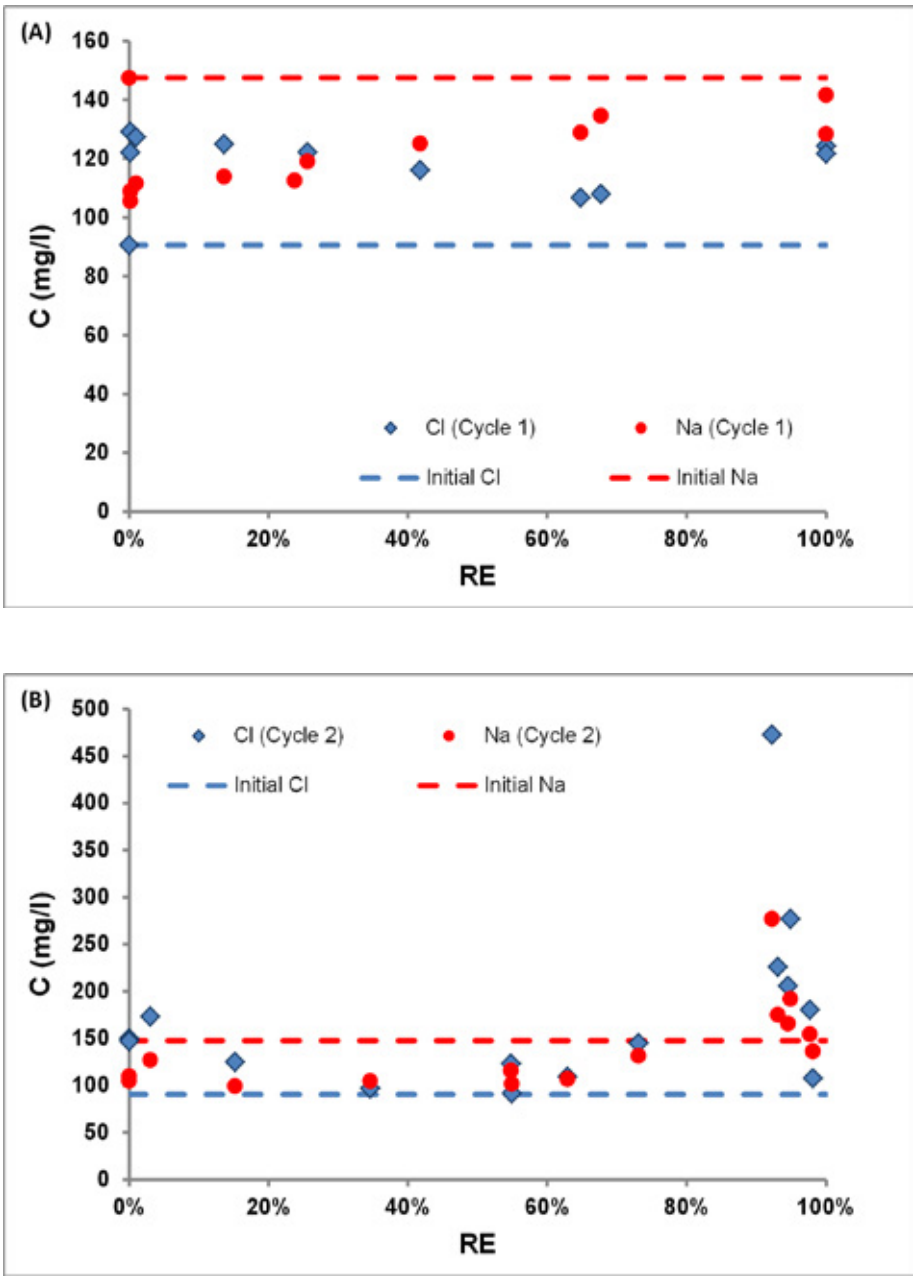

Figure 6-9: (A):Observed Cl and Na concentrations in the abstracted freshwater at HDDW1 during Cycle 1. B: Observed Cl and Na concentrations in the abstracted freshwater at HDDW1 during Cycle 2.

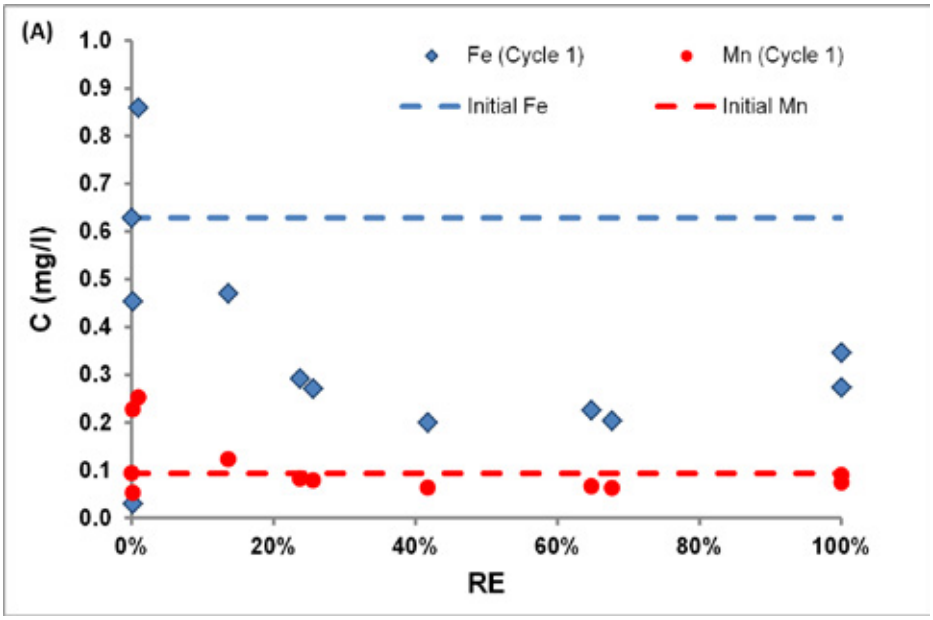

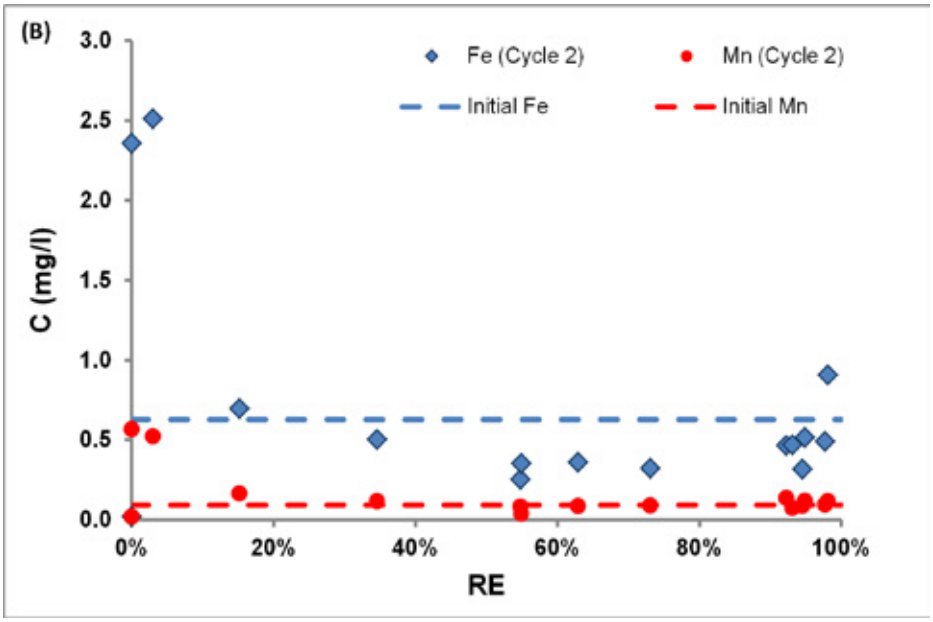

Figure 6-10: (A):Observed Fe and Mn concentrations in the abstracted freshwater at HDDW1 during Cycle 1. B: Observed Fe and Mn concentrations in the abstracted freshwater at HDDW1 during Cycle 2.

6.5 Discussion and conclusions

Abstraction of freshwater during ASR operation in coastal aquifers is generally troublesome due to buoyancy effects. A 'Freshmaker' set-up to enlarge thin fresh groundwater lenses in shallow aquifers by the use of two parallel, superimposed horizontal directional drilled wells (HDDWs) was tested using 2-D SEAWAT groundwater transport modelling preceding its field operation. A shallow HDDW was used to inject and abstract freshwater surpluses and a deeper HDDW was used to intercept deeper saline groundwater. SEAWAT transport modelling showed that a freshwater volume equal to the injected volume could be abstracted yearly, and that the abstracted water consisted of both injected water and native, fresh groundwater. Due to the use of the HDDWs, regional hydrological effects can be expected to be limited.

A prerequisite is continuous interception of the deeper saline groundwater by the deeper HDDW. Conventional ASR set-ups (although using HDDWs) predicted limited freshwater abstraction (~50% of the injected volume). The origin of this significant reduction in ASR performance compared to the Freshmaker set-up can be found in the basics of a freshwater lens in saline groundwater. As with natural freshwater lenses in these relatively homogenous aquifers, the depth of the freshwater lens relative to the local drainage level is controlled by the Ghyben-Herzberg relation. This means that the extending head in the freshwater lens compared to this drainage level and the density difference between the fresh and saline groundwater control the thickness of the lens (Verruijt, 1968). The modelling results showed that the head increase in the freshwater lens compared to the reference situation in the conventional ASR scenario (scenario A and B) is limited due to the low injection rates. However, a much higher head increase in this phreatic aquifer will lead to root deterioration of orchard trees or even groundwater exfiltration. Furthermore, in storage phases (with neither freshwater availability, nor demand), the relative head increase cannot be maintained, resulting in thinning of the freshwater lens and a loss of freshwater. Upconing of saltwater is favored in the abstraction phase due to the abstraction from a shallow freshwater lens, underlain by saline groundwater and is found in various studies (e.g., Aliewi et al., 2001; Asghar et al., 2002; Oude Essink, 2001; Reilly and Goodman, 1987a; Schmork and Mercado, 1969; Werner et al., 2013; Werner et al., 2009). To safely increase the thickness of the lens in limited time, prevent losses during storage, and abstract a large freshwater volume in periods of demand, abstraction by the deeper HDDW proves to be indispensable.

The depth and discharge of the intercepting, deeper HDDW is a relevant design parameter as (1) this HDDW can abstract costly freshwater when it is installed too

shallow or abstracts at a rate which is too high, or (2) provide insufficient protection of the upper HDDW when it is installed too deep or abstracts at a rate which is too low. SEAWAT modelling with an extra fictitious, conservative tracer in the injection water showed that no injected freshwater should enter the top of the deeper HDDW2 in the Ovezande trial for the operational parameters of Scenario D. Only a part of the brackish mixing zone may be abstracted in the model, as shown by the modelled Cl^- concentrations at HDDW2 (Figure 6-11). SEAWAT modelling also showed that placement of the deeper HDDW at 20 m-BSL led to early salinization of upper HDDW in the first two years. Lowering of the fresh-salt interface was less below HDDW1 in this case and extended laterally. Although the target aquifer was modelled as being homogeneous and anisotropic, intervening clay layers may further decrease the functionality of the deeper, intercepting HDDW in field applications. This emphasizes the need for a priori aquifer characterization, for instance using cone penetration tests. Altogether, the modelling results indicate that appropriate placement depths were chosen for the Ovezande field trial.

SEAWAT modelling also showed that under the local hydrological conditions simulated (freshwater lens, net recharge, controlled drainage levels) the interception of deep saltwater eventually enables abstraction of the targeted freshwater volumes, even without injection of freshwater surpluses. However, this operation may affect the local hydrology stronger than the proposed 'Freshmaker' operation, or cause mining of the existing freshwater lens. Additionally, beneficial effects on the produced freshwater are anticipated with the injection by the 'Freshmaker', such as subsurface iron removal from the otherwise iron containing natural freshwater lens by injection of oxygen-rich water (e.g., Antoniou et al., 2013; van Halem et al., 2010).

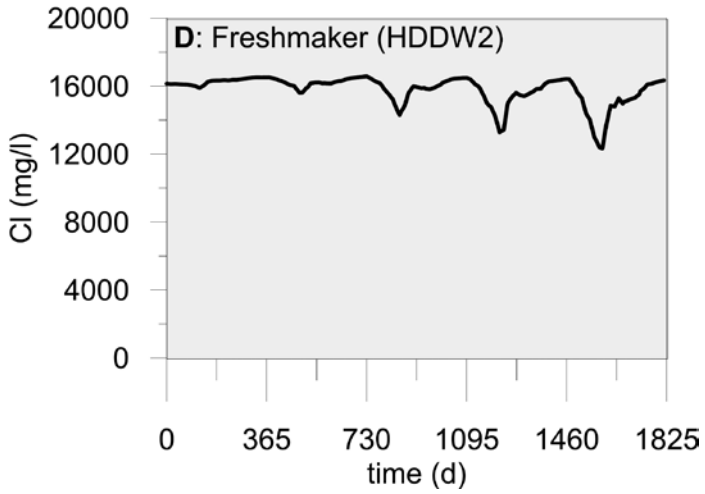

Figure 6-11: Chloride concentrations at the deeper HDDW of the Freshmaker (Scenario D).

The field results revealed some operational constraints for successful implementation of the Freshmaker: rapid recovery of a large freshwater volume (~160 m^3/d) while keeping the saltwater interception constant may induce rapid upconing of saltwater below the upper HDDW1. This can be mitigated by interception of more saltwater by the deeper HDDW, but it can be expected that limiting the abstractions and thereby the drawdown is preferred to limit upconing and recover the maximal volume of freshwater, likewise the SEAWAT simulations performed (with average abstraction rates of 35 and 70 m^3/d). Essentially this means that the Freshmaker provides the build-up of large freshwater volumes, which can, however, only be produced over a longer timeframe. Further on, it is important to mention that like during MPPW-ASR (Chapter 4), exchange of Ca^{2+} and Na^{+} on exchanger sites in the deeper aquifer will cause Na-enrichment in unmixed water during freshening and a retarded arrival of Na^{+} during salinization. At the Ovezande field site, deeply anoxic water was initially recovered upon storage, which is most presumably caused by mineralization of biomass which had accumulated during injection of the surface water with (presumably) high concentrations of dissolved organic carbon (DOC). An accompanying reduction of Fe-hydroxides and Mn-oxides close to ASR wells has been observed in earlier ASR studies (Antoniou et al., 2012; Greskowiak et al., 2005), where moderate to high DOC concentrations were present in the injection water. A more extensive interpretation of the field results and calibration of the SEAWAT model based on the observations is a topic of further study, but beyond the scope of this thesis.

In this chapter, the theoretical viability of the Freshmaker principle is confirmed preceding and during the first field application. The findings suggest that a robust ASR configuration is available for coastal areas with similar hydrological settings worldwide, where ASR was previously considered unviable. This means that for the first time, valuable freshwater surpluses can be stored in these relevant areas without claiming vast surface areas aboveground due to recent developments in hydrologic engineering. With this increased freshwater availability at hand, coastal areas can remain (or become) interesting for agriculture, industries, and inhabitants. Despite the additional complexity, the estimated cost-price for the water supplied by the Freshmaker is 0.35 €/m^3, which is less than the local alternative (piped water: 0.70 €/m^3). Future studies should focus on further and closer field verification of the outcomes of this study, as well as observation and modelling of HDDW edge effects, potential aquifer heterogeneities, water quality changes from aquifer reactivity, and potential well clogging.

6.6 Acknowledgements

The study presented in this chapter was funded by the Dutch national research program 'Knowledge for Climate' and the parties involved in GO-Fresh ('Geohydrological Opportunities Fresh Water Supply'). Maatschap Rijk-Boonman, Bos Grijpskerke, and Meeuwse Handelsonderming Goes are thanked for their contribution in the Ovezande field trial. Three anonymous reviewers are thanked for their comments to the earlier version of this chapter.

Chapter 7

Scientific and social-technical implications

Illustration by Irene Goede (www.irenegoede.nl)

Partly based on:

Zuurbier, K.G., Raat, K.J., Paalman, M., Oosterhof, A.T., Stuyfzand, P.J., 2016. How Subsurface Water Technologies (SWT) can Provide Robust, Effective, and Cost-Efficient Solutions for Freshwater Management in Coastal Zones. Water resources Management: 1-17. DOI: 10.1007/s11269-016-1294-x.

7.1 Introduction

The outcomes of this PhD research are summarized and discussed in this chapter to mark their socio-technical and scientific impact. Following a summary of the findings, I will elaborate on the implications for the performance of aquifer storage and recovery (ASR) in coastal areas. Subsequently, I will discuss the implications on freshwater management in coastal areas in general, since the generated insights and reported techniques also impact the prospects for management of fresh (ground)water (reserves) and salinization in these areas. Finally, I will identify the implications and perspectives based on the outcomes of this thesis for futures scientific research.

7.2 Summary of the findings

The main objective of this research was to *quantify and increase the potential performance of relatively small-scale ASR systems in coastal areas with brackish-saline aquifers, taking into account recently developed well configurations for performance optimization*. The research executed to meet the objective is discussed in detail in Chapter 2 to Chapter 6 and is summarized below.

In **Chapter 2**, the application of two recently published ASR performance estimation methods (Ward et al. (2009) and Bakker (2010)) to map the potential ASR performance in a Dutch coastal area was discussed. This area is characterized by brackish to saline groundwater with locally high lateral flow velocities. ASR performance of existing systems in the study area showed good agreement with both performance estimation methods, although the method by Bakker (2010) showed a slightly better prediction of the loss by buoyancy effects. Deviations between actual and predicted ASR performance may originate from simplifications in the conceptual model and uncertainties in the hydrogeological and hydrochemical input. As the estimation methods prove suitable to predict ASR performance, feasibility maps were generated for different scales of ASR to identify favorable ASR sites. The potential for small (<100m^3/d) to medium (<500 m^3/d)-scale ASR varies spatially in the study area, emphasizing the relevance of reliable a priori spatial mapping. Even in slightly brackish aquifers (<1,000 mg/l Cl), the predicted performance of small- to medium-scale ASR may already be low by buoyancy effects.

A new ASR configuration to increase the RE was introduced in **Chapter 3**. Freshwater losses could be reduced by applying deep injection and shallow recovery via independently operated multiple partially penetrating wells (MPPW) in a single bore-

hole. A small-scale ASR system with such an MPPW was installed in January 2012 and its operation was extensively monitored until October 2012. A SEAWAT model was built and calibrated on the field measurements of this first ASR cycle. The model was used to compare the MPPW with a conventional, fully and partially penetrating well. The simulated Cycle 1 freshwater recovery of those wells was 15 and 30% of the injected water, respectively, which was significantly less than the 40% recovered by the MPPW. Modelling indicated that, in subsequent cycles, around 60% could be recovered by the MPPW. A further RE increase was hampered by mixing in the periodically salinizing lower half of the aquifer. This remained a source of freshwater losses. The unrecoverable freshwater (mixed with some ambient groundwater) moved laterally from the ASR well in the upper zone of the target aquifer. The RE obtained was significantly higher than the RE of the conventional well types, while additional costs were limited. Therefore, even for less ideal ASR conditions, a viable system can still be realized using the MPPW.

In **Chapter 4**, the observed water quality changes by reactive transport processes in the field MPPW-ASR system (presented in Chapter 3) and their impact on RE were presented. It was shown that the freshwater injected in the deepest of four wells became enriched with sodium (Na) and other dominant cations from the brackish groundwater due to cation exchange upon 'freshening'. This enriched freshwater was predominantly recovered at the shallowest well. During recovery periods, the breakthrough of Na was retarded in the deeper and central parts of the aquifer due to cation exchange induced by 'salinization'. The buoyancy effects precluded a progressively improving water quality with subsequent cycles as observed at conventional ASR systems lacking buoyancy affects. The process of cation exchange can either increase or decrease the RE of MPPW-ASR operation, depending on the maximum permissible limits for Na (being 0.5 mmol/l in Nootdorp), the cation exchange capacity and native groundwater and injected water composition.

In **Chapter 4** it was also shown that dissolution of Fe and Mn-containing carbonates led to contamination with Fe and Mn in injected water. This dissolution was stimulated by CO_2-production (by oxidation of adsorbed Fe and Mn, mainly in the first cycle) and by proton-buffering upon pyrite oxidation particularly in the pyrite and Fe/Mn-carbonate-rich deeper sections of the aquifer. As pyrite consumed virtually all oxygen in the deeper aquifer sections in Cycle 2, Fe and Mn remained mobile in the anoxic water upon release. During recovery, Fe precipitated to Fe-hydroxide via reduction of MnO_2. Recovery at this interval was therefore marked by a severe and continuous contamination with predominantly Mn. However, the field pilot indicated that recovery of Mn and Fe could be prevented by regular injections of small volumes

of oxygen-rich water via the shallowest well. This process is similar to subsurface iron removal (SIR) applied during abstraction of (natural) groundwater.

The essentially upward flow paths in the MPPW-ASR system expose a significant part of the injected water to the (sub)horizontal geochemical stratification of the aquifer. In **Chapter 4** it was demonstrated that the vertical positions of reactive layers control the mobilization of undesired elements during MPPW-ASR, rather than the average geochemical composition of the target aquifer. This calls for a more detailed geochemical characterization of target aquifers for MPPW-ASR, as well as an optimized operation of its injection and recovery wells, depending on which elements control the recovery efficiency.

ASR in coastal areas is vulnerable to natural or man-made connections between overlying aquifers. In **Chapter 5** it is shown how artificial connections between originally separated coastal aquifers ('conduits') have a negative effect on the freshwater RE during ASR. In the reported study, ASR was applied in a shallow brackish water aquifer overlying a deeper more saline aquifer used for aquifer thermal energy storage (ATES). Although both aquifers were considered well separated by a thick regionally continuous clay layer, intrusion of deeper saltwater prematurely terminated the freshwater recovery. The most likely pathway was identified by field measurements, hydrochemical analyses, and SEAWAT transport modelling. It was shown that the borehole of an ATES well provided a pathway for short-circuiting of deeper saltwater. Transport modelling underlined that the potentially rapid short-circuiting during storage and recovery can reduce the RE to null. When only negligible mixing with ambient groundwater is allowed, a linear RE decrease by short-circuiting with increasing distance from the ASR well within the radius of the injected injected freshwater body was observed. Field observations and groundwater transport modelling showed that intercepting the deep short-circuiting water can mitigate the observed RE decrease. Complete compensation of the RE decrease will generally be unattainable since also injected freshwater gets intercepted. Finally, it was found that brackish water was upconing from the underlying aquitard towards the shallow recovery wells of the MPPW-ASR system. This can prevent an increased RE by the use of MPPWs when virtually unmixed water must be recovered. Detailed characterization of the underlying aquitard (hydraulic conductivity, thickness) is therefore another critical aspect during site characterization.

In **Chapter 6**, the use of a pair of parallel, superimposed horizontal wells was presented to combine shallow ASR with deep interception of underlying saltwater. A shallow, fresh groundwater lens can be enlarged and protected by such a configuration. This 'Freshmaker' set-up was successfully placed in a coastal aquifer in The

Netherlands using horizontal directional drilling to install two 70 m long horizontal directional drilled wells (HDDWs). With this Freshmaker prototype, it was aimed to inject a specific volume of freshwater and abstract the same volume of water (consisting of injected water and ambient native fresh groundwater) with the desired water quality. Groundwater transport modelling demonstrated that this set-up should be able to inject and abstract a water volume of at least 4,200 m^3 without exceeding strict salinity limits. This would be unattainable with conventional ASR. The field pilot supported the model outcomes, as almost 4,500 m^3 of freshwater could be successfully abstracted during the summer of 2014 upon infiltration of an equal freshwater volume. During the ASR operation, a clear increase and decrease of the freshwater lens were observed. The study presented in this chapter was the first to demonstrate the potential benefits of HDDWs for a field ASR application.

7.3 Implications of the findings for ASR

Knowing the particular outcomes of spatial ASR performance analyses and the various well-monitored field pilots, it is relevant to discuss the broader implications for ASR. The main finding is that due the increasing data availability, ASR performance estimation methods, and drilling and operational techniques, a significant increase in the performance and therefore reliability of ASR in coastal areas can be achieved. This is very relevant, since negative or uncertain prospects have often led to investments in less sustainable or more expensive techniques for freshwater supply, such as desalination and aboveground storage. Moreover, the outcomes indicate that the feasibility perspectives of ASR in coastal aquifers worldwide require revision thanks to recent developments in hydrologic engineering.

The main controls for a potential increase in especially coastal ASR performance are, as based on the results of this study:

1. Select the ASR site carefully.

Heterogeneity is no exception in coastal areas. Both physical and hydrochemical aquifer properties may vary significantly over relatively short distances and may cause complete failure at a targeted ASR site, even if successful systems are relatively close by. Using the GIS approach from Chapter 2, one can identify suitable sites (simple, small-scale ASR successful), unsuitable sites (virtually no success), and intermediate sites (large-scale ASR successful, or optimized well configurations enable small-scale ASR). The findings from Chapter 6 also indicate that caution during site-selection

should be maintained if previous activities at a site occurred that may have disturbed hydrogeologically confining strata. Particularly, there is a significant risk of contamination via hydraulic connections caused by improperly sealed or burst boreholes (Chapter 6).

2. *Control the sections of the aquifer used for injection and recovery, and actively intercept undesired water to increase the RE.*

A standard ASR well (single well screen, generally fully penetrating) may provide the best option to realize a relatively cheap, high-capacity pumping well, but offers no controls on the depth at which the freshwater is recovered and abstracted. The MPPW offers an opportunity to counteract at least part of the freshwater losses induced by buoyancy effects, through anticipation of the upward movement of the injected freshwater. Deep injection and shallow recovery can significantly extend the freshwater recovery in less suitable aquifers (Chapter 3). Despite the significant increases in RE that can be obtained, mixing remains a continuous source of freshwater losses, prohibiting an RE of 100%. Under even more challenging conditions, a significant increase in freshwater recovery by the MPPW may still be realized, but will require interception of the deeper saltwater during the shallow recovery of freshwater with a 'Freshkeeper' (Stuyfzand and Raat, 2010).

3. *Take the geochemical interactions with the injected water and vertical heterogeneity of the target aquifer into account.*

Compared to conventional, fully-penetrating vertical ASR wells, the use of an MPPW or a horizontal well can lead to more geochemical interaction with (sub)horizontal, reactive units. This is due to the vertical flow induced by buoyancy and the preferential infiltration via the deepest wells while abstracting via the shallowest wells. Therefore, especially the deepest aquifer interval affects the hydrochemical development of the injected water: most geochemical interaction occurs here rapidly after injection. Additionally, there is more interaction with intercalated, but potentially highly reactive layers in between the injection and the recovery wells: a relatively large part of the injected water will have to pass and interact with these units before recovery.

One evident water quality deterioration occurs by desorbing cations originating from the native brackish-saline water, like Na, during each injection phase. The resulting water quality deterioration will not significantly decrease upon subsequent cycles due to the frequent salinization of deeper aquifer segments with a NaCl water type. Dosing of Ca to the injection water can limit the contaminated volume of injected water, but also leads to a more significant enrichment in this volume. Additionally,

especially Fe and Mn may mobilize in deeper intervals of the target aquifer during residence and can travel toward shallow recovery wells unhampered, as found in this study (Chapter 4). Similar mobilization during ASR was observed elsewhere (Antoniou et al., 2013; Antoniou et al., 2012). This can, however, be counteracted by applying subsurface iron removal at the recovery wells (Chapter 4), or even by oxidative pre-treatment of injection intervals (Antoniou et al., 2014). The forced additional vertical transport and aquifer residence time may, however also enhance removal of for instance organic micro pollutants, viruses, and chlorination by-products (Dillon et al., 2006; Miotliński et al., 2014).

4. Select horizontal wells in a setting with shallow freshwater lenses.
In many coastal areas worldwide, shallow freshwater lenses fed by a (temporal) rainwater surplus are present. Exploitation of these lenses by abstraction of the freshwater is generally hampered by upconing and/or depletion. In Chapter 6 it is shown that a combination of horizontal wells (like HDDWs), ASR, and interception and disposal of deeper saltwater in a 'Freshmaker' configuration enables storage and recovery of significant freshwater volumes. The maximal volume that to be abstracted with the Freshmaker is controlled by the depths and lengths of the wells, the initial thickness of the freshwater lens, the salinity of the saltwater, the duration of the ASR phases, the hydraulic conductivity and the effective porosity.

5. Add information and communication technology (ICT) and sensoring.
This thesis demonstrates that the introduction of flexibility offers a valuable increase in ASR performance. At the same time, such flexible ASR systems are more complicated for the end users (generally not hydrogeologists). Computerization as demonstrated in the Nootdorp pilot is significantly more important than during conventional ASR to: prevent mistakes, optimize injection (e.g., deep in the aquifer), optimize recovery, prevent overflows of aboveground buffers (for instance, by shortly enabling injection via all well screens of the MPPW during extreme rainfall eventsw, or, better still, even anticipate on predicted rainfall), and efficiently intercept deep saltwater to maximize shallow freshwater recovery.

7.4 Implications of the findings for freshwater management in coastal areas

7.4.1 The role of ASR as a freshwater management tool in coastal areas

ASR is not a new tool for freshwater management. Since deep well injection became more common in the fifties, also saline aquifers were considered for freshwater storage in the sixties (Bear and Jacobs, 1965; Esmail and Kimbler, 1967). However, few reports on successful applications of especially small-scale coastal ASR can be found (Maliva and Missimer, 2010; Pyne, 2005), although research continued (Merritt, 1986; Molz and Bell, 1977; Peters, 1983). Some emergency supplies enabled freshwater availability for several days in case of disasters (Pyne, 2005), which, however, results in very low REs. In the eighties, an ASR system using a conventional long, vertical well screen was realized close to the Ovezande area of the Freshmaker field pilot in similar hydrogeological settings (Projectgroep Zoetwateronderzoek Goes, 1986). Due to low REs and clogging issues, this site was decommissioned after initial cycle testing. In the Eastland area, the first ASR system was realized in 1983, but variable success and absence of monitoring and evaluation limited the widespread introduction, even after introduction of MPPWs (although operated more like a fully penetrating well) in the nineties (Zwinkels, 2010).

The implications of this thesis for ASR in freshwater management are mainly in the increased reliability of ASR in brackish-saline aquifers. By reducing the chance of ASR failure by limited freshwater recovery, the technique becomes more interesting to provide a reliable freshwater supply. At the same time, the findings will also moderate expectations, as it is demonstrated that an RE of 100% will normally be unattainable in brackish or saline aquifers. Only when saline water is intercepted with a separate well, such as in case of the Freshmaker, an (eventual) RE of 100% is feasible.

In the Netherlands, this increased ASR reliability is very much welcomed with the prospects of longer periods of drought, despite an increase in yearly gross precipitation (Royal Netherlands Meteorological Institute, 2014) induced by climate change. Furthermore, water is increasingly recognized as a scarce resource (World Economic Forum, 2015). The need for water harvesting and storage is therefore expected to increase. Finally, an increase in extreme rainfall events is expected in the Netherlands (Royal Netherlands Meteorological Institute, 2014), which requires better exploitation of aboveground water reservoirs for retention of intense rainfall. ASR provides means to lower the levels of these reservoirs by early infiltration once potential extreme rainfall events are predicted, and to provide retention, without having to discharge (and lose) the water to sea. Therefore, the water remains available for later times of

demand, while the unrecoverable part can counteract the ongoing salinization.

An alternative for ASR to increase freshwater availability is desalination of brackish groundwater or seawater via reverse osmosis (RO). Despite the generally higher costs and energy consumption, RO may be preferred as it imposes less risks and unknowns than ASR in coastal areas. However, disposal of the saline waste stream from RO ('concentrate') accumulates at the sea floor (Shiau et al., 2007), which may have undesirable ecological effects (Del-Pilar-Ruso et al., 2008; Del Bene et al., 1994; Einav et al., 2003). Or it will lead, in the case of disposal via wells, to potential salinization or depletion of the groundwater system. This is the case when the net abstraction of freshwater is not compensated by infiltration of freshwater, but resulting in sea water intrusion or declining groundwater tables. For this reason, this deep disposal will be banned in The Netherlands in 2022, after a negative evaluation of its consequences (Technische Commissie Bodem, 2010). The combination of ASR and RO in one system using MPPWs as realized at the ASR site in the Westland (Chapter 5) can yield several interesting benefits, such as reduction of the volume requiring the RO treatment, a lower salinity of RO feedwater, a more robust water supply, and a balance in freshwater injection (aquifer replenishment) and recovery.

7.4.2 Broader evaluation of the dedicated well configurations to improve freshwater management

To explore the broader applicability of the dedicated well configurations discussed in this thesis for freshwater management in coastal zones, the efficiency of the MPPW, the Freshkeeper well, and the Freshmaker to solve four common hydrogeological problems in coastal areas was assessed:

- *Brackish water upconing (Reilly and Goodman, 1987b)*: resorting from shallow abstraction from a stratified aquifer (i.e., freshwater overlying brackish/saline water);
- *Seawater intrusion (SWI; Werner et al. (2013))*: 'the landward incursion of seawater' via the subsurface;
- *Thin target aquifers for abstraction / storage*: this may imply a low yield per well, requiring placement of expensive well galleries with many wells and pumps;
- *Saline seepage in deep polder areas (de Louw et al., 2010)*: ongoing land subsidence, sea-level rise, and occasionally (former) peat excavations intensify saline seepage in delta areas, which causes salinization of inland surface waters.

Based on the outcomes and insights from this thesis and previous Freshkeeper studies (Oosterhof et al., 2013; Stuyfzand and Raat, 2010; Wolthek et al., 2012), the

applicability of new dedicated well configurations to solve common hydrogeological problems and improve freshwater supply in coastal zones was evaluated. The outcomes are discussed below:

- *Brackish water upconing*: this process can be delayed by MPPW-ASR, but elimination cannot be guaranteed as upconing may still occur during recovery, especially when storage periods are long and deeper water is saline, a situation similar to scenario A and B of the Freshmaker in Chapter 6. Upconing may still threaten shallow abstraction wells when a Freshkeeper is applied and brackish water is not desalinated or removed permanently from the groundwater system, but only re-injected, as recently demonstrated by Alam and Olsthoorn (2014). The Freshkeeper and Freshmaker in their presented form (injecting membrane concentrate in a deeper confined aquifer or discharging abstracted saltwater to sea) can sufficiently eliminate upconing by the net abstraction of brackish water, as demonstrated by field monitoring (Oosterhof et al., 2013) and modelling scenarios C and D in Chapter 6. For both the Freshkeeper and Freshmaker it is required that freshwater abstraction rates and saltwater interception rates are coupled: overabstraction of freshwater in combination with limited interception of saltwater will still result in upconing;
- *Seawater intrusion*: MPPW-ASR may only prevent saltwater intrusion if the net injection exceeds the saltwater intrusion, making it a freshwater hydraulic barrier (e.g. Luyun et al., 2011; Mahesha, 1996), with deep injection at the optimal aquifer interval (Abarca et al., 2006). One may expect, however, that the Freshkeeper and the Freshmaker can prevent saltwater intrusion, provided that the well placement and their abstraction rates are such that the entire intruding saltwater wedge is intercepted and disposed of or desalinated. This was confirmed using density-dependent transport modelling in combination with an optimization model (Abd-Elhamid and Javadi, 2011), which indicated that coupled interception and abstraction (ADR: abstraction, desalination, recharge) can then be considered most (cost-)efficient;
- *Thin target aquifers for abstraction / storage*: MPPW-ASR and the Freshkeeper will be hard to apply in thin aquifers. However, the use of HDDWs in the Freshmaker set-up can make thin aquifers viable for abstraction/storage, since a single, high-capacity well can be realized;
- *Saline seepage in deep polders*: MPPW-ASR may freshen the diffusive seepage component sourced by shallow groundwater in the upper aquifer, but is less effective in counteracting seepage of deeper, saline groundwater via boils, which can be the largest salt contributor in polder areas (de Louw et al., 2010).

The Freshkeeper concept was previously suggested as a suitable technique to counteract saline seepage (Olsthoorn, 2008; Stuyfzand and Raat, 2010) Specific Consequences of Density Dependent Flow, and Positive Environmental Consequences </title><secondary-title>20th Saltwater Intrusion Meeting (SWIM, although it was considered unviable when all abstracted water is directly re-injected in deeper aquifers because of hydrological effects in the surrounding areas and the required high pumping rates (De Louw et al., 2007). This underlines that a net abstraction via aboveground disposal or concentration of the abstracted brackish water is desirable to actually reduce seepage. The Freshmaker can decrease the saline seepage in polder areas based on the modelling performed for the Ovezande field pilot. As the intercepted saltwater is disposed to a local water course here, the current set-up does not contribute to a reduction in salt load to the local surface water system. Disposal of intercepted brackish-saline groundwater (or membrane concentrate when desalination is applied) can therefore be expected to become a key element in coastal freshwater management.

Finally, the MPPWs studied in this thesis can be used to separate different water quality during abstraction from aquifers with a stratified water quality, also in non-coastal areas. Treatment efforts at, for instance, drinking water well fields may be reduced this way as the flux requiring treatment can be reduced, while clogging of abstraction wells by redox zonation (Bustos Medina et al., 2013; Van Beek, 2012) can also be reduced or even prevented by separation of iron and oxygen containing groundwater.

7.4.3 Impacts on the (ground)water system

The ASR techniques that are discussed in this thesis involve use of the relatively shallow subsurface. Impact on the shallow groundwater and potentially the surface water system may therefore be anticipated. If ASR is accompanied by saltwater interception and disposal to the surface water system, there is even a direct impact. Based on the findings in this thesis, a few observations can already be made in this context.

First of all, it is important to note that during ASR in brackish aquifers, only a part of the injected freshwater can be recovered (Chapter 3). This results in a net freshening of the aquifer by the introduction of ASR. Unrecovered freshwater surpluses which are otherwise discharged to sea, will move to the top of the shallow aquifers, creating stratification in the aquifer's groundwater quality. This will decrease the salinity of diffuse seepage towards the land surface in the study area of this thesis. For boil seepage, which may be a larger contributor to the surface water's salinity (de Louw

et al., 2010), positive effects will be less significant, however, since these boils can attract water from the whole thickness of the aquifer (de Louw et al., 2013).

In the study area of this thesis, groundwater levels are controlled by drainage systems. Therefore, to balance the freshwater infiltration during ASR using rainwater surpluses, more groundwater must become drained and discharged to sea. A local increase of seepage of deeper groundwater can therefore be anticipated close to the ASR systems during infiltration stages. This can especially be expected when the rainwater is collected and by-passes the upper aquitard without replenishing the shallow groundwater, like in the case of the MPPW-ASR systems in Chapter 3-5. When the ASR systems use aboveground buffers for temporal freshwater surpluses, the discharge via the drainage systems will also become better distributed over time; the aboveground retention will reduce peak discharges during intense rainfall events, while the subsequent slow infiltration will enhance seepage and discharge in the following dry(er) period. During recovery, abstraction of freshwater from the ASR bubble will result in relatively low hydraulic heads in the target aquifer in the system's surroundings, which may locally reduce seepage to the drainage system and cause additional lowering of the groundwater table. These processes may limit salinization of the drainage system, but may also induce subsidence.

In the case of the Freshmaker, where shallow freshwater lenses are thickened by shallow infiltration of freshwater and deep interception of saltwater, the results indicate that the shallow groundwater will freshen. Additionally, saltwater upconing towards draining water courses can become eliminated due to the deep interception of saltwater, or even infiltration from the watercourses may occur during recovery periods. Only the disposal of deep saltwater will therefore remain as a source of saltwater to the surface water system. On a catchment scale, it can therefore be relevant to regulate the saltwater interception and discharge, especially when many Freshmakers are installed, to prevent severe salinization of the surface water system.

7.5 Scientific implications and research perspectives

7.5.1 Scientific implications of this thesis: validation of theoretical analysis and improvement of ASR performance

Recently, new methods to either evaluate (Bakker, 2010; Ward et al., 2007; Ward et al., 2008; Ward et al., 2009) or improve (Maliva and Missimer, 2010; Van Ginkel et al., 2014) the performance of ASR in coastal areas were proposed in (scientific)

literature. This thesis provides essential scientific insights to the practical implementation of these methods. First of all, it is shown in Chapter 2 that a priori estimations on the performance of ASR can be used to map suitable ASR sites without rigorous numerical modelling. Based on the comparison with the performance of existing ASR systems, the proposed estimation methods proved to be reliable. The method provided by Bakker (2010) provided the most quantitative and accurate predictions of ASR performance in brackish-saline aquifers. Yet, this method is only reliable for stagnant groundwater bodies, fully penetrating wells and isotropic aquifers. Additionally, the groundwater transport modelling at the Westland ASR site (Chapter 5) demonstrates that upconing might occur when the underlying, confining aquitard is not sufficiently impermeable. The existing performance estimations indicate the potential ASR performance based on the target aquifer only, and not based on its confinement. For this reason, it is of major importance to know if an underlying aquitard can be considered virtually impermeable prior to implementation of the current ASR performance estimation methods.

The hypothetical improvement of ASR performance by the introduction of independently operating well screens at different depths was validated by integrated scientific research, comprising field experiments, (geo)chemical and geophysical analyses, and numerical modelling. This coupling of methods provides a sound and reliable scientific basis for future implementation. Measurements during operation at two field sites indicate that a reliable MPPW can be constructed, as short-circuiting via the MPPW-borehole was not observed. Besides the gains in freshwater recovery, this study is also the first to demonstrate that a complete mitigation of freshwater losses with MPPW-ASR cannot be obtained. It is also the first to recognize how reactive transport processes during MPPW-ASR have a distinct impact on recovered freshwater. The potential of HDDWs for ASR in coastal aquifers was also addressed briefly. However, preliminary benefits of this shift to horizontal well screens during ASR may boost the scientific research on the functioning of horizontal wells (and HDDWs in particular), which is still scant in comparison with vertical wells.

7.5.2 Future scientific research

7.5.2.1 Optimization of well configurations and operations

Although the dedicated well configurations and the adjusted operation proved to be beneficial in this thesis research, the optimization of both is still lacking. Scientific research is required to identify the most optimal or robust configurations and operations to further maximize the freshwater recovery if possible, and to quantify their cost-effectiveness. Similarly, scientific research should be performed to enable effi-

cient interception of saltwater during operation of a Freshkeeper (during recovery) or a Freshmaker (injection, storage, and recovery). Dedicated real-time sensoring in the target aquifer will provide essential information to efficiently operate the more dedicated coastal ASR systems. The recent use of, for instance, fiber optic cables (Bakker et al., 2015) inserted with direct push might be effective for this purpose, if a fiber optic cable to measure electrical conductivity instead of temperature is developed. Compact element specific sensors measuring, for instance, Na, Fe, and Mn can also contribute to further optimization of the ASR performance. Scientific research should indicate if these additional, detailed data enable a substantial increase in freshwater production, compared to the current data availability (online EC of abstracted water, sporadically CTD divers in observation wells). Altogether, it is scientific research that should provide relevant input for automated central control units to increase the robustness and applicability of the dedicated coastal ASR systems presented in this thesis.

This thesis also shows that successful ASR in brackish-saline aquifers is not solely controlled by the admixing of injected water with more saline groundwater. Unmixed water can become unsuitable for use upon aquifer residence due to geochemical interactions, especially when the deepest aquifer sections are the most reactive, for instance due to a high CEC or a tendency to release (trace) metals. Preparation of this aquifer section prior to injection of the water that is to be recovered can be successful, but fundamental controls need to become known to efficiently pre-treat this aquifer zone with either strong oxidant (e.g. Antoniou et al., 2014) or exchanging ions like Ca (e.g., Brown and Silvey, 1977; Konikow et al., 2001). The same holds for the apparently successful subsurface iron removal during MPPW-ASR, which justifies further scientific research to improve the recovered water quality.

7.5.2.2 RE increase in geologically differing aquifers

All findings in this thesis are based on case studies involving sandy unconsolidated aquifers in The Netherlands, which are dominated by intergranular flow. However, limestone aquifers are also frequently found in coastal zones, and are targeted for freshwater supply worldwide. Transport processes may differ significantly in such aquifers due to dual-porosity (Bibby, 1981). This can lead to underperforming ASR-systems due to extremely early salinization via preferential flow paths (e.g., Maliva and Missimer, 2010; Missimer et al., 2002; Pyne, 2005), comparable to the man-made connection between different aquifers presented in Chapter 5. In the same way, this may reduce the effectiveness of the improvements suggested, since flow patterns are less predictable and preferential flow paths may hamper for instance the interception of brackish-saline water by for instance a Freshkeeper or a Freshmaker. Scientific

research is required to validate the efficiency of the dedicated well configurations for aquifers with a different texture. A logical first step would be modelling of the dedicated configurations in such aquifers, followed by field validation in case the modelling exercises predict positive effects on the RE.

7.5.2.3 Impacts on the (ground)water system

Although some impacts on the (ground)water system could be reasoned based on the outcomes of this thesis (Section 7.4.3), a more detailed scientific analysis of the effects of the relatively shallow ASR techniques on the (ground)water system is justified. Only recently, a better scientific understanding of the current groundwater-surface water interactions in coastal areas was obtained by field and modelling studies (De Louw, 2013; Delsman, 2015; Pauw, 2015). In a next step, a sound scientific understanding of the effect of relatively shallow ASR on the current groundwater – surface water interaction should be obtained. This way, the true potential of ASR to simultaneously counteract broader water management issues like (pluvial) flooding and water quality deterioration (salinization, eutrophication) should be assessed.

Similarly, the effects of upscaling should be assessed, since an uncontrolled expansion of ASR may lead to interference and suboptimal performance, as illustrated by recent aquifer thermal energy storage systems (ATES; Bloemendal et al., 2014). In the case of ASR, however, less interference can be expected since most users store only one type of water (freshwater), whereas during ATES both warm and cold water is stored. Furthermore, it can be expected that the conditions for ASR in coastal aquifers will generally improve upon widespread application, due to the freshening of target aquifers.

7.5.2.4 Quality of recovered water upon aquifer residence

In Chapter 4, the reactive transport controls on the chemical water quality were scientifically assessed. It was shown that introduction of the MPPW-ASR system leads to deviating hydrochemical processes in comparison with conventional ASR, which can lead to continuous enrichment with Fe and Mn. Hydrochemical monitoring at the Freshmaker (Chapter 0) highlighted enrichment with Fe and Mn especially during the start of recovery. A further scientific diagnosis of the cause of the enrichment at the Freshmaker and the apparently successful subsurface removal of Fe and Mn at the MPPW-ASR site in Nootdorp is essential to obtain better controls on the chemical water quality for the ASR end users, who demand an impeccable water quality. In line with the chemical water quality, advanced agriculture demands microbial reliability of the irrigation water, which is often not provided by surface waters. Similarly, surface

water and storm water (also: greenhouse roofwater) may contain organic micropollutants, which can pose a threat to the groundwater system. Therefore, the functioning of ASR or aquifer storage transfer and recovery (ASTR) as a treatment step by degradation of pathogens and (emerging) micropollutants deserves further scientific attention, despite the relevant research already performed (e.g. Dillon, 2005; Dillon et al., 2006; Dillon et al., 2010; Patterson et al., 2011; Pavelic et al., 2006). An additional water quality aspect forms the dispersion of clay minerals upon freshening during infiltration, which was observed especially at the Westland field site and in literature (Konikow et al., 2001; Torkzaban et al., 2015; Zheng et al., 2014). Especially when the mixed injected water – groundwater is used for desalination via reverse osmosis to enhance the freshwater recovery, this may lead to operational problems such as membrane clogging.

Chapter 8

Dankwoord

Na ruim 4 jaar intensief onderzoek ben ik bijzonder veel mensen dank verschuldigd. Een dergelijk praktijkgericht en tegelijkertijd wetenschappelijk onderzoek in zo'n korte tijd opzetten, uitvoeren en laten accumuleren in een thesis kun je immers niet alleen. De volgorde die ik in dit dankwoord aanhoud zal enigszins chronologisch zijn.

Allereerst bedank ik Geert-Jan Vis en Kees Kasse van de VU. Hun wetenschappelijke bedrevenheid in de laatste fase van mijn Bacheloropleiding gaf mij de eerste duw richting de wetenschap, een sector die voor mij tot die tijd even onbekend als onbemind was. Geert-Jan en Kees hebben daarnaast tijdens mijn promotieonderzoek een belangrijke bijdrage geleverd aan de verwerking en de interpretatie van de in Nootdorp gestoken kernen.

Een volgende forse zet richting de wetenschap gaven Boris van Breukelen en Vincent Post van de VU en Johan Valstar (Deltares), Eric van Nieuwkerk (thans BECA, NZ) en Niels Hartog (thans KWR). De onderzoeksprojecten tijdens mijn Masteropleiding Applied Environmental Geosciences onder hun supervisie zorgden voor een zeer solide basis met zowel hydrologische als chemische kennis en kunde, inclusief het vertalen naar accurate, heldere, en compact beschreven uitkomsten. Trots ben ik nog altijd op mijn eerste peer-reviewed paper als eerste auteur die hieruit volgde, welke helaas onvoldoende in de scope van dit proefschrift paste.

In mei 2010 benaderde Pieter Stuyfzand mij om invulling te geven aan een promotiepositie aan de VU, gekoppeld aan een aanstelling bij KWR in Nieuwegein. Iets met ondergronds bergen en terugwinnen van zoetwater bij agrariërs, een heel nieuwe doelgroep (voor KWR, althans). Een goede kop koffie met Pieter op station Utrecht Centraal en een kennismaking met betrokkenen bij KWR leidde ertoe dat ik op 1 september 2010 van start kon als PhD.

Dit onderzoek vond plaats binnen Kennis voor Klimaat, binnen het thema 'Zoetwatervoorziening' onder leiding van Ad Jeuken en Eelco van Beek. Met veel plezier heb ik binnen Kennis voor Klimaat samengewerkt met andere onderzoekers en programmamanagers. In het bijzonder vermeld ik daarbij naast Ad en Eelco ook de nauw betrokken onderzoekers Pieter Pauw, Joost Delsman, Gualbert Oude Essink (allen Deltares en zeer bedreven met zoet-zout), Jeroen Veraart (Alterra) en Kim van Nieuwaal en Monique Slegers (Kennis voor Klimaat).

Binnen KWR heb ik met veel plezier en in een goede sfeer aan mijn onderzoek kunnen werken. Alle collega's binnen de afdeling Watersysteemtechnologie ben ik hiervoor dankbaar. Bijzondere dank ben ik verschuldigd aan mijn kamergenoot en strijdmakker Marcel Paalman. Samen zijn we een avontuur aangegaan waarbij het af en toe best spannend werd, maar de overtuiging rondom ASR bleef. Het heeft goed uitgepakt. Dank voor jouw inzicht en relativering tijdens de lange en soms vermoei-

ende processen met de verschillende partijen. Uiteraard dank ik mijn teamleiders Gert-Jan Zwolsman en Jan Willem Kooiman en kennisgroepmanager Jos Boere voor hun continue support in soms risicodragende, moeilijke (veld)projecten. Kees Vink en Femke Rambags wil ik bedanken voor hun gedegen voorbereidende werk aan de Freshmaker.

Ondanks het feit dat promotie plaats heeft aan de TU Delft, vond het gros van onderzoek plaats aan de VU. Totdat vreemde besluiten een eind maakten aan de Amsterdam Critical Zone Hydrology Group heb ik daar met veel plezier kunnen werken. Joost, Andreas en Hans-Peter, dank voor jullie goede gezelschap in de verschillende kamers. Met name roommate Matthijs wil ik bedanken voor zijn praktische tips rondom boren, putten, meten, labanalyses, publiceren, promoveren, et cetera. John en Martine bedank ik voor hun hulp bij de verwerking van inmiddels 1216 watermonsters en 504 sedimentmonsters van verschillende pilots. Ook de staf van de groep wil bedanken voor hun hulp, goede koffie en zeer prettige gezelschap: Koos, Maarten, Boris, Henk, Ilja en Sampurno. Michel en Frans bedank ik in het bijzonder voor de ondersteuning bij het vele veldwerk en de goede gesprekken. De betrokken studenten bedank ik voor hun onmisbare bijdrage aan mijn onderzoek: Guido, Robert, Vera, Bas en Siebren. Mark Bakker en Willem Jan Zaadnoordijk van de TU Delft wil ik bedanken voor de hulp bij het toepassen van methoden om aan ASR te rekenen en het tot stand brengen van Hoofdstuk 2. Willem Jan bedank ik tevens voor zijn hulp bij het modelleren en rapporteren van het systeem in Nootdorp.

Al vroeg in mijn onderzoeksproject ontmoette ik via Guus Meis (LTO-Glaskracht) een pionier binnen de Zuid-Hollandse ASR-wereld: Eef Zwinkels van B-E De Lier. Door zijn bevlogenheid en bekendheid met de waarde van (en de problemen met) ASR in de glastuinbouw hebben we de veldproeven Nootdorp en Westland kunnen realiseren. Dit zijn uiteindelijk pijlers geworden waar het proefschrift op staat. Dus Eef: ik ben je hier zeer erkentelijk voor. Later is de goede samenwerking met (inmiddels) Codema B-E De Lier voortgezet, waarvoor ik met name Dick, Danny, Patrick, Ed en Richard wil bedanken. Piet en Peter Meeuwse van Meeuwse Handelsonderneming Goes speelden tezamen met Carla Michielsen en John Bal van de ZLTO een minstens zo belangrijke rol bij het tot stand brengen, in de lucht houden en monitoren van de Freshmaker. Het is te danken aan de inzet van deze lokale (markt)partijen dat uitgebreide veldproeven in relatief zeer korte tijd tot stand konden komen.

Zodoende kom ik bij de tuinders die het aandurfden om met ASR te gaan werken op hun bedrijf. Water is geen speeltje binnen de hoogwaardige tuinbouw en dagelijkse beschikbaarheid van voldoende water van uitmuntende kwaliteit is een vereiste. Ik ben jullie dan ook zeer dankbaar dat jullie de ruimte en medewerking hebben

geschonken om de beproefde ASR-systemen in jullie bedrijfsvoering in te passen, te bemeten en testen. Hans en André van der Goes, Jan en Paula Rijk, en Marco, René en met name Cornelis van Prominent Tomaten: dank voor jullie medewerking. Jullie inspanning, kennis, passie en kunde om te komen tot uitmuntende orchideeën, appels/peren en tomaten zijn doorgaans onderbelicht en ondergewaardeerd, maar verdienen veel respect.

Uiteraard bedank ik ook de belangrijkste personen om de thesis en de promotie te voltooien. De leden van de promotiecommissie voor hun beoordeling van het proefschrift en de deelname aan de publieke verdediging. David, thank you for the fascinating ASR discussions we had. En natuurlijk: Pieter en Niels, dank voor jullie supervisie gedurende de laatste jaren. Jullie stonden vrijwel altijd en op adequate wijze voor mij paraat, ondanks zeer drukke werk- en privéagenda's. Jullie hebben mij gevormd tot een scherpe en efficiënte onderzoeker.

Tot slot, dank aan mijn familie voor de steun voor en de afleiding tijdens dit promotieproject. Ondanks dat jullie van het wetenschappelijke deel soms niet echt een beeld hadden, hadden jullie dit beeld voor het agrarische en menselijke deel zoveel meer. Inge, bedankt voor je steun, zorg en met name afleiding gedurende de laatste jaren. Zonder jou was de opgave vele malen groter geweest.

Chapter **9**

Curriculum Vitea

Koen Gerardus Zuurbier was born in 1985 in Heerhugowaard. He studied Applied Environmental Geosciences at the Free University (VU) in Amsterdam. From 2006 until 2010, he worked part-time as field engineer at Grondslag BV and MWH. During his Master education programme in 2009, he worked on the execution and data-processing of a large field monitoring campaign at the Banisveld Landfill site in the Southern-Netherlands. This study was followed by a coupled groundwater transport/chemical modelling study of aquifer thermal energy storage (ATES) systems in 2010 at Deltares (Master Thesis).

After graduating, Koen Zuurbier started as a scientific researcher at KWR Watercycle Research Institute in the 'Knowledge for Climate' Research Program, coupled with a PhD-candidacy at the VU in Amsterdam and later the Technical University of Delft. In his research he focuses on water management and water quality issues during aquifer storage and recovery (ASR) of freshwater. Examples of research topics are the design, operation, and field monitoring of ASR systems in coastal aquifers and the (reactive) groundwater transport modelling involved.

Koen Zuurbier aims to form a bridge between science and practice, linking science with the daily practice of end users and technicians to enable efficient and sustainable use of the subsurface for freshwater supply.

Peer reviewed publications

Zuurbier, K.G. and Stuyfzand, P.J., submitted-a. Consequences and mitigation of saltwater intrusion induced by short-circuiting during aquifer storage and recovery (ASR) in a coastal, semi-confined aquifer. Submitted to: Hydrology and Earth Systems Science.

Zuurbier, K.G., Hartog, N., Stuyfzand, P.J., submitted-b. Reactive transport impacts on recovered freshwater quality for a field MPPW-ASR system in a brackish and geochemically heterogeneous coastal aquifer. Submitted to Applied Geochemistry.

Zuurbier, K.G., Raat, K.J., Paalman, M., Oosterhof, A.T., Stuyfzand, P.J., 2016. How Subsurface Water Technologies (SWT) can Provide Robust, Effective, and Cost-Efficient Solutions for Freshwater Management in Coastal Zones. Water resources Management: 1-17. DOI: 10.1007/s11269-016-1294-x.

Zuurbier, K.G., Kooiman, J.W., Groen, M.M.A., Maas, B., Stuyfzand, P.J., 2015. Enabling Successful Aquifer Storage and Recovery of Freshwater Using Horizontal Directional Drilled Wells in Coastal Aquifers. Journal of Hydrologic Engineering, 20(3): B4014003.

Zuurbier, K.G., Zaadnoordijk, W.J., Stuyfzand, P.J., 2014. How multiple partially penetrating wells improve the freshwater recovery of coastal aquifer storage and recovery (ASR) systems: A field and modeling study. Journal of Hydrology, 509(0): 430-441.

Zuurbier, K.G., Hartog, N., Valstar, J., Post, V.E.A., van Breukelen, B.M., 2013b. The impact of low-temperature seasonal aquifer thermal energy storage (SATES) systems on chlorinated solvent contaminated groundwater: Modeling of spreading and degradation. Journal of Contaminant Hydrology, 147(0): 1-13.

Zuurbier, K.G., Bakker, M., Zaadnoordijk, W., Stuyfzand, P., 2013a. Identification of potential sites for aquifer storage and recovery (ASR) in coastal areas using ASR performance estimation methods. Hydrogeology Journal, 21(6): 1373-1383.

Vis, G.-J., Bohncke, S. J. P., Schneider, H., Kasse, C., Coenraads-Nederveen, S., Zuurbier, K., and Rozema, J. ,2010. Holocene flooding history of the Lower Tagus Valley (Portugal). Journal of Quaternary Science, 25(8): 1222-1238.

Conference proceedings

Gertjan Zwolsman, Peter van Thienen, Koen Zuurbier, Cees van Leeuwen & Erdem Görgün, 2015. Watershare®: An international network for efficient knowledge transfer within the water sector – Potential applications in Turkey. Sustainable Water Management, Izmir, Turkey.

Zuurbier, K.G. et al., 2014. How subsurface water technologies provide robust, effective and cost-efficient freshwater solutions IWA - World Water Congress. IWA, Lisbon, Portugal.

Zuurbier, K.G., Zaadnoordijk, W.J., Stuyfzand, P.J., 2013a. Towards successful aquifer storage and recovery (ASR) in coastal aquifers: use of ASR feasibility mapping and multiple partially penetrating wells, International symposium on managed aquifer recharge (ISMAR) 8, Beijing, China.

Zuurbier, K.G., Stuyfzand, P.J., Kooiman, J.W., 2013b. The Freshmaker: enabling aquifer storage and recovery (ASR) of freshwater using horizontal directional drilled wells (HDDWs) in coastal areas, International symposium on managed aquifer recharge (ISMAR) 8, Beijing, China.

Zuurbier, K.G., Stuyfzand, P.J., 2012. Optimizing small- to medium-scale aquifer storage and recovery in coastal aquifers for irrigation water supply, Saltwater Intrusion Meeting (SWIM) 22, Armacao dos Buzios, Brazil, pp. 144-146.

Zuurbier, K.G., Paalman, M., Stuyfzand, P.J., 2011. Making innovative water technologies feasible in practice: use of Aquifer Storage and Recovery (ASR) in irrigation water supply and water reuse, International Water Week 2011, Amsterdam.

Professional publications

Zuurbier, K.G., Hartog, N., Valstar, J., Van Nieuwkerk, E., 2011 - Sterk verbeterde analyse van interactie warmte/koude-opslag en verontreinigd grondwater. Vakblad H2O.

Zuurbier, K.G., Stuyfzand, P.J., 2013. Sophisticated well configurations to enable aquifer

storage and recovery (ASR) in coastal aquifers, Zout grondwater in kustgebieden: van probleem tot oplossing, Utrecht, pp. 1.

Zuurbier, K.G., Paalman, M., Van der Linde, S., De Gelder, D., Meeuwse, P.J., 2015. Innovatieve putconcepten maken zoetwaterreservoir in verzilte ondergrond mogelijk. Vakblad H2O.

Zuurbier, K.G., Stuyfzand, P.J., Van Loon, A., 2013. Deltafact Ondergrondse Waterberging, STOWA, STOWA - Deltaproof.

Chapter **10**

Bibliography

Abarca, E. et al., 2006. Optimal design of measures to correct seawater intrusion. Water Resources Research, 42(9): W09415.

Abd-Elhamid, H., Javadi, A., 2011. A Cost-Effective Method to Control Seawater Intrusion in Coastal Aquifers. Water resources Management, 25(11): 2755-2780.

Alam, N., Olsthoorn, T.N., 2014. Punjab scavenger wells for sustainable additional groundwater irrigation. Agricultural Water Management, 138(0): 55-67.

Aliewi, A.S. et al., 2001. Numerical Simulation of the Movement of Saltwater under Skimming and Scavenger Pumping in the Pleistocene Aquifer of Gaza and Jericho Areas, Palestine. Transport in Porous Media, 43(1): 195-212.

Antoniou, E.A., Hartog, N., van Breukelen, B.M., Stuyfzand, P.J., 2014. Aquifer pre-oxidation using permanganate to mitigate water quality deterioration during aquifer storage and recovery. Applied Geochemistry, 50(0): 25-36.

Antoniou, E.A., Stuyfzand, P.J., van Breukelen, B.M., 2013. Reactive transport modeling of an aquifer storage and recovery (ASR) pilot to assess long-term water quality improvements and potential solutions. Applied Geochemistry, 35(0): 173-186.

Antoniou, E.A., van Breukelen, B.M., Putters, B., Stuyfzand, P.J., 2012. Hydrogeochemical patterns, processes and mass transfers during aquifer storage and recovery (ASR) in an anoxic sandy aquifer. Applied Geochemistry, 27(12): 2435-2452.

Appelo, C.A.J., 1994a. Some Calculations on Multicomponent Transport with Cation Exchange in Aquifers. Ground water, 32(6): 968-975.

Appelo, C.A.J., 1994b. Cation and proton exchange, pH variations, and carbonate reactions in a freshening aquifer. Water Resources Research, 30(10): 2793-2805.

Appelo, C.A.J., Postma, D., 2005. Geochemistry, groundwater and pollution, 2. A.A. Balkema, Leiden, The Netherlands, 649 pp.

Arnell, N.W., 1999. Climate change and global water resources. Global Environmental Change, 9, Supplement 1(0): S31-S49.

Asghar, M.N., Prathapar, S.A., Shafique, M.S., 2002. Extracting relatively-fresh groundwater from aquifers underlain by salty groundwater. Agricultural Water Management, 52(2): 119-137.

Bakker, M., 2010. Radial Dupuit interface flow to assess the aquifer storage and recovery potential of saltwater aquifers. Hydrogeology Journal, 18(1): 107-115.

Bakker, M., Caljé, R., Schaars, F., van der Made, K.-J., de Haas, S., 2015. An active heat tracer experiment to determine groundwater velocities using fiber optic cables installed with direct push equipment. Water Resources Research, 51(4): 2760-2772.

Bakr, M., van Oostrom, N., Sommer, W., 2013. Efficiency of and interference among multiple Aquifer Thermal Energy Storage systems; A Dutch case study. Renewable Energy, 60(0): 53-62.

Barends, B.J., Brouwer, F.J.J., Schröder, F.H., 1995. Land subsidence, natural causes, measuring techniques, the Groningen gasfields. Balkema, Rotterdam, The Netherlands, 409 pp.

Bear, J., 1972. Dynamics of fluids in porous media. American Elsevier, New York, U.S.A.

Bear, J., Jacobs, M., 1965. On the movement of water bodies injected into aquifers. Journal of Hydrology, 3(1): 37-57.

Berner, R.A., 1984. Sedimentary pyrite formation: An update. Geochimica et Cosmochimica Acta, 48(4): 605-615.

Bibby, R., 1981. Mass transport of solutes in dual-porosity media. Water Resources Research, 17(4): 1075-1081.

Bloemendal, M., Olsthoorn, T., Boons, F., 2014. How to achieve optimal and sustainable use of the subsurface for Aquifer Thermal Energy Storage. Energy Policy, 66: 104-114.

Bonte, M. et al., 2013a. Impacts of Shallow Geothermal Energy Production on Redox Processes and Microbial Communities. Environmental Science & Technology, 47(24): 14476-14484.

Bonte, M., Stuyfzand, P.J., Hulsmann, A., Van Beelen, P., 2011a. Underground Thermal Energy Storage: Environmental Risks and Policy Developments in the Netherlands and European Union. Ecology and Society, 16.

Bonte, M., Stuyfzand, P.J., Van den Berg, G.A., Hijnen, W.A.M., 2011b. Effects of aquifer thermal energy storage on groundwater quality and the consequences for drinking water production: a case study from the Netherlands. Water science and technology, 63(9): 1922-1931.

Bonte, M., van Breukelen, B.M., Stuyfzand, P.J., 2013b. Temperature-induced impacts on groundwater quality and arsenic mobility in anoxic aquifer sediments used for both drinking water and shallow geothermal energy production. Water Research, 47(14): 5088-5100.

Bonte, M., Zaadnoordijk, W.J., Maas, K., 2014. A Simple Analytical Formula for the Leakage Flux Through a Perforated Aquitard. Groundwater: n/a-n/a.

Breeuwsma, A., Wösten, J.H.M., Vleeshouwer, J.J., van Slobbe, A.M., Bouma, J., 1986. Derivation of Land Qualities to Assess Environmental Problems from Soil Surveys1. Soil Sci. Soc. Am. J., 50(1): 186-190.

Broers, H.P., 2001. A strategy for sampling reactive aquifer sediments in drinking water well fields, Impact of Human Activity on Groundwater Dynamics. IAHS, Maastricht, pp. 247-253.

Brown, D.L., Silvey, W.D., 1977. Artificial recharge to a freshwater-sensitive brackish-water sand aquifer, Norfolk, Viginia. U.S. Geological Survey Professional Paper, 953: 53.

Buscheck, T.A., Doughty, C., Tsang, C.F., 1983. Prediction and analysis of a field experiment on a multilayered aquifer thermal energy storage system with strong buoyancy flow. Water Resources Research, 19(5): 1307-1315.

Busschers, F.S. et al., 2005. Sedimentary architecture and optical dating of Middle and Late Pleistocene Rhine-Meuse deposits – fluvial response to climate change, sea-level fluctuation and glaciation. Netherlands Journal of Geosciences, 84(1): 25-41.

Bustos Medina, D., Berg, G., Breukelen, B., Juhasz-Holterman, M., Stuyfzand, P., 2013. Iron-hydroxide clogging of public supply wells receiving artificial recharge: near-well and in-well

hydrological and hydrochemical observations. Hydrogeology Journal: 1-20.
CBS, 2013. Hernieuwbare energie in Nederland 2012, CBS, available via: www.cbs.nl.
Ceric, A., Haitjema, H., 2005. On using simple time-of-travel capture zone delineation methods. Ground Water, 43(3): 408-412.
Chesnaux, R., 2012. Uncontrolled Drilling: Exposing a Global Threat to Groundwater Sustainability Journal of Water Resource and Protection, 4(9): 4.
Chesnaux, R., Chapuis, R., 2007. Detecting and quantifying leakage through defective borehole seals: a new methodology and laboratory verification. Geotechnical Testing Journal, 30(1): 17.
Chesnaux, R., Rafini, S., Elliott, A.-P., 2012. A numerical investigation to illustrate the consequences of hydraulic connections between granular and fractured-rock aquifers. Hydrogeology Journal, 20(8): 1669-1680.
Cirkel, D.G., Van der Wens, P., Rothuizen, R.D., Kooiman, J.W., 2010. Water extraction with HDD drillings - One horizontal well for multiple vertical wells. Land+Water, access via www.hddw.nl.
Clinton, T., 2007. Reclaimed water Aquifer Storage and Recovery; potential changes in water quality. WateReuse Foundation WRF-03-009, Alexandria VA, USA.
De Louw, P.G.B., 2013. Saline seepage in detaic areas, VU University, Amsterdam, 200 pp.
de Louw, P.G.B. et al., 2011. Shallow rainwater lenses in deltaic areas with saline seepage. Hydrol. Earth Syst. Sci., 15(12): 3659-3678.
De Louw, P.G.B., Oude Essink, G.H.P., Maljaars, P., 2007. Background study: seepage reduction techniques (in Dutch), TNO.
de Louw, P.G.B., Oude Essink, G.H.P., Stuyfzand, P.J., van der Zee, S.E.A.T.M., 2010. Upward groundwater flow in boils as the dominant mechanism of salinization in deep polders, The Netherlands. Journal of Hydrology, 394(3–4): 494-506.
de Louw, P.G.B., Vandenbohede, A., Werner, A.D., Oude Essink, G.H.P., 2013. Natural saltwater upconing by preferential groundwater discharge through boils. Journal of Hydrology, 490(0): 74-87.
Del-Pilar-Ruso, Y., De-la-Ossa-Carretero, J.A., Giménez-Casalduero, F., Sánchez-Lizaso, J.L., 2008. Effects of a brine discharge over soft bottom Polychaeta assemblage. Environmental Pollution, 156(2): 240-250.
Del Bene, J.V., Jirka, G., Largier, J., 1994. Ocean brine disposal. Desalination, 97(1–3): 365-372.
Delsman, J.R., 2015. Saline groundwater - surface water interaction in coastal lowlands, VU University, Amsterdam, 185 pp.
Delta Commission, 2014. Delta Program 2015: Delta Decision Freshwater Strategy, Ministry of Infrastructure and Environment, The Hague.
Dillon, P., 2005. Future management of aquifer recharge. Hydrogeology Journal, 13(1): 313-316.
Dillon, P. et al., 2006. Role of aquifer storage in water reuse. Desalination, 188(1-3): 123-134.
Dillon, P. et al., 2010. Managed aquifer recharge: rediscovering nature as a leading edge technology.

Water science and technology, 62(10): 2338-2345.
Einav, R., Harussi, K., Perry, D., 2003. The footprint of the desalination processes on the environment. Desalination, 152(1–3): 141-154.
Esmail, O.J., Kimbler, O.K., 1967. Investigation of the technical feasibility of storing fresh water in saline aquifers. Water Resour. Res., 3(3): 683-695.
European Commission, 2012. A Blueprint to Safeguard Europe's Water Resources, Brussel.
Ferguson, B.K., 1990. Urban storm water infiltration: Purposes, implementation, results. Journal of Soil and Water Conservation, 45(6): 605-609.
Fortuin, N.P.M., Willemsen, A., 2005. Exsolution of nitrogen and argon by methanogenesis in Dutch ground water. Journal of Hydrology, 301(1–4): 1-13.
Gasda, S., Nordbotten, J., Celia, M., 2008. Determining effective wellbore permeability from a field pressure test: a numerical analysis of detection limits. Environmental Geology, 54(6): 1207-1215.
Greskowiak, J., Prommer, H., Vanderzalm, J., Pavelic, P., Dillon, P., 2005. Modeling of carbon cycling and biogeochemical changes during injection and recovery of reclaimed water at Bolivar, South Australia. Water Resources Research, 41(10): W10418.
Hantush, M.S., 1966. Wells in homogeneous anisotropic aquifers. Water Resour. Res., 2(2): 273-279.
Harbough, A.W., Banta, E.R., Hill, M.C., McDonald, M.G., 2000. Modflow-2000, the U.S. Geological Survey modular groundwater model - User guide to modularization concepts and the Groundwater Flow Process. Open-File Report 00-92, U.S. Geological Survey.
Hartog, N., Griffioen, J., van der Weijden, C.H., 2002. Distribution and Reactivity of O2-Reducing Components in Sediments from a Layered Aquifer. Environmental Science & Technology, 36(11): 2338-2344.
Hermann, R., 2005. ASR well field optimization in unconfined aquifers in the Middle East, ISMAR5. United Nations Educational, Scientific and Cultural Organization, Berlin, Germany.
Houben, G.J., Hauschild, S., 2011. Numerical Modeling of the Near-Field Hydraulics of Water Wells. Ground water, 49(4): 570-575.
Hubber, M.K., Willis, D.G., 1972. Mechanics of hydraulic fracturion. AAGP, Memoir 18: 199-217.
Intergovernmental Panel on Climate Change (IPCC), 2007. Climate Change 2007 - The Physical Science Basis New York, USA.
Jiménez-Martínez, J., Aravena, R., Candela, L., 2011. The Role of Leaky Boreholes in the Contamination of a Regional Confined Aquifer. A Case Study: The Campo de Cartagena Region, Spain. Water, Air, & Soil Pollution, 215(1-4): 311-327.
Jones, G.W., Pichler, T., 2007. Relationship between pyrite stability and arsenic mobility during aquifer storage and recovery in southwest central Florida. Environ. Sci. Technol, 41(3): 723-730.

Koltermann, C.E., Gorelick, S.M., 1995. Fractional packing model for hydraulic conductivity derived from sediment mixtures. Water Resources Research, 31(12): 3283-3297.

Konert, M., Vandenberghe, J., 1997. Comparison of laser grain size analysis with pipette and sieve analysis: a solution for the underestimation of the clay fraction. Sedimentology, 44(3): 523-535.

Konikow, L.F., August, L.L., Voss, C.I., 2001. Effects of Clay Dispersion on Aquifer Storage and Recovery in Coastal Aquifers. Transport in Porous Media, 43(1): 45-64.

Kooi, H., 2000. Land subsidence due to compaction in the coastal area of The Netherlands: the role of lateral fluid flow and constraints from well-log data. Global and Planetary Change, 27(1-4): 207-222.

Kronzucker, H.J., Britto, D.T., 2011. Sodium transport in plants: a critical review. New Phytologist, 189(1): 54-81.

Kumar, A., Kimbler, O.K., 1970. Effect of Dispersion, Gravitational Segregation, and Formation Stratification on the Recovery of Freshwater Stored in Saline Aquifers. Water Resources Research, 6(6): 1689-1700.

Kwadijk, J.C.J. et al., 2010. Using adaptation tipping points to prepare for climate change and sea level rise: a case study in the Netherlands. Wiley Interdisciplinary Reviews: Climate Change, 1(5): 729-740.

Langevin, C.D., 2008. Modeling Axisymmetric Flow and Transport. Ground Water, 46(4): 579-590.

Langevin, C.D., Thorne, D.T., Dausman, A.M., Sukop, M.C., Guo, W., 2007. SEAWAT version 4: a computer program for simulation of multi-species solute and heat transport. In: U.S.G.S. (Ed.), Techniques and Methods, book 6, Reston, Virginia, USA.

Lazareva, O., Druschel, G., Pichler, T., 2015. Understanding arsenic behavior in carbonate aquifers: Implications for aquifer storage and recovery (ASR). Applied Geochemistry, 52(0): 57-66.

Leonard, B.P., 1988. Universal limiter for transient interpolation modeling of the advective transport equations: the ULTIMATE conservative difference scheme. NASA Technical Memorandum 100916 ICOMP-88-11.

Lu, C., Werner, A.D., Simmons, C.T., Robinson, N.I., Luo, J., 2013. Maximizing Net Extraction Using an Injection-Extraction Well Pair in a Coastal Aquifer. Ground Water, 51(2): 219-228.

Luyun, R., Momii, K., Nakagawa, K., 2011. Effects of Recharge Wells and Flow Barriers on Seawater Intrusion. Ground water, 49(2): 239-249.

Ma, R., Zheng, C., 2010. Effects of Density and Viscosity in Modeling Heat as a Groundwater Tracer. Ground Water, 48(3): 380-389.

Maas, C., 2011. Leakage via unsealed boreholes (in Dutch), KWR watercycle research institute, Nieuwegein.

Mahesha, A., 1996. Steady-State Effect of Freshwater Injection on Seawater Intrusion. Journal of Irrigation and Drainage Engineering, 122(3): 149-154.

Maliva, R.G., Guo, W., Missimer, T.M., 2006. Aquifer storage and recovery: Recent hydrogeological advances and system performance. Water Environment Research, 78(13): 2428-2435.

Maliva, R.G., Missimer, T.M., 2010. Aquifer Storage and Recovery and Managed Aquifer Recharge using wells; planning, hydrogeology, design and operation. Methods in Water Resources Evolution. Schlumberger, Texas, USA, 578 pp.

McNeill, J.D., Bosnar, M., Snelgrove, J.B., 1990. Technical Note 25: Resolution of an Electromagnetic Borehole logger for Geotechnical and groundwater applications.

Meinardi, C.R., 1994. Groundwater recharge and travel times in the sandy regions of the Netherlands, Vrije Universiteit Amsterdam, Amsterdam, The Netherlands, 211 pp.

Merritt, M.L., 1986. Recovering Fresh Water Stored in Saline Limestone Aquifers. Ground Water, 24(4): 516-529.

Mettler, S. et al., 2001. Characterization of iron and manganese precipitates from an in situ ground water treatment plant. Groundwater, 39(6): 921-930.

Metzger, L.F., Izbicki, J.A., 2013. Electromagnetic-Induction Logging to Monitor Changing Chloride Concentrations. Ground water, 51(1): 108-121.

Miotliński, K., Dillon, P.J., Pavelic, P., Barry, K., Kremer, S., 2014. Recovery of Injected Freshwater from a Brackish Aquifer with a Multiwell System. Groundwater, 52(4): 495-502.

Missimer, T.M., Guo, W., Walker, C.W., Maliva, R.G., 2002. Hydraulic and density considerations in the design of aquifer storage and recovery systems. Florida Water Resources Journal, 55(2): 30-36.

Misut, P.E., Voss, C.I., 2007. Freshwater-saltwater transition zone movement during aquifer storage and recovery cycles in Brooklyn and Queens, New York City, USA. Journal of Hydrology, 337(1-2): 87-103.

Molz, F.J., Bell, L.C., 1977. Head gradient control in aquifers used for fluid storage. Water Resour. Res., 13(4): 795-798.

Molz, F.J., Melville, J.G., Güven, O., Parr, A.D., 1983a. Aquifer thermal energy storage: An attempt to counter free thermal convection. Water Resources Research, 19(4): 922-930.

Molz, F.J., Melville, J.G., Parr, A.D., King, D.A., Hopf, M.T., 1983b. Aquifer thermal energy storage : A well doublet experiment at increased temperatures. Water Resources Research, 19(1): 149-160.

Morris, B.L. et al., 2003. Groundwater and its susceptiblity to degradation: A global assessment of the problem and options for management., United Nations Environment Programme, Nairobi.

Mos Grondmechanica, 2006. Interpretation pilot drilling for ATES system grower's association Prominent at Groeneweg-II, Mos Grondmechanica, Rotterdam.

Negenman, A.J.H. et al., 1996. Landelijke hydrologische systeemanalyse; deelrapport 3: 'Deelgebied Noord- en Zuid-Holland ten zuiden van het Noordzeekanaal'. (National hydrologic system analysis; report 3: 'Part of the provinces of North and South Holland, South of the

Northsea Canal', in Dutch), IGG-TNO, Utrecht, The Netherlands.
Neil, C.W., Yang, Y.J., Schupp, D., Jun, Y.-S., 2014. Water Chemistry Impacts on Arsenic Mobilization from Arsenopyrite Dissolution and Secondary Mineral Precipitation: Implications for Managed Aquifer Recharge. Environmental Science & Technology.
Oele, E. et al., 1983. Surveying The Netherlands: sampling techniques, maps and their implications. Geologie en Mijnbouw, 62: 355-372.
Olsthoorn, T.N., 1982. KIWA announcement 71: Clogging of injection wells (in Dutch), Keuringsinstituut voor waterartikelen, Niewegein.
Olsthoorn, T.N., 2008. Brackish Groundwater as a New Resource for Drinking Water, Specific Consequences of Density Dependent Flow, and Positive Environmental Consequences 20th Saltwater Intrusion Meeting (SWIM), Naples, Florida, USA.
Oosterhof, A., Raat, K.J., Wolthek, N., 2013. Reuse of salinized well fields for the production of drinking water by interception and desalination of brackish groundwater, 9th Conference on water reuse. International Water Association (IWA), Windhoek, Namibia.
Oude Essink, G.H.P., 2001. Improving fresh groundwater supply--problems and solutions. Ocean & Coastal Management, 44(5-6): 429-449.
Oude Essink, G.H.P., van Baaren, E.S., de Louw, P.G.B., 2010. Effects of climate change on coastal groundwater systems: A modeling study in the Netherlands. Water Resources Research, 46: W00F04.
Paalman, M. et al., 2012. Vergroten zelfvoorzienendheid watervoorziening Glastuinbouw: Watervraag Glastuinbouw Haaglanden (deel 1). (Enlarging selfsufficient horticultural freshwater supply: Greenhouse areas Haaglanden (part 1), in Dutch). Knowledge for Climate, Utrecht, The Netherlands.
Parkhurst, D.L., Appelo, C.A.J., 1999. User's guide to PHREEQC (version 2): a computer program for speciation, batch-reaction, one-dimensional transport, and inverse geochemical calculations. Water-resources investigations report ; 99-4259. U.S. Geological Survey : Earth Science Information Center, Open-File Reports Section [distributor], Denver, Colorado, USA.
Patterson, B.M. et al., 2011. Behaviour and fate of nine recycled water trace organics during managed aquifer recharge in an aerobic aquifer. Journal of Contaminant Hydrology, 122(1-4): 53-62.
Pauw, P.S., 2015. Field and model investigations of freshwater lenses in coastal aquifers, Wageningen University, Wageningen, 158 pp.
Pavelic, P., Dillon, P., Simmons, C.T., 2002. Lumped parameter estimation of initial recovery efficiciency during ASR. In: Dillon, P.J. (Ed.), Fourth International Symposium on Artificial Recharge (ISAR4) Swerts & Zeitlinger, Adelaide, pp. 285-290.
Pavelic, P., Dillon, P.J., Nicholson, B.C., 2006. Comparative evaluation of the fate of disinfection byproducts at eight aquifer storage and recovery sites. Environ. Sci. Technol, 40(2): 501-508.

Peters, J.H., 1983. The movement of fresh water injected in salaquifers. KIWA, Nieuwegein.

Post, V.E.A., 2003. Groundwater salinization processes in the coastal area of the Netherlands due to transgressions during the Holocene, Vrije Universiteit, Amsterdam.

Post, V.E.A., 2011. Electrical Conductivity as a Proxy for Groundwater Density in Coastal Aquifers. Ground Water, 50(5): 5.

Postma, D., 1985. Concentration of Mn and separation from Fe in sediments—I. Kinetics and stoichiometry of the reaction between birnessite and dissolved Fe(II) at 10°C. Geochimica et Cosmochimica Acta, 49(4): 1023-1033.

Postma, D., Appelo, C.A.J., 2000. Reduction of Mn-oxides by ferrous iron in a flow system: column experiment and reactive transport modeling. Geochimica et Cosmochimica Acta, 64(7): 1237-1247.

Price, R.E., Pichler, T., 2006. Abundance and mineralogical association of arsenic in the Suwannee Limestone (Florida): Implications for arsenic release during water–rock interaction. Chemical Geology, 228(1–3): 44-56.

Projectgroep Zoetwateronderzoek Goes, 1986. Zoetwaterinfiltratieproef Kapelle, Commissie Waterbeheersing en Verzilting.

Prommer, H., Stuyfzand, P.J., 2005. Identification of temperature-dependent water quality changes during a deep well injection experiment in a pyritic aquifer. Environ. Sci. Technol, 39(7): 2200-2209.

Pyne, R.D.G., 2005. Aquifer Storage Recovery - A guide to Groundwater Recharge Through Wells. ASR Systems LLC, Gainesville, Florida, USA, 608 pp.

Reilly, T., Goodman, A., 1987a. Analysis of saltwater upconing beneath a pumping well. Journal of Hydrology, 89(3): 169-204.

Reilly, T.E., Goodman, A.S., 1987b. Analysis of saltwater upconing beneath a pumping well. Journal of Hydrology, 89(3–4): 169-204.

Richard, S. et al., 2014. Field evidence of hydraulic connections between bedrock aquifers and overlying granular aquifers: examples from the Grenville Province of the Canadian Shield. Hydrogeology Journal: 1-16.

Royal Netherlands Meteorological Institute, Precipitation surplus 1981-2010, http://www.knmi.nl, cited: 2013.

Royal Netherlands Meteorological Institute, Royal Netherlands Meteorological Institute - Precipitation weather station Rotterdam, http://www.knmi.nl, cited: 2011.

Royal Netherlands Meteorological Institute, 2014. KNMI'14 climate scenarios for The Netherlands; guideline for professionals in climate adaptation, KNMI, De Bilt.

Russel, M., (ed.), 2013. Clogging issues associated with managed aquifer recharge methods, 212 pp.

Santi, P., McCray, J., Martens, J., 2006. Investigating cross-contamination of aquifers. Hydrogeology

Journal, 14(1-2): 51-68.
Schmork, S., Mercado, A., 1969. Upconing of Fresh Water—Sea Water Interface Below Pumping Wells, Field Study. Water Resources Research, 5(6): 1290-1311.
Schothorst, C.J., 1977. Subsidence of low moor peat soils in the western Netherlands. Geoderma, 17(4): 265-291.
Schröter, D. et al., 2005. Ecosystem Service Supply and Vulnerability to Global Change in Europe. Science, 310(5752): 1333-1337.
Shiau, B.S., Yang, C.L., Tsai, B.J., 2007. Experimental Observations on the Submerged Discharge of Brine into Coastal Water in Flowing Current. Journal of Coastal Research, 50: 5.
Simcore Software, 2010. Processing Modflow 8: An Integrated Modeling Environment for the Simulation of Groundwater Flow, Transport and Reactive Processes.
Steeneveldt, R., Berger, B., Torp, T.A., 2006. CO2 Capture and Storage: Closing the Knowing–Doing Gap. Chemical Engineering Research and Design, 84(9): 739-763.
Stichting Infrastructuur Kwaliteitsborging Bodembeheer, 2013a. Protocol 2100 (version 3.1): Mechanical drilling (in Dutch). Stichting Infrastructuur Kwaliteitsborging Bodembeheer (SIKB), Gouda.
Stichting Infrastructuur Kwaliteitsborging Bodembeheer, 2013b. Protocol 11001: Design, realisation, and control of the subsurface elements of aquifer thermal energy storage systems (in Dutch). Stichting Infrastructuur Kwaliteitsborging Bodembeheer (SIKB), Gouda, pp. 74.
Stoeckl, L., Houben, G., 2012. Flow dynamics and age stratification of freshwater lenses: Experiments and modeling. Journal of Hydrology, 458–459(0): 9-15.
Stuyfzand, P., Raat, K., 2010. Benefits and hurdles of using brackish groundwater as a drinking water source in the Netherlands. Hydrogeology Journal, 18(1): 117-130.
Stuyfzand, P.J., 1993. Hydrochemistry and Hydrology of the Coastal Dune area of the Western Netherlands, Vrije Universiteit, Amsterdam, The Netherlands, 366 pp.
Stuyfzand, P.J., 1994. Geohydrochemical aspects of methane in Dutch groundwater (in Dutch). H2O, 27(17): 500 - 510.
Stuyfzand, P.J., 1998. Quality changes upon injection into anoxic aquifers in the Netherlands: Evaluation of 11 experiments In: Peter, J.H. (Ed.), Artificial recharge of groundwater, Proc. 3rd Intern. Symp. on Artificial Recharge. Balkema, Amsterdam, The Netherlands, 283-291 pp.
Stuyfzand, P.J., 2008. Base Exchange Indices as Indicators of Salinization or Freshening of (Coastal) Aquifers Saltwater Intrusion Meeting. IFAS Research, Napels, Florida, USA, pp. 262-265.
Stuyfzand, P.J., Nienhuis, P., Antoniou, E.A., Zuurbier, K.G., 2012. Feasibility of subterranean storage via A(S/T)R in the coastal dunes of Holland (Western Netherlands). KWR Report 2012.082 (in Dutch), KWR.
Stuyfzand, P.J., Van Rossum, P., Mendizabal, I., 2006. Does arsenic, in groudnwater of

the compound Rhine-Meuse-Scheldt-Ems delta, menace drinking water supply in The Netherlands?. In: Appelo, C.A.J. (Ed.), Arsenic in Groundwater, a world problem, Utrecht.

Technische Commissie Bodem, 2010. Advies Lozingen van brijn bij agrarische activiteiten A064(2010).

TNO-NITG, TNO-NITG DINOloket, http://www.dinoloket.nl, cited: 2011.

TNO, 1995. Interpolated isohypses (28-4-1995). In: TNO (Ed.), Utrecht, The Netherlands.

Torkzaban, S. et al., 2015. Colloid Release and Clogging in Porous Media: Effects of Solution Ionic Strength and Flow Velocity. Journal of Contaminant Hydrology(181): 161-171.

Tsang, C.-F., Birkholzer, J., Rutqvist, J., 2008. A comparative review of hydrologic issues involved in geologic storage of CO_2 and injection disposal of liquid waste. Environmental Geology, 54(8): 1723-1737.

United Nations, 2010. UN Atlas of the Oceans. In: United Nations (Ed.), UN Atlas of the Oceans. United Nations, Rome, Italy.

Vacher, H.L., Hutchings, W.C., Budd, D.A., 2006. Metaphors and Models: The ASR Bubble in the Floridan Aquifer. Ground Water, 44(2): 144-154.

Valocchi, A.J., Street, R.L., Roberts, P.V., 1981. Transport of ion-exchanging solutes in groundwater: Chromatographic theory and field simulation. Water Resour. Res., 17(5): 1517-1527.

Van Beek, C.G.E.M., 1985. Experiences with underground water treatment in the Netherlands. Water Supply, 3(2): 1-11.

Van Beek, C.G.E.M., 2012. Cause and prevention of clogging of wells abstracting groundwater. IWA Publishing, London

van den Hurk, B. et al., 2007. New climate change scenarios for the Netherlands., Water Science and Technology, pp. 27-33.

van Ginkel, M., 2015. Aquifer design for freshwater storage and recovery in artificial islands and coastal expansions. Hydrogeology Journal, 23(4): 615-618.

Van Ginkel, M., Olsthoorn, T.N., Bakker, M., 2014. A New Operational Paradigm for Small-Scale ASR in Saline Aquifers. Groundwater, 52(5): 685-693.

Van Ginkel, M., Olsthoorn, T.N., Smidt, E., Darwish, R., Rashwan, S., 2010. Fresh Storage Saline Extraction (FSSE) wells, feasibility of freshwater storage in saline aquifer with a focus on the Red Sea coast, Egypt, ISMAR, 2010, Abu Dhabi, United Arab Emirates.

van Halem, D. et al., 2010. Subsurface iron and arsenic removal for shallow tube well drinking water supply in rural Bangladesh. Water Research, 44(19): 5761-5769.

van Halem, D., Vet, W.d., Verberk, J., Amy, G., van Dijk, H., 2011. Characterization of accumulated precipitates during subsurface iron removal. Applied Geochemistry, 26(1): 116-124.

Van Helvoort, P.J., 2003. Complex confining layers: a physical and geochemical characterization of heterogeneous unconsolidated fluvial deposits using a facies-based approach, Utrecht University, Utrecht.

Vanderzalm, J.L. et al., 2011. Arsenic mobility and impact on recovered water quality during aquifer storage and recovery using reclaimed water in a carbonate aquifer. Applied Geochemistry, 26(12): 1946-1955.

Verruijt, A., 1968. A note on the Ghyben-Herzberg formula. Bulletin of the International Association of Scientific Hydrology (Delft, Netherlands: Technological University), 13(4): 43-46.

Vienken, T., Dietrich, P., 2011. Field evaluation of methods for determining hydraulic conductivity from grain size data. Journal of Hydrology, 400(1–2): 58-71.

Wallis, I. et al., 2011. Process-Based Reactive Transport Model To Quantify Arsenic Mobility during Aquifer Storage and Recovery of Potable Water. Environmental Science & Technology, 45(16): 6924-6931.

Wallis, I., Prommer, H., Post, V., Vandenbohede, A., Simmons, C.T., 2013. Simulating MODFLOW-Based Reactive Transport Under Radially Symmetric Flow Conditions. Groundwater, 51(3): 398-413.

Wallis, I., Prommer, H., Simmons, C.T., Post, V., Stuyfzand, P.J., 2010. Evaluation of Conceptual and Numerical Models for Arsenic Mobilization and Attenuation during Managed Aquifer Recharge. Environmental Science & Technology, 44(13): 5035-5041.

Ward, J.D., Simmons, C.T., Dillon, P.J., 2007. A theoretical analysis of mixed convection in aquifer storage and recovery: How important are density effects? Journal of Hydrology, 343(3-4): 169-186.

Ward, J.D., Simmons, C.T., Dillon, P.J., 2008. Variable-density modelling of multiple-cycle aquifer storage and recovery (ASR): Importance of anisotropy and layered heterogeneity in brackish aquifers. Journal of Hydrology, 356(1-2): 93-105.

Ward, J.D., Simmons, C.T., Dillon, P.J., Pavelic, P., 2009. Integrated assessment of lateral flow, density effects and dispersion in aquifer storage and recovery. Journal of Hydrology, 370(1-4): 83-99.

Weber, W.J., Smith, E.H., 1987. Simulation and design models for adsorption processes. Environmental Science & Technology, 21(11): 1040-1050.

Weltje, G.J., Tjallingii, R., 2008. Calibration of XRF core scanners for quantitative geochemical logging of sediment cores: Theory and application. Earth and Planetary Science Letters, 274(3–4): 423-438.

Werner, A.D. et al., 2013. Seawater intrusion processes, investigation and management: Recent advances and future challenges. Advances in Water Resources, 51(0): 3-26.

Werner, A.D., Jakovovic, D., Simmons, C.T., 2009. Experimental observations of saltwater up-coning. Journal of Hydrology, 373(1-2): 230-241.

Wolthek, N., Raat, K., de Ruijter, J.A., Kemperman, A., Oosterhof, A., 2012. Desalination of brackish groundwater and concentrate disposal by deep well injection. Desalination and Water Treatment, 51(4-6): 1131-1136.

World Economic Forum, 2015. Global Risks 2015, World Economic Forum, Davos, Switzerland.

Zheng, X.-l., Shan, B.-b., Chen, L., Sun, Y.-w., Zhang, S.-h., 2014. Attachment–detachment dynamics of suspended particle in porous media: Experiment and modeling. Journal of Hydrology, 511(0): 199-204.

Zuurbier, K.G., Hartog, N., Valstar, J., Post, V.E.A., van Breukelen, B.M., 2013. The impact of low-temperature seasonal aquifer thermal energy storage (SATES) systems on chlorinated solvent contaminated groundwater: Modeling of spreading and degradation. Journal of Contaminant Hydrology, 147(0): 1-13.

Zuurbier, K.G., Paalman, M., Zwinkels, E., 2012. Haalbaarheid Ondergrondse Waterberging Glastuinbouw Westland. KWR 2012.003, KWR Watercycle Research Institute, Nieuwegein.

Zwinkels, E., 2010. Installed ASR systems in the Eastland area. Personal communication.

Aquifer storage and recovery using groundwater wells can provide a robust, cost-effective, and sustainable freshwater supply. However, buoyancy effects force the freshwater to float upwards in brackish-saline aquifers, resulting in an early and often unacceptable recovery of too saline ambient groundwater by lower parts of the well. This raises the question of ASR optimization for brackish-saline aquifers.

In this PhD thesis, a broadened scientific understanding of the performance of ASR in brackish-saline aquifers is described. Meaningful a priori indication of the ASR performance could be mapped and highlighted a highly-variable ASR-performance in coastal areas. A potential increase in freshwater recovery can be attained by implementing dedicated well configurations at ASR-systems in brackish-saline aquifers. This was confirmed during field pilots using multiple partially penetrating wells (MPPW) and horizontal directional drilled wells (HDDWs). These dedicated well configurations are primarily based on an increased vertical control on freshwater injection and recovery, optionally complemented by interception of deeper brackish or saline groundwater.

The findings in this thesis provide important means to achieve a local, self-reliant freshwater supply in especially coastal areas using temporally available freshwater sources via ASR. In these areas, which suffer most from decreasing freshwater availabilities and growing demands, ASR can now become a viable cost-effective freshwater management option, whereas it was previously neglected due to the limited success of conventional ASR systems.